

# **Impact of *APOE* genotype and age on large-scale MTL neurocognitive networks**

Rikki Lissaman

A thesis submitted for the degree of Doctor of Philosophy

School of Psychology, Cardiff University

September 2021



## Statements and declarations

### Statement 1

This thesis is being submitted in partial fulfilment of the requirements for the degree of PhD.

Signed ..... (candidate) Date .....

### Statement 2

This work has not been submitted in substance for any other degree or award at this or any other university or place of learning, nor is it being submitted concurrently for any other degree or award (outside of any formal collaboration agreement between the University and a partner organisation).

Signed ..... (candidate) Date .....

### Statement 3

I hereby give consent for my thesis, if accepted, to be available in the University's Open Access repository (or, where approved, to be available in the University's library and for inter-library loan), and for the title and summary to be made available to outside organisations, subject to the expiry of a University-approved bar on access if applicable.

Signed ..... (candidate) Date .....

### Declaration

This thesis is the result of my own independent work, except where otherwise stated, and the views expressed are my own. Other sources are acknowledged by explicit references. The thesis has not been edited by a third party beyond what is permitted by Cardiff University's Use of Third Party Editors by Research Degree Students Procedure.

Signed ..... (candidate) Date .....

In loving memory of my brother,  
Josh.

## Acknowledgements

First and foremost, I would like to thank my supervisors: Dr Carl Hodgetts, Professor Andrew Lawrence, and Professor Kim Graham. Your guidance – both professional and personal – has made me a better, more confident researcher. This PhD is a testament to your supervision.

I would also like to thank Dr Mark Postans and Dr Angharad Williams for their support. I consider myself lucky to have found myself in a lab with such kind, encouraging post-docs. Additional thanks to Dr Raluca Petrican for taking the time to answer my many questions about partial least squares analysis.

Outside of CUBRIC, I owe a great deal of gratitude to my friends: Marshall, Gillies, Anton, and Tomos. Thank you for reminding me that there is more to life than my PhD. I look forward to celebrating with you all.

Thanks also to my family, the self-titled “Morris mafia”. There are too many of you to thank individually, but I am grateful for all that you have done for me over the years.

Special thanks go to my parents. Your unwavering support and unconditional love made all of this possible. I could not ask for better parents. Thank you for everything.

Last, but by no means least, I would like to thank my partner Debs for supporting me throughout this journey. I haven’t been the easiest person to deal with, but you have been there every step of the way. You truly are my better half, and I cannot wait to see what the future holds for us. Inñobbok ñafna.



## Thesis summary

Research on medial temporal lobe (MTL) function converges on the notion that the hippocampus and perirhinal cortex (PRC) are specialised for different types of representational content: scenes and objects. The evolutionary accretion model advances this further, proposing that these MTL structures constitute key nodes within the extended hippocampal navigation and feature networks, respectively. The former network is considered more vulnerable to the impact of age and age-related neurodegenerative disease, including Alzheimer's disease (AD). Additionally, young carriers of the apolipoprotein E (*APOE*)  $\epsilon$ 4 allele – an AD risk factor – have been shown to exhibit alterations within this network, supporting lifespan accounts of cognitive decline. Recently, however, this network-selective vulnerability has been challenged by reports of object-related impairments in ageing and AD risk.

This thesis therefore investigated the impact of *APOE* genotype – especially *APOE*  $\epsilon$ 4 – and age on these two neurocognitive networks and their representations. To achieve this, web-based cognitive testing (Chapter 2), magnetic resonance imaging (MRI)-based structural covariance analysis (Chapter 3), and diffusion MRI-based tractography (Chapter 4) were used.

In middle-aged and older adults, *APOE*  $\epsilon$ 4 and *APOE*  $\epsilon$ 2 – a risk-reducing allele – were associated with divergent age trends in perceptual discrimination independent of condition (Chapter 2). Conversely, in a sample spanning the adult lifespan, age and gender/sex – but not *APOE*  $\epsilon$ 4 – were associated with the structural covariance of the hippocampus and PRC (Chapter 3). Finally, in younger adults, *APOE*  $\epsilon$ 4 impacted the lateralisation of inferior longitudinal fasciculus (ILF) microstructure – a key tract in the feature network (Chapter 4).

The findings of this thesis provide evidence that *APOE* genotype and age impact aspects of these networks and their representations, but it remains

challenging to interpret them collectively. Nonetheless, this research addresses pre-existing limitations, and provides a foundation for studies that could aid our understanding of age- and *APOE*-related impact(s) on the brain and cognition.

## Table of contents

<b>Chapter 1: General introduction</b>	<b>1</b>
1.1. Representational content in large-scale medial temporal lobe neurocognitive networks	1
1.1.1. The medial temporal lobe: More than a unitary system	1
1.1.2. From nodes to neurocognitive networks	12
1.1.2.1. The extended hippocampal navigation network	12
1.1.2.2. The feature network	15
1.1.2.3. Connecting it all together: Network disconnection and amnesia	17
Box 1. Approaches to studying connectivity in the living human brain	22
1.2. Impact of age and age-related neurodegenerative disease	29
1.2.1. Age and the extended hippocampal navigation network	30
1.2.1.1. Spatial memory and navigation	30
1.2.1.2. Episodic memory	32
1.2.1.3. Scene-related cognition	33
1.2.2. Alzheimer's disease and the extended hippocampal navigation network	34
1.2.3. Age and the feature network	41
1.2.4. Alzheimer's disease and the feature network	43
1.3. <i>APOE</i> $\epsilon$ 4 as a risk factor for age-related cognitive decline	45
1.4. Aims of the thesis	54

<b>Chapter 2: Impact of <i>APOE</i> genotype and age on different-view scene and face odd-one-out perceptual discrimination in middle-aged and older adults</b>	<b>57</b>
2.1. Introduction	57
2.2. Methods	67
2.2.1. Participants	67
2.2.2. Procedure	70
2.2.3. Odd-one-out perceptual discrimination task (Lee, Buckley et al., 2005)	70
2.2.4. Family history of dementia questionnaire	74
2.2.5. <i>APOE</i> genotype	75
2.2.6. Statistical analyses	76
2.3. Results	82
2.3.1. Sample characteristics	82
2.3.2. Four-choice odd-one-out perceptual discrimination performance	87
2.3.2.1. Mean correct RTs	87
2.3.2.2. Proportion correct	90
2.3.2.3. Difference scores	93
2.4. Discussion	96
2.5. Summary	105
<b>Chapter 3: Impact of <i>APOE</i> <math>\epsilon</math>4, gender/sex, and age on the structural covariance of the hippocampus and perirhinal cortex across the adult lifespan</b>	<b>107</b>
3.1. Introduction	107
3.2. Methods	114
3.2.1. Participants	114
3.2.2. <i>APOE</i> genotype	116
3.2.3. MRI acquisition	117
3.2.4. MRI pre-processing	118
3.2.5. Cognitive tasks	118
3.2.6. Statistical analyses	121

3.2.6.1.	Sample characteristics	121
3.2.6.2.	Structural covariance analysis	121
3.2.6.3.	Cognitive correlates of the structural covariance patterns	124
3.3.	Results	125
3.3.1.	Sample characteristics	125
3.3.2.	Structural covariance analysis	126
3.3.3.	Cognitive correlates of the structural covariance pattern	131
3.4.	Discussion	135
3.5.	Summary	142
<b>Chapter 4: Impact of <i>APOE</i> <math>\epsilon</math>4 on parahippocampal cingulum bundle microstructure in healthy young adults</b>		<b>144</b>
4.1.	Introduction	144
4.2.	Methods	152
4.2.1.	Participants	152
4.2.2.	<i>APOE</i> genotype	154
4.2.3.	MRI acquisition	156
4.2.4.	Diffusion MRI	157
4.2.4.1.	Pre-processing	157
4.2.4.2.	Tractography	158
4.2.4.3.	Automated tract reconstruction	158
4.2.4.4.	TBSS	159
4.2.5.	Statistical analyses	160
4.2.5.1.	Primary (replication) analyses	162
4.2.5.2.	Secondary (extension) analyses	163
4.2.5.2.1.	HMOA	163
4.2.5.2.2.	Hemispheric asymmetry in PHCB and ILF microstructure: Impact of <i>APOE</i> $\epsilon$ 4 and sex	163
4.3.	Results	164
4.3.1.	Sample characteristics	164

4.3.2.	Primary (replication) analyses	165
4.3.2.1.	Impact of <i>APOE</i> $\epsilon$ 4 on bilateral PHCB FA and MD	165
4.3.2.2.	Impact of <i>APOE</i> $\epsilon$ 4 on bilateral ILF and MD	168
4.3.2.3.	TBSS	169
4.3.3.	Secondary (extension) analyses	170
4.3.3.1.	Impact of <i>APOE</i> $\epsilon$ 4 on bilateral PHCB and ILF HMOA	170
4.3.3.2.	Hemispheric asymmetry in PHCB and ILF microstructure: Impact of <i>APOE</i> $\epsilon$ 4 and sex	172
4.4.	Discussion	178
4.5.	Summary	186
<b>Chapter 5: General discussion</b>		<b>187</b>
5.1.	Summary of main findings	189
5.1.1.	Odd-one-out perceptual discrimination accuracy differs as a function of <i>APOE</i> genotype and age in middle-aged and older females	189
5.1.2.	Gender/sex and age but not <i>APOE</i> $\epsilon$ 4 impact the shared structural covariance of the anteromedial hippocampus and PRC	192
5.1.3.	<i>APOE</i> $\epsilon$ 4 does not impact PHCB microstructure in young adults but does impact ILF lateralisation	194
5.2.	Theoretical implications	196
5.3.	Methodological considerations and implications	203
5.3.1.	Reliance on cross-sectional designs and the treatment of age as an independent variable	204
5.3.2.	Lack of $A\beta$ and tau PET imaging	206
5.3.3.	Inability to account for ethnicity/ancestry	207

5.3.4.	Lack of statistical power to investigate the impact of all <i>APOE</i> allele combinations	209
5.3.5.	Inability to examine polygenic effects	210
5.4.	Outstanding questions and future directions	211
5.4.1.	How does the <i>APOE</i> $\epsilon$ 2 allele fit into lifespan systems vulnerability accounts?	212
5.4.2.	Do <i>APOE</i> $\epsilon$ 4 carriers and non-carriers undergo different patterns of white matter maturation during childhood/adolescence?	213
5.4.3.	Are hippocampal subfields differentially vulnerable to the impact of <i>APOE</i> $\epsilon$ 4 and age?	214
5.5.	Concluding remarks	216
<b>References</b>		<b>218</b>
<b>Appendix</b>		<b>307</b>

## List of abbreviations

The table below lists the various abbreviations, acronyms, and initialisms used throughout this thesis. The page on which each is first used or defined is also provided. Abbreviations, acronyms, and initialisms used in specific figures or tables – but not in text – are not included.

---

Abbreviation	Meaning	Page
$\alpha$	Alpha	81
A $\beta$	Amyloid-beta	36
ABCD study	Adolescent Brain Cognitive Development study	214
AD	Alzheimer's disease	34
ALSPAC	Avon Longitudinal Study of Parents and Children	55
ANOVA	Analysis of variance	76
APOE	Apolipoprotein E	46
BFs	Bayes factors	161
BMI	Body mass index	76
BSR	Bootstrap ratio	122
BOLD	Blood oxygenation level-dependent	26
CAT12	Computational Anatomy Toolbox (version 12)	118
CUBRIC	Cardiff University Brain Research Imaging Centre	152
CWTCH	Cardiff Web Tools for Cognitive health	66
EC	Entorhinal cortex	1
DLBS	Dallas Lifespan Brain Study	113
DMTS	Delayed match-to-sample	112
dRL	Damped Richardson Lucy	158
DTI	Diffusion tensor imaging	24
FA	Fractional anisotropy	23
fMRI	Functional magnetic resonance imaging	10
fODF	Fibre orientation distribution function	25
FWE	Free water elimination	157



GWAS	Genome wide association study	47
HARDI	High angular diffusion imaging	156
HMOA	Hindrance modulated orientational anisotropy	151
IES	Inverse efficiency score	79
ILF	Inferior longitudinal fasciculus	15
LDL	Low-density lipoprotein	83
LIs	Lateralisation indices	152
LVs	Latent variables	122
MCI	Mild cognitive impairment	35
MD	Mean diffusivity	23
MEG	Magnetoencephalography	52
MoCA	Montreal Cognitive Assessment	44
MNI	Montreal Neurological Institute	118
MRI	Magnetic resonance imaging	10
MTL	Medial temporal lobe	1
NHST	Null hypothesis significance testing	122
PCC	Posterior cingulate cortex	13
PET	Positron emission tomography	34
PHC	Parahippocampal cortex	1
PHCB	Parahippocampal cingulum bundle	13
PLS	Partial least squares	121
PRC	Perirhinal cortex	1
PRS	Polygenic risk score	211
RTs	Response times	77
ROI	Region of interest	27
RSC	Retrosplenial cortex	11
SNP	Single nucleotide polymorphism	116
TBSS	Tract-based spatial statistics	23
TFCE	Threshold-free cluster enhancement	160
WAIS-III	Wechsler Adult Intelligence Scale-III	113

---

## Chapter 1: General introduction

### 1.1. Representational content in large-scale medial temporal lobe neurocognitive networks

#### 1.1.1. *The medial temporal lobe: More than a unitary memory system*

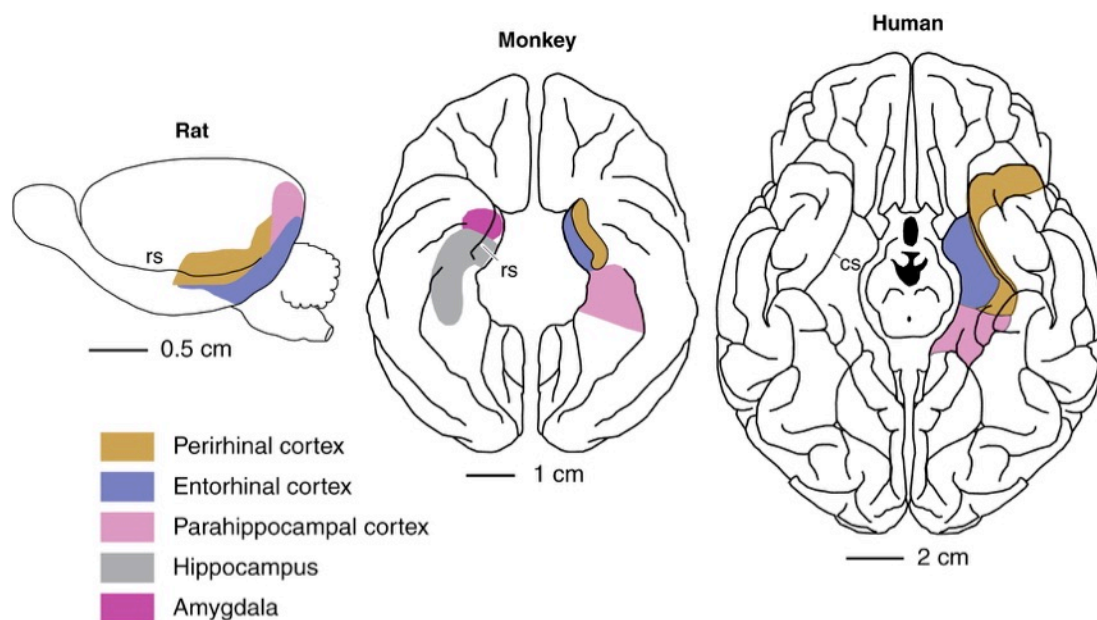
On August 25, 1953, Henry Gustav Molaison underwent a radical surgical procedure that would change his life and the field of memory research forever (Eichenbaum, 2013; Rosenbaum et al., 2014). The surgery, which aimed to control his intractable epileptic seizures, involved the removal of a substantial portion of the temporal lobe, including much of the hippocampus (Scoville, 1954; for more recent evaluations of Henry's surgical lesion, see Annese et al., 2014; Corkin et al., 1997). Although successful in reducing the frequency of Henry's seizures (Maguière & Corkin, 2015), the surgery had an unforeseen yet profound effect: it left him densely amnesic. This severe memory impairment, first fully described in the seminal case report by Scoville and Milner (1957), inspired a generation of research investigating the neural basis of memory, and established Henry – better known as patient H.M. – as part of neuroscientific lore (Squire, 2009).

In subsequent years, memory research became heavily centred on the hippocampus and its neighbouring neocortical structures, namely the entorhinal cortex (EC), perirhinal cortex (PRC) and parahippocampal cortex (PHC). These structures, illustrated in Figure 1.1, are often referred to collectively as the “medial temporal lobe” (MTL; Squire et al., 2004). Over time, this research led to the development of the extremely influential MTL memory system account (Squire & Zola-Morgan, 1991; see also Squire, 2004; Squire & Dede, 2015; Squire & Wixted, 2011). The central premise of this account is that the MTL constitutes an anatomically and functionally distinct system that is specialised for so-called declarative or explicit memory (Cohen & Squire, 1980) – that is, memory for facts (i.e. semantic memory) and events (i.e. episodic memory; Tulving, 1972, 1983, 2002). Perception

and other aspects of cognition are instead proposed to arise via alternative systems (Squire & Zola, 1996). The MTL memory system account further predicts that the degree of damage to its components should be proportional to the degree of declarative memory impairment observed (Zola-Morgan et al., 1994). In short, this account claims that 1) the MTL constitutes a specialised memory system, and 2) that there is no meaningful division of function *within* the MTL.

**Figure 1.1.**

*Approximate Size and Location of MTL Structures in the Rat, Monkey, and Human Brain*



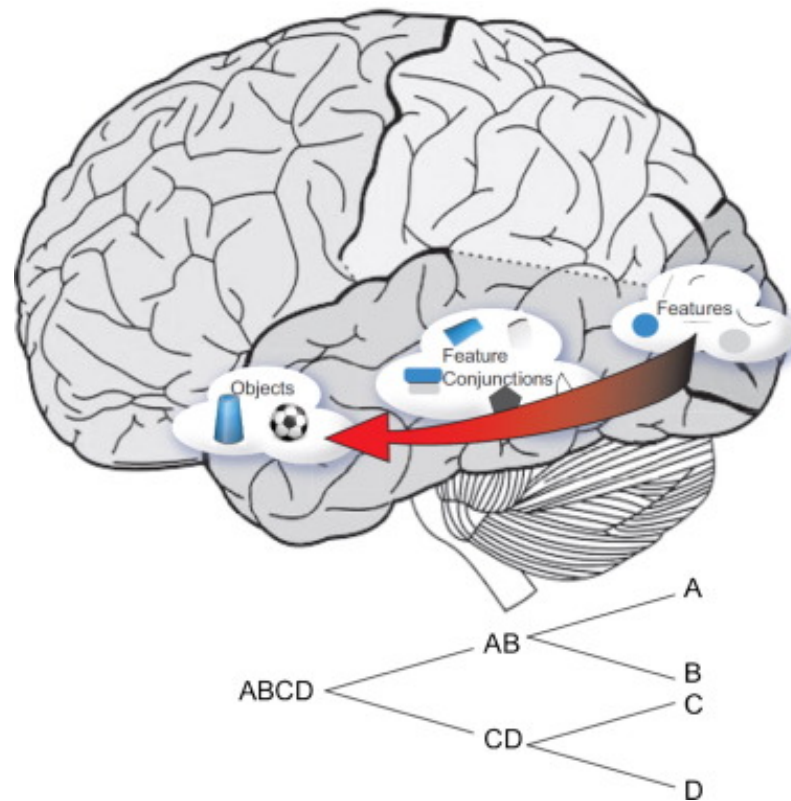
*Note.* Structures typically included as part of the MTL (Squire et al., 2004), as well as the amygdala, are shown on the lateral surface of a rat brain (left) and the ventral surface of a monkey brain (middle) and a human brain (right). Although the PHC is shown in the rat, this actually corresponds to a homologous structure called the postrhinal cortex (Burwell et al., 1995; Burwell, 2001). Abbreviations: rs = rhinal sulcus, cs = collateral sulcus. Reprinted from Murray et al. (2007).

Despite its popularity, accumulating evidence has challenged the unitary MTL memory system account, demonstrating that MTL structures can be

functionally differentiated from one another and contribute to functions other than declarative memory (for relevant reviews and commentaries, see Eichenbaum et al., 2012; Gaffan, 2002; Graham et al., 2010; Hassabis & Maguire, 2009; Lee, Barense, & Graham, 2005; Lee et al., 2012; Maguire et al., 2016; Maguire & Mullally, 2013; Murray et al., 2007, 2017; Murray & Wise, 2004, 2010, 2012; Ranganath & Ritchey, 2012; Ritchey et al., 2015; Saksida & Bussey, 2010; Schacter et al., 2017). For example, studies in primates have long shown that lesions to the hippocampus and its major input/output pathway – the fornix – selectively impair scene-specific memory (Gaffan, 1994), whereas lesions to the PRC selectively impair no-delay object recognition (Eacott et al., 1994) and concurrent object discrimination learning (Buckley & Gaffan, 1997, 1998). Subsequent patient work in humans has provided comparable evidence, demonstrating that the hippocampus and PRC are crucial for accurate perceptual discrimination of complex conjunctive scene and object/face stimuli, respectively (Aly et al., 2013; Barense et al., 2005; Buckley & Gaffan, 2006; Behrmann et al., 2016; Lee, Buckley et al., 2005; Lee, Bussey et al., 2005; Mundy et al., 2013). Inspired by such findings, contemporary accounts of MTL function have proposed that its component structures are functionally specialised to encode and store different types of representational content, which can then be called upon to support various aspects of cognition, such as attention (Ruiz et al., 2020), perceptual learning (Mundy et al., 2013), working memory (Lee & Rudebeck, 2010), imagination (Schacter et al., 2017), and social cognition (Schafer & Schiller, 2018).

One such account, referred to as the “representational-hierarchical” account (Bussey & Saksida, 2007; Cowell et al., 2010a, 2010b, 2019; Saksida & Bussey, 2010), proposes that structures within the MTL form part of a continuum or pathway within the ventral visual stream (Ungerleider & Haxby, 1994). Proponents of this view argue that there is no sharp separation between perception and memory in the brain, as suggested by the MTL memory system (for a recent discussion, see Cowell et al., 2019). Instead, MTL structures – notably the PRC – form part of a hierarchical pathway that represents visual information at increasing levels of complexity (Figure 1.2).

This pathway begins in early visual areas, located at the most posterior end of the ventral visual stream, where lower-level features (e.g. orientation, colour) are represented. As this information is then passed on to more anterior regions of the ventral visual stream, increasingly complex conjunctions of these features are represented, ultimately reaching the point at which a complete object is represented in the PRC. It is important to note, however, that this account emphasises the importance of the PRC in representing complex conjunctions of features at the object-level rather than objects per se. In this regard, the PRC is hypothesised to resolve “feature ambiguity” (Barense et al., 2005; Bussey & Saksida, 2002; Bussey et al., 2002; O’Neil et al., 2009). That is, the PRC is required whenever an individual must discriminate between stimuli with overlapping features, whether “true” objects or not (e.g. faces). Although heavily focused on the PRC, this account further places the hippocampus at the apex of the PRC-ventral visual processing stream, where it houses complex conjunctions of both object and spatial information (Lee et al., 2012; Saksida & Bussey, 2010). As such, this view proposes that hippocampal representations may help to resolve “spatial ambiguity” – that is, situations in which stimuli share spatial features (Cowell et al., 2010a; for a related view, see Turk-Browne, 2019), as assessed using tasks that manipulate properties such as the distance between objects or the visual angle of object features. Evidence in support of this view comes from a variety of sources, including research on rodents showing that lesions to the hippocampus impair the ability to discriminate between similar spatial locations (McTighe et al., 2009; for a relevant example in monkeys, see Buckley et al., 2004).

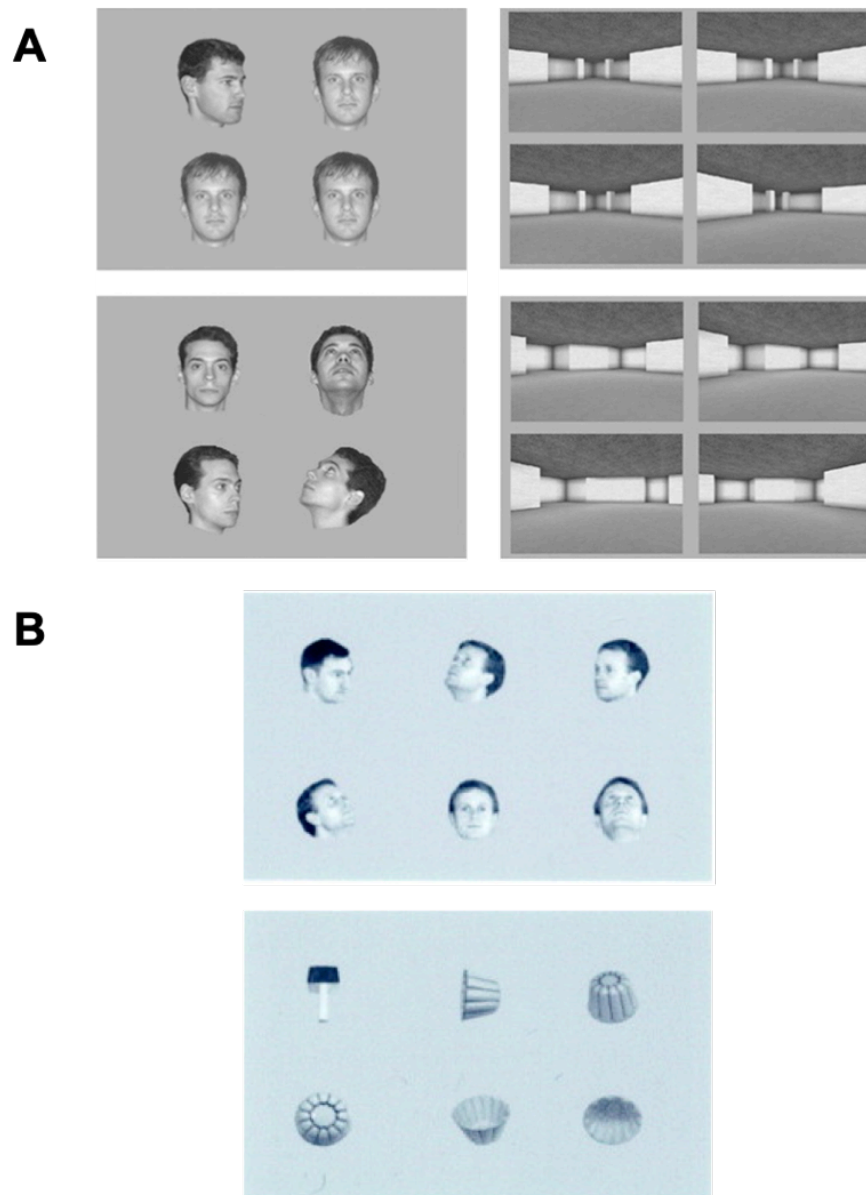
**Figure 1.2.***The Representational-Hierarchical Account*

*Note.* The arrow shows how representations of visual features in the brain become increasingly complex as information passes from posterior to anterior regions along the PRC-ventral visual processing stream. This is also reflected by the letters, whereby the individual features (A, B, C, D) are ultimately represented as a complex conjunction of these features (ABCD). Reprinted from Kent et al. (2016).

Building on the representational-hierarchical view, the emergent memory account (Graham et al., 2010) likewise rejects the existence of a sharp dichotomy between perception and memory in the brain. Rather, its proponents argue that the hippocampus and PRC create complex conjunctive scene and object (including face) representations, which can support perception and memory, as well as other aspects of cognition (Graham et al., 2010; Lee, Barense, & Graham, 2005). A key prediction of the emergent memory account is that MTL engagement in a given task will be driven not by cognitive function (e.g. declarative memory; Squire & Wixted, 2011) or process (e.g. familiarity and recollection; for reviews of this

literature, see Aggleton & Brown, 1999; Yonelinas, 2002), but the degree to which the task in question taxes these complex conjunctive representations. In this regard, both the representational-hierarchical account and the emergent memory account emphasise the role of MTL structures in supporting different forms of representational content. Over the last two decades, a number of tasks have been developed in non-human species, and translated into humans, to test this prediction. These include concurrent configural discrimination tasks, pairwise “morph” discrimination tasks, and odd-one-out perceptual discrimination (a.k.a. oddity or oddity judgment) tasks (for detailed discussions of these tasks, see Graham et al., 2010; Lee et al., 2012; Saksida & Bussey, 2010).

Here, I focus specifically on the odd-one-out perceptual discrimination task, as studies using it provide some of the strongest evidence in support of representational accounts of MTL function. The goal of this task is to identify the odd-one-out from a visual array of same-category stimuli that are presented simultaneously, typically containing three or four items in total (Figure 1.3). Non-target stimuli in the array are the same stimulus presented either from the same viewpoint (i.e. same-view condition) or different viewpoint (i.e. different-view condition). Successful identification of the odd-one-out depends more heavily on conjunctive/configural processing in the different-view condition than in the same-view condition, as the variation in viewpoint means that all stimuli differ at the level of simple features. As such, only processing the configuration – that is, the arrangement of the various features – will lead to the odd-one-out. While early animal studies using this task measured performance by trials to criterion and may therefore reflect learning rather than perception (Buckley et al., 2001; for a critique of this methodology, see Hampton, 2005), more recent versions used in humans utilise trial-unique stimuli, meaning that there is little – if any – demand on memory. Variations of this task have been increasingly used in recent years, including both patient studies and neuroimaging studies of cognitively unimpaired individuals.

**Figure 1.3.***The Odd-One-Out Perceptual Discrimination Task*

*Note.* Example oddity stimuli from human (A) and monkey (B) studies. In panel A, stimuli for four conditions are shown: same-view face (top-left), different-view face (bottom-left), same-view scene (top-right), and different-view scene (bottom-right). Note how the local features of the non-target stimuli are the same in the same-view face and scene conditions but not in the different-view face and scene conditions. In panel B, stimuli for two conditions are shown: different-view human face (top) and different-view object (bottom). Other types of stimuli are sometimes used in these tasks (e.g. greebles; Gauthier & Tarr, 1997), although these are not shown here. Panel A reprinted from Lee, Buckley et al. (2005). Panel B adapted from Buckley et al. (2001).



In one of the first applications of this paradigm, Buckley et al. (2001) examined perceptual discrimination accuracy in monkeys with PRC lesions. Several different conditions were included – some involving stimuli that could be identified based on single features (e.g. shapes, colours, and sizes), others involving stimuli that could be identified based on conjunctions of features (e.g. human faces, monkey faces, objects with various levels of perceptual noise, scenes). Compared to control monkeys, those with PRC lesions were found to be unimpaired on colour, shape, and size oddity, even when the conditions were made harder (e.g. by manipulating the difference in hue between stimuli in the colour oddity). By contrast, the monkeys with PRC lesions were impaired relative to controls on object oddity, particularly when the non-target stimuli were presented from different viewpoints. PRC-related impairments were further evident in the human face, monkey face, and scene oddity conditions. Thus, Buckley et al. (2001) concluded that their results indicate that the PRC supports perception for specific types of stimuli, which rely on more abstract, object-level representations (see also Buckley & Gaffan, 2006). To account for the scene deficit, the authors speculated that the monkeys might have treated the scene stimuli as objects in and of themselves. However, at around the same time, a study using a similar version of the oddity task with human amnesia patients failed to replicate these observations (Stark & Squire, 2000). Instead, patients with damage including the PRC performed normally on all conditions, including those involving object discrimination (Stark & Squire, 2000). Moreover, as mentioned previously, Buckley et al.'s (2001) study was later criticised for conflating learning/memory and perception by measuring performance via trials to criterion (Hampton, 2005; although for a response, see Buckley, 2005).

Lee, Buckley et al. (2005) sought to address this criticism in one of two experiments on human amnesia patients by examining performance on the odd-one-out task using trial-unique stimuli. Adapting the task for human use in this way made it possible to minimise any reliance on learning/memory, thereby addressing a critical “translational gap” in the literature. Two groups of patients were included: those with selective hippocampal damage and

those with wider MTL damage (including the PRC). Four types of stimuli were used: same-view faces, different-view faces, same-view scenes, and different-view scenes. Results showed that, relative to age-matched controls, patients with damage restricted to the hippocampus were selectively impaired in the different-view scene condition. By contrast, patients with more extensive damage to the MTL – including the hippocampus *and* the PRC – were impaired on both different-view scene and face discrimination relative to controls. No differences were evident between patients and controls for same-view stimuli, suggesting that the representations housed by the hippocampus and PRC are necessary for viewpoint-independent perception. Given these findings and those of related studies (e.g. Lee, Bussey et al., 2005), Lee, Buckley et al. (2005) concluded that the hippocampus and PRC contribute to perception, a finding attributed to their role in supporting complex conjunctive representations of scene and object stimuli, respectively. Subsequent patient research using the odd-one-out task, or other closely aligned tasks (e.g. concurrent configural discrimination tasks), has reported strikingly similar patterns of impairment (Barens et al., 2007; Behrmann et al., 2016; Devlin & Price, 2007; Erez et al., 2013; Hartley et al., 2007; Lee et al., 2006; Mundy et al., 2013; Taylor et al., 2007). These findings therefore add weight to the view that the hippocampus and PRC – two MTL structures – support perception *and* memory, and do so via their highly specialised representations. Such evidence cannot easily be reconciled by the MTL memory system account (Squire & Zola-Morgan, 1991).

While this pattern of impairment is relatively consistent across studies, as highlighted above, there are a small number of studies in the literature reporting that damage to the hippocampus or wider MTL does not impair performance on variations of the odd-one-out task, whether using scene or object/face stimuli (Kim et al., 2011; Stark & Squire, 2000; see also Levy et al., 2005; Shrager et al., 2006). Citing these findings, proponents of the MTL memory system account argue that the perceptual impairments reported by Lee, Buckley et al. (2005), in addition to those reported in other studies (e.g. Lee, Bussey et al., 2005), may be due to damage beyond the MTL, notably

area TE (Kim et al., 2011; Suzuki, 2009). This region has been implicated in higher order visual perception (for a relevant discussion, see Suzuki, 2010) and is considered by some researchers to be the final stage in the ventral visual processing stream (Eldridge et al., 2018; although for a counter-view, refer back to the representational-hierarchical account). Moreover, these same authors posit that the visual inspection scheme used to assess the extent of damage in some studies – specifically, Lee, Buckley et al. (2005) and Lee, Bussey et al. (2005) – exacerbate this concern. However, it has subsequently been shown that impaired oddity performance was evident in patients whose damage did not include area TE (Baxter, 2009). Alternative explanations have been put forward to explain the discrepancy in results, including the performance of control participants across studies, the way in which stimuli were generated, and the role of different hippocampal subfields (for relevant discussions, see Baxter, 2009; Buckley & Gaffan, 2006; Graham et al., 2010; Hodgetts, Voets et al., 2017; Lee et al., 2012). It might also be the case that the impact of brain damage in the patients might be better explained by taking a network-level approach, focusing not only on the regions that are damaged but also their structural and functional connectivity. I return to this idea later in this chapter. Regardless, in light of these differing findings, it is necessary to examine whether converging evidence from other sources, such as neuroimaging, provide additional insight.

A number of functional neuroimaging studies have since examined the brain structures supporting scene and object/face oddity judgments. For example, Lee et al. (2008) used a form of magnetic resonance imaging (MRI) – specifically, functional MRI (fMRI) – to identify regions throughout the brain that were activated by different-view scene oddity and different-view face oddity (using size oddity as a single feature baseline condition). Consistent with the patient studies described above (Behrmann et al., 2016; Lee, Buckley et al., 2005; Mundy et al., 2013), Lee et al. (2008) observed that scene oddity judgments were associated with greater activation in the posterior hippocampus and PHC, whereas face oddity judgments were associated with greater activation in the anterior hippocampus/amygdala and PRC. Several fMRI studies have since observed similar findings (Barens et

al., 2007, 2010; Clarke & Tyler, 2014; Devlin & Price, 2007; Kafkas et al., 2017; Lee et al., 2013; Martin et al., 2013, 2016; Watson et al., 2012), with the hippocampus (and PHC) linked to scene processing and the PRC linked to face/object processing.

Building on this, Hodgetts, Voets et al. (2017) used ultra-high resolution (7T) fMRI to explore whether specific hippocampal subfields (i.e. CA1-CA3, dentate gyrus, subiculum) support scene oddity discrimination. Analysis revealed that activation in the subiculum – specifically, the anteromedial subiculum – was greater for scene oddity judgments than face and object oddity judgments. This finding is interesting for several reasons. First, it further confirms the importance of the hippocampus in visual scene discrimination, which is consistent with representational accounts (Graham et al., 2010; Saksida & Bussey, 2010). Second, unlike other fMRI studies cited here (e.g. Lee et al., 2008), this finding implicates the anterior hippocampus in scene odd-one-out discrimination. Additional work is needed to clarify the locus of scene representations in the hippocampus, but this finding is consistent with a relatively large-scale fMRI analysis of group- and individual-level scene activations during a one-back working memory task (Hodgetts et al., 2016; see also Baldassano et al., 2016; Dalton et al., 2018; McCormick et al., 2021; Zeidman & Maguire, 2016). This might also help to explain the divergent pattern of oddity results observed in patient studies, discussed previously, as the precise location of hippocampal damage may vary from patient to patient, potentially impacting oddity performance. Third, as the subiculum is a crucial source of hippocampal projections to regions that have likewise been implicated in memory, such as the anterior thalamic nuclei, mammillary bodies, and retrosplenial cortex (RSC; Aggleton & Christiansen, 2015), this finding highlights how hippocampal function is not self-contained but rather emerges from its connectivity within an extended network. Again, I return to this idea in detail later. Collectively, the fMRI evidence discussed here clearly adds weight to the majority of patient studies reporting that MTL structures differentially support aspects of perception and memory via their specialised neural representations (for a relevant systematic review, see Robin et al., 2019).

### 1.1.2. *From nodes to neurocognitive networks*

Although this chapter has thus far been focused on the hippocampus and PRC in isolation, most memory researchers now acknowledge that the specialised representations supported by these structures emerge via large-scale, distributed neurocognitive networks (Mesulam, 1990, 1994). Broadly defined, the term “neurocognitive network” refers to a collection of structurally and/or functionally connected brain regions that are organised in a manner that subserves particular cognitive functions or representations (Bressler & Menon, 2010; Mesulam, 2009). While the focus on localised brain structures has provided great insight into MTL function, such an approach ignores the interaction or *connectivity* between structures and cannot necessarily explain how such unique, specialised representations emerge (Behrmann & Plaut, 2013; Mesulam, 2009; Petersen & Sporns, 2015). Consequently, there is a growing shift in focus from specific structures toward these dynamic, interactive large-scale neurocognitive networks (for recent discussions, see Ekstrom et al., 2017; Inhoff & Ranganath, 2017). Two such networks are of particular interest in this thesis: the so-called “extended hippocampal navigation network” and the so-called “feature network” (Murray et al., 2017). Through their interactions with highly specialised representations supported by the human prefrontal cortex, these networks are proposed to support aspects of human memory (Murray & Wise, 2010; Murray et al., 2017).

#### 1.1.2.1. *The extended hippocampal navigation network*

According to the evolutionary accretion model (Murray et al., 2017), a homologue of the hippocampus emerged in early vertebrates, supporting “map-like” representations that were crucial for navigation. This view is broadly in line with cognitive map theory (O’Keefe & Nadel, 1978; Tolman, 1948), which proposes that the hippocampus supports memory by mapping experiences according to when and where they took place (for a contemporary discussion, see Ranganath, 2019). Later, as anthropoids began to rely on foveal vision for foraging choices made at a distance,

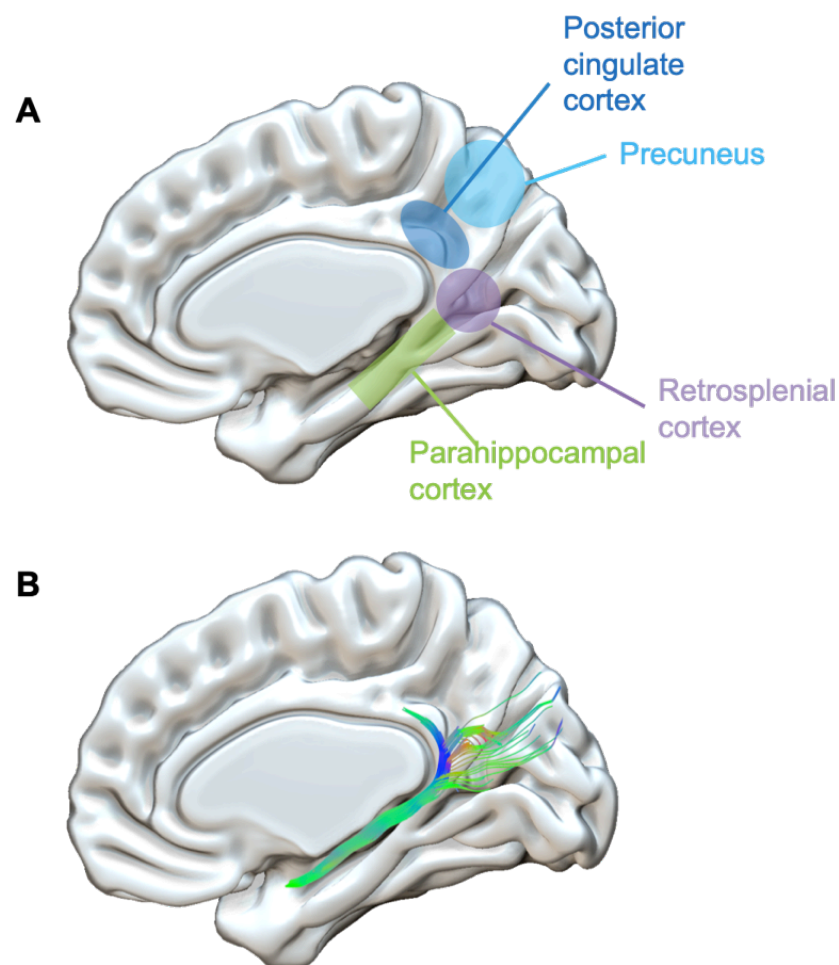
hippocampal representations of visual scenes became favoured and were ultimately selected for (Murray et al., 2018; see also Ryan & Shen, 2020; Schilder et al., 2019). This builds upon earlier representational accounts (Graham et al., 2010; Saksida & Bussey, 2010), which argue that the hippocampus houses specialised conjunctive representations of complex scenes.

Going beyond this, however, the evolutionary accretion model proposes that the hippocampus forms an extended navigation network with the PHC, RSC, and posterior cingulate cortex (PCC; Figure 1.4). Neural tract tracing studies in rats and monkeys substantiate this, highlighting that these structures are heavily inter-connected, with a prominent white matter tract – the cingulum bundle – mediating much of this connectivity (Aggleton, 2012; Bubb et al., 2017, 2018). The posterior portion of this tract – the parahippocampal cingulum bundle (PHCB) – is perhaps most relevant in this context (Jones, Christiansen et al., 2013; Heilbronner & Haber, 2014), a topic I return to later in Section 1.1.3 and in Chapter 4. Through this connectivity, as well as connectivity with the prefrontal cortex, these additional structures then enrich and elaborate on hippocampal scene representations, constructing internal “scene models” (for a related account, see Ranganath & Ritchey, 2012; Ritchey et al., 2015). It is hypothesised that these scene models facilitate the construction of coherent, detailed mental views of spatial scenes or places, which can extend beyond available sensory information and are thus important not only for memory but also future thinking and imagination. Indeed, consistent with cognitive map theory (O’Keefe & Nadel, 1978), multiple theoretical accounts now converge on the idea that scene/spatial context representations are crucial for aspects of spatial navigation and, in addition, act as a foundation or “spatial scaffold” for episodic memories (Gaffan, 1991; Hassabis & Maguire, 2007, 2009; Maguire & Mullaly, 2013; Murray et al., 2017; Nadel & Peterson, 2013; Robin, 2018; Rubin et al., 2019; Rubin & Umanath, 2015; Zeidman & Maguire, 2016). Put another way, these accounts propose that scene/spatial context representations support the construction of episodic memories. Behavioural research provides evidence in accordance with this (Robin, 2018), showing that the presence of

scene/spatial context information facilitates vivid remembering (Robin et al., 2016), associative memory and integration across memories (Robin & Olsen, 2019), and even recollection of single words (Lalla et al., 2020).

**Figure 1.4.**

*Extra-Hippocampal Nodes and Primary White Matter Tract of the Extended Hippocampal Navigation Network*

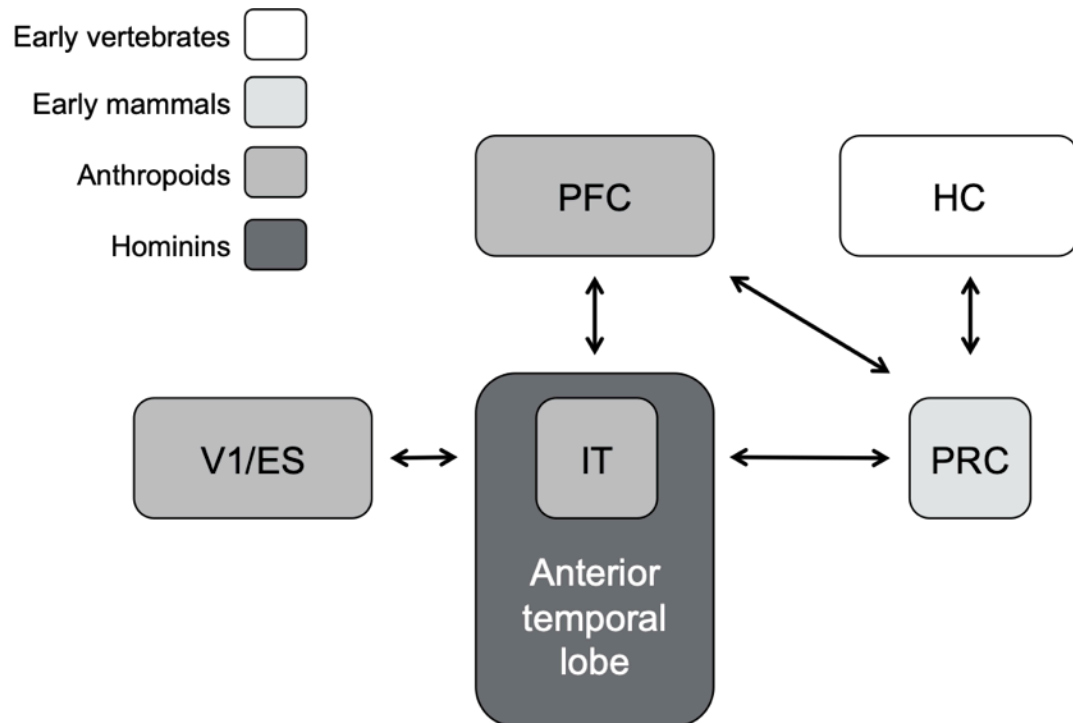


*Note.* The extra-hippocampal nodes and primary white matter tract of the extended hippocampal navigation network, as defined by the evolutionary accretion model (Murray et al., 2017), are shown. Panel A highlights the approximate locations of the PHC, RSC, and PCC, as well as the precuneus. The hippocampus is not shown, but its location relative to the PHC is highlighted in Figure 1.1. Panel B highlights the approximate location of the PHCB – reconstructed using diffusion MRI-based tractography (see Box 1) – and underscores its pivotal placement in the network. Panel A adapted from Robin (2018).

### 1.1.2.2. *The feature network*

The feature network, as it is named in the evolutionary accretion model, is proposed to have emerged as anthropoid primates adapted to diurnal foraging (Murray et al., 2017). This network is comprised of two components, which are sometimes referred to as the dorsal and ventral visual streams (Ungerleider & Mishkin, 1982; see also the description of the representational-hierarchical account in Section 1.1.1). According to Murray et al. (2017), the dorsal component of the feature network included the posterior parietal regions of early primates, which housed specialised representations of visuomotor metrics. Later, as these regions enlarged over evolutionary time, the representations of these regions came to support perception *and* memory for metrics relevant to resources (e.g. number, distance, order). By contrast, the ventral component of this network (Figure 1.5) – connected in part by a long association tract called the inferior longitudinal fasciculus (ILF; Catani et al., 2003; Herbet et al., 2018) – included the temporal regions of early primates, as well as sensory regions that evolved earlier (e.g. PRC). As with the dorsal component, the ventral component enlarged and became more sophisticated over time, such that its specialised representations came to support perception *and* memory for visual and acoustic attributes (i.e. features) relevant to resources (Murray et al., 2017). This proposal is somewhat similar to that put forward by the representational-hierarchical account (Bussey & Saksida, 2007; Saksida & Bussey, 2010), in that both emphasise the importance of a ventral pathway from early visual areas to the PRC. In addition, the evolutionary accretion model postulates that temporal regions, including the PRC, provide more evolutionarily recent parts of the prefrontal cortex with information necessary to generate goals appropriate to a given context and outcome (Eldridge et al., 2021; Murray et al., 2017; Passingham & Wise, 2012).



**Figure 1.5.***Key Nodes and Connections of the Ventral Component of the Feature Network*

*Note.* Key nodes of the ventral (a.k.a. occipital-temporal) component of the feature network are shown, as are connections with other regions (e.g. the hippocampus, PFC). Regions are shaded according to when they emerged in evolutionary time. Arrows represent the bi-directionality of connectivity between regions. Abbreviations: ES = extrastriate cortex, HC = hippocampus, IT = inferior temporal cortex, PFC = prefrontal cortex, PRC = perirhinal cortex, V1 = primary visual cortex. Adapted from Murray et al. (2017).

As the ape-human lineage separated from other anthropoids, temporal regions representing attributes relevant to resources, such as the inferior temporal cortex and PRC, underwent a period of expansion (Kaas, 2013; Van Essen & Dierker, 2007). During this expansion, the evolutionary accretion model proposes that these regions – referred to as a “hub” – further adapted to more general, higher-order functions, especially relating to semantic memory (Murray et al., 2017). Broadly defined, semantic memory refers to stored knowledge about the world, including facts, concepts, and

categories acquired throughout life (Tulving, 1972, 1983, 2002). This form of memory differs from episodic memory in that it is largely context-independent – that is, it does not include source information per se (for recent discussions on the episodic-semantic distinction, see Irish & Vatansever, 2020; Renoult & Rugg, 2020). Support for this account comes from a range of sources. For example, fMRI studies have reported that PRC activation is associated with the ability to discriminate between words with high levels of semantic overlap (i.e. ambiguity; Clarke & Taylor, 2014; see also Clarke, 2020; Clarke & Taylor, 2015; Martin et al., 2018; Wright et al., 2015). This suggests that, in hominins, the PRC came to represent conjunctions of both perceptual and semantic features (Murray et al., 2017). Adding to this, studies on patients with semantic dementia provide yet more evidence that the anterior temporal lobe is specialised for semantic memory. Semantic dementia is one of the main clinical variants of frontotemporal dementia, predominantly affecting the anterior and ventral temporal lobe (Hodges et al., 2010; Hodges & Patterson, 2007; La Joie et al., 2014). This includes the PRC and anterior hippocampus, although the former is particularly affected early in the course of the disease (Davies et al., 2004, 2009). In terms of its clinical presentation, patients with semantic dementia commonly present with word-finding problems and thereafter progressively lose conceptual and categorical semantic knowledge (Fletcher & Warren, 2011). Episodic memory is usually unaffected, at least not as severely as semantic memory (Nestor et al., 2006). Given the selectivity of this memory impairment, as well as the fact that anterotemporal regions and their white matter connections with the frontal lobe (e.g. the uncinate fasciculus) are heavily affected (Acosta-Cabronero et al., 2011; La Joie et al., 2014), patients with semantic dementia underscore the importance of this anterior temporal lobe hub – part of the ventral feature network – in semantic memory (Murray et al., 2017).

### *1.1.2.3. Connecting it all together: Network disconnection and amnesia*

As outlined above, the evolutionary accretion model goes beyond earlier representational accounts of MTL function, such as the emergent memory account (Graham et al., 2010), by explicitly placing the hippocampus and

PRC within broader neurocognitive networks, namely the extended hippocampal navigation network and the feature network (Murray et al., 2017). The former is proposed to elaborate on the complex conjunctive scene representations supported by the hippocampus, whereas the latter – particularly the ventral component – is proposed to represent complex conjunctive representations of features, enabling individuals to disambiguate between perceptual (e.g. object-level) and more abstract (e.g. semantic) attributes/features. In addition, the evolutionary accretion model proposes that these networks, and their respective interactions with the prefrontal cortex, are crucial for aspects of everyday memory, including both episodic and semantic memory (Murray & Wise, 2010; Murray et al., 2017). This emphasis on interactions, or connectivity, differs from the focus on individual regions discussed in Section 1.1. Moreover, adopting such a network-based approach to understanding memory function further helps to re-frame previously discussed lesion studies, focusing instead on how damage to a particular structure results in it being disconnected from other parts of the brain.

Studies conducted on monkeys provide support for the view that these large-scale networks and their interactions with regions of the prefrontal cortex mediate aspects of memory. For instance, Gaffan (1994) lesioned the fornix of monkeys to examine whether this major hippocampal connection contributes to object and/or scene-related memory. It was observed that fornix lesions produced notable scene-specific memory impairments, while leaving object memory largely intact (see also Gaffan & Parker, 1996; Gaffan et al., 2001; Parker & Gaffan, 1997; for a relevant review, see Eacott & Gaffan, 2005). Similar scene memory deficits have likewise been observed in humans with fornix damage (Aggleton et al., 2000), indicating that the importance of hippocampal connections is not species-specific. Cingulum bundle lesions, and PHCB lesions in particular, have not been extensively examined in monkeys, largely because its location makes selective interventions extremely difficult (Bubb et al., 2018). Nevertheless, lesions to the mammillary bodies, which connect to the PCC via a pathway including the mamillo-thalamic tract, anterior thalamic nuclei, and cingulum bundle

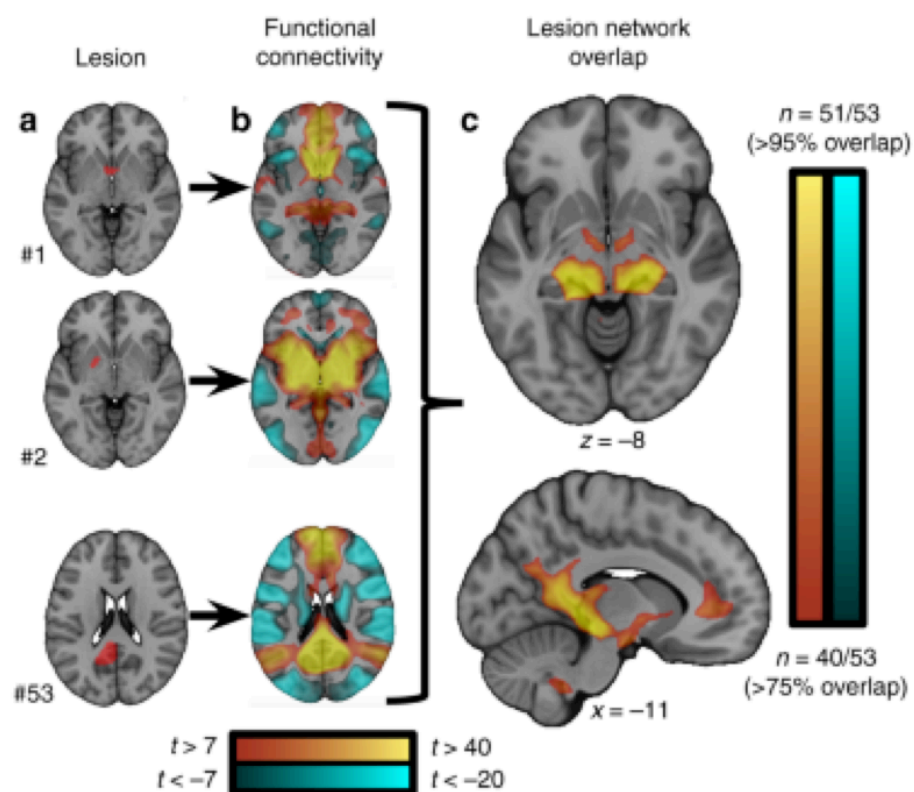
have been shown to produce severe impairments in scene learning (Parker & Gaffan, 1997). Studies in monkeys further demonstrate that frontal-temporal disconnection produces impairments on a variety of tasks purported to tap episodic-like memory, such as object-in-place learning (Browning et al., 2005, 2007, 2013; Browning & Gaffan, 2008a, 2008b; Parker & Gaffan, 1998; for a relevant discussion, see Gaffan & Wilson, 2008). Disconnecting the PRC from parts of the frontal lobe has also been shown to impair visual object recognition (Parker & Gaffan, 1998). In humans, studies of patients with congenital prosopagnosia – a condition characterised by deficits in identifying faces – have identified alterations in the microstructure and macrostructure of the ILF (Gomez et al., 2015; Grossi et al., 2014; Thomas et al., 2009). These findings collectively highlight the importance of connections within the extended hippocampal navigation network and feature network, as well as connections between these networks and the frontal lobe, in aspects of memory.

Adopting the network-based account espoused by the evolutionary accretion model (Murray et al., 2017), human amnesia can arguably be considered a disconnection syndrome. Consider the case of patient H.M., who I introduced in Section 1.1. Although H.M.'s lesion inspired considerable interest in the hippocampus and broader MTL (Squire & Zola-Morgan, 1991), a structural MRI scan and subsequent post-mortem examination later revealed that H.M. likely experienced significant damage to the uncinate fasciculus, fornix, and cingulum bundle (Thiebaut de Schotten et al., 2015). These more recent findings complicate matters, demonstrating that H.M. actually had damage to key white matter connections in both the extended hippocampal network and the feature network. In this regard, H.M.'s profound memory impairment – including an inability to remember new facts and events – can be attributed not only to the structures removed by his surgery, but also the fact that several memory-related regions were disconnected from one another. Recent work using lesion network mapping substantiates this. Ferguson et al. (2019) examined 53 lesion locations previously reported to cause severe episodic memory deficits and then used resting-state fMRI (see Box 1) in a separate sample to identify brain regions that were functionally connected with each

one. Individual lesion network maps were overlapped to identify regions that were commonly connected to the amnesia-causing lesions. Strikingly, analysis revealed that the vast majority (>95%) of lesion locations were functionally connected with one particular site at the junction of the hippocampus – specifically, the subiculum – and the RSC (Figure 1.6). Given that both the hippocampus (subiculum) and RSC form part of the extended hippocampal navigation network, this finding supplements the view that this network and its connectivity is important for episodic memory, while also underscoring the broader point that memory impairment is a product not necessarily of lesion site but of regions disconnected with that site.

**Figure 1.6.**

*Overlapping Patterns of Functional Connectivity Associated With Amnesia-Causing Lesions*



*Note.* Example lesion locations (a) are pictured alongside their respective functional connectivity networks (b). Positive correlations are shown as warm colours, whereas negative correlations are shown as cool colours. The overlapping pattern of connectivity across these lesion-specific maps is shown (c). Reprinted from Ferguson et al. (2019).

A small number of recent studies have examined how microstructural variation in key white matter tracts within each of these networks is relevant to their specialised representations. In one particularly notable example, Hodgetts et al. (2019) used diffusion MRI-based tractography (see Box 1) to examine whether the microstructure of the PHCB is related to hippocampal, PHC, and PCC activation during scene oddity performance. This was motivated by a prior research, discussed above, as well as a relevant fMRI study that observed increased PCC activation during scene, but not face, odd-one-out perceptual discrimination in individuals at increased risk of AD (see Section 1.3; Shine et al., 2015; see also Hodgetts, Voets et al., 2017). Given that the PHCB links these structures together (Figure 1.4), and they appear important for the representation of scenes (Murray et al., 2017), it was hypothesised that tract microstructure would correlate with scene oddity activation in these structures. Analysis revealed that microstructure of the PHCB was in fact correlated with scene oddity-related activation in the hippocampus, PHC, and PCC (Shine et al., 2015), directly implicating this tract in the extended hippocampal navigation network. Consistent with this, another recent study demonstrated that PHCB microstructure is associated with the generation of event element and spatiotemporal context details during autobiographical remembering (Memel et al., 2020). Regarding the ILF, which is an important connection within the ventral component of the feature network, diffusion MRI-based tractography studies have linked the microstructure of this tract with both face perception (Bourbon-Teles et al., 2021; Hodgetts et al., 2015; Postans et al., 2014) and semantic memory (Hodgetts, Postans et al., 2017). These findings dovetail with the previously mentioned studies of patients with congenital prosopagnosia (Gomez et al., 2015; Grossi et al., 2014; Thomas et al., 2009), thereby providing evidence that the ILF has a role in object/face processing. While more work is needed in this area (see Chapter 4), such findings add to the accumulating evidence that the key white matter tracts in the aforementioned networks play a role in supporting their respective representations.

---

**Box 1. Approaches to studying connectivity in the living human brain**

Traditionally, cognitive neuroscience research has attempted to map specific cognitive functions onto localised brain structures (for a relevant discussion, see Kanwisher, 2017). Such an approach ignores the interaction between brain structures, however, and thus cannot account for certain aspects of cognition (Betzel, 2020; Mesulam, 2009; Petersen & Sporns, 2015). In this chapter, I introduced the evolutionary accretion model (Murray et al., 2017), an account that emphasises the importance of large-scale MTL neurocognitive networks and their connections, rather than focusing on a select few brain structures (e.g. Zola-Morgan & Squire, 1991). The advent of modern neuroimaging methods has partly driven the development of such accounts, making it possible to indirectly probe structural and functional connectivity in the living human brain. The two most popular methods are diffusion MRI and resting-state or task-free fMRI. An additional analytical method that typically relies on structural MRI to identify networks based on morphometric features – structural covariance – has also gained prominence.

**Diffusion MRI**

Diffusion MRI measures the random, microscopic movement of water molecules (i.e. diffusion) in brain tissue (for relevant reviews, see Assaf et al., 2019; Jbabdi & Behrens, 2013; Jones, 2008; Jones, Knösche, & Turner, 2013). In nerve fibres, or axons, diffusion is constrained in a particular direction – that is, water molecules are less hindered along a given axon than across it. Therefore, by measuring the diffusion MRI signal at each voxel in multiple different directions, this method is capable of examining local fibre orientations. The resulting voxel-wise orientation information can then be pieced together in order to reconstruct white matter fibre tracts. This method is referred to as “fibre tractography” or simply “tractography” (for a review, see Jeurissen et al, 2019). An alternative approach is simply to examine the voxel-wise measures of diffusion properties (i.e. microstructure),

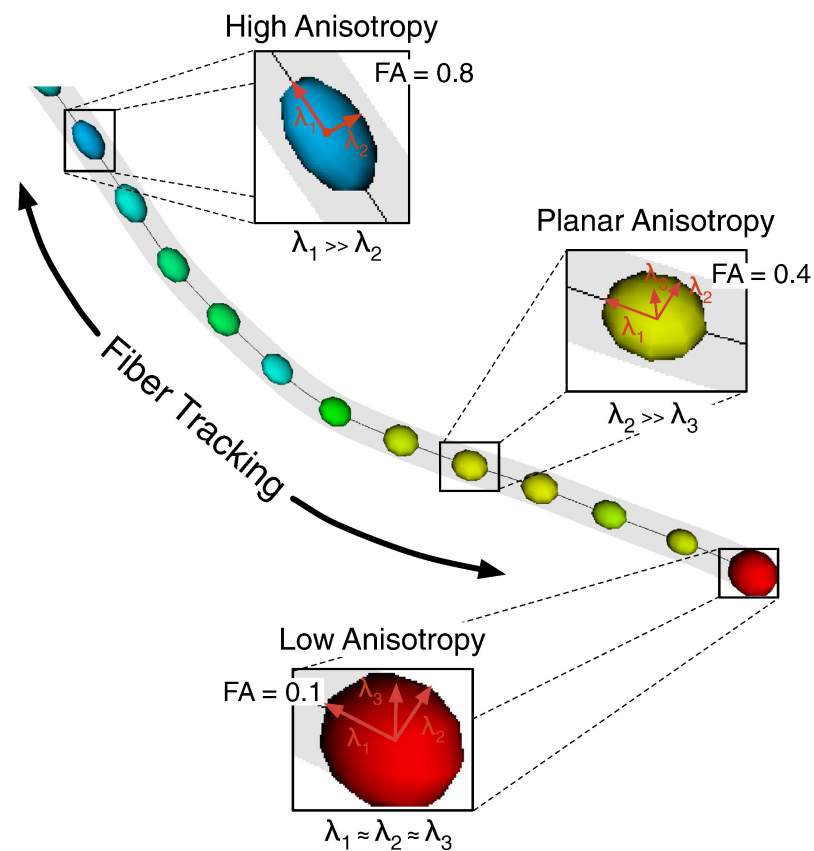
such as in tract-based spatial statistics (TBSS; Smith et al., 2006). Here, I focus primarily on the former, as this is arguably the best available approach for visualising and measuring tract microstructure in *individual* brains.

To obtain information about fibre orientation for tractography, a model must be fit to each voxel. The most common model is the diffusion tensor, whose main eigenvector captures the primary direction of diffusion. This is assumed to represent the underlying orientation of fibres within a voxel, which can be linked together – voxel-to-voxel – in order to estimate streamlines as part of tract reconstruction (Figure 1.7). Broadly speaking, there are two classes of tractography algorithms: deterministic (Alexander, 2010) and probabilistic (Parker, 2010). These algorithms differ in that deterministic tractography assumes a single orientation at each voxel, whereas probabilistic tractography assumes a distribution of orientations (Jones, Knösche, & Turner, 2013). The latter is, as a result, much more computationally intensive than the former. Tractography algorithms aside, it is also possible to derive voxel-wise measures of tissue microstructure from this tensor, notably fractional anisotropy (FA) and mean diffusivity (MD). FA is a scalar value that represents the degree to which diffusion is constrained in a particular direction, ranging from 0 (fully isotropic; diffusion unconstrained) to 1 (fully anisotropic; diffusion entirely constrained in a given direction). By contrast, MD ( $10^{-3}\text{mm}^2 \text{s}^{-1}$ ) represents an average of axial diffusion (i.e. diffusion along the main axis) and radial diffusion (i.e. diffusion along the orthogonal axis). Higher levels of FA and lower levels of MD are commonly associated with increased axon density and to some extent myelination (Beaulieu, 2002), although they are not specific to any one particular aspect of microstructure (Jones, Knösche, & Turner, 2013). Both of these measures can be averaged across tracts to obtain tract-wise, rather than voxel-wise, measures of microstructure. Crucially, these measures reflect the physical characteristics of white matter tracts, which have consequences for their function and may be related to variation cognitive/behavioural output (Assaf et al., 2019).



**Figure 1.7.**

*Visual Illustration of the Diffusion Tensor Model and its Application to Tractography*



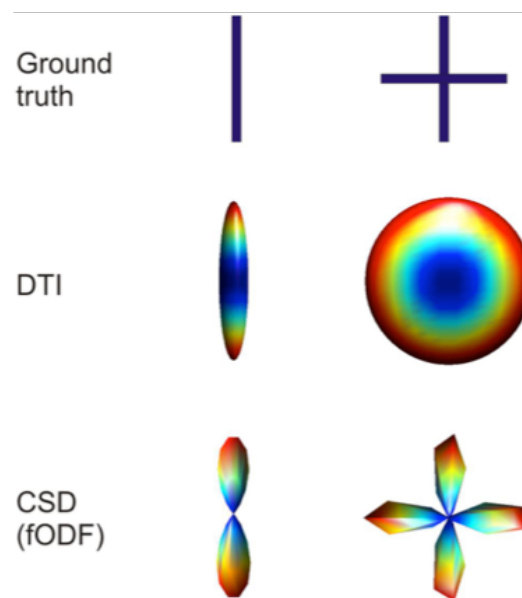
*Note.* The process of fibre tracking (or “fiber tracking”) is shown. The trajectory of the streamline – illustrated as a thin black line with grey shading – is based on voxel-to-voxel orientation information. This orientation information is derived from diffusion tensors, which are displayed as ellipsoids. The colour of the tensor corresponds to the FA value (blue = high, yellow = medium, red = low). As can be seen, when anisotropy is low, the streamline terminates. Reprinted from O’Donnell and Pasternak (2015).

While this approach – diffusion tensor imaging (DTI) – has been extremely popular, it has a number of limitations. In the context of tractography, the most important is the inability of the tensor to capture more than one fibre population per voxel (O’Donnell & Pasternak, 2015). Given that each voxel contains thousands of fibres, this constitutes an unrealistic assumption, and thus the diffusion tensor can produce relatively poor fibre orientation estimates. For example, in the presence of crossing fibres, the diffusion

tensor may appear “flat”, ultimately leading to the incorrect termination of streamlines (Figure 1.8). For this reason, more advanced, “higher-order” models have been introduced (Jeurissen et al., 2019). One such approach, spherical deconvolution, models the fibre orientations as a continuous function of a sphere – the so-called fibre orientation distribution function (fODF; Tournier et al., 2004). I use a variation of this approach in Chapter 4.

**Figure 1.8.**

*Visual Illustration of the Effect of Crossing Fibres on the Diffusion Tensor and the fODF*



*Note.* The way in which the diffusion tensor and fODF model one (left) or two (right) fibres populations is illustrated. In the former, the diffusion tensor performs well, although such an occurrence is anatomically unlikely. In the more realistic example, the diffusion tensor performs poorly, incorrectly suggesting that the hypothetical voxel is characterised by low anisotropy. By contrast, the fODF – estimated using spherical deconvolution – performs much better, accurately capturing the more complex fibre arrangements. Abbreviations: CSD = constrained spherical deconvolution, DTI = diffusion tensor imaging, fODF = fibre orientation density function. Adapted from Bastiani and Roebroek (2015).

In recent years, much has been written about the methodological strengths and limitations of diffusion MRI-based tractography more broadly. Validation studies comparing tractography with gold-standard neural tract tracing in mice (Calabrese et al., 2015), ferrets (Delettre et al., 2019), and monkeys (van den Heuvel et al., 2015) indicate that diffusion MRI tractography provides reasonably accurate reconstructions, although there are limits (Schilling et al., 2019). Comparisons between diffusion MRI-based tractography and neural tract tracing in post-mortem human tissue suggests a similar conclusion; it is useful and reasonably accurate but far from perfect (Seehaus et al., 2013). Moreover, there is also some concern about the replicability and reproducibility of tractography results (Rheault et al., 2020; Schilling et al., 2020, 2021). This remains an active topic of research and will no doubt lead to important advances.

### **Resting-state fMRI**

Resting-state or task-free fMRI measures spontaneous, low frequency (< 0.1Hz) fluctuations in the blood oxygenation level-dependent (BOLD) signal in the absence of a cognitive task (for relevant reviews, see Lee et al., 2013; Lv et al., 2018; Smitha et al., 2017). The temporal correlation of these fluctuations between regions is assumed to represent synchronous neural activity, or communication, and is thus a proxy for intrinsic functional connectivity. Fundamentally, functional connectivity is a statistical concept; it identifies statistical dependencies, estimated via correlation or covariance, between regional fMRI time series. Measures of functional connectivity are therefore correlational rather than causal, and do not provide insight into directionality (although for relevant attempts, see Almgren et al., 2020; Friston et al., 2014; Park et al., 2018; Razi et al., 2015). Despite this limitation, resting-state fMRI-based functional connectivity has become increasingly popular in recent years, in part due to its ease of use.

Seed-based analysis was the first analytical approach applied to resting-state fMRI data (Biswal et al., 1995) and remains popular today. Other widely used analytical methods include independent components analysis and

graph theoretical analysis. At its core, seed-based analysis examines the association between the BOLD signal in an a priori selected seed region, also referred to as a region of interest (ROI), with other a priori selected seed regions or with all voxels throughout the brain. This approach has proven extremely useful, identifying a number of robust group-level and individual-level intrinsic connectivity networks (e.g. Power et al., 2011; Yeo et al., 2011), including the so-called “default mode network” and its MTL sub-component (for relevant reviews, see Buckner & DiNicola, 2019; Raichle, 2015). Large parts of this network, notably the MTL sub-component, overlap extensively with structures that are activated during episodic memory retrieval, including the PHC, RSC, and PCC (Benoit & Schacter, 2015; Ferguson et al., 2019; Kim, 2010; Rugg & Vilberg, 2013; Spaniol et al., 2009). Moreover, functional connectivity between these structures and the hippocampus (i.e. the extended hippocampal navigation network) has been associated with task-related activation during an associative memory task (Ritchey et al., 2014), as well as inter-individual differences in task-based recollection (King et al., 2015) and naturalistic/subjective remembering (Sheldon et al., 2016). This underscores the relevance of resting-state fMRI-based functional connectivity for not only understanding connectivity in the living brain, but also how this relates to aspects of cognition.

Despite this, there are important methodological limitations to consider with resting-state fMRI. An arguably underappreciated issue in this area is the need to control for physiological confounds relating to cardiac and respiratory processes (Murphy et al., 2013). Another issue is the degree to which functional connectivity maps are reliable and reproducible. It has been argued that resting-state fMRI produces connectivity maps that are reliable across session and subjects (Lee et al., 2013), although a recent review found poor levels of test-retest reliability (Noble et al., 2019). Finally, while some studies have reported that resting-state functional connectivity is in some way related to diffusion MRI-based structural connectivity (e.g. Greicius et al., 2009), the relationship between these two forms of connectivity is imperfect and fairly complex (for a review, see Suárez et al., 2020).

## **Structural covariance**

Structural covariance refers to the correlation between morphological features of one brain structure with morphological features in other brain structures (for a review, see Alexander-Bloch, Giedd, & Bullmore, 2013). In this regard, structural covariance is not a method like diffusion MRI or resting-state fMRI, but is instead an analytical approach that is commonly applied to structural MRI. There are several different approaches to structural covariance, but the most common is seed-based analysis (for an overview of this approach, see “Resting-state fMRI”). Other methods include principal components analysis and graph theoretical analysis. Numerous morphological features can be investigated, although the most common are grey matter volume, cortical thickness, and surface area.

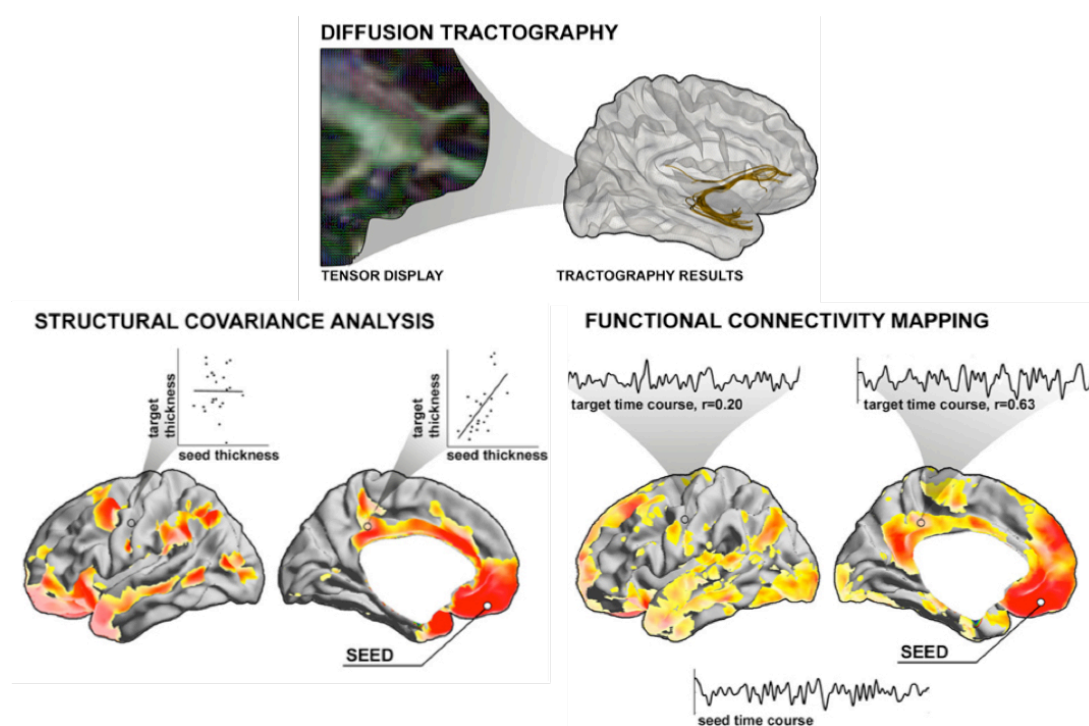
The assumption underpinning structural covariance is that shared morphological properties (e.g. size) across brain structures are a reflection of genetic and/or environmental influences (Alexander-Bloch, Raznahan et al., 2013; Mechelli et al., 2005; Romero-Garcia et al., 2018; Yee et al., 2018; Zielinski et al., 2010), or are perhaps due to a shared involvement in some aspect of cognition. The latter proposal indicates that structural covariance may in some way index connectivity. While this is an area of on-going investigation, initial findings suggest that patterns of structural covariance do in fact overlap with patterns of functional connectivity (Clos et al., 2014; Guo et al., 2015; Kelly et al., 2012; Spreng et al., 2019). Overlap has also been reported with diffusion MRI-based tractography (Gong et al., 2012) and anatomical connectivity more broadly (Yee et al., 2018), but the overlap appears weaker than that observed with functional connectivity (Alexander-Bloch, Giedd, & Bullmore, 2013).

In spite of this, there is a key methodological drawback of structural covariance relative to diffusion MRI or resting-state fMRI: structural covariance is estimated on the basis of a group of images. This makes it challenging to draw inferences at the individual-level, limiting individual differences research. However, recent methodological advances have

attempted to rectify this (Raamana & Strother, 2018, 2020; Seidlitz et al., 2018), and certain multivariate methods make it possible to extract “brain scores” that represent the degree to which an individual expresses a group-level pattern of covariance (Spreng & Turner, 2013). I use the latter in this thesis (see Chapter 3).

**Figure 1.9.**

*Methods of Studying Connectivity in Humans*



*Note.* Figure shows a diffusion MRI-based tractography reconstruction of the uncinate fasciculus (top), the whole-brain structural covariance pattern associated with the medial orbitofrontal cortex (left), and the whole-brain functional connectivity pattern associated with the medial orbitofrontal cortex (right). Adapted from Bernhardt et al. (2013).

## 1.2. Impact of age and age-related neurodegenerative disease

The number of people reaching older age is increasing throughout the world. Today, there are an estimated 727 million people aged 65 years or older, representing approximately 9.3% of the global population (United Nations

[UN], 2020). It is projected that this figure will continue to increase in coming years, reaching 1.5 billion by 2050 (UN, 2020). Given these trends in longevity, there is a growing need to understand how the brain and cognition are impacted by age and age-related neurodegenerative disease. In Section 1.1, I introduced two large-scale neurocognitive networks: the so-called extended hippocampal navigation and feature networks (Murray et al., 2017). The former is proposed to enrich and elaborate on hippocampal scene representations, facilitating the construction of mental views of scenes that are thought to underpin spatial navigation, scene perception, and episodic memory (for variations of this idea, see Gaffan, 1991; Hassabis & Maguire, 2007, 2009; Maguire & Mullaly, 2013; Murray et al., 2017; Nadel & Peterson, 2013; Robin, 2018; Rubin et al., 2019; Rubin & Umanath, 2015; Zeidman & Maguire, 2016). The latter – especially its ventral component – is proposed to represent objects-level features, as well as semantic concepts and categories. This raises a critical question: to what extent does age and age-related neurodegenerative disease impact these two networks and their corresponding representations? Much of the relevant research conducted to date has suggested that the extended hippocampal navigation system and aspects of cognition that depend on its representations are more vulnerable to healthy and pathological ageing, but this has recently been disputed.

### *1.2.1. Age and the extended hippocampal navigation network*

#### *1.2.1.1. Spatial memory and navigation*

Multiple lines of evidence indicate that spatial memory and navigation abilities, particularly allocentric spatial processing, decline with age (for relevant reviews, see Colombo et al., 2017; Li & King, 2019; Lester et al., 2017). An allocentric representation – defined as a “mental representation of where things are in space with respect to each other independent of our own location” (Ekstrom et al., 2014, p.2) – is in many ways akin to a cognitive map (Byrne et al., 2007; Fidalgo & Martin, 2016; see also Section 1.1.2.1). An illustrative example can be found in research using the Morris water maze. Briefly, the Morris water maze is a task in which an animal, typically a

rat, is placed in a circular pool of opaque water and must locate a submerged platform in order to escape (Morris, 1981; Morris et al., 1982). No local landmarks are present, only distal landmarks – that is, the only landmarks present are those outside the pool. In one of the more common variants of the Morris water maze task, the animal is then placed back in the pool from different locations, but the platform remains in a fixed location. To complete the task, therefore, the animal must learn to navigate based on its knowledge of the relationship between the goal location and the distal landmarks, as opposed to a fixed route from its starting viewpoint or position. In this regard, the task requires the animal to utilise allocentric or viewpoint-independent representations rather than egocentric or viewpoint-dependent representations (although for critiques of this interpretation, see Ekstrom et al., 2014; Wolbers & Wiener, 2014). Hippocampal lesions have been shown to impair performance on this task, as measured by escape latency and swim path (D’Hooge & De Deyn, 2001). In the context of ageing, it has also been observed that older rats learn to perform the task at a slower rate than younger rats, and are less direct when doing so (Gallagher et al., 1993; Gallagher & Rapp, 1997).

In humans, virtual analogues of the Morris water maze have been used to examine whether equivalent age-related effects are evident. Consistent with the rodent literature, it has been reported that older adults generally take more circuitous routes, spend more time searching for the platform, and are less accurate when recalling the location of the platform (e.g. Gazova et al., 2013; Moffat & Resnick, 2002; for a review, see Li & King, 2019). Moreover, when compared to younger adults, older adults tend to exhibit difficulties when switching from an egocentric to an allocentric reference frame (Harris et al., 2012; Harris & Wolbers, 2014). While it has been shown that younger but not older adults exhibit bilateral hippocampal activation during allocentric processing (Antonova et al., 2009), age-related decline in spatial navigation is further reflected in the structure and function of a number of regions, including the PHC and RSC/PCC (Ekstrom et al., 2014; Zhong & Moffat, 2018). Together, these findings suggest that age impacts allocentric spatial



memory and navigation, and that this age-related decline is related to the functional integrity of the extended hippocampal navigation network.

#### *1.2.1.2. Episodic memory*

Complaints of memory impairment are commonly reported in otherwise healthy middle-aged and older adults (Luck et al., 2018). Given that scene/spatial context representations are important to both navigation and episodic memory (Hassabis & Maguire, 2007, 2009; Murray et al., 2017; Nadel & Peterson, 2013; Robin, 2018; Rubin & Umanath, 2015), it is perhaps unsurprising that episodic memory in particular is thought to be vulnerable to ageing (Grady, 2012; Hedden & Gabrieli, 2004; Tromp et al., 2015). Although substantial individual variability exists (Olaya et al., 2017), some studies suggest that episodic memory decline may begin as early as the third decade of life (Park & Reuter-Lorenz, 2009; Salthouse, 2003, 2009). Notably, this age-related decline is characterised by an especially prominent inability to retrieve scene/spatial context information (Cansino, 2009), which may provide a scaffold for representations of events (see Section 1.1.2.1). Indeed, age-related decline in memory for spatial context is typically much greater than that observed in memory for previously presented items (Kessels et al., 2007; Old & Naveh-Benjamin, 2008; Spencer & Raz, 1995; Talamini & Gorree, 2012; although for a counter-example, see Diamond et al., 2018). Ageing thus appears to affect the ability to retrieve the often rich, detailed spatial information that accompanies an event, rather than the ability to remember events per se (Addis et al., 2008; Levine et al., 2002). Brain structures commonly activated while remembering spatial context information include the hippocampus, PHC, RSC/PCC, and precuneus (Robin, 2018). These structures feature prominently in the extended hippocampal navigation network, which is consistent with its proposed role in supporting representations of scenes (Murray et al., 2017; see also Ranganath & Ritchey, 2012). Given the above, one might expect that the impact of age on episodic memory, and scenes/spatial context specifically, to be related to alterations in the extended hippocampal navigation network. A large body of research provides support for this prediction, with numerous studies

reporting that age-related decline in episodic memory is related to alterations in the activation of key structures within this network, as well as alterations in the structural and functional connectivity between them (Cansino et al., 2015; Daselaar et al., 2006; Edde et al., 2020; Ezzati et al., 2016; Foster et al., 2019; Persson et al., 2012; Salami et al., 2014; Staffaroni et al., 2018; Wang et al., 2010; for a relevant review, see Nyberg, 2017). In line with the proposed salience of spatial context, recent fMRI work has likewise reported that age-related differences in memory for this type of information are associated with alterations in frontoparietal-hippocampal connectivity (Ankudowich et al., 2019; see also Ankudowich et al., 2016). On this basis of the research, it appears that ageing impacts episodic memory, and scenes/spatial context in particular, which is related to dysfunction in the extended hippocampal navigation network.

#### *1.2.1.3. Scene-related cognition*

As scene/place representations are argued to be important for spatial navigation and episodic memory, it stands to reason that older adults may demonstrate deficits on tasks that more directly tap into these representations. However, there is a paucity of studies examining decline in scene-related cognition during “normal” ageing, with only a few reported to date. In one such example, Robin and Moscovitch (2017) presented younger and older participants with high- and low-familiarity spatial cues in the form of real-world landmarks. For each cue presented, participants were asked to picture the scene around the landmark (scene condition), to recall events at or around the landmark (autobiographical/episodic memory condition), or to imagine a plausible future event involving the landmark (future condition). A number of interesting findings were reported but one in particular is relevant here – across all conditions, including the scene condition, older participants reported fewer internal details (i.e. details relating to perceptions, thoughts, or feelings, as well as time and place information) than younger participants. This age-related difference in the production of internal details replicated prior findings pertaining to autobiographical/episodic memory and future thinking (Gaesser et al., 2011), while further demonstrating that this extends

to scene-related memory. Interpreted alongside the aforementioned research on allocentric spatial navigation and episodic memory, Robin and Moscovitch's (2017) findings are consistent with the notion that age impacts the network supporting scene representations, which in turn underpin each of these cognitive functions.

Thus far in this section, I have only discussed research on normal or "healthy" ageing, while noting that there are individual differences at play. However, it is important to note that it is extremely difficult to separate normal ageing from age-related pathological changes. Underscoring this point, two decades of research using positron emission tomography (PET) has overwhelmingly demonstrated that various forms of neuropathology are often present in the ageing brain, despite the absence of overt clinical impairment (for a relevant discussion, see Jagust, 2018). Consequently, it remains unclear as to whether alterations in the brain and cognition, such as those discussed, are the result of age-related neurodegenerative disease, or if there is a "pure" form of age-related decline (for relevant discussions, see Fjell et al., 2014; Jagust, 2013; Walhovd et al., 2014). Given this current inability to accurately distinguish between normal and pathological ageing, it appears relevant to examine the impact of age-related neurodegenerative disease (and risk for them) on the networks introduced in Section 1.1, as well as their corresponding representations. Here, I consider the case of Alzheimer's disease (AD), which has traditionally been linked to dysfunction of the extended hippocampal navigation network.

### *1.2.2. Alzheimer's disease and the extended hippocampal navigation network*

AD is a chronic, progressive neurodegenerative disease and the most common cause of dementia worldwide (World Health Organisation [WHO], 2017). Dementia itself is an umbrella term for a particular group of cognitive and behavioural symptoms that interfere with daily living and worsen over time. In the U.K., more than 850,000 people are thought to have dementia, of which approximately 60% is caused by AD (Alzheimer's Society, 2014).

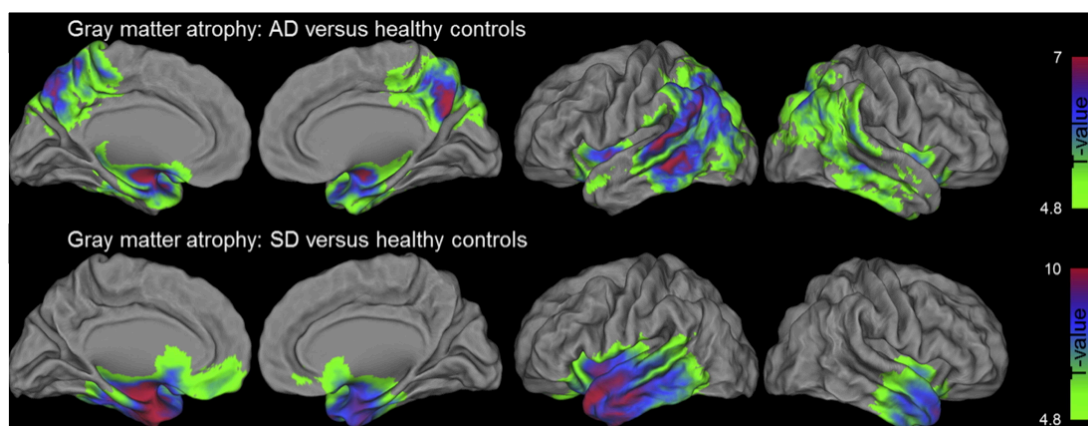
Prevalence of AD increases with advancing age and is thus considered age-related. In the U.S., for example, 3% of people aged 65-74 are estimated to have AD dementia, whereas the figure for people aged 85 or above is 32% (Alzheimer's Association, 2020). In typical cases, the initial and most severe impairment is in memory (McKhann et al., 2011), specifically episodic memory (Dubois et al., 2007, 2014). This is sometimes referred to as the amnesic variant of AD (McKhann et al., 2011). Other less common variants begin with different symptoms, including visuospatial skills (i.e. posterior cortical atrophy) and language (i.e. logopenic primary progressive aphasia; McKhann et al., 2011). Regardless of the nature of the initial impairment, however, a diagnosis of AD can only be made if multiple aspects of cognition are affected, producing a profound impact on daily functioning. In mild cognitive impairment (MCI), by contrast, the impact on cognition is more selective and daily functioning is relatively preserved (Albert et al., 2011). MCI is thought to represent a transition phase between normal ageing and AD, although not all individuals diagnosed with MCI go on to convert (for a discussion, see Richard & Brayne, 2014). Interestingly, the extent of decline in episodic memory has been suggested as a potentially useful line of enquiry for predicting conversion from amnesic MCI to AD (Irish et al., 2011).

The profound episodic memory impairment that typifies the amnesic presentation of AD is commonly attributed to the pattern of atrophy that characterises the disease. At post-mortem, marked atrophy is often evident in the MTL, notably in the hippocampus (DeTure & Dickson, 2019). There is also increasing recognition of post-mortem atrophy in posterior parietal regions, such as the PCC (DeTure & Dickson, 2019). These same regions are characterised by decreased glucose metabolism and decreased functional connectivity with the hippocampus in early stages of the disease (Chetelat et al., 2003; Greicius et al., 2004; Minoshima et al., 1997; Pengas, Hodges et al., 2010; Reiman et al., 2001). Adding to this, structural MRI has revealed that patients with AD, relative to healthy age-matched controls, exhibit a prominent reduction in grey matter in the medial temporal and posterior parietal cortices (Figure 1.10; La Joie et al., 2014). This pattern

differs relative to other dementias, such as semantic dementia, and has been related to the prominent episodic memory deficits observed in AD (La Joie et al., 2014; Nestor et al., 2006). Atrophy in these structures, which overlap considerably with the key components of the extended hippocampal navigation network, is thought to reflect the downstream consequences of amyloid-beta ( $A\beta$ ) accumulation. Extra-cellular  $A\beta$ -containing plaques are a hallmark pathological feature of AD (DeTure & Dickson, 2019; Serrano-Pozo et al., 2011), and the dominant hypothesis of AD – the amyloid cascade hypothesis – argues that the initial deposition and accumulation of  $A\beta$  is the key precipitating factor in AD pathogenesis (Hardy & Allsop, 1991; Hardy & Higgins, 1992; Selkoe, 1991; for a review, see Selkoe & Hardy, 2016). In fact, according to the recently proposed ATN (i.e.  $A\beta$ , tau, neurodegeneration) framework (Jack et al., 2018; see also Jack et al., 2016), the presence of aggregated  $A\beta$  in the brain is indicative of AD pathogenic change irrespective of whether tau tangles – another hallmark pathological feature of AD (DeTure & Dickson, 2019; Serrano-Pozo et al., 2011) – or neurodegeneration are present (Table 1.1). While the ATN framework is flexible regarding the order of pathological events in AD, one possibility – referred to as the “modified amyloid cascade hypothesis” (Jack et al., 2018) – proposes that increasing  $A\beta$  levels may lead to the propagation of tau (He et al., 2018; Hurtado et al., 2010; Pooler et al., 2015; Therneau et al., 2021).

**Figure 1.10.**

*Grey Matter Volume Reduction in Patients with AD and Semantic Dementia Relative to Healthy Controls*



*Note.* The pattern shown represents regions whereby grey matter volume was lower (i.e. atrophy) for patients with AD (upper panel) or semantic dementia (lower panel) than for healthy, age-matched controls. Darker colours signify stronger effects. Reprinted from La Joie et al. (2014).

**Table 1.1.**

*Biomarker Profiles of AD According to the ATN Framework*

ATN profiles	Biomarker category	
A-T-N-	Normal Alzheimer's biomarkers	
A+T-N-	Alzheimer's pathologic change	Alzheimer's continuum
A+T+N-	Alzheimer's disease	
A+T+N+	Alzheimer's disease	
A+T-N+	Alzheimer's and concomitant suspects non-Alzheimer's pathologic change	
A-T+N-	Non-Alzheimer's pathologic change	
A-T-N+	Non-Alzheimer's pathologic change	
A-T+N+	Non-Alzheimer's pathologic change	

*Note.* ATN profiles capture the state of three AD-related biomarkers – the presence of  $A\beta$  (A), the presence of tau (T), and the presence of neurodegeneration (N) – according to whether they are normal (-) or abnormal (+). Biomarker categories are shaded to indicate no pathological change (white), AD-related pathological change (light grey), or non-AD-related pathological change (dark grey). Adapted from Jack et al. (2018).

The primacy of A $\beta$  is particularly relevant here, as A $\beta$  PET studies in cognitively normal individuals indicate that posterior parietal regions, including the PCC/RSC, are among the earliest sites of A $\beta$  deposition (Oh et al., 2016; Mattsson et al., 2019; Palmqvist et al., 2017; Villeneuve et al., 2015). Such findings suggest that the extended hippocampal navigation network is selectively vulnerable to A $\beta$  deposition and accumulation, which may in turn explain why patients with AD later demonstrate prominent impairment in episodic memory and related aspects of cognition. Such a suggestion is consistent with the concept of network vulnerability, which posits that neurodegenerative diseases, including AD, impact specific networks (Seeley et al., 2009; for a review, see Seeley, 2017). That said, it is important to acknowledge that the association between A $\beta$ , neurodegeneration, and subsequent episodic memory impairment is relatively weak (Jagust, 2018). In fact, another hallmark pathological feature of AD – tau-containing neurofibrillary tangles – is more strongly associated with neurodegeneration (e.g. La Joie et al., 2020) and decline in memory (e.g. Chen et al., 2021). One way to account for this, briefly mentioned above, is that the accumulation of A $\beta$  may ultimately lead to the further spread of tau, which then produces neurodegeneration and cognitive decline (Jack et al., 2018). This would help explain why the direct association between A $\beta$ , neurodegeneration, and episodic memory decline is weak albeit significant (Jansen et al., 2018; for a relevant discussion, see Jagust, 2018). To briefly summarise, the findings mentioned here suggest that the extended hippocampal navigation network is particularly vulnerable to at least one aspect of AD pathology (i.e. A $\beta$ ) and that ultimately the resulting alterations (i.e. metabolic changes, atrophy, etc.) in the network's components may explain the observed deficits in episodic memory.

A growing number of studies have further reported AD-related impairments in spatial navigation and spatial memory (for a relevant review, see Coughlan et al., 2018; see also Ekstrom et al., 2018; Lester et al., 2017). Wandering behaviour is relatively common in patients with dementia and is even more pronounced in patients with AD dementia specifically (Klein et al., 1999). When examined in the laboratory, either using virtual reality or real-world

navigation tasks, patients with AD and MCI often demonstrate a marked impairment in various forms of navigation, including those relying on allocentric processing (Allison et al., 2016; Cushman et al., 2008; Hort et al., 2007; Parizkova et al., 2020; Verghese et al., 2017). Given that patients with AD exhibit hypo-metabolism and atrophy in the extended hippocampal navigation network (Figure 1.10), which supports allocentric representations of space, this is perhaps unsurprising. Notably, such deficits have further been found to discriminate AD from other dementias, such as frontotemporal dementia, with the integrity of the RSC linked to performance (Tu et al., 2015). Recently, it has also been reported that deficits in navigational ability are predictive of AD clinical progression (Levine et al., 2020). This has led to the suggestion that spatial navigation impairment may constitute a useful preclinical marker for AD (Coughlan et al., 2018). In the context of spatial memory, it has been reported that patients with AD and MCI are impaired on topographical short-term memory, as assessed by the Four Mountains task (Chan et al., 2016), relative to both matched controls and patients with frontotemporal dementia (Bird et al., 2010). Notably, performance on this task has been linked to hippocampal volume and cortical thickness of the precuneus (Moodley et al., 2015). Related impairment in virtual route learning – a measure of navigationally relevant spatial memory – has been shown to discriminate patients with AD from healthy controls, as well as AD from semantic dementia (Pengas, Patterson et al., 2010). These findings provide evidence that impairment in allocentric navigation and spatial memory is evident early in AD, and implicates components of the extended hippocampal navigation network in both of these cognitive functions.

In addition, scene perception deficits have been observed in AD. Given that representations of scenes – arguably the canonical form of spatial context (Robin et al., 2018) – are theorised to support spatial navigation and episodic memory (Gaffan, 1991; Hassabis & Maguire, 2007, 2009; Maguire & Mullaly, 2013; Murray et al., 2017; Nadel & Peterson, 2013; Robin, 2018; Rubin et al., 2019; Rubin & Umanath, 2015; Zeidman & Maguire, 2016), such findings are entirely consistent with the aforementioned research relating to AD. In one prominent example, Lee et al. (2006) assessed performance on a variation of



the odd-one-out perceptual discrimination task in patients with AD and patients with semantic dementia, as well as their respective controls. Unlike AD, semantic dementia predominantly affects frontal and anterior temporal regions, including the PRC (Davies et al., 2004; La Joie et al., 2014; Nestor et al., 2006). In this regard, the feature network is more heavily affected by semantic dementia than the extended hippocampal navigation network, whereas the reverse is true in AD (Figure 1.10). Activation in components of the former has been linked to oddity discrimination for conjunctive face/object stimuli, whereas activation in components of the latter has been linked to oddity discrimination for conjunctive scene stimuli (e.g. Lee et al., 2008). This raises the possibility that patients with semantic dementia may be selectively impaired on different-view object/face oddity but patients with AD may be selectively impaired on different-view scene oddity. To test this, Lee et al. (2006) examined performance using same-view and different-view scene and face odd-one-out stimuli. As suggested, patients with AD (relative to patients with SD and controls) were impaired when making different-view scene oddity judgments, while patients with semantic dementia (relative to patients with AD and controls) were impaired when making different-view face oddity judgments (see also Lee et al., 2007). Somewhat surprisingly, mild deficits were also observed in the AD group for same-view scenes, a pattern that differs relative to studies on patients with hippocampal amnesia (e.g. Lee, Buckley et al., 2005). One possible explanation for these findings is that hippocampal damage selectively impacts viewpoint-independent (i.e. allocentric) scene representations housed by this structure, but AD impacts the broader extended navigation network.

Viewed together, the aforementioned findings indicate that AD-related pathology (i.e. A $\beta$ ) and atrophy impacts many of the regions comprising the extended hippocampal navigation network, which in turn produces observable impairments in episodic memory, spatial navigation and memory, as well as scene perception. This is consistent with the view that this network is critical for the construction of coherent scene representations, which in turn serve to support spatial navigation and provide a scaffold for episodic memory (Murray et al., 2017; see also Hassabis & Maguire, 2009; Maguire &

Mullaly, 2013; Nadel & Peterson, 2013; Robin, 2018; Robin et al., 2018; Zeidman & Maguire, 2016). Moreover, these impairments are similar to those discussed in relation to normal ageing. It is thus persuasive to argue that age and age-related neurodegenerative disease, in this case AD, disproportionately impacts the extended hippocampal navigation network and its putative scene representations. However, contemporary research on ageing and AD has called this conclusion into question, implicating the ventral component of the feature network and its corresponding object representations.

### *1.2.3. Age and the feature network*

There are now a number of studies reporting age-related impairments in object relative to scene/spatial discrimination (e.g. Güsten et al., 2021; Reagh et al., 2016, 2018; Ryan et al., 2012; Stark & Stark, 2017). For example, Reagh et al. (2016) examined mnemonic discrimination for object identity and spatial location in younger and older adults. Building on prior work (Reagh et al., 2014), the older participants were split into “impaired” and “unimpaired” groups depending on their performance on a word-learning task argued to be sensitive to episodic memory dysfunction. The primary experimental task involved study-test blocks, with object and spatial memory tested separately. In object test blocks, the goal was to correctly identify if a given object had been presented previously (i.e. target) or if it was a different albeit perceptually similar object (i.e. lure). In the scene/spatial test blocks, the goal was to identify if a given object occupied the same location as shown previously (i.e. target) or if it was shown in a different location (i.e. lure). Object and spatial lure similarity was manipulated to create high, mid, and low levels of similarity. A number of interesting findings were reported. First, no group differences were evident in object or spatial target recognition – that is, age did not have a meaningful impact on the ability to correctly recognise object identity or spatial location. Second, unimpaired older adults were better able to correctly reject object lures relative to spatial lures at all similarity levels. Third, both the impaired and unimpaired older groups were less able to discriminate object lures than the younger group, particularly at

mid and low levels of similarity. Fourth, only the impaired older group was less able to discriminate spatial lures than the younger group. These findings point to an age-related difference in object mnemonic discrimination, with the exception being that impaired older adults are impaired in both object and spatial mnemonic discrimination.

Functional neuroimaging studies have shed additional light on this issue. Ryan et al. (2012) used fMRI to investigate differences in object discrimination between younger and older adults. In terms of behaviour, it was reported that older adults were poorer at object discrimination than younger adults, although only when the stimuli were more complex. Importantly, this was unlikely to be the result of a general perceptual impairment, because the two groups did not differ when discriminating between size stimuli. In terms of brain activation, Ryan et al. (2012) observed that older adults exhibited lower levels of activation in the posterior portion of the left PRC. This is consistent with the notion that age impacts ventral components of the feature network, producing age-related deficits in tasks reliant on conjunctive (object) feature representations (Burke et al., 2018). Adding further weight to this hypothesis, Reagh et al. (2018) used fMRI to identify age-related differences in activation for the task described previously (see Reagh et al., 2016). In this particular study, older participants were less able than younger participants to discriminate between object and spatial lures, although the difference was more marked for objects (for a somewhat similar behavioural result, see Stark & Stark, 2017). Regarding the functional results, there was an age-related difference in activation of the anterolateral portion of the EC, such that older adults showed lower levels of activation than younger adults (Reagh et al., 2018). Prior research has shown that the anterolateral EC is strongly connected with the PRC and responds preferentially to object rather than scene stimuli (Maass et al., 2015; Navarro Shröder et al., 2015; see also Aggleton, 2012; Suzuki & Amaral, 1994). As such, Reagh et al.'s (2018) findings appear to indicate that age impacts structures within, or connected to, the feature network, and that this is linked to relative impairments in objects versus spatial/scene discrimination.

However, a limitation of the studies discussed so far is that the authors compared groups of younger and older adults. Treating age as a categorical variable can be useful, as shown, but it potentially masks changes that occur across the lifespan (Hedden & Gabrieli, 2004). Moreover, it tells us little about when decline becomes evident, or the nature of the relationship with age (e.g. linear/nonlinear). In a recent study, Güsten et al. (2021) sought to address this limitation by recruiting a large sample of adults ( $N > 1500$ ) from across the adult lifespan (18-77 years). Performance was assessed using a web-based two-back task incorporating both object and scene stimuli. Web-based tasks provide a unique opportunity to obtain large samples of cognitive data, which can rarely be matched by in-person testing (Huentelman et al., 2020). I further discuss the benefits of web-based tasks in Chapter 2. The goal of this particular task is to identify whether the stimulus is the same or different than the stimulus presented two images prior. Results revealed a linear age-related decline in performance for objects, which was stronger than that observed for scenes (Güsten et al., 2021). This was driven by an increase in the false alarm rate rather than a decline in the hit rate – that is, with advancing age, participants were more likely to identify non-target object stimuli as target object stimuli. Interestingly, increased false alarm rates have been observed following PRC lesions, which proponents of the representational-hierarchical account argue is due to an increased reliance on low-level object representations following the loss of high-level object representations supported by the PRC (Cowell et al., 2006; Yeung et al., 2013). Given that a prior study using the same task as that employed by Güsten et al. (2021) found that older adults exhibit a reduction in domain specificity in the PRC (Berron et al., 2018), these findings suggest that the PRC and the broader feature network are preferentially impacted by age (Burke et al., 2018).

#### *1.2.4. Alzheimer's disease and the feature network*

Several studies relating to MCI and AD have similarly observed deficits in object-related memory, some of which have further shown that this is stronger than the impairment observed in scene/spatial memory. It has been

reported in older adults, for example, that performance on the Montreal Cognitive Assessment (MoCA) – a test sensitive to amnesic MCI – is more strongly related with object than scene recognition performance (Fidalgo et al., 2016). Indeed, complex object discrimination has been proposed as potentially useful measure for the detection of early MCI (Gaynor et al., 2019). Even more intriguing, especially in the context of this thesis, is a recent study by Mason et al. (2017) that used a variation of the odd-one-out perceptual discrimination task discussed in Section 1.1. Two groups of middle-aged participants were studied: those with and those without a family history of AD. Performance was assessed for four types of different-view stimuli: faces, objects, greebles (i.e. complex, novel objects; Gauthier & Tarr, 1997), and scenes. Contrary to evidence specifically relating to AD (Lee et al., 2006), only one type of stimulus was found to show an effect of AD family history, namely the greebles (Mason et al., 2017). Mason et al. (2017) argued that greebles, which are complex and often unfamiliar to participants, are likely to invoke the greatest degree of feature ambiguity. As discussed in Section 1.1, the PRC and the ventral feature network are theorised to resolve feature ambiguity, which implies that early AD-related alterations in those at-risk (indicated by a positive family history) may be affecting this network.

At this point, one might wonder how AD might impact the feature network. As briefly mentioned earlier, tau-containing neurofibrillary tangles are a hallmark pathological feature of AD (DeTure & Dickson, 2019; Serrano-Pozo et al., 2011) and are closely linked to neurodegeneration and memory decline over the course of the disease (e.g. Chen et al., 2021; La Joie et al., 2020; for a relevant discussion, see Jagust, 2018). Tau pathology is thought to begin in the so-called “transentorhinal region” (Braak & Braak, 1997), a transition area between two components of the feature network: the lateral portion of the EC and the PRC (Braak & Braak, 1985). Crucially, recent tau PET studies have shown that this occurs many years before clinical symptoms of AD (e.g. Berron et al., 2021; Maass et al., 2017; for a discussion, see Jagust, 2018), with one post-mortem study suggesting that this may even begin in early adulthood (Braak & Del Tredici, 2011). Notably, tau later appears to spread to other regions of the brain as A $\beta$  accumulates in posteromedial

structures (Jagust, 2018), possibly via the cingulum bundle (Jacobs et al., 2018). The notion that tau might accumulate in the MTL during normal ageing and only spread further in the presence of A $\beta$  is currently a topic of intense research (for a recent example, see Iaccarino et al., 2021). Nevertheless, evidence for network-selective vulnerability to differential aspects of AD pathology is starting to emerge, with A $\beta$  in posteromedial regions linked to poorer scene mnemonic discrimination and tau in anterotemporal regions linked to poorer object mnemonic discrimination (Maass et al., 2019).

Overall, the reviewed findings present a mixed picture. On the one hand, there is a relatively large body of research suggesting that age – whether normal or pathological (i.e. MCI, AD), if such a discrepancy exists – impacts the extended hippocampal navigation network and its corresponding scene representations. On the other hand, more recent evidence indicates that the PRC and ventral parts of feature network, along with its corresponding object representations, are vulnerable to ageing, as well as MCI and AD-related pathology. In this regard, the question posed at the start of this section remains – as yet – unanswered. One of the aims of this thesis is to add to this emerging literature, refining our collective understanding of the differential impact that age has on these two representational networks.

### **Section 1.3. *APOE* $\epsilon$ 4 as a risk factor for age-related cognitive decline**

An important challenge for cognitive neuroscience research on ageing is to better understand the factors that increase or decrease vulnerability to age-related decline. This line of research often refers to such factors – whether genetic or environmental – as increasing or decreasing “reserve”, a hypothesised capacity of neural resources that attenuates vulnerability to the effects of age and age-related neurodegenerative disease (Cabeza et al., 2018; Stern et al., 2019). In this regard, while certain brain networks and their corresponding representations may be particularly vulnerable to the effects of age (Section 1.2), additional factors may exacerbate or alleviate these vulnerabilities. Characterising how these factors interact with age-

related processes is therefore important, as it may improve our collective understanding of why certain individuals are more (or less) likely to experience particular forms of late-life cognitive decline. In this thesis, I focus on apolipoprotein E (*APOE*) genotype and the *APOE*  $\epsilon 4$  allele in particular.

Located on chromosome 19q13, the human *APOE* gene encodes a multi-functional protein of the same name, APOE, which is comprised of 299 amino acids (Huang & Mahley, 2014). There are three common allelic variants – *APOE*  $\epsilon 2$ , *APOE*  $\epsilon 3$ , *APOE*  $\epsilon 4$  – and thus six possible *APOE* genotypes:  $\epsilon 2/\epsilon 2$ ,  $\epsilon 2/\epsilon 3$ ,  $\epsilon 3/\epsilon 3$ ,  $\epsilon 2/\epsilon 4$ ,  $\epsilon 3/\epsilon 4$ , and  $\epsilon 4/\epsilon 4$ . Although DNA sequencing in primates and early humans indicates that *APOE*  $\epsilon 4$  is the ancestral allele (Fullerton et al., 2000; McIntosh et al., 2012), it is the  $\epsilon 3$  allele that is most common in humans today. Indeed, these three alleles – *APOE*  $\epsilon 2$ ,  $\epsilon 3$ , and  $\epsilon 4$  – are estimated to have a worldwide frequency of approximately 8%, 78%, and 14%, respectively (Liu et al., 2013). The APOE isoforms produced by these three alleles differ only at two positions, specifically positions 112 and 158 (Rall et al., 1982; Weisgraber et al., 1981). An overview of these isoforms and their three-dimensional (lipid-free) structure is shown in Figure 1.11. Critically, although small, these single amino acid changes significantly alter the structure and function of APOE isoforms at the molecular and cellular level, which in turn have a profound effect on AD risk (Huang & Mahley, 2014; Mahley, 2016; Mahley & Huang, 2012a, 2012b).

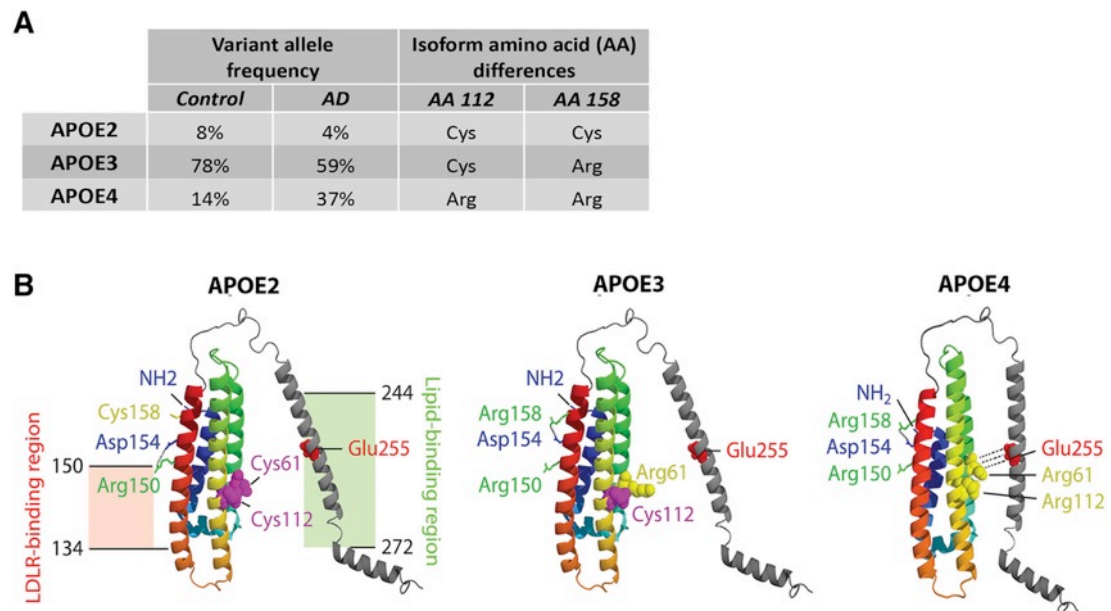
The association between the *APOE*  $\epsilon 4$  allele and AD was first identified in a series of studies published in 1993 (Corder et al., 1993; Saunders et al., 1993; Strittmatter et al., 1993). Shortly thereafter, the *APOE*  $\epsilon 2$  allele was identified as a possible protective factor (Chartier-Harlin et al., 1994; Corder et al., 1994; see also Suri et al., 2013). In a subsequent meta-analysis of the many ensuing studies, Farrer et al. (1997) examined the odds ratios for AD according to different *APOE* genotypes (relative to the most common genotype:  $\epsilon 3/\epsilon 3$ ). Despite odds ratios varying according to sex and ancestral background, the results confirmed that *APOE*  $\epsilon 4$  was associated with AD in a dose-dependent manner ( $\epsilon 3/\epsilon 3 < \epsilon 3/\epsilon 4 < \epsilon 4/\epsilon 4$ ). Results also confirmed that

the  $\epsilon 2$  allele was associated with a mild reduction in risk, although not for individuals with the  $\epsilon 2/\epsilon 4$  genotype. Recent evidence has substantiated this latter point, observing that the  $\epsilon 2\epsilon 4$  genotype is associated with increased AD-related pathology (e.g.  $A\beta$ ) and overall AD risk (Goldberg et al., 2020; Jansen et al., 2015; Oveisgharan et al., 2018; Reiman et al., 2020). While large-scale genome-wide association studies (GWAS) have identified additional genetic loci associated with AD (Jansen et al., 2019; Lambert et al., 2013; Marioni et al., 2018), all are attributed with odds ratios considerably smaller ( $\sim 1.1$ - $1.3$ ) than those attributed to *APOE*  $\epsilon 4$  (heterozygotes:  $\sim 4$ , homozygotes:  $\sim 12$ ). Interestingly, this increase in AD risk appears to be moderated by sex, such that female  $\epsilon 4$  carriers are more at-risk than male  $\epsilon 4$  carriers (Neu et al., 2017; Riedel et al., 2016; Ungar et al., 2014). Contemporary work examining lifetime risk, rather than odds ratios, further indicates that the risk conferred by *APOE*  $\epsilon 4$  is near equivalent to that conferred by *BRCA1* for breast cancer (Genin et al., 2011). According to this analysis, by age 85, AD lifetime risk reaches 51% and 60% for male and female  $\epsilon 4$  homozygotes, respectively (Genin et al., 2011). Based on these findings, as well as the observation that *APOE*  $\epsilon 4$  reduces the age of AD onset (Ashford, 2004; Blacker et al., 1997; Corder et al., 1993; Sando et al., 2008), this allele is now widely recognised as a major susceptibility gene for AD (Yu et al., 2014).



**Figure 1.11.**

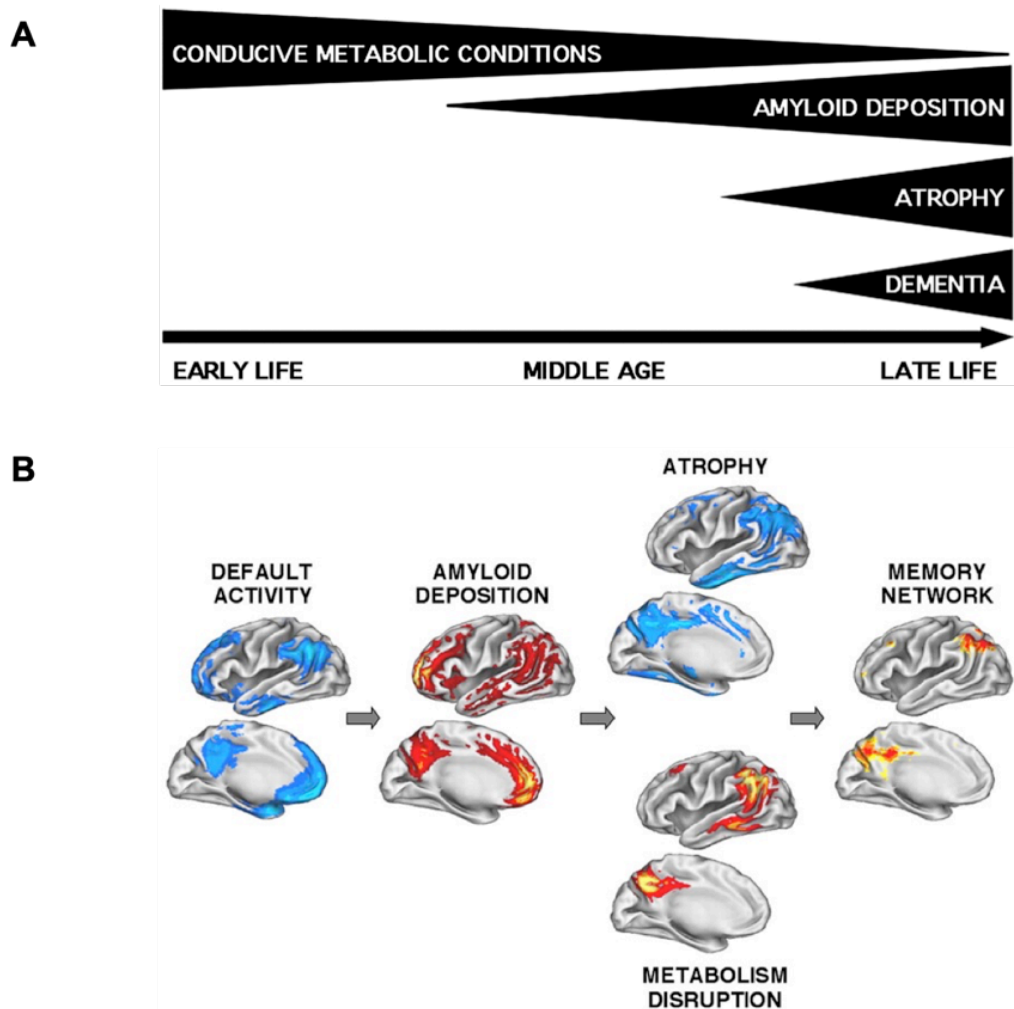
*Allelic Frequencies, Isoform Amino Acid Differences, and Protein Structure of Human APOE*



*Note.* The frequency of each *APOE* allele in the general population and in AD patients is shown, as are the amino acid differences associated with each allele (A). Three-dimensional models of lipid-free *APOE* isoforms are also shown (B). Reprinted from Belloy et al. (2019).

However, the relationship between *APOE*  $\epsilon$ 4 and AD goes beyond susceptibility alone. A recent line of research suggests that the  $\epsilon$ 4 allele affects the clinical presentation of AD, such that patients with one or more copies are increasingly likely to present with the amnesic variant of the disease (for a recent review, see Emrani et al., 2020). Supporting this, there are numerous reports indicating that the presence of the *APOE*  $\epsilon$ 4 allele is related to more marked memory impairments in AD (Kim et al., 2018; Snowden et al., 2007; van der Vlies et al., 2007; Wolk et al., 2010). The reverse has also been reported, with *APOE*  $\epsilon$ 4 negative AD patients presenting with prominent non-memory related impairment (e.g. Scheltens et al., 2017). As such, possession of the *APOE*  $\epsilon$ 4 allele not only affects risk and age of onset for AD, but also appears to impact the clinical presentation of the disease.

Given the link between *APOE*  $\epsilon 4$  and AD, there has been a considerable amount of research seeking to understand how this allele impacts the brain (for a recent review, see Belloy et al., 2019). One set of related perspectives, referred to here as lifespan systems vulnerability accounts (Figure 1.12), seek to frame the effect(s) of *APOE*  $\epsilon 4$  in the context of lifelong patterns of brain activation and metabolism (Bero et al., 2011; Buckner et al., 2005, 2009; Jagust & Mormino, 2011). According to these accounts, factors such as the  $\epsilon 4$  allele reduce reserve (i.e. “neural efficiency”) in a way that leads to hyper-activation/hyper-metabolism early in life, which in turn increases susceptibility to later  $A\beta$  accumulation. With advancing age, the growing burden of  $A\beta$  then leads to network dysfunction, ultimately giving rise to hypo-activation/hypo-metabolism and cognitive decline (Busche et al., 2008; Busche & Konnerth, 2016; Palop & Mucke, 2010). Animal work provides evidence of a plausible mechanistic explanation for this view. Across several studies employing different methods, it has been reported that neural activity modulates the release of  $A\beta$  (Bero et al., 2011; Cirrito et al., 2005; Kamenetz et al., 2003; Yamamoto et al., 2015; Yuan & Grutzendler, 2016). Mouse models of AD further indicate that the increasing presence of  $A\beta$  may potentiate the spread of tau – deposited as a function of age – beyond structures in the MTL (He et al., 2018; Hurtado et al., 2010; Pooler et al., 2015; Therneau et al., 2021), perhaps via structural connections between regions (Ahmed et al., 2014; Iaccarino et al., 2018; for a relevant discussion, see Lewis & Dickson, 2016). Although direct mechanistic support in humans is lacking, neuroimaging studies have established that structures characterised by high levels of functional activation and metabolic activity at rest, such as the PCC/RSC, are among the earliest sites of  $A\beta$  accumulation (Oh et al., 2016; Mattsson et al., 2019; Palmqvist et al., 2017; Villeneuve et al., 2015). These findings provide support for a link between brain activation/metabolic activity and amyloid accumulation, and suggest that the extended hippocampal navigation network is vulnerable to  $A\beta$ . A key test for lifespan systems vulnerability accounts, however, is whether individuals who possess one or more copies of the *APOE*  $\epsilon 4$  allele show alterations in brain activation and metabolic activity early in the lifespan.

**Figure 1.12.***Lifespan Systems Vulnerability Accounts of Cognitive Decline and AD*

*Note.* The hypothetical progression from early-life metabolic alterations to later  $A\beta$  accumulation, atrophy, and ultimately cognitive decline and dementia are shown. Panel A shows a schematic illustration of this progression, while panel B shows the overlap between regions characterised by hyper-activation/hyper-metabolism,  $A\beta$  accumulation, and atrophy/hypo-metabolism. Adapted from Buckner et al. (2005).

In line with this view, a number of studies have observed hyper-activation and hyper-metabolism in young *APOE*  $\epsilon 4$  carriers within the extended hippocampal navigation network. Two separate fMRI studies have observed greater activation (i.e. hyper-activation) in the hippocampus of young  $\epsilon 4$  carriers, relative to non-carriers, during episodic memory encoding (Dennis

et al., 2010; Filippini et al., 2009). In another relevant study, Kunz et al. (2015) applied an fMRI modelling approach that enabled the authors to detect grid-cell-like activation in the EC (Doeller et al., 2010), a region of the brain impacted early by tau pathology (see Section 1.2.4). The authors observed that young  $\epsilon 4$  carriers demonstrated reduced grid-cell-like activation in the EC relative to non-carriers, which was linked to poorer spatial memory performance. Reduced grid-cell-like activation was further associated with increased activation in the hippocampus (Kunz et al., 2015). Moreover, it has also been reported that young *APOE*  $\epsilon 4$  carriers exhibit hyper-activation in the PCC during scene odd-one-out perceptual discrimination (Shine et al., 2015), which is broadly consistent with reports of  $A\beta$ -related posteromedial and hippocampal hyper-activation (Huijbers et al., 2012, 2014; Leal et al., 2017; Mormino et al., 2012; Oh et al., 2016; Sperling et al., 2009; Vannini et al., 2013), as well as scene oddity deficits in AD (Lee et al., 2006; see also Lee et al., 2007). Collectively, the results of these studies are broadly in line with the view that the  $\epsilon 4$  allele may reduce neural efficiency (Busche & Konnerth, 2016), leading to hyper-activation/hyper-metabolism and increased  $A\beta$  accumulation, triggering a cascade that ultimately disrupts functional activation and metabolic activity in later life. Supporting this, a cross-sectional study of the interaction between *APOE*  $\epsilon 4$  carrier status and age demonstrated reduced activation during episodic encoding in older  $\epsilon 4$  carriers relative to younger  $\epsilon 4$  carriers (Filippini et al., 2011).

These alterations in functional activation and metabolic activity suggest that the *APOE*  $\epsilon 4$  allele reduces neural efficiency (Jagust & Mormino, 2011), or reserve, in young adults. This is particularly evident in regions comprising the extended hippocampal navigation network, such as the PCC/RSC. Adding to this, it has also been reported that young *APOE*  $\epsilon 4$  carriers demonstrate alterations in functional connectivity within this network. For instance, Filippini et al. (2009) observed that young  $\epsilon 4$  carriers relative to non-carriers showed greater intrinsic fMRI-based functional connectivity (i.e. hyper-connectivity) between the hippocampus and PCC/RSC. It should be noted that there are reasons to doubt the replicability of this finding (Mentink et al.,

2021), despite conceptually similar results having been reported (Zheng et al., 2021). Nonetheless, hippocampal-PCC hyper-connectivity (a.k.a. increased synchronisation) has also been reported in middle-aged and older *APOE*  $\epsilon 4$  carriers relative to non-carriers, which was in turn related to poorer memory performance (Westlye et al., 2011). This finding provides support for the view that hyper-connectivity within the extended hippocampal navigation network is a product of reduced neural efficiency rather than compensatory mechanisms (Elman et al., 2014). Extending this work, it has been proposed that a period of hyper-connectivity is subsequently followed by a period of hypo-connectivity in the course of AD (Schultz et al., 2017). This is consistent with the argument that hyper-connectivity, as well as hyper-activation/hyper-metabolism, may be an important driver of  $A\beta$  accumulation (Busche & Konnerth, 2015), which later results in hypo-connectivity in AD (Greicius et al., 2004). In accordance with this, a recent study using magnetoencephalography (MEG) observed patterns of hyper-connectivity in young *APOE*  $\epsilon 4$  carriers and hypo-connectivity in AD patients (Koelewijn et al., 2019). Whether hyper-activation/hyper-metabolism and hyper-connectivity reflect distinct mechanisms is unclear, but the evidence discussed nonetheless suggests that early-life alterations in task-related activation, metabolic activity, and intrinsic functional connectivity are evident in young *APOE*  $\epsilon 4$  carriers.

Given the close but imperfect relationship between structural and functional connectivity (Suárez et al., 2020; see also Box 1), it is possible that the  $\epsilon 4$  allele may induce early-life changes in structural connectivity, perhaps via reduced or delayed axonal pruning (Chung et al., 2016), that drive alterations in functional connectivity (Navlakha et al., 2018). To investigate this possibility, Hodgetts et al. (2019) examined the effect of *APOE*  $\epsilon 4$  on PHCB and ILF microstructure in a sample of healthy, young individuals. As mentioned in Section 1.1, the PHCB represents an important tract in the extended hippocampal navigation network, mediating much of the connectivity between the hippocampus, PHC, RSC, and PCC (Jones, Christiansen et al., 2013; Heilbronner & Haber, 2014). The ILF, by contrast, is proposed to connect ventral components of the feature network (Catani et

al., 2003; Herbet et al., 2018). *APOE*  $\epsilon$ 4 carriers showed higher FA and lower MD than non-carriers in the PHCB but not the ILF (Hodgetts et al., 2019). As higher FA and lower MD partially reflect increased axon density and potentially myelination (Beaulieu, 2002), including other aspects of microstructure (Box 1), this result indicates that *APOE*  $\epsilon$ 4 carriers exhibit increased structural connectivity in the PHCB relative to non-carriers, perhaps due to axonal over-connectivity. As discussed previously (Section 1.1), Hodgetts et al. (2019) further observed that these alterations in PHCB microstructure were associated with scene oddity related activation in the PCC, as well as the hippocampus and PHC (see also Shine et al., 2015). To account for this, Hodgetts et al. (2019) speculated that *APOE*  $\epsilon$ 4 carriers and non-carriers may undergo different patterns of white matter maturation, perhaps via reduced axonal pruning of the late-maturing cingulum bundle (Lebel & Beaulieu, 2011; Lebel et al., 2012; see also Tamnes et al., 2018), leading to an initial “overshoot” in PHCB microstructure and a related increase in functional activation and connectivity (i.e. hyper-activation and -connectivity) within this important, large-scale MTL neurocognitive network.

These findings from young *APOE*  $\epsilon$ 4 carriers provide support for the lifespan systems vulnerability view. Together, they suggest that the *APOE*  $\epsilon$ 4 allele may bring about early-life brain changes that reduce neural efficiency or reserve, which over time lead to increased A $\beta$  accumulation and ultimately dysfunction in the extended hippocampal navigation network. In this regard, *APOE*  $\epsilon$ 4 can be conceptualised as a risk factor for late-life cognitive decline within a broader lifespan framework. However, one might wonder how this line of research can be squared with findings implicating the feature network, in ageing and MCI/AD (e.g. Fidalgo et al., 2016). One of the aims of this thesis is to provide insight into the impact of *APOE* genotype – and *APOE*  $\epsilon$ 4 in particular – on these networks at particular points in the lifespan and, to a degree, across the lifespan.

## Section 1.4. Aims of the thesis

In this chapter, I began by discussing the shift from the concept of a unitary MTL memory system to the role of representations in large-scale MTL neurocognitive networks (Section 1.1). I introduced two particular networks: the extended hippocampal navigation network and the feature network (Murray et al., 2017). The former is proposed to enrich and elaborate on hippocampal scene representations, supporting spatial navigation and acting as a scaffold for episodic memory. The latter – especially its ventral component – is proposed to represent object-level features, as well as semantic concepts and categories. However, as highlighted in Section 1.2, the relative impact of age and age-related neurodegenerative disease on these networks remains unclear. Some evidence suggests that the navigation network is particularly vulnerable to age, whereas a growing body of work implicates aspects of the feature network. Given current trends in longevity (UN, 2020), there is an urgent need to refine our collective understanding of how age and age-related neurodegenerative disease, as well as risk for such disease, impacts these brain networks and their corresponding representations. Addressing this knowledge gap represents one of the core aims of the thesis. Relatedly, in Section 1.3, I outlined how the *APOE*  $\epsilon 4$  allele may be related to early-life alterations in the extended hippocampal navigation network, which give rise to hyper-activation and hyper-metabolism. This in turn is thought to lead to vulnerability to AD-related pathology (i.e.  $A\beta$  accumulation) and ultimately network dysfunction (Bero et al., 2011; Buckner et al., 2005, 2009; Jagust & Mormino, 2011). Despite this, further research is needed to characterise the impact of *APOE*  $\epsilon 4$  – and *APOE* genotype more broadly – on these networks and their corresponding representations at various points in the lifespan, including in early adulthood. This represents another core aim of this thesis.

In Chapter 2, I examine the relative impact of *APOE* genotype and age on different-view scene and different-view face oddity performance in a sample of middle-aged and older adults using a web-based task. I described this experimental paradigm previously (Section 1.1), outlining how it is sensitive

to the specialised representations supported by the extended hippocampal navigation and feature networks, respectively. Moreover, as mentioned in relation to the results of Güsten et al.'s (2021) study, the use of a web-based task provided an opportunity to obtain large samples of sensitive cognitive data (see also Huentelman et al., 2020). In fact, the experiment reported in Chapter 2 includes oddity data from more than 500 female participants, who were recruited from the Avon Longitudinal Study of Parents and Children (ALSPAC; <http://www.bristol.ac.uk/alspac/>). The focus on female participants was motivated not only by their availability, but also by prior reports showing that female  $\epsilon 4$  carriers are more at risk of AD than male  $\epsilon 4$  carriers (Riedel et al., 2016; Ungar et al., 2014; for further discussion, see Chapter 2, Section 2.1). An additional benefit of examining perceptual discrimination in this sample was the ability to examine the impact of the *APOE*  $\epsilon 2$  allele, the so-called “forgotten *APOE* allele” (Suri et al., 2013, p.2879). This allele has been shown to be protective against cognitive decline and AD (Chartier-Harlin et al., 1994; Corder et al., 1994; Farrer et al., 1997; for more recent work, see Reiman et al., 2020), but little is known about its role in mid-life (Salvato, 2015).

In Chapter 3, I examine the relative impact of *APOE*  $\epsilon 4$ , gender/sex, and age on the structural covariance (see Box 1) of key components within the two networks: the hippocampus and the PRC. Given that structural covariance may reflect connectivity to some degree (Alexander-Bloch, Giedd, & Bullmore, 2013; Yee et al., 2018; see also Box 1), this method makes it possible to investigate how connectivity of these network nodes is impacted by *APOE*  $\epsilon 4$ , gender/sex, and age. The functional relevance of these structural covariance patterns was assessed via the NeuroSynth decoder (<https://neurosynth.org/decode/>; Yarkoni et al., 2011) and via associations with performance on particular cognitive tasks. Moreover, by including self-identified males and females from across the adult lifespan, this chapter addresses the role of gender/sex and age more explicitly, which was not possible in Chapter 2.



In Chapter 4, I examine the impact of *APOE*  $\epsilon 4$  carrier status on PHCB and ILF microstructure (FA, MD) in healthy young adults. As mentioned previously, these white matter tracts feature prominently in the extended hippocampal navigation and feature networks. This chapter largely serves as a replication of Hodgetts et al. (2019) study, which reported that *APOE*  $\epsilon 4$  carriers relative to non-carriers exhibit higher FA and lower MD (i.e. higher structural connectivity) in the PHCB but not the ILF. If replicated in a larger sample, as attempted here, this finding would provide insight relevant for lifespan systems vulnerability accounts. Additional analyses are also included in this chapter. For example, I report an analysis investigating whether hemispheric asymmetry in PHCB/ILF microstructure is affected by *APOE*  $\epsilon 4$  carrier status and sex.

Finally, in Chapter 5, I conclude this thesis by summarising the results from the three experimental chapters. I then discuss their wider theoretical implications, especially in relation to *APOE* genotype and age. Following this, I move on to consider the various limitations of the work presented, drawing on relevant research. I conclude by identifying outstanding questions and outline how future research might provide answers.

## **Chapter 2: Impact of *APOE* genotype and age on different-view scene and face odd-one-out perceptual discrimination in middle-aged and older adults**

### **2.1. Introduction**

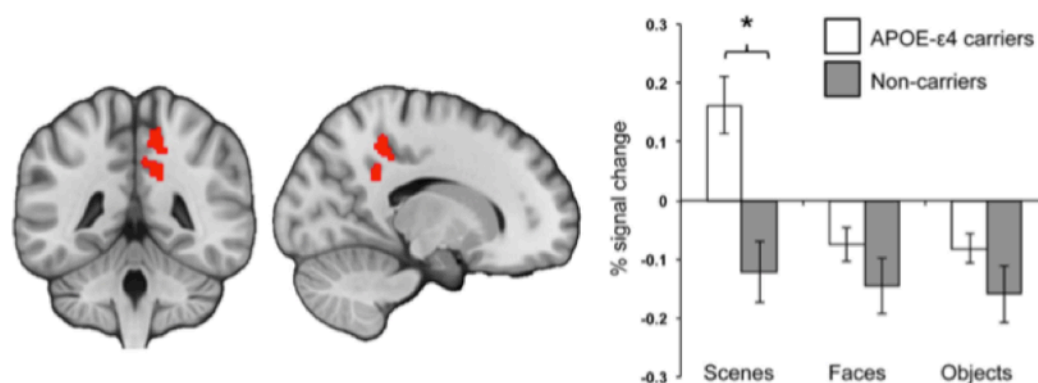
In Chapter 1, I introduced a contemporary representational account of visual perception and memory: the evolutionary accretion model (Murray et al., 2017). Consistent with other representational accounts, such as the emergent memory account (Graham et al., 2010) and the representational-hierarchical model (Saksida & Bussey, 2010), the evolutionary accretion model proposes that the hippocampus and PRC – two MTL structures – support highly specialised representations of scene and object/face feature conjunctions, respectively (Section 1.1.1). Crucially, these highly specialised, conjunctive representations are argued to emerge via large-scale, distributed neurocognitive networks (Mesulam, 1990, 1994). I discussed two such networks in Chapter 1: the so-called extended hippocampal navigation network and the so-called feature network (Murray et al., 2017). The former is proposed to enrich and elaborate on hippocampal scene representations, facilitating the construction of coherent views of scenes or places (for a related account, see the PMAT framework - Ranganath & Ritchey, 2012; Ritchey et al., 2015). These scene representations are thought to be important for navigation and, in addition, act as a foundation or “spatial scaffold” for episodic memories (Murray et al., 2017; see Section 1.1.2.1). The latter – especially its ventral component – is proposed to represent object-level features, as well as semantic concepts and categories (Murray et al., 2017; see also Lambon Ralph et al., 2017). Through interactions with specialised representations supported by the human prefrontal cortex, both of these networks are thought to contribute to aspects of human memory (Murray & Wise, 2010; Murray et al., 2017). Despite their proposed role in cognition, however, it is currently unclear whether the *APOE*  $\epsilon$ 4 allele – the best-established genetic risk factor for AD (Serrano-Pozo et al., 2021) –

and/or age differentially impact these two networks (see Sections 1.2 and 1.3).

In recent years, a growing body of evidence has suggested that the *APOE*  $\epsilon$ 4 allele detrimentally impacts fMRI and behavioural markers of allocentric spatial navigation and scene-based cognition. In one such study, Kunz et al. (2015) observed that young  $\epsilon$ 4 carriers demonstrated reduced grid-cell-like representations in the EC relative to non-carriers, which was in turn linked to poorer spatial memory performance and increased hippocampal task activation. Somewhat consistent with this finding, impairment in path integration – that is, the ability to ascertain one’s current position based on previous positions, head direction, speed, and time elapsed – has been reported in *APOE*  $\epsilon$ 4 carriers, especially when the use of compensatory strategies was restricted (Bierbrauer et al., 2020). Path integration is thought to be dependent on grid cells (Hafting et al., 2005), including in humans (Stangl et al., 2018), and has long been considered as an example of allocentric processing (McNaughton et al., 1991; although for critique of this view, see Ekstrom et al., 2014). This therefore bolsters the notion that allocentric scene processing is impacted by *APOE*  $\epsilon$ 4. Regarding spatial memory, Laczó et al. (2011) reported that *APOE*  $\epsilon$ 4 carriers with amnesic MCI are impaired on the Morris water maze task relative to *APOE*  $\epsilon$ 4 non-carriers with amnesic MCI. As discussed in Section 1.2.1.1, completion of this task is thought to be reliant on an allocentric strategy (although for critiques of this view, see Ekstrom et al., 2014; Wolbers & Wiener, 2014). In addition, the  $\epsilon$ 4 allele has been linked with impairment in wayfinding among middle-aged and older adults, despite the absence of an episodic memory deficit between carriers and non-carriers (Coughlan et al., 2019; see also Gellersen, Trelle et al., 2021). This suggests that navigation deficits may precede episodic memory deficits in the context of *APOE* and ageing (Coughlan et al., 2018).

Further evidence linking the *APOE*  $\epsilon$ 4 allele with scene-related processing comes from the odd-one-out perceptual discrimination (a.k.a. oddity or oddity judgment) task. I reviewed this task in detail in Section 1.1. Briefly, the goal

of this task is to select the odd-one-out from a visual array of same-category stimuli, all of which are presented at the same time. When the non-target stimuli are presented from different viewpoints, successful identification of the odd-one-out can only be made on the basis of feature conjunctions. This is important in the context of the scene condition, as it means that the task taxes the conjunctive scene representations of the hippocampus (Graham et al., 2010; Murray et al., 2017), which can be considered equivalent to, or a precursor of, allocentric “cognitive maps” (Byrne et al., 2007; Fidalgo & Martin, 2016). Utilising this task, Shine et al. (2015) investigated whether young *APOE*  $\epsilon$ 4 carriers relative to non-carriers demonstrate functional alterations in posteromedial regions – notably, the PCC – during different-view scene but not different-view face or different-view object oddity discrimination. As highlighted in Figure 2.1, Shine et al. (2015) observed increased activation – interpreted as hyper-activation in Section 1.3 – in the PCC during different-view scene discrimination (see also Hodgetts et al., 2019). No other differences were observed between *APOE*  $\epsilon$ 4 carriers and non-carriers. This finding points to an alteration in scene-related activation within the extended hippocampal navigation network, which is consistent with the notion that the  $\epsilon$ 4 allele detrimentally impacts allocentric navigation and scene processing.

**Figure 2.1.***Scene-Related PCC Alterations in APOE  $\epsilon$ 4 carriers*

*Note.* Percentage BOLD signal change for each type of oddity stimulus type (vs. a baseline shape condition) is shown. Data are separated according to *APOE*  $\epsilon$ 4 carrier status, with the white bars representing carriers and the grey bars representing non-carriers. Hyper-activation in the PCC, which was defined using a separate functional localiser task, is evident only for scene odd-one-out discrimination. Reprinted from Shine et al. (2015).

Notably, these  $\epsilon$ 4-related alterations in scene processing may offer insight into the early episodic memory impairment that characterises the amnesic variant of AD (Dubois et al., 2007, 2014; McKhann et al., 2011). Multiple theoretical accounts, including the evolutionary accretion model, converge on the notion that scene representations provide a scaffold on which episodic/autobiographical memories can be constructed (Gaffan, 1991; Hassabis & Maguire, 2007, 2009; Maguire & Mullaly, 2013; Murray et al., 2017; Nadel & Peterson, 2013; Robin, 2018; Rubin et al., 2019; Rubin & Umanath, 2015; Zeidman & Maguire, 2016). In this regard, the extended hippocampal navigation network and its detailed, complex scene representations are theorised to make important contributions to the rich spatial information that accompanies an event (i.e. spatial context). Returning to *APOE*  $\epsilon$ 4, it stands to reason therefore that if this allele detrimentally impacts the scene representations supported by the aforementioned network, it may also be more strongly linked with episodic memory problems in AD, specifically in relation to the generation of detailed

context information. Support for this comes from a range of studies reporting that the presence of the  $\epsilon 4$  allele is related to more severe memory impairments in AD (Kim et al., 2018; Snowden et al., 2007; van der Vlies et al., 2007; Wolk et al., 2010; for a relevant review, see Emrani et al., 2020). Moreover, it has recently been shown that middle-aged and older adults in possession of the  $\epsilon 4$  allele generate fewer internal details (i.e. details including time and place information) than non-carriers when recalling autobiographical memories (Grilli et al., 2018).

One possible mechanism for *APOE*  $\epsilon 4$ -related alterations in scene processing and spatial context information centres on  $A\beta$ . Although controversial (Herrup, 2015), the deposition and accumulation of  $A\beta$  is still widely regarded as the primary precipitating factor in the development of AD (Selkoe & Hardy, 2016). Furthermore, the *APOE*  $\epsilon 4$  allele is associated with increased longitudinal accumulation of  $A\beta$  (Mishra et al., 2018). Whether this is due to enhanced  $A\beta$  production or reduced  $A\beta$  clearance, among other possibilities, remains an active topic of research (Safieh et al., 2019; Serrano-Pozo et al., 2021; Wisniewski & Drummond, 2020). Regardless, given that the earliest sites of  $A\beta$  accumulation include posterior parietal regions that feature prominently in the extended hippocampal navigation network (Oh et al., 2016; Mattsson et al., 2019; Palmqvist et al., 2017; Villeneuve et al., 2015), it is plausible that this network may be particularly vulnerable to  $A\beta$  and – crucially – may be more heavily impacted in  $\epsilon 4$  carriers relative to non-carriers. Consistent with this, lifespan systems vulnerability accounts (Bero et al., 2011; Buckner et al., 2005, 2009; Jagust & Mormino, 2011) propose that the  $\epsilon 4$  allele reduces neural efficiency in a way that leads to hyper-activation/hyper-metabolism in specific regions and/or networks early in life, which in turn increases susceptibility to later  $A\beta$  accumulation (see Section 1.3). This explains the overlap between regions characterised by scene-related hyper-activation (Shine et al., 2015; see also Hodgetts et al., 2019) and regions characterised by early  $A\beta$  accumulation, such as the PCC. The link between *APOE*  $\epsilon 4$  and  $A\beta$  thus provides a mechanism by which this allele may impact the extended hippocampal navigation network and, in turn, its corresponding scene representations.

In contrast to the link between *APOE*  $\epsilon 4$  and scene processing, a growing number of studies have reported that the ability to discriminate between objects sharing many features (e.g. complex objects, faces) is more prominently impacted by ageing. These studies (e.g. Reagh et al., 2016, 2018; Ryan et al., 2012; Stark & Stark, 2017) are reviewed in detail in Section 1.2.3. To briefly summarise, when comparing groups of younger adults relative to groups of older adults on object mnemonic discrimination, older adults often exhibit poorer performance. Although such age-related differences in task performance are sometimes evident in both object *and* scene mnemonic discrimination (Berron et al., 2018), these differences tend to be larger for objects (Stark & Stark, 2017). Functional neuroimaging studies provide additional insight into the neural correlates of this age effect, reporting that older adults relative to younger adults exhibit lower levels of activation in the PRC (Ryan et al., 2012; see also Berron et al., 2018) and anterolateral EC (Reagh et al., 2018) during object mnemonic discrimination. The latter structure is strongly connected to the PRC and has been previously shown to respond preferentially to object rather than scene stimuli (Maass et al., 2015; Navarro Shröder et al., 2015; see also Aggleton, 2012; Suzuki & Amaral, 1994). Based on these findings, it appears that age may detrimentally impact the ventral component of the feature network, as well its corresponding object-level representations (Burke et al., 2018).

A caveat to these studies, however, is that they may exaggerate age effects by comparing younger and older groups (although for an exception, see Güsten et al, 2021). To illustrate this point, consider the example of face stimuli. Prior research provides some evidence that faces are particularly salient in younger adults, especially during adolescence (Scherf et al., 2012). Therefore, if a study compares face discrimination in a group of younger adults (~18-21 years) relative to a group of older adults (~70 years), differences in performance may be much larger than if the same study compared the older group to a slightly older set of younger adults (e.g. 25-30 years) or even a set of middle-aged adults. In the sense, the age of the participants in the two groups has the potential to bias the observed effect(s), especially if age-related differences in stimulus processing are evident. This

is especially relevant, as the impact of *APOE*  $\epsilon 4$  on the brain and cognition in mid-life is currently unclear (Salvato, 2015). To address this limitation here, I focus primarily on middle-aged and older participants, while also treating age as a continuous variable. Although this does not address the bias associated with cross-sectional studies of ageing more broadly (Hedden & Gabrieli, 2004), it is superior to group comparisons and provides a framework for better understanding the effects of *APOE*  $\epsilon 4$  and age on scene and object-related task at the middle-to-upper end of the adult lifespan.

Intriguingly, emerging evidence indicates that individuals at risk of AD likewise demonstrate alterations in object-related discrimination. Using the odd-one-out task, Mason et al. (2017) found that middle-aged participants with a family history of AD were impaired (relative to those without a family history of AD) for only one type of stimuli: greebles (Gauthier & Tarr, 1997). Mason et al. (2017) posit that greebles, which are complex and often novel to participants, are likely to invoke the greatest degree of feature ambiguity. The evolutionary accretion model (Murray et al., 2017), in addition to earlier representational accounts (e.g. Saksida & Bussey, 2010), proposes that the PRC and ventral parts of the feature network help to resolve feature ambiguity, which implies that AD risk – as indicated by a positive family history – may impact this network. That said, given the findings mentioned previously, it is difficult to know whether this reflects non-pathological ageing or AD risk specifically. Other research provides support for the latter, identifying complex object discrimination as a potentially useful measure for detecting MCI (Gaynor et al., 2019), which itself is thought to represent a transition phase between normal ageing and AD (Albert et al., 2011). In addition, another study reported that performance on the MoCA – a test sensitive to amnesic MCI – is more strongly related with object than scene recognition performance (Fidalgo et al., 2016). These studies thus provide evidence that object-related memory performance is impaired in individuals at risk of AD, which appears inconsistent with the research on *APOE*  $\epsilon 4$ . However, it is important to note here that no study to date has yet directly investigated the effect of *APOE*  $\epsilon 4$  in this context, leaving open the question



of whether this allele has differential impacts on scene and object/face discrimination in middle-aged and older adults.

Another as yet unanswered question is to what extent *APOE*  $\epsilon 2$  impacts scene and object/face discrimination at this point in the lifespan. The  $\epsilon 2$  allele, in contrast to  $\epsilon 4$ , is protective against AD, reducing risk for the disease (Chartier-Harlin et al., 1994; Corder et al., 1994; Farrer et al., 1997). Recent evidence indicates that the protective effect of *APOE*  $\epsilon 2$  is largely driven by reduced A $\beta$  burden (Goldberg et al., 2020; Reiman et al., 2020; Salvadó et al., 2021). Despite this, research on *APOE* has historically focused on the  $\epsilon 4$  allele, largely due to the low prevalence of  $\epsilon 2$  in the population (O'Donoghue et al., 2018). *APOE*  $\epsilon 2$  has thus been dubbed the “forgotten *APOE* allele” (Suri et al., 2013, p.2879). Nevertheless, some studies have examined the effect of the  $\epsilon 2$  allele on aspects of cognition in middle-aged and older adults, although rarely using modern cognitive tasks that are sensitive to the specialised representations supported by the previously discussed networks (e.g. the odd-one-out perceptual discrimination task; see Section 1.1). In a longitudinal study of community-based older adults, for instance, Reas et al. (2019) observed that  $\epsilon 2$  carriers exhibited slower levels of age-related decline in executive function relative to  $\epsilon 3$  carriers (i.e.  $\epsilon 3/\epsilon 3$ ), whereas  $\epsilon 4$  carriers exhibited faster age-related decline in the same cognitive function. Consistent with this finding, Sinclair et al. (2017) reported that younger/middle-aged  $\epsilon 2$  carriers performed better than  $\epsilon 3$  carriers and  $\epsilon 4$  carriers on tasks tapping executive function but also episodic memory and working memory. These findings are congruent with the notion that the  $\epsilon 2$  allele confers a protective advantage against cognitive decline, as well as more general increases in longevity (Sebastiani et al., 2019; Shinohara et al., 2020; Wolters et al., 2019; for a relevant discussion, see Li et al., 2020). However, other studies have reported patterns of findings that do not neatly map onto the  $\epsilon 2$  allele's proposed role as a protective factor against AD. Lancaster, Forster et al. (2017) investigated whether genotype differences ( $\epsilon 2$  vs.  $\epsilon 3$  vs.  $\epsilon 4$ ) were evident in performance on a visuospatial attention task. The authors observed that, among their middle-aged participants, the  $\epsilon 2$  carrier group displayed less efficient visual search performance. No such

differences were evident between the  $\epsilon 3$  or  $\epsilon 4$  carrier groups (Lancaster, Forster et al., 2017). In an fMRI study of *APOE* genotype differences on the Stroop task and an episodic encoding task, Trachtenberg, Filippini, Cheeseman et al. (2012) observed that  $\epsilon 2$  and  $\epsilon 4$  carriers, relative to  $\epsilon 3$  carriers, exhibited increased activation in MTL structures such as the hippocampus and PHC, despite not showing differences in performance. Moreover, the same group reported a similar finding relating to functional connectivity of MTL structures, as well as other regions (Trachtenberg, Filippini, Ebmeier et al., 2012). As such, there is a question as to whether scene and object/face perceptual discrimination – and cognition more broadly – differs in *APOE*  $\epsilon 2$  carriers relative to  $\epsilon 3$  and  $\epsilon 4$  carriers and, if so, whether this is evident in mid-life.

Studying the impact of *APOE* genotype and age on cognition in mid-life requires relatively large samples of participants. Indeed, it has been argued previously that the effect of the *APOE*  $\epsilon 4$  allele on more traditional (i.e. clinic-based) measures of cognition is relatively small (Wisdom et al., 2011; for a comparison with the autobiographical memory interview, see Grilli et al., 2018), while research on ageing is generally underpowered to detect realistic effect sizes (Brydges, 2019). Obtaining large samples from in-person cognitive testing is challenging, however, as it is often both expensive and time-intensive. Fortunately, it is now possible to collect data from much larger samples using web-based cognitive tasks (for a discussion, see Huentelman et al., 2020). There are several notable advantages to web-based research, including the ability to recruit larger, more diverse samples (Vaughn et al., 2018; Woods et al., 2015). By utilising web-based tasks, therefore, it is possible to obtain sample sizes that provide sufficient power to detect realistic effect sizes, thereby reducing the likelihood of falsely rejecting the null – put another way, the likelihood of committing a Type II error (Button et al., 2013). In this regard, the use of web-based cognitive tests makes it possible to conduct large-scale, well-powered research on *APOE* genotype at various points throughout the lifespan.

Here, I utilised an online research platform designed and built by Ounce Technology ([www.ouncetech.co.uk](http://www.ouncetech.co.uk)) in collaboration with researchers at Cardiff University: Cardiff Web Tools for Cognitive Health (CWTCH; [www.cwtch.ounce.ac](http://www.cwtch.ounce.ac)). The goal of this platform is to provide a secure, easily accessible online space in which to examine individual differences in spatial perception and memory. To this end, CWTCH incorporates two cognitive tasks: an odd-one-out perceptual discrimination task (a.k.a. oddity task; Lee, Buckley et al., 2005) and a spatial n-back task (Lee & Rudebeck, 2010). An image of the task menu, as seen by participants, is shown in the appendix (Section 6.1). Both tasks have been used in prior research but, crucially, have been adapted for use on a laptop or desktop computer. Given that the odd-one-out task appears sensitive to *APOE*-related functional brain changes in early-life (Shine et al., 2015), as well as clinical impairment early in the course of AD (Lee et al., 2006), the CWTCH platform provides a unique opportunity to conduct relatively well-powered research on the impact of this allele on scene (and object/face) processing in middle-aged and older adults prior to the onset of clinical symptoms.

In the current chapter, I report a study that aimed to examine the impact of *APOE* genotype and age on different-view scene and different-view face perceptual oddity discrimination in a sample of middle-aged and older adult females. Prior research pertaining to the effects of *APOE* and age on scene and object (including face) discrimination presents a mixed picture, as discussed, and the study reported here will therefore help to further refine our collective understanding. The exclusive focus on female participants was driven in part by their availability and the amount of historic phenotypic data made available, as part of their involvement in ALSPAC (see Section 2.2.1). However, there were also good theoretical reasons to focus exclusively on females (for relevant reviews, see Riedel et al., 2016; Ungar et al., 2014). It has long been known that female *APOE*  $\epsilon 4$  carriers are more at risk of AD than male *APOE*  $\epsilon 4$  carriers (Farrer et al., 1997; Payami et al., 1994, 1996). Conversion to MCI and AD is also highest among female  $\epsilon 4$  carriers (Altmann et al., 2014). Similarly, faster rates of memory decline have been reported in female versus male  $\epsilon 4$  carriers (Wang et al., 2019). Although the

precise mechanism underpinning this increased susceptibility to AD remains to be resolved (Gamache et al., 2020), it is notable that higher levels of AD pathology, including A $\beta$  (Corder et al., 2004) but especially pathological tau (Babapour Mofrad et al., 2020; Buckley et al., 2019; Hohman et al., 2018; Wang et al., 2021), are evident in female *APOE*  $\epsilon$ 4 carriers. It is clear, as a result, that there is good reason to focus specifically on female participants.

## 2.2. Methods

### 2.2.1. Participants

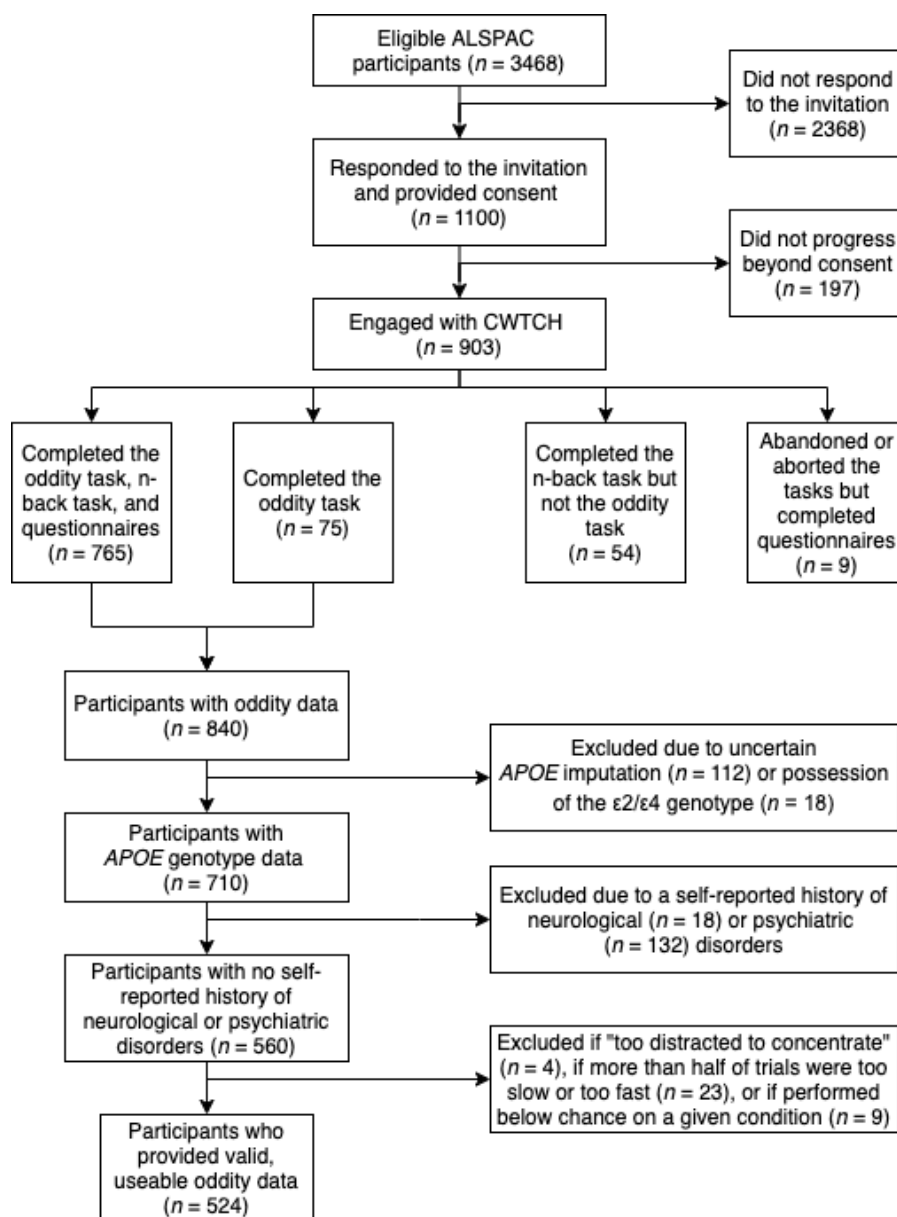
Participants were identified and recruited through ALSPAC (<http://www.bristol.ac.uk/alspac/>). ALSPAC is a prospective birth cohort study that initially recruited pregnant females residing in the historic county of Avon (South West England), with an expected due date between April 1991 and December 1992. After exclusions were applied, the initial sample included 13,761 participants. Additional participants who were eligible at the outset but did not enroll were recruited when the oldest children were approximately seven years of age. All ALSPAC participants have since been followed up at regular intervals via postal questionnaires and clinical assessments (for more information, see Boyd et al., 2012, 2019; Fraser et al., 2013). Note also that the ALSPAC website contains details of all the data that is available through a fully searchable data dictionary and variable search tool (<http://www.bristol.ac.uk/alspac/researchers/our-data/>).

Inclusion criteria for the current study were: the availability of genome-wide genetic data and an active involvement in ALSPAC including attendance at one or more “Focus on Mothers” clinical assessment. Four such assessments have been completed to date, with the most recent taking place between April 2014 and March 2015. ALSPAC participants who met these criteria were subsequently invited to take part via email or letter, depending on the contact information available. Participants were asked to self-exclude prior to testing if they had a non-correctable visual impairment or if they

lacked access to a laptop/computer and the internet. Smartphones and tablets were not allowed, as the CWTCH platform was not optimised for their use at the time of test. The aim was to recruit the maximum sample size possible with the available resources, as opposed to a specific number of participants based on an a priori power calculation. In total, 1100 participants responded to the invitation and provided informed consent to participate. However, not all participants progressed beyond this stage, and of those who did, not all completed the cognitive tasks and questionnaires (for more on the procedure, see Section 2.2.2). For the purpose of this chapter, I focus specifically on participants who completed the odd-one-out task, had no prior self-reported history of neurological or psychiatric conditions, and passed further quality control procedures (described below). A detailed diagram capturing the flow of participants into the final analysis is provided in Figure 2.2. As shown, the final sample comprised 524 women aged between 46 and 70 years ( $M = 58.8$ ,  $SD = 4.2$ ). All participants received a £10 voucher in return for their involvement. Ethical approval for the study was obtained from the ALSPAC Ethics and Law Committee and the Cardiff University School of Psychology Research Ethics Committee.

Figure 2.2.

## Flowchart of Participant Engagement



*Note.* Approximately one third of those invited responded to the invitation (31.72%). Although not all progressed beyond consent, more than 900 participants engaged with the CWATCH platform in some way. In all, 840 participants provided data for the oddity task. Following further exclusions, described here in full, the final sample comprised 524 participants.

### 2.2.2. Procedure

In each letter or email invite, participants were provided with a link to the CWTCH research platform and a unique username and password. Once successfully logged-on, participants were presented with an information sheet outlining the rationale, aims, and requirements of the study. They were then presented with a checkbox consent form, which had to be completed in order for participants to progress further. After consenting, participants were tested on one of two tasks: an odd-one-out perceptual discrimination task (a.k.a. oddity task; Lee, Buckley et al., 2005) or a spatial n-back task (Lee & Rudebeck, 2010). The order of the two tasks was presented randomly to each participant (see also Section 6.1). It was not possible to move on to the second task until the participant had engaged with the first task. Note that this does not mean the participant necessarily completed the first task; for example, if they started the task but closed their browser or lost connection to the internet part way through, the task was instead listed as abandoned/aborted. Nonetheless, if participants engaged with both tasks, they were then presented with four short questionnaires, including one covering family history of dementia. Completion of all tasks and questionnaires took approximately 50-70 minutes. In this chapter, I focus specifically on the data from the odd-one-out task.

### 2.2.3. Odd-one-out perceptual discrimination task (Lee, Buckley et al., 2005)

Two versions of the odd-one-out task were conducted – one in which three stimuli were presented (i.e. three-choice oddity), and one in which four stimuli were presented (i.e. four-choice oddity). In both versions of the task, one of the stimuli was perceptually similar to but distinct from the other stimuli (i.e. the odd-one-out). There were two conditions in each version of the task – one containing different-view scenes and one containing different-view faces. To ensure that performance did not vary according to presentation order, task version (three-choice, four-choice) and condition (different-view scene, different-view face) were counterbalanced across participants (Figure 2.3). This gave four different counterbalancing versions,

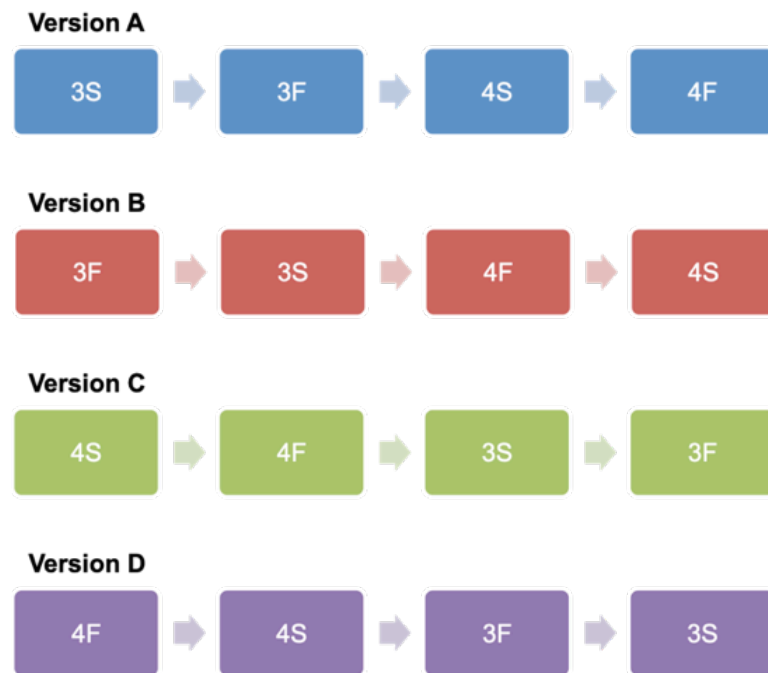
referred to here as versions A, B, C, and D. Of the 524 participants included in this chapter, the number in each counterbalancing version was as follows: A ( $n = 114$ ), B ( $n = 145$ ), C ( $n = 135$ ), and D ( $n = 130$ ). A chi-square goodness of fit test revealed that this distribution did not differ relative to that expected by chance ( $\chi^2(3, N = 524) = 3.83, p = .28$ ). Throughout this chapter, I focus exclusively on data from the four-choice oddity. I do so as exploratory analysis indicated that ceiling effects were present in the three-choice oddity (Figure 2.4), limiting its value for research seeking to examine how *APOE* genotype and age impact performance. The presence of ceiling effects in the three-choice oddity does, however, provide evidence against the presence of sensory or low-level perceptual deficits that could explain differences in performance on the four-choice oddity (see also Erez et al., 2013).

In the four-choice version of the task, there were 2 practice trials (with feedback) and 40 experimental trials (without feedback) per condition. Participants were instructed to respond as quickly and as accurately as possible, while stimuli remained on-screen until a response was recorded. Trials were separated by an inter-trial interval of 2000ms. The stimuli used for these trials were taken from Lee, Buckley et al.'s (2005) different-view scene and different-view face oddity conditions (Figure 2.5; for examples of other studies using these stimuli, see Behrman et al., 2016; Erez et al., 2013). Each trial in the different-view scene condition involved four virtual reality scenes generated using a commercially available computer game (Deus Ex, Ion Storm L.P., Austin, TX) and a freeware software editor (Deus Ex Software Development Kit v1112f). Three of these stimuli were of the same scene from a different viewpoint, whereas one (i.e. the odd-one-out) was of a different scene. Each trial in the different-view face condition involved four unfamiliar male faces (Caucasian, aged 20-40 years, short hair, no facial hair or spectacles) presented in one of six viewpoints. Three of these stimuli were of the same face from a different viewpoint, whereas one (i.e. the odd-one-out) was of a different face.

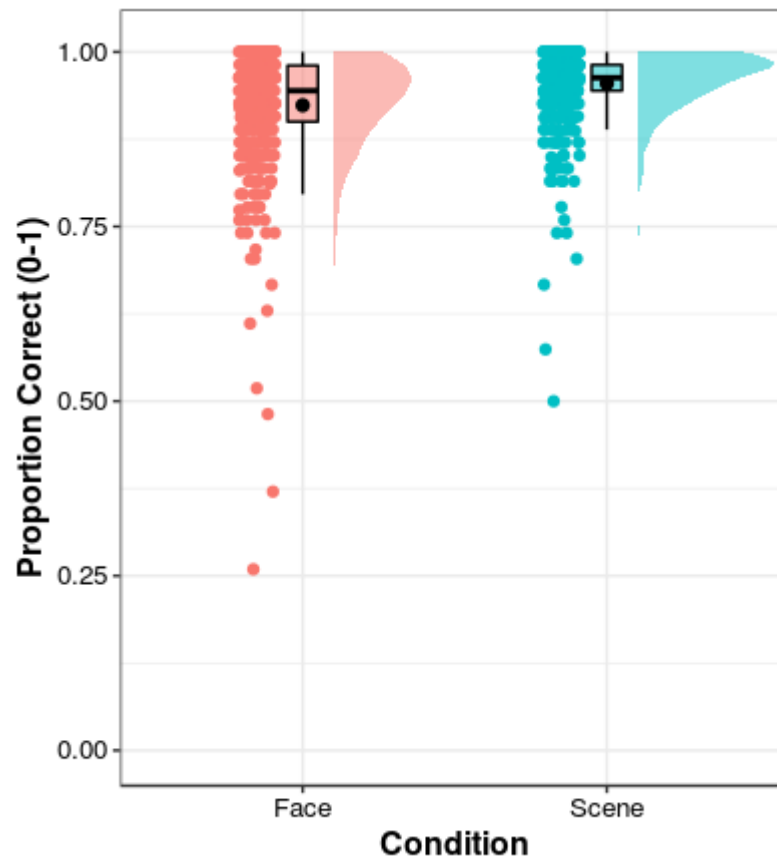


**Figure 2.3.**

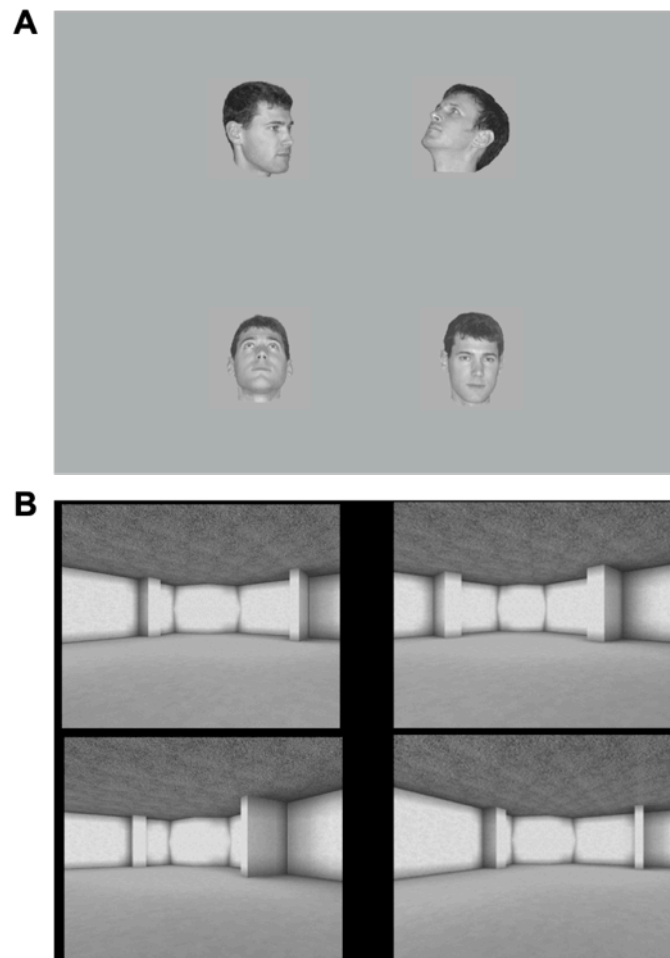
*Counterbalancing for the Odd-One-Out Perceptual Discrimination Task*



*Note.* Four different counterbalancing versions were used (A, B, C, and D), each with a different order of task version (three-choice, four-choice) and condition (different-view scene, different-view face). Participants were pseudo-randomly allocated to one of these four versions. Abbreviations: 3S = three-choice oddity, scene condition; 3F = three-choice oddity, face condition; 4S = four-choice oddity, scene condition; 4F = four-choice oddity, face condition.

**Figure 2.4.***Proportion Correct in the Three-Choice Oddity Task*

*Note.* Proportion correct (0-1) is shown for the different-view face and different-view scene condition in the three-choice oddity task. Individual data points, each representing a single participant, are shown alongside boxplots and density plots. A small amount of jitter has been added to each point for clarity. To facilitate interpretation, the mean value (black circle) and median value (a black line) for each group are both shown. Note that one participant performed below chance (~33%) in the different-view face condition. This participant was not removed from analysis here as they performed well on both conditions in the four-choice oddity task (four-choice face proportion correct = 0.85, four-choice scene proportion correct = 0.74), arguing against a sensory or low-level perceptual problem. Moreover, further inspection revealed that they belonged to counterbalancing version B, in which three-choice face oddity is the first condition (see Figure 2.3). This raises the possibility that the participant did not quite understand the task at first but came to understand it.

**Figure 2.5.***Four-Choice Oddity Task Stimuli*

*Note.* Example stimuli are shown for an individual four-choice oddity trial in the different-view face condition (A) and the different-view scene condition (B). Stimuli were taken from Lee, Buckley et al.'s (2005) study.

#### *2.2.4. Family history of dementia questionnaire*

A bespoke two-item questionnaire was used to establish whether a participant had a positive family history of dementia. Participants were asked whether one of their biological parents or siblings – first-degree relatives – had ever been diagnosed with any form of dementia. From this, it was possible to generate a binary score (yes/no), signifying whether each participant had a positive family history of dementia or not. This

questionnaire, including the information given to participants, is provided in the appendix (Section 6.2).

### 2.2.5. *APOE* genotype

*APOE* genotype was inferred from imputed (1000G phase 1, version 3) genome-wide genetic data provided by ALSPAC. To obtain “best-guess” genotypes from the imputed (i.e. probabilistic) data, a hard-call threshold of 0.8 was used. Genotypes below this threshold were considered missing, and the corresponding participants were removed from further analysis. Prior research has shown that inferring *APOE* genotype from imputed genome-wide genetic data, as done in this chapter (i.e. using similar hard-call thresholds), produces high levels of correspondence with directly measured *APOE* genotypes (Lupton et al., 2018; Oldmeadow et al., 2014; Radmanesh et al., 2014; Vuoksimaa et al., 2020). To check this formally, percentage correspondence was examined between best-guess genotypes and a subset of directly measured genotypes provided by ALSPAC. Results are provided in the appendix (Section 6.3). To generate three *APOE* genotype groups (*APOE*  $\epsilon$ 2 carriers, *APOE*  $\epsilon$ 3 carriers, and *APOE*  $\epsilon$ 4 carriers), participants with the  $\epsilon$ 2/ $\epsilon$ 4 genotype were removed from analysis (for a similar approach, see Lancaster, Forster et al., 2017). In later chapters, I adopt a different approach, instead including individuals with the  $\epsilon$ 2/ $\epsilon$ 4 genotype as part of *APOE*  $\epsilon$ 4 carrier groups. The reason for this discrepancy is that the current sample (but not those in subsequent chapters) provides a sufficient number of  $\epsilon$ 2 carriers in order to meaningfully analyse these individuals as a separate group. This offers an opportunity to examine the effects of AD risk enhancing and risk reducing *APOE* alleles, addressing a limitation in the literature (for a detailed discussion, see Suri et al., 2013). The genotypic distribution of the available sample was as follows: 76  $\epsilon$ 2 carriers (5  $\epsilon$ 2/ $\epsilon$ 2, 71  $\epsilon$ 2/ $\epsilon$ 3), 334  $\epsilon$ 3 carriers (334  $\epsilon$ 3/ $\epsilon$ 3), and 114  $\epsilon$ 4 carriers (107  $\epsilon$ 3/ $\epsilon$ 4, 7  $\epsilon$ 4/ $\epsilon$ 4).

### 2.2.6. Statistical analyses

All statistical analyses reported in this chapter were conducted using R (version 3.6.0; R Core Team, 2019) in RStudio (version 1.3.1093; RStudio Team, 2020). Differences in sample characteristics according to *APOE* genotype group were examined using chi-square tests of independence for categorical variables and robust one-way analysis of variance (ANOVA) tests for continuous variables. In the case of chi-square tests, Cramer's  $V$  was calculated as a measure of effect size, where relevant, using the *effectsize* package (version 0.4.4-1; Ben-Shachar et al., 2020). In the case of one-way ANOVAs, although  $F$  tests are commonly thought to be robust to violations of normality and homoscedasticity, it is increasingly recognised that this is not the case, especially when group sizes are unequal (Field & Wilcox, 2017; Mair & Wilcox, 2020). As such, robust one-way ANOVAs based on trimmed means (20% trimming level) were conducted using the *t1way* function from the *WRS2* package (version 1.1-1; Mair & Wilcox, 2020). A robust explanatory measure of effect size,  $\xi$ , is likewise reported (Wilcox & Tian, 2011). Values of  $\xi$  equal to 0.1, 0.3, and 0.5 roughly correspond to small, medium, and large effect sizes (Mair & Wilcox, 2020). Robust post-hoc tests on trimmed means were conducted using the *lincon* function, also from the *WRS2* package (Mair & Wilcox, 2020).

These analyses, described above, were carried out primarily to examine whether the three *APOE* genotype groups differed in terms of any characteristics that have previously been linked with cognitive decline, poorer brain health, and dementia (for relevant discussions and reviews, see Carroll & Turkheimer, 2018; Jaroudi et al., 2017; Tucker-Drob et al., 2019). Body mass index (BMI), for example, has been positively associated with dementia incidence (Ma et al., 2020). Other vascular factors such as smoking, hypertension, and diabetes – in addition to BMI – have been linked to lower grey matter volume in the hippocampus, as well as alterations in white matter microstructure affecting a variety of tracts (Cox et al., 2019). Variables relating to menopause have further been linked to cognition and dementia (Pertesi et al., 2019). Indeed, all of the variables included here are to some

extent considered risk factors for cognitive decline and dementia (Livingston et al., 2020; Yu et al., 2020). Given the current focus on *APOE* genotype differences, it is important to rule out – or at least identify – other ways in which these groups differ, especially in relation to characteristics that have themselves been linked to later life decline in cognitive function. Although such characteristics could serve as moderators, or even mediators, of *APOE* genotype effects, the current study does not have sufficient statistical power to detect interactions between four or more variables. As such, I simply report these for completeness.

Regarding the oddity task, although web-based cognitive testing provides a number of advantages over in-person cognitive testing (Huentelman et al., 2020), rigorous pre-processing is often needed to ensure that the data are of sufficient quality for analysis. Here, as a first step, responses were checked to determine whether any participant repeatedly clicked in the same location throughout. Given that the odd-one-out appeared in each of the four possible locations an equal number of times, participants adopting this strategy could achieve chance-level (25%) performance without truly engaging with the task. Reassuringly, the highest number of responses in the same location made by a single participant in either condition was 19 (47.5% of their face condition trials; proportion correct = 0.625 [62.5%]). As such, no participants were excluded on this basis. Next, trials associated with response times (RTs) below 300ms or above 30s were removed. While this lower limit is broadly consistent with prior work using web-based cognitive tasks (e.g. Güsten et al., 2021), the upper limit is quite liberal. Despite this, the lower limit led to the removal of just two trials (> 0.01% of all trials collapsed across participants and conditions), whereas the upper limit led to the removal of 3188 trials (7.6% of all trials collapsed across participants and conditions). A figure showing the distribution of all trial RTs associated with either condition – collapsed across participants – is provided in the appendix (Section 6.4). To minimise the impact of participants who provided a large number of fast and/or slow trials, additional exclusions were applied. More specifically, participants were removed entirely if more than half of their trials in a given condition were removed for being below 300ms or above 30s. Thereafter,

accuracy (i.e. proportion correct) was examined across stimuli in each condition. This led to the identification of two trials – one in the different-view face condition, one in the different-view scene condition – that were associated with below chance accuracy across all participants (25%). Both trials were then removed from analysis, leaving a maximum number of 39 trials per participant, per condition. Finally, as the last pre-processing step, proportion correct was calculated for each participant in each condition. Participants who recorded a score below chance (25%) in either the different-view face or different-view scene oddity were subsequently removed from analysis.

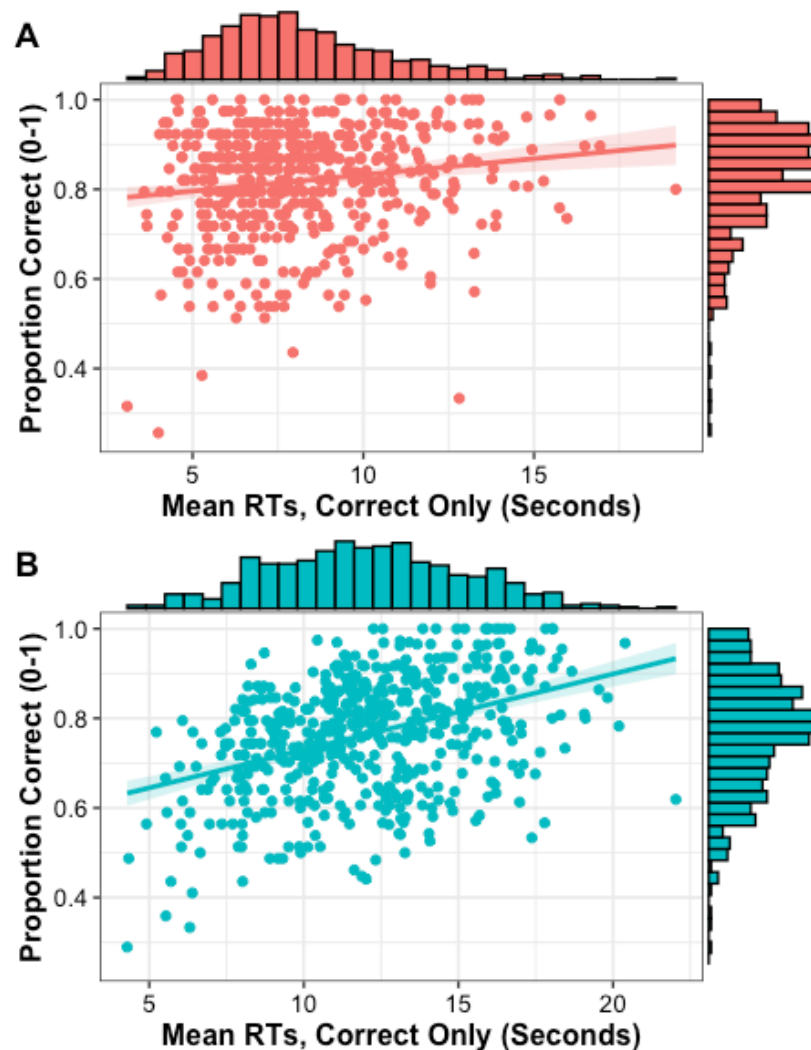
In line with prior studies using the oddity task (for examples, see Barense et al., 2007, 2010; Behrmann et al., 2016; Erez et al., 2013; Hodgetts et al., 2015, 2019; Hodgetts, Voets et al., 2017; Lee et al., 2008; Shine et al., 2015), performance was primarily assessed by proportion correct (0-1) and mean RTs for correct trials (seconds). To determine whether these two performance measures were related in a manner that might impact interpretation, an exploratory analysis was conducted. Figure 2.6 shows proportion correct as a function of mean RTs for correct trials. As is evident, there was a positive correlation between these two performance indicators in both the different-view face (Pearson's  $r(522) = 0.158$ ,  $p < .001$ ) and different-view scene (Pearson's  $r(522) = 0.404$ ,  $p < .001$ ) conditions, such that participants who were slower to respond on average were also more accurate on average. A Steiger z-test (Steiger, 1980) was conducted to statistically compare these correlations using the *cocor* package (version 1.1-3; Diedenhofen & Musch, 2015)<sup>1</sup>. This revealed that the relationship between proportion correct and mean correct RTs was stronger in the different-view scene condition than in the different-view face condition ( $z = -4.851$ ,  $p < .001$ ). As such, it appears that a speed-accuracy trade-off was evident (for a relevant review, see Heitz, 2014) and that this was stronger in the different-view scene condition.

---

<sup>1</sup> *cocor.dep.groups.nonoverlap*( $r.jk = 0.158$ ,  $r.hm = 0.404$ ,  $r.jh = 0.596$ ,  $r.jm = 0.263$ ,  $r.kh = 0.279$ ,  $n = 524$ , alternative = "two-sided")

**Figure 2.6.**

*Relationship Between Proportion Correct and Mean RTs (Correct Trials) in the Four-Choice Oddity Task*



*Note.* The relationship between the two primary performance measures – proportion correct (0-1) and mean RTs (correct trials only; seconds) – is shown for the different-view face condition (A) and different-view scene condition (B), respectively. Each point represents a single participant. The distribution of proportion correct scores and mean RTs are shown opposite the corresponding axis. Given that participants were removed from the current analysis if they performed below chance, the y-axis starts at 0.25. Abbreviations: RTs = response times.

Accounting for speed-accuracy trade-offs is far from straightforward. One approach is to use a combined measure of performance such as the inverse



efficiency score (IES; Townsend & Ashby, 1978; see also Townsend & Ashby, 1983). This measure has been implemented in prior research using the oddity task (for an example, see Berhmann et al., 2016). However, as noted by Bruyer and Brysbaert (2011), the IES does not have a simple relationship with RTs and it is unclear whether this measure appropriately weights speed and accuracy. It is also important to note that Townsend and Ashby (1983) actually recommended that the IES *not* be used when RTs and proportion correct (i.e. the inverse of proportion of errors) are positively correlated – that is, when a speed-accuracy trade-off is evident. Based on a series of simulation studies, Vandierendonck (2017, 2018, 2021) recently extended this recommendation to all combined speed-accuracy measures, arguing that “these integrated measures should not be used to neutralise or to circumvent SAT [speed-accuracy trade-off] effects” (Vandierendonck, 2021, p.23). Given the limited utility of these measures in situations akin to that observed here, as well as the desire to limit the number of statistical tests performed (Liesefeld & Janczyk, 2019), a combined measure was not included in the current chapter. When interpreting the results, however, it is important to consider the presence of this speed-accuracy trade-off.

To investigate how mean correct RTs and proportion correct varied according to condition, *APOE* genotype, and age, data were analysed using linear mixed-effects models. Mixed-effects models refer to a family of models that contain both fixed and random effects terms – hence the name “mixed” (for contemporary introductions to mixed-effects modelling in the context of psychological research, see Brown, 2021; DeBruine & Barr, 2021). Fixed effects represent effects that are expected to influence the dependent variable(s) – in this particular case, mean RTs for correct responses, proportion correct, and difference scores – in a predictable manner across different samples. The independent variables (a.k.a. explanatory variables) of interest are thus typically included as fixed variables. By contrast, random effects represent the degree to which fixed effects vary across levels of a grouping variable, such as participants. The inclusion of random effects makes it possible to explicitly model the way in which participants and other relevant variables – all of which are typically sampled from a larger

population – vary in their influence on these fixed (i.e. population-level) effects. An additional benefit of mixed-effects models – pertinent to the current chapter – is that they are able to deal with missing data and imbalanced designs (Baayen et al., 2008; see also Brown, 2021).

Here, linear mixed-effects models were fitted using the *lme4* package (version 1.1-26; Bates et al., 2015). Condition (different-view scene, different-view face), *APOE* genotype group (*APOE*  $\epsilon$ 2, *APOE*  $\epsilon$ 3, *APOE*  $\epsilon$ 4), and age were entered as fixed effects. Counterbalancing version (A, B, C, D) was also entered as a fixed effect albeit only to control for its potential influence on task performance. A random by-participant intercept was included to account for variance due to individual differences (for conceptually similar examples of linear mixed-effects model usage, see Gellersen, Trelle et al., 2021; Güsten et al., 2021; Liang et al., 2020; Lim et al., 2021; Son et al., 2021; Subramaniapillai et al., 2019). The fitted linear mixed-effects models thus took the following form:

$$\text{Dependent variable} \sim \text{condition} \times \text{APOE genotype group} \times \text{age} + \\ \text{counterbalancing version} + (1 \mid \text{participant})$$

Age – the only continuous independent variable – was centred and scaled (i.e. standardised). The categorical variables were coded using deviation coding. Consistent with current best practice guidance (Meteyard & Davies, 2020; see also Luke, 2017), statistical significance of the fixed effects was determined via Satterthwaite approximations as implemented by the *lmerTest* package (version 3.1-3; Kuznetsova et al., 2017). Results were deemed to be statistically significant if the *p*-value was smaller than, or equal to, the alpha ( $\alpha$ ) criterion of 0.05. Post-hoc comparisons on estimated marginal means were conducted using the *emmeans* package (version 1.5.4; Lenth, 2020). The Tukey method of *p*-value adjustment for multiple comparisons was employed where relevant.

To examine whether within-participant differences in mean correct RTs and accuracy between the different-view scene and face conditions varied

according to *APOE* genotype and age, difference scores were calculated (difference score = faces - scenes). For any given participant, a negative score indicates that the value for mean correct RTs/proportion correct was higher in the scene condition, whereas a positive score indicates that the value for mean correct RTs/proportion correct was higher in the face condition. Unlike the analysis discussed above, which examined performance between conditions across all participants, the focus on this analysis was the degree to which within-participant performance was better or worse across conditions. Such difference scores have been used in other studies in this research area (for relevant examples, see Berron et al., 2018; Gellersen, Trelle et al., 2021; Maass et al., 2019). Subsequently, these difference scores were analysed using robust multiple linear regression, which was conducted using the *lmrob* function from the *robustbase* package (version 0.93-7; Maechler et al., 2021; see also Chapter 3). This method fits a robust variant of the model – described below – based on an M-estimator (Koller & Stahel, 2011; Yohai, 1987) using iteratively re-weighted least squares estimation (for an example of its utility, see Field & Wilcox, 2017). The fitted model was as follows:

Difference scores  $\sim$  *APOE*  $\epsilon$ 4 carrier status x age + counterbalancing version

Difference scores were entered as dependent variables. *APOE*  $\epsilon$ 4 carrier status was coded using deviation coding. Age was centred and scaled. Counterbalancing version was again included as a covariate of no interest. As above, results were deemed statistically significant if the observed *p*-value was smaller than, or equal to, the nominal  $\alpha$  level of 0.05.

## 2.3. Results

### 2.3.1. Sample characteristics

As highlighted in Section 2.2.1, the final sample comprised 524 women aged between 46 and 70 years ( $M = 58.8$ ,  $SD = 4.2$ ). Table 2.1 provides an overview of the sample characteristics separated by *APOE*  $\epsilon$ 2,  $\epsilon$ 3, and  $\epsilon$ 4

genotype groups. Only three variables showed a significant group difference: age ( $F(2, 101.67) = 3.739, p = .027, \xi = 0.22, 95\% \text{ CI } [0.08, 0.39]$ ), total cholesterol levels ( $F(2, 104.86) = 11.512, p < .001, \xi = 0.36, 95\% \text{ CI } [0.20, 0.52]$ ), and low-density lipoprotein (LDL) levels ( $F(2, 100.63) = 12.169, p < .001, \xi = 0.36, 95\% \text{ CI } [0.21, 0.50]$ ). In terms of age, robust post-hoc tests revealed that the  $\epsilon 4$  group was significantly older – on average – than the  $\epsilon 2$  group ( $\Psi = -1.627, p = .041$ ) and the  $\epsilon 3$  group ( $\Psi = -1.307, p = .04$ ). The  $\epsilon 2$  and  $\epsilon 3$  groups did not significantly differ in terms of age ( $\Psi = 0.32, p = .579$ ). An overview of the age distribution separated by *APOE* genotype group is shown in Figure 2.7. In terms of total cholesterol, robust post-hoc tests revealed that the  $\epsilon 2$  group had significantly lower levels than the  $\epsilon 3$  group ( $\Psi = 0.486, p < .001$ ), and the  $\epsilon 4$  group ( $\Psi = -0.578, p < .001$ ). By contrast, no significant difference was observed between the  $\epsilon 3$  and  $\epsilon 4$  groups ( $\Psi = -0.092, p = .338$ ). A similar pattern was evident in terms of LDL levels, such that robust post-hoc tests revealed that the  $\epsilon 2$  group had significantly lower levels than the  $\epsilon 3$  group ( $\Psi = 0.431, p < .001$ ), and the  $\epsilon 4$  group ( $\Psi = -0.533, p < .001$ ). Again, no significant difference between the  $\epsilon 3$  and  $\epsilon 4$  groups was identified ( $\Psi = -0.102, p = .237$ ). The lower levels of total cholesterol and LDL cholesterol in the *APOE*  $\epsilon 2$  group is consistent with recent large-scale analyses ( $N > 300,000$ ) of UK Biobank data (Kuo et al., 2020; Lumsden et al., 2020), which are in turn consistent with *APOE*'s well-documented role in cholesterol metabolism (for a review, see Mahley, 2016). These findings provide further reassurance that the method used to infer *APOE* genotype from genome-wide genetic data – described in Section 2.2.4 – was sufficiently accurate. Adding to this, although the effect of *APOE* genotype on family history of dementia was not statistically significant, it is noteworthy that the trend followed the pattern one would expect based on AD risk ( $\epsilon 2 < \epsilon 3 < \epsilon 4$ ).

**Table 2.1.***Sample Characteristics Separated by APOE Genotype Group*

	<i>APOE Genotype Group</i>		
	<i>APOE ε2</i>	<i>APOE ε3</i>	<i>APOE ε4</i>
<i>Demographics</i>			
<b>Age (years)*</b>	<b>58.4 (3.9)</b>	<b>58.6 (4.2)</b>	<b>59.9 (4.3)</b>
Education level <sup>a</sup>			
No qualifications	4.05%	3.45%	0%
Vocational qualification	5.41%	5.02%	1.80%
O-level or equivalent	37.84%	31.97%	34.23%
A-level or equivalent	31.08%	30.41%	30.63%
Teaching/nursing qualification or university degree	21.62%	29.15%	33.33%
BMI <sup>b</sup>	27.4 (5.8)	26.2 (5.0)	25.9 (5.1)
Systolic blood pressure (mmHg) <sup>b</sup>	120 (13.2)	120 (14.4)	120 (14.4)
Diastolic blood pressure (mmHg) <sup>b</sup>	69.6 (9.15)	70.5 (8.77)	70.5 (9.39)
Current smoker (%yes) <sup>c</sup>	8.82%	5.65%	4.90%
Diabetic (%yes) <sup>d</sup>	1.33%	1.55%	2.70%
Menopause (%yes) <sup>b</sup>	38.67%	34.58%	46.85%
Cholesterol (mmol/l) <sup>b</sup>			
<b>Total***</b>	<b>4.93 (0.88)</b>	<b>5.40 (0.88)</b>	<b>5.47 (0.86)</b>
HDL	1.59 (0.31)	1.60 (0.42)	1.55 (0.34)
<b>LDL***</b>	<b>2.92 (0.82)</b>	<b>3.34 (0.76)</b>	<b>3.44 (0.73)</b>
C-reactive protein (mmol/l) <sup>b</sup>	2.59 (3.91)	2.0 (3.28)	1.70 (2.15)
<i>Questionnaires</i>			
Family history of dementia (%yes) <sup>e</sup>	18.06%	24.27%	27.1%
<i>Cognitive Tasks</i>			
WMS Logical memory <sup>f</sup>			
Immediate recall score	16.2 (3.21)	15.9 (3.28)	15.7 (3.57)
Delayed recall score	15.2 (3.62)	14.9 (3.56)	14.7 (4.03)
WAIS-III digit span backward score <sup>f</sup>	7.53 (2.10)	7.42 (2.56)	7.24 (2.34)
WAIS-III digit symbol coding score <sup>f</sup>	83.4 (12.1)	83.2 (14.3)	83.7 (13.3)
Spot-the-word score <sup>f</sup>	45.0 (7.64)	45.7 (7.17)	45.5 (6.18)
CFL verbal fluency score <sup>f</sup>	44.4 (13.0)	45.0 (12.4)	46.7 (11.1)

*Note.* Values represent the mean and standard deviation (in parentheses) or percentage (%) of participants. Age (years) was the only variable for which

all participants provided data. All other variables were associated with varying degrees of missingness (mean = 8.94%, range = 3.05%-40.08%), and the values reported here were calculated without these missing values. Moreover, of the variables reported in the table, only age and family history of dementia were collected at the time of test (year administered = 2020). Abbreviations: BMI = body mass index, HDL = high-density lipoprotein, LDL = low-density lipoprotein, WMS = Wechsler Memory Scale (Wechsler, 1998), WAIS-III = Wechsler Adult Intelligence Scale III (Wechsler, 1997).

<sup>a</sup> The highest level of educational qualification obtained by each participant was self-reported at 32 weeks gestation (approx. year administered = 1992). No questions were asked about qualifications higher than undergraduate degree or equivalent (e.g. master's degree, PhD/MD, etc.). It is possible that some participants have since obtained further qualifications, although more recent data relating to this have much higher amounts of missingness. For a recent example of a study using this measure of educational attainment, see Stergiakouli et al. (2017).

<sup>b</sup> Values for these variables were obtained from the most recent Focus on Mothers (FOM) clinic available, representing the most up-to-date information for each participant (clinic dates: FOM1 = December 2008-July 2011; FOM2 = July 2011-June 2013; FOM3 = March 2013-March 2014; FOM4 = April 2014-May 2015). Given that even the most recent clinic was 5 years prior to this study, however, these values may not reflect the participant's current status. This might explain why, for example, the percentage of participants who are going through or have been through menopause is lower than might be anticipated given the mean age of the groups at the time of test.

<sup>c</sup> Participants were asked if they currently smoke via questionnaire (approx. year administered = 2010). It is possible that some participants have since quit, or that participants have subsequently taken up smoking.

<sup>d</sup> Values for this variable were obtained by examining responses across multiple questionnaires (approx. years administered = 1992, 1999, 2002, 2010) and coding any prior "yes" response as indicating that the participant has diabetes. As with other variables, it remains possible that these values have changed in recent years.

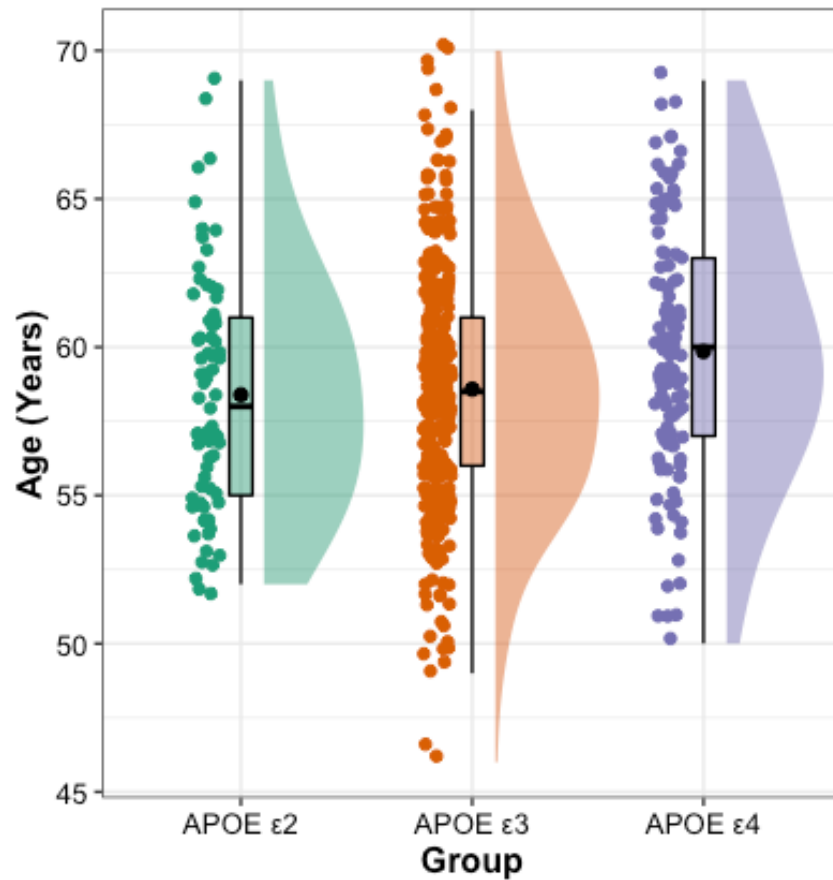
<sup>e</sup> Values for the questionnaires were obtained via the CWTCH online research platform. The family history of dementia questionnaire simply required participants to indicate whether one of their biological parents or siblings – first-degree relatives – had ever been diagnosed with any form of dementia. From this, a binary score (yes/no) was generated.

<sup>f</sup> Values for these variables were obtained from the first FOM clinic available, preventing practice effects from influencing the results.

\*  $p < .05$ , \*\*  $p < .01$ , \*\*\*  $p < .001$  (highlighted in bold, described in text).

**Figure 2.7.**

*Age Distribution of the Sample Separated by APOE Genotype Group*



*Note.* Participant ages are shown for each of the three *APOE* genotype groups (*APOE* ε2, *APOE* ε3, *APOE* ε4). Individual data points, each representing a single participant, are shown alongside boxplots and density plots. A small amount of jitter has been added to each point for clarity. To facilitate interpretation, the mean value (black circle) and median value (a black line) for each group are both shown.

### 2.3.2. Four-choice odd-one-out perceptual discrimination performance

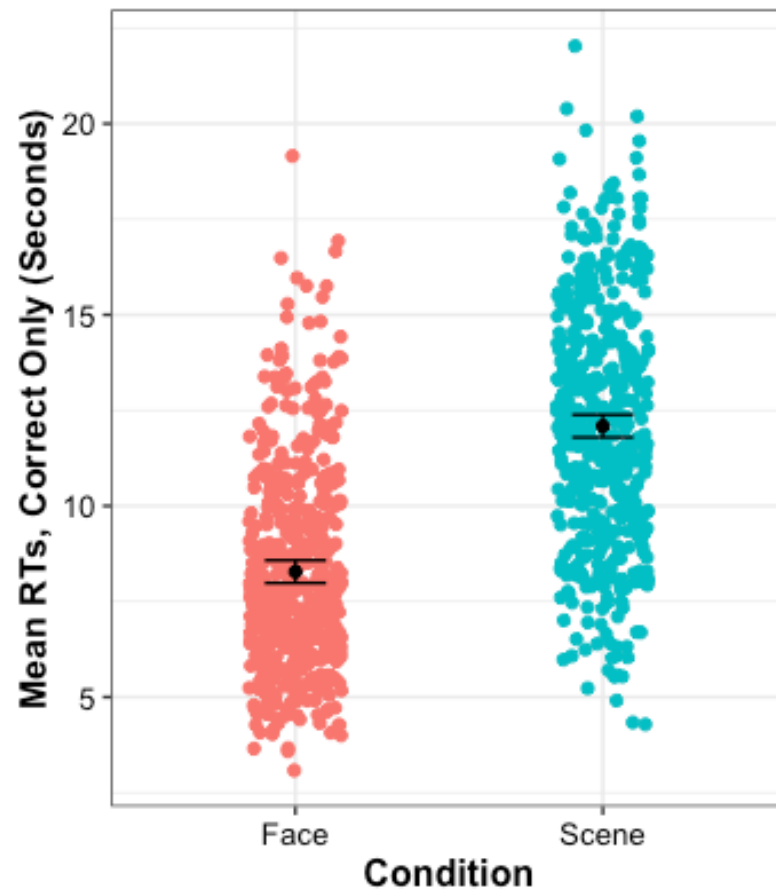
#### 2.3.2.1. Mean correct RTs

Starting with mean RTs for correct trials, there was a significant main effect of condition ( $F(1, 518) = 737.337, p < .001$ ). This was driven by quicker mean RTs for correct trials in the different-view face condition (estimated marginal  $M = 8.28$ s) than the different-view scene condition (estimated marginal  $M = 12.09$ s). An overview is provided in Figure 2.8. There was also a significant main effect of age ( $F(1, 515) = 18.065, p < .001$ ) on mean RTs for correct trials, such that older participants were slower on average than younger participants (Figure 2.9). Notably, there was no significant main effect of *APOE* genotype group ( $F(2, 515) = 0.869, p = .42$ ). In addition, there was no significant two-way interaction between condition and *APOE* genotype group ( $F(2, 518) = 0.059, p = .942$ ), condition and age ( $F(1, 518) = 0.002, p = .961$ ), and *APOE* genotype group and age ( $F(2, 515) = .889, p = .412$ ). No significant three-way interaction was observed either ( $F(2, 518) = .761, p = .468$ ). Taken together, these results indicate that while older participants were slower than younger participants on average, participants were also generally faster in the different-view face oddity condition than the different-view scene oddity condition.



**Figure 2.8.**

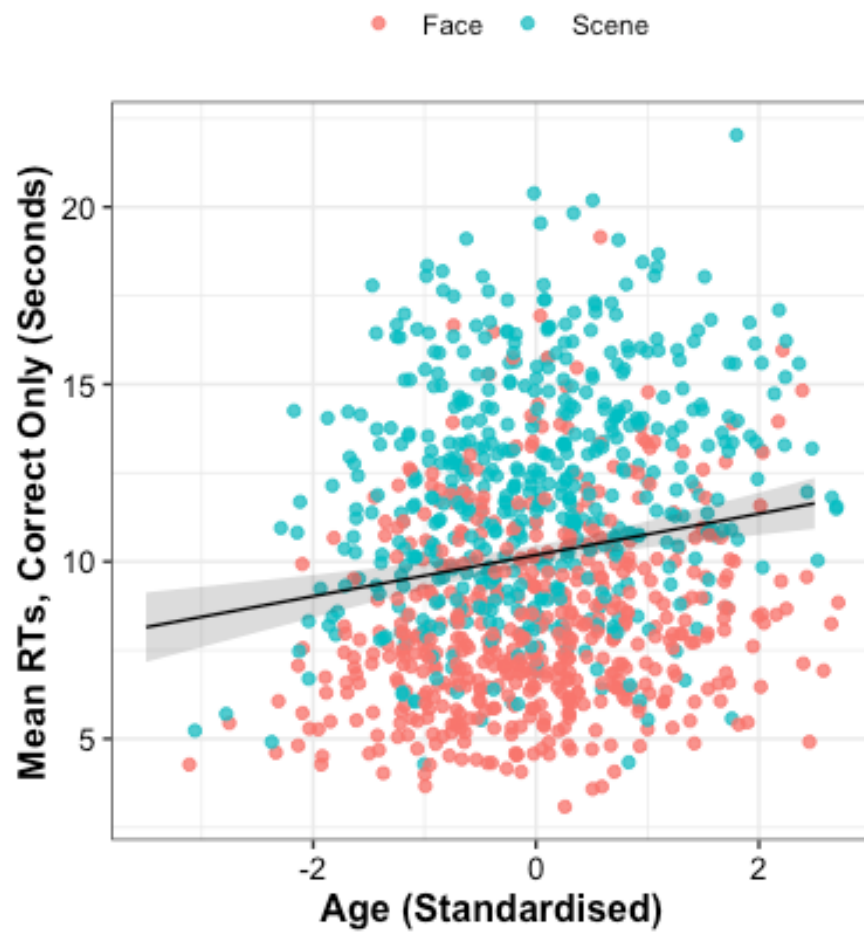
*Main Effect of Condition on Mean Correct RTs in the Four-Choice Oddity Task*



*Note.* Estimated marginal means and their corresponding error bars (95% confidence interval) are shown for mean correct RTs in the different-view face and scene conditions, respectively. Individual data points represent each participant's mean correct RT. A small amount of jitter has been added to each point for clarity. Abbreviations: RTs = response times.

**Figure 2.9.**

*Main Effect of Age on Mean Correct RTs in the Four-Choice Oddity Task*



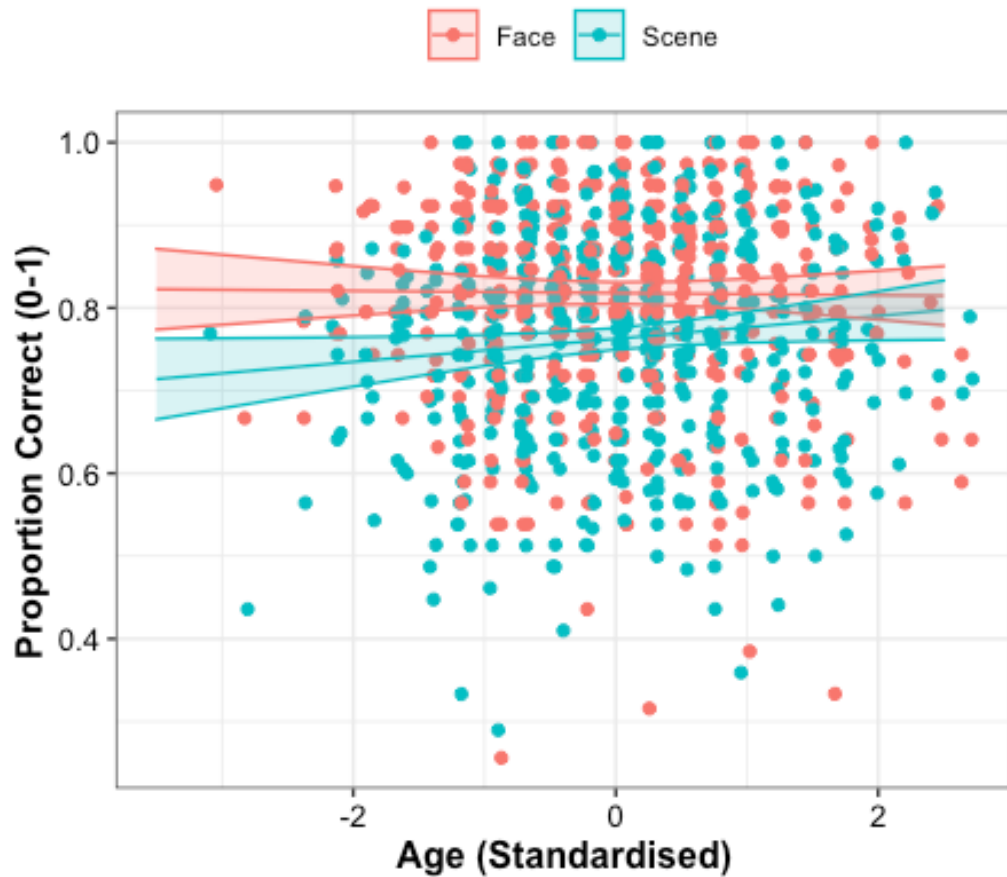
*Note.* The fitted line and 95% confidence interval is based on predicted values from the linear mixed-effects model. Individual data points represent each participant's mean correct RT in the different-view face condition and the different-view scene condition. As such, two data points are evident for each participant in the current sample. A small amount of jitter has been added to each point for clarity. Abbreviations: RTs = response times.

### 2.3.2.2. Proportion correct

Turning to proportion correct, there was a significant main effect of condition ( $F(1, 515) = .53.963, p < .001$ ) but not *APOE* genotype group ( $F(2, 515) = 2.866, p = .058$ ) or age ( $F(1, 515) = 1.255, p = .263$ ). This was driven by higher proportion correct in the different-view face condition (estimated marginal  $M = 0.82$ ) than the different-view scene condition (estimated marginal  $M = 0.76$ ). However, caution is required when interpreting this main effect, as a marginally significant two-way interaction was observed between condition and age ( $F(1, 518) = 3.871, p = .05$ ). Post-hoc comparisons revealed that there was a marginally significant difference in the slope of the age trend between the different-view face and scene condition ( $t(518) = -1.968, p = .05$ ), such that the former was characterised by a relative flat trend and the latter was characterised by a positive trend (Figure 2.10). This finding suggests that older participants (relative to younger participants) tended to be more accurate on the different-view scene condition but that accuracy was relative consistent irrespective of age on the different-view face condition. Beyond this, there was also a significant interaction between *APOE* genotype group and age ( $F(2, 515) = 4.366, p = .013$ ). Post-hoc comparisons (corrected for multiple comparisons) revealed a significant difference in the slope of the age trend between *APOE*  $\epsilon 2$  carriers and *APOE*  $\epsilon 4$  carriers ( $t(515) = 2.947, p = .009$ ). No significant difference was observed between  $\epsilon 2$  and  $\epsilon 3$  carriers ( $t(515) = -1.996, p = .114$ ) or between  $\epsilon 3$  and  $\epsilon 4$  carriers ( $t(515) = 1.706, p = .204$ ). Figure 2.11 provides an overview of this interaction, highlighting how the  $\epsilon 2$  group were more accurate with advancing age whereas the  $\epsilon 4$  group were less accurate with advancing age. This finding indicates that individuals in possession of the  $\epsilon 2$  and  $\epsilon 4$  alleles exhibited different age-related trends in accuracy on the odd-one-out perceptual discrimination task across conditions. For completeness, it should be noted that the two-way interaction between condition and *APOE* genotype group was not statistically significant ( $F(2, 518) = 1.239, p = .291$ ), nor was the three-way interaction between these variables and age ( $F(2, 518) = 0.072, p = .931$ ).

**Figure 2.10.**

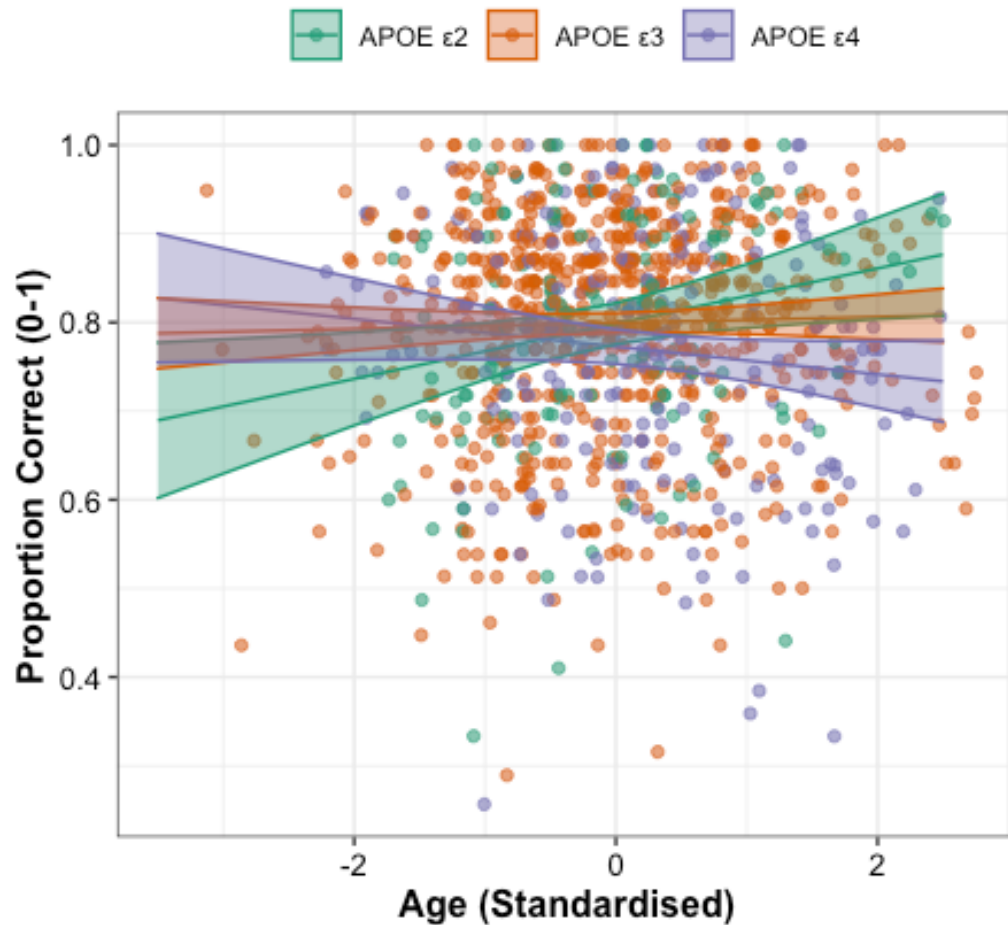
*Interaction Between Condition and Age on Proportion Correct in the Four-Choice Oddity Task*



*Note.* The fitted lines and 95% confidence intervals are based on predicted values from the linear mixed-effects model. Individual data points represent proportion correct for each participant in the different-view face condition and the different-view scene condition. As such, two data points are evident for each participant in the current sample. A small amount of jitter has been added to each point for clarity.

**Figure 2.11.**

*Interaction Between APOE genotype and Age on Proportion Correct in the Four-Choice Oddity Task Independent of Condition*



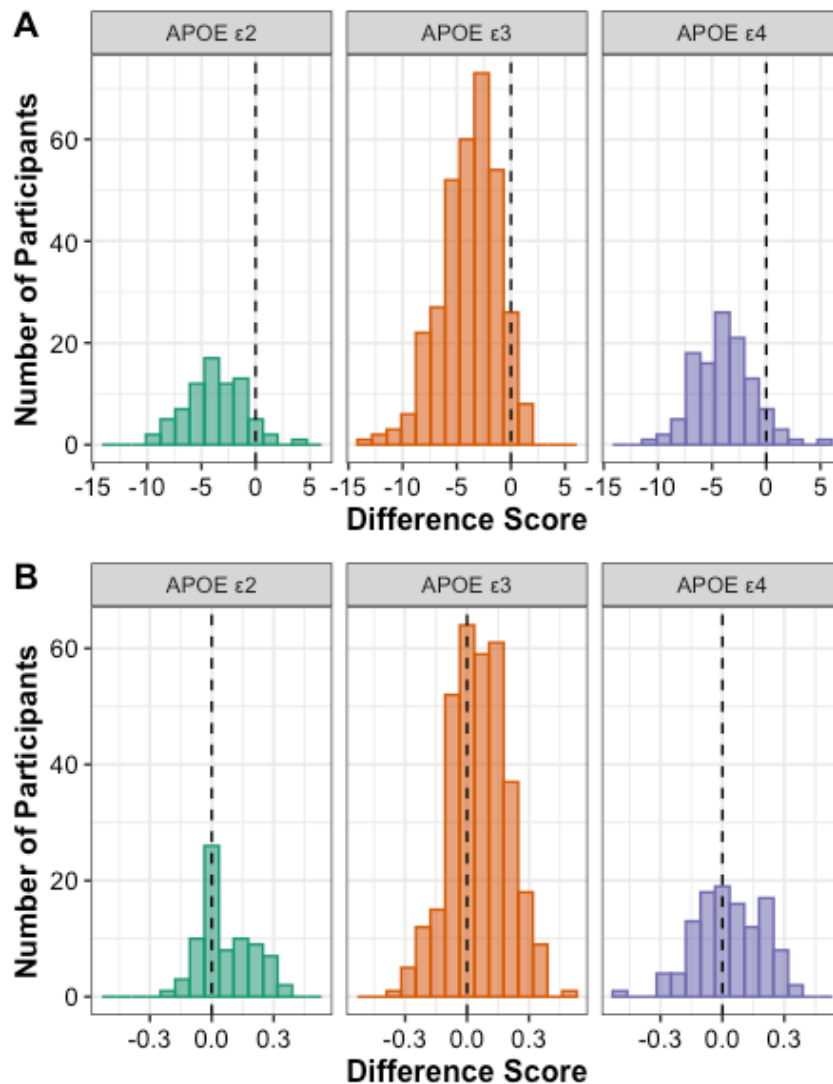
*Note.* The fitted lines and 95% confidence intervals are based on predicted values from the linear mixed-effects model. Individual data points represent proportion correct for each participant as a function of age. A small amount of jitter has been added to each point for clarity.

### 2.3.2.3. Difference scores

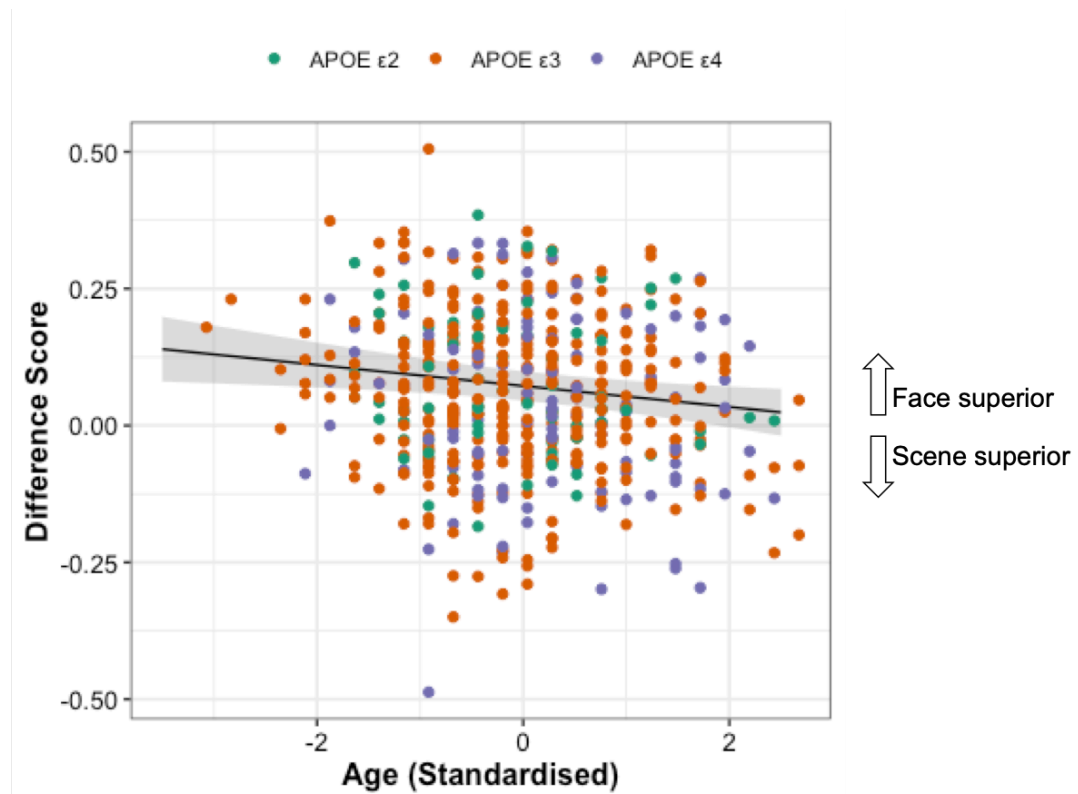
As a final step, difference scores for mean correct RTs and proportion correct were analysed. An overview of these differences scores – separated by *APOE* genotype group – is shown in Figure 2.12. For correct RT difference scores, no significant associations were observed for *APOE* genotype, age, or their interaction (all  $p$ s > .123). This therefore suggests that the within-participant difference in mean correct RTs between conditions, which generally involved slower responses in the scene condition, did not vary as a function of *APOE* genotype or age. For proportion correct difference scores, a significant association was observed for age ( $b = -0.019$ ,  $p = .009$ ). This association is shown in Figure 2.13. All other associations were not significant (all  $p$ s > .324). This result indicates that the within-participant difference in proportion correct between conditions – that is, the superior accuracy in the different-view face versus different-view scene condition – was lower in older adults, becoming almost non-existent. Given the results reported in Section 2.3.2.2, this seemed to be driven by higher accuracy in the different-view scene condition among older participants, rather than lower accuracy in the different-view face condition among older participants.

**Figure 2.12.**

*Distribution of Difference Scores for Mean Correct RTs and Proportion Correct as a Function of APOE Genotype*



*Note.* The distribution of difference scores for mean correct RTs (A) and proportion correct (B) as a function of APOE genotype group are shown. The dashed line identifies the value for 0 (i.e. no difference). Negative difference scores indicate that values for mean correct RTs/proportion correct were higher in the scene condition, whereas positive difference scores indicate that values for mean correct RTs/proportion correct was higher in the face condition.

**Figure 2.13.***Association Between Age and Proportion Correct Difference Scores*

*Note.* The fitted line and 95% confidence interval is based on predicted values from the robust multiple linear regression model. Individual data points represent difference scores for each participant as a function of age. A small amount of jitter has been added to each point for clarity. As shown by the arrows on the right of the figure, negative difference scores indicate that values for proportion correct were higher in the scene condition, whereas positive difference scores indicate that values for proportion correct was higher in the face condition.



## 2.4. Discussion

Several studies – discussed in Section 2.1 – indicate that *APOE*  $\epsilon 4$  impacts allocentric navigation/scene-based processing, which is proposed to depend on the extended hippocampal navigation network (Murray et al., 2017). However, it is currently challenging to reconcile these findings with numerous reports suggesting that age and AD risk, as defined by MCI or a positive family history of AD, preferentially impact complex object discrimination. This is especially true as complex object (including face) discrimination is proposed to depend on the ventral component of the feature network (Murray et al., 2017). Adding to this, there is a relative dearth of information about the impact of the *APOE*  $\epsilon 2$  allele – the so-called “forgotten *APOE* allele” (Suri et al., 2013, p.2879) – on scene and object discrimination, especially in mid-life. In this chapter, therefore, the primary aim was to examine the impact of *APOE* genotype ( $\epsilon 2$ ,  $\epsilon 3$ ,  $\epsilon 4$ ) and age on different-view scene and face odd-one-out perceptual discrimination in a sample of middle-aged and older female participants. The exclusive focus on female participants was driven in part by their availability, as part of ALSPAC, but also by previous studies that convincingly show that the link between *APOE*  $\epsilon 4$  and AD is stronger in females than in males (Gamache et al., 2020; Riedel et al., 2016; Ungar et al., 2014). A web-based version of the four-choice oddity task was utilised as part of the CWTCH research platform, facilitating the recruitment of a final sample incorporating 524 participants. In this regard, the study reported in the current chapter represents a novel addition to the literature.

Young *APOE*  $\epsilon 4$  carriers have previously been shown to exhibit increased activation (i.e. hyper-activation) in the PCC – a core component of the extended hippocampal navigation network – during different-view scene but not different-view object or face oddity discrimination (Shine et al., 2015). Scene oddity-related activation in the PCC, as well as the hippocampus and PHC, has in turn been linked to the microstructural properties of the PHCB in young *APOE*  $\epsilon 4$  carriers relative to non-carriers (Hodgetts et al., 2019). As highlighted in Chapter 1 (see Section 1.1.2.1), the PHCB constitutes a critical white matter tract within the extended hippocampal navigation network.

These early alterations within this key network mirror the scene-specific deficits observed in early AD using the oddity task (Lee et al., 2006; see also Lee et al., 2007), potentially pointing to network vulnerability to AD-related pathology. Despite these findings, however, no comparable scene-specific effects were observed here. Specifically, there was no interaction between condition and *APOE* genotype for proportion correct or mean correct RTs, indicating that oddity performance in the  $\epsilon 2$ ,  $\epsilon 3$ , and  $\epsilon 4$  groups did not differ according to condition. In addition, the relationship between age and performance in the different-view face condition and in the different-view scene condition – regardless of the measure used (mean correct RTs, proportion correct) – did not differ between the three groups. There was also no association between *APOE* genotype and within-participant difference scores for either mean correct RTs or proportion correct. These findings, therefore, seemingly run counter to the notion that the  $\epsilon 4$  allele is linked with alterations in the extended hippocampal navigation network and, as a consequence, poorer scene oddity discrimination. It is important to note, however, that the effect of *APOE* genotype on proportion correct was near the threshold for significance ( $p = .058$ ) and, more importantly, that the relationship between age and proportion correct did vary significantly as a function of *APOE* genotype group independent of oddity condition. In particular, it was found that *APOE*  $\epsilon 4$  and  $\epsilon 2$  carriers exhibited opposite age trends, with the former demonstrating lower accuracy with advancing age and the latter demonstrating higher accuracy with advancing age. Neither group differed significantly relative to the *APOE*  $\epsilon 3$  carrier group.

Given that the extended hippocampal navigation and (ventral) feature networks are proposed to support scene and object (including face) perceptual discrimination (Murray et al., 2017), respectively, the interaction between *APOE* genotype and age prima facie suggests that possession of the  $\epsilon 4$  and  $\epsilon 2$  alleles differentially affect these two networks, at least in middle-aged and older females. Following on from this finding, a key question is *how* the *APOE*  $\epsilon 4$  and  $\epsilon 2$  alleles differentially affect these networks, thereby resulting in divergent age-related trends in accuracy on the oddity task. The underlying mechanism(s) behind the pattern of

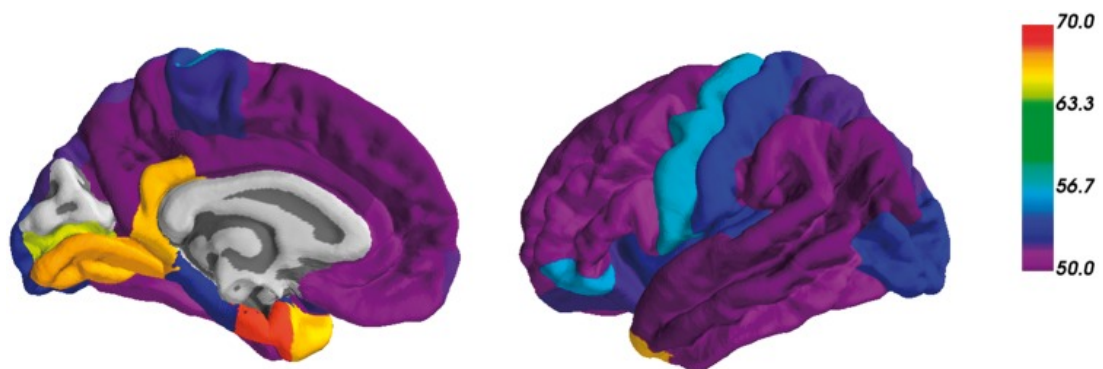
performance may differ and, as such, I consider potential reasons for each group's age trend in turn. It is important nonetheless to recognise that it was the difference between the two groups that was significant, rather than the within-group trends in and of themselves.

Differences in region-specific rates of A $\beta$  accumulation between *APOE*  $\epsilon$ 4 carriers and non-carriers offer one potential explanation for the lower levels of accuracy observed with advancing age in the  $\epsilon$ 4 group (relative to the  $\epsilon$ 2 group). Although the earliest sites of A $\beta$  accumulation are in regions comprising the extended hippocampal navigation network, such as the PCC, it remains the case that the deposition and accumulation of A $\beta$  increases over time (Jansen et al., 2015; Ossenkoppele et al., 2015; Roberts et al., 2018). Moreover, this increase is not uniform across the brain – that is, different brain regions demonstrate different rates of A $\beta$  accumulation (Grothe et al., 2017; Rodrigue et al., 2012; Villain et al., 2012). Of particular relevance here, differences in the region-specific rate of A $\beta$  accumulation also differ between *APOE*  $\epsilon$ 4 carriers and non-carriers (Mishra et al., 2018). As shown in Figure 2.14, these differences (i.e. increased A $\beta$  in  $\epsilon$ 4 carriers) first become apparent around age 50, but more region-specific differences are observed with advancing age. Given that the majority of participants in the current sample were aged between 55 and 65 years ( $n = 412$ , 78.63%), it is not only plausible that a proportion had A $\beta$  pathology, but that those with the  $\epsilon$ 4 allele (relative to those without) had higher rates of A $\beta$  in numerous brain regions, potentially including parts of the feature network (Figure 2.14). Adding to this, the  $\epsilon$ 4 group were also older on average than the  $\epsilon$ 2 and  $\epsilon$ 3 groups, increasing the likelihood that significant A $\beta$  pathology was present, including in regions beyond the extended hippocampal navigation network. The possible presence of A $\beta$  in both networks can thus explain why accuracy – measured as proportion correct – declined with advancing age in the  $\epsilon$ 4 group independent of condition. This explanation further raises the possibility that the selective effects of *APOE*  $\epsilon$ 4 on allocentric navigation and scene-based processing may be confined to earlier stages in the lifespan (Hodgetts et al., 2019; Kunz et al., 2015; Shine et al., 2015), where significant A $\beta$  burden is unlikely or at least more limited. It should be noted, however, that

studies in young adults have not always compared allocentric navigation/scene-based tasks against alternative tasks (e.g. Kunz et al., 2015), limiting our collective knowledge as to whether the *APOE*  $\epsilon 4$  allele's effect is selective to navigation/scene processing or whether it likewise impacts complex object (including face) processing (although see Shine et al., 2015) and other aspects of cognition.

**Figure 2.14.**

*Region-Specific Rates of A $\beta$  Accumulation Between APOE  $\epsilon 4$  Carriers and Non-Carriers*



*Note.* The age at which *APOE*  $\epsilon 4$  carriers and non-carriers exhibit different rates of A $\beta$  accumulation in a given region is shown. The colour bar identifies the age at which these differences become apparent, ranging from 50 years to 70 years. Reprinted from Mishra et al. (2018).

The above explanation focuses entirely on A $\beta$  but tau pathology may likewise have a role. In vivo tau PET studies suggest that some of the earliest accumulation of tau occurs in the PRC and anterolateral EC (Berron et al., 2021; Yushkevich et al., 2021). Both of these regions form part of the feature network that, as discussed, is proposed to have a role in representing object-level features (Murray et al., 2017). The age at which tau pathology typically becomes evident is not yet clear, but post-mortem data indicate that tau is relatively common in the so-called transentorhinal region by age 60 (Braak & Braak, 1997) and may even be present in early adulthood (Braak &

Del Tredici, 2011). Additionally, recent research indicates that higher levels of tau pathology are evident in female *APOE*  $\epsilon 4$  carriers relative to non-carriers (Babapour Mofrad et al., 2020; Buckley et al., 2019; Hohman et al., 2018; Wang et al., 2021). As such, it is plausible that older *APOE*  $\epsilon 4$  carriers in the current sample had higher levels of tau relative to non-carriers, especially in key regions within the feature network, potentially impacting performance on the task. Consistent with the notion that tau and  $A\beta$  pathology in both networks may have impacted performance here, one contemporary study of cognitively unimpaired adults reported that anterotemporal tau burden was associated with poorer object discrimination while posteromedial  $A\beta$  burden was associated with poorer scene discrimination (Maass et al., 2019). The precise neurobiological mechanism by which  $A\beta$  and tau in these regions may produce selective scene and object impairments is currently unclear. One potential explanation – derived from recent human research – is that  $A\beta$  and tau differentially impact synaptic and axonal function, the former occurring first (Pereira et al., 2021; for a commentary, see Jagust, 2021). Further research is necessary to explore this possibility and, more broadly, to bridge the gap between AD-related pathology and cognitive performance on tasks such as the oddity.

Beyond *APOE*  $\epsilon 4$ , the higher level of accuracy observed with advancing age in the  $\epsilon 2$  group merits discussion. As highlighted in Section 2.1, research on *APOE* has traditionally focused exclusively on the presence or absence of the  $\epsilon 4$  allele (Suri et al., 2013), in part due to the low prevalence of  $\epsilon 2$  in the wider population (O'Donoghue et al., 2018). It is for this reason that, despite having a protective role against AD (Chartier-Harlin et al., 1994; Corder et al., 1994; Farrer et al., 1997), little is known about the effects of this allele on the brain and cognition at various points in the lifespan, including mid-life (Salvato, 2015). In the study reported in the current chapter, it was observed that higher levels of accuracy – independent of condition – were associated with advancing age in the *APOE*  $\epsilon 2$  group, differing relative to the pattern in the *APOE*  $\epsilon 4$  group. This finding is somewhat consistent with the results from Sinclair et al. (2017), who observed that young/middle-aged  $\epsilon 2$  carriers outperformed  $\epsilon 3$  and  $\epsilon 4$  carriers on tasks measuring a number of domains,

including episodic memory (see also Zokaei et al., 2021). It is also in line with more general longevity effects associated with this allele (Sebastiani et al., 2019; Shinohara et al., 2020; Wolters et al., 2019).

Reduced levels of A $\beta$  accumulation may partially account for the age-related pattern of perceptual discrimination accuracy observed in the *APOE*  $\epsilon$ 2 group, which differed to that of the *APOE*  $\epsilon$ 4 group. Recent evidence indicates that the protection against AD conferred by this allele is a product of reduced A $\beta$  burden (Goldberg et al., 2020; Reiman et al., 2020; Salvadó et al., 2021). As the earliest A $\beta$  accumulation tends to occur in regions comprising the extended hippocampal navigation network (Oh et al., 2016; Mattsson et al., 2019; Palmqvist et al., 2017; Villeneuve et al., 2015), it is reasonable to speculate that  $\epsilon$ 2-related protection against A $\beta$  resulted in preserved scene perceptual discrimination performance with advancing age. In addition, if the presence of A $\beta$  potentiates the spread of tau beyond structures in the MTL (He et al., 2018; Hurtado et al., 2010; Pooler et al., 2015; Therneau et al., 2021), it might further be the case that parts of both network were relatively unaffected by tau pathology, as well as A $\beta$ , thereby explaining the lack of a condition-dependent effect of age. It is curious nonetheless as to why this group showed not just preserved levels of accuracy with age on the oddity task but *higher* levels of accuracy. One possibility is that performance in the  $\epsilon$ 2 carriers may have been biased by selective attrition. This phenomenon – selective attrition – refers to the tendency of some people, defined by particular characteristics, to drop out from longitudinal studies such as ALSPAC (Asendorpf et al., 2014). Previous research on longitudinal studies of cognitive ageing has shown that participants who drop out (versus those who do not) are more likely to perform poorly on cognitive tests at baseline (Matthews et al., 2004; Salthouse, 2014; Van Beijsterveldt et al., 2002). This is especially true of participants aged 50 or older (Salthouse, 2014). If this occurred in ALSPAC (for a discussion, see Fraser et al., 2013) and in the *APOE*  $\epsilon$ 2 group in particular, then it is possible that the higher age-related performance on the task is a by-product of the resulting bias. It is worth noting, however, that a recent analysis of participation in the UK Biobank study observed that *APOE*

$\epsilon 4$  homozygotes were less likely to complete optional questionnaires compared to *APOE*  $\epsilon 2$  homozygotes, rather than the reverse (Tyrrell et al., 2021). This therefore casts doubt on the selective attrition argument as it pertains to  $\epsilon 2$  carriers, but such an explanation cannot be ruled out based on the current data.

The current chapter also observed differences in performance across the four-choice oddity conditions independent of *APOE* genotype. In particular, higher levels of accuracy were observed with advancing age in the different-view scene condition, whereas accuracy in the different-view face condition was relatively consistent across the age span of the largely middle-aged participants. Examined using within-participant difference scores, it was found that the accuracy advantage for the different-view face condition over the different-view scene condition was lower in older adults, which is in line with what one would expect given the previously mentioned relationship between age and accuracy in the different-view scene condition. Put simply, the “face advantage” diminished with advancing age, but this was driven by higher age-related accuracy in the different-view scene condition rather than lower age-related accuracy in the different-view face condition.

Past studies – discussed in detail in Chapter 1 (see Section 1.2.3) and briefly mentioned here in Section 2.1 – have reported that older adults (versus younger adults) are differentially impaired on object discrimination relative scene/spatial location discrimination (Güsten et al., 2021; Reagh et al., 2016, 2018; Stark & Stark, 2017). These age-related deficits have in turn been linked to reduced functional activation in the PRC (Ryan et al., 2012; see also Berron et al., 2018) and anterolateral EC (Reagh et al., 2018), both of which form part of the feature network (Murray et al., 2017). Based on these findings, therefore, one might predict that age detrimentally impacts this network, affecting its corresponding object-level representations (Burke et al., 2018). This would be somewhat consistent with the diminished face advantage observed in older adults, but only if this was driven by poorer accuracy in the different-view face condition. As highlighted in this section, this is not what was observed in the current chapter. Instead, higher levels of

accuracy on the different-view scene oddity condition in older adults drove the reduction in the face advantage. Accuracy on the different-view face oddity condition, by contrast, was relatively consistent across the sample (i.e. independent of age). As such, the results observed do not necessarily align with those reported previously.

An alternative explanation for these results centres on the presence of a speed-accuracy trade-off in the data. Indeed, as shown in Figure 2.6, a speed-accuracy trade-off (i.e. a positive association between mean correct RTs and proportion correct) was evident in both conditions, although more so for the different-view scene condition. If older participants tended to opt for a strategy emphasizing accuracy at the expense of speed, as suggested previously (Dully et al., 2018; Hedge et al., 2018; Starns & Ratcliffe, 2010, 2012; for a brief discussion, see Heitz, 2014), then one would expect to see higher levels of accuracy and slower mean correct RTs with older age on the odd-one-out task. Consistent with this, the current chapter found higher levels of accuracy with advancing age in the different-view scene condition, mentioned already, as well as slower mean correct RTs with age independent of condition. Importantly, advancing age was not associated with higher levels of accuracy in the face condition. Viewed alongside the weaker trade-off in the different-view face condition (versus the different-view scene condition), this implies that while older participants emphasised accuracy at the expense of RTs across conditions, younger participants were able to attain comparable levels of accuracy at lower RTs in the different-view face condition but not the different-view scene condition. This seems to fit with the attenuated speed-accuracy trade-off observed in the different-view face condition. An intriguing question for future research is why exactly age-related slowing of RTs provided a greater accuracy benefit for the different-view scene condition relative to different-view face condition. Moreover, it would be interesting to conduct a follow-up study using a RT cut-off, as is common in neuroimaging studies using the oddity task (Barens et al., 2010; Costigan et al., 2019; Hodgetts et al., 2015, 2019; Hodgetts, Voets et al., 2017; Lee et al., 2008; Shine et al., 2015), to establish whether



the findings observed here would replicate if participants were actively prevented from placing a greater emphasis on accuracy than speed.

It should be noted that the study reported in the current chapter had a number of limitations. First and foremost, a cross-sectional design was used to investigate the effects of *APOE* genotype and age. Given that participants were born in different years or even decades, it is possible that they differed in characteristics (e.g. experience with technology; Olson et al., 2011) that are not necessarily related to age per se. That is, cohort effects may have been present (Hedden & Gabrieli, 2004; Ganguli, 2017; Grady, 2012), potentially affecting performance on the task. An additional limitation is the exclusive focus on female participants. Although there were good practical and theoretical motivations for this decision (see Section 2.1), including the higher rates of AD-related pathology in female *APOE*  $\epsilon 4$  carriers (Babapour Mofrad et al., 2020; Buckley et al., 2019; Corder et al., 2004; Hohman et al., 2018; Wang et al., 2021), it is unclear whether the results observed here generalise to males. This is important, as it may be the case that the interaction between *APOE* genotype and age in middle-aged and older adults is only evident in females, raising pressing questions about the underlying mechanism(s) (Gamache et al., 2020). I attempt to (partially) address this in Chapter 3 by including both males and females. The lack of information about A $\beta$  and tau in the current sample constitutes a further limitation, making it challenging to test the explanations offered for the observed findings. Prior research highlights the potential impact of A $\beta$  and tau on scene and object mnemonic discrimination (Maass et al., 2019), underscoring their relevance to the current chapter. Moving forward, future research on *APOE* genotype and age would greatly benefit from the inclusion of PET imaging where possible, helping to identify whether these effects are driven by underlying AD pathology (Jagust, 2013).

In addition to the above, the use of a web-based version of the four-choice oddity task warrants specific consideration. In the study reported here, the use of a web-based task made it possible to obtain data from a sample large enough to ensure that the analyses conducted were sufficiently powered to

detect more realistic effects, if such effects exist. This reduces the likelihood of committing a Type II error (Button et al., 2013). The ability to recruit larger samples is one of the many advantages of web-based cognitive testing (Huentelman et al., 2020). A concern regarding web-based testing pertains to the quality of the data (Vaughn et al., 2018; Woods et al., 2015). For example, the data collected for this chapter included a relatively large number of slow trials (see Section 2.2.6), which could indicate that participants failed to appropriately engage with the task. Following rigorous pre-processing, however, the data collected as part of this study was deemed to be of good quality, with participants showing high levels of task performance. Indeed, even mean correct RTs were found to be comparable with earlier laboratory studies using this task, especially when examining healthy older adults and when no time limit was present (for relevant examples, see Behrmann et al., 2016; Erez et al., 2013). This is in line with research suggesting that laboratory-based testing and web-based testing can produce data of equivalent quality (Germine et al., 2012), as well as recent applied research using web-based tasks (e.g. Güsten et al., 2021; Talboom et al., 2019). Despite this, a limitation of the current study is that the device used was not controlled for. There is some evidence to suggest that the type of device used can influence performance on cognitive tasks (Germine et al., 2019; Passell et al., 2021). It seems unlikely that this can account for results such as the interaction between *APOE* genotype and age, unless individuals in the  $\epsilon 2$ ,  $\epsilon 3$ , and  $\epsilon 4$  groups by chance happened to use different devices. Although unlikely, this possibility cannot be definitively excluded. The results reported here form part of a growing, promising literature on web-based tasks and applications, which may prove to be useful in the assessment of preclinical AD (Öhman et al., 2021).

## 2.5. Summary

In summary, this chapter demonstrated that *APOE* genotype and age impact odd-one-out perceptual discrimination in mid-life. Contrary to expectations based on prior research (e.g. Hodgetts et al., 2019; Shine et al., 2015), there were no scene-selective effects linked to the *APOE*  $\epsilon 4$  allele. There was also

no evidence of age-related impairment in face discrimination relative to scene discrimination, as one might expect based on recent studies (Güsten et al., 2021; Reagh et al., 2016, 2018; Stark & Stark, 2017). Instead, it was found that accuracy – measured as proportion correct – varied as a function of both *APOE* genotype group and age *independent of condition* (i.e. different-view scene, different-view face). To be more specific, it was observed that lower accuracy was linked with advancing age in *APOE*  $\epsilon 4$  carriers, whereas higher accuracy was linked with advancing age in *APOE*  $\epsilon 2$  carriers. This finding suggests that the extended hippocampal navigation and (ventral) feature networks may be impacted by *APOE* genotype and age, potentially via  $A\beta$ - and tau-related mechanisms. Independent of *APOE* genotype, there were further differences in performance on the four-choice oddity task. Higher levels of accuracy were observed with advancing age in the scene oddity condition, while accuracy in the face oddity condition was relative consistent across the age range of the studied participants. Within-participant difference scores supplemented this, showing that higher scene oddity accuracy with advancing age led to a diminished “face advantage” in performance. These results were largely attributed to the presence of a speed-accuracy trade-off in the data, which was stronger in the different-view scene than the different-view face condition.

In the next chapter, I use structural covariance analysis to examine whether *APOE*  $\epsilon 4$ , age, and sex impact the covariance patterns of the hippocampus and the PRC. These two structures are argued to represent key nodes within the extended hippocampal navigation network and feature network, respectively. Given that this method is thought to reflect aspects of connectivity (see Chapter 1, Box 1), the reported analysis provides insight into the impact of *APOE*  $\epsilon 4$  and age on key connections within these large-scale neurocognitive networks. The inclusion of males and females further builds on the work reported in the current chapter, as only females were studied. Based on the findings reported here, one might to observe reduced structural covariance in both networks with advancing age, particularly in  $\epsilon 4$  carriers relative to non-carriers. It might also be the case that this pattern is only evident in females, representing a sex by *APOE* interaction.

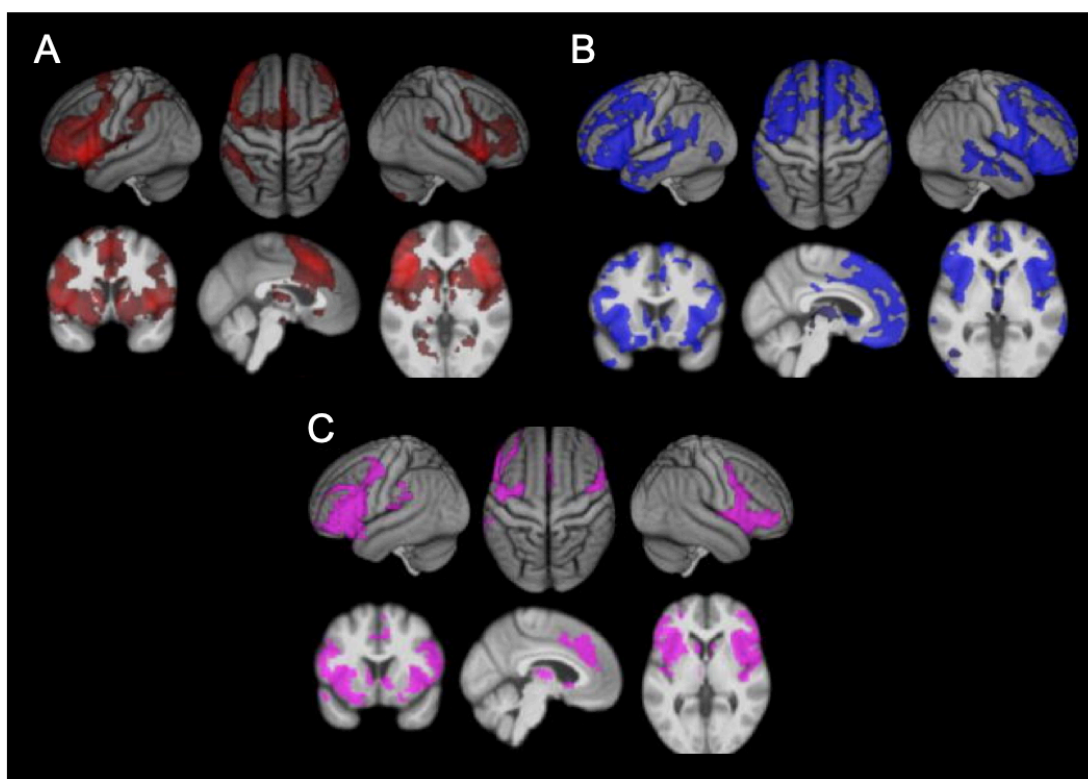
## **Chapter 3: Impact of *APOE* $\epsilon$ 4, gender/sex, and age on the structural covariance of the hippocampus and perirhinal cortex across the adult lifespan**

### **3.1. Introduction**

Chapter 2 investigated the impact of *APOE* genotype and age on different-view scene and face odd-one-out perceptual discrimination in a sample of middle-aged and older females. Contrary to prior research indicating that *APOE*  $\epsilon$ 4 preferentially impacts fMRI and behavioural markers of allocentric navigation and scene-based cognition (Bierbrauer et al., 2020; Hodgetts et al., 2019; Kunz et al., 2015; Shine et al., 2015), analysis revealed that this allele was not linked with poorer scene discrimination. Rather, an interaction between *APOE* genotype and age was observed independent of condition (i.e. different-view scenes, different-view faces), such that lower levels of accuracy were observed with advancing age in  $\epsilon$ 4 carriers whereas higher levels of accuracy were observed with advancing age in  $\epsilon$ 2 carriers. According to representational accounts of MTL function (Graham et al., 2010; Murray et al., 2017; Saksida & Bussey, 2010), the hippocampus and its wider network support complex conjunctive scene representations, whereas the PRC and its wider network support complex conjunctive object-level representations. As such, one might reasonably conclude that *APOE*  $\epsilon$ 4 and  $\epsilon$ 2 differentially affect these two networks, particularly in middle-aged and older females. In this chapter, I focus specifically on *APOE*  $\epsilon$ 4, with the aim of examining the patterns of whole-brain structural covariance associated with the hippocampus and PRC, and whether these patterns are modulated by this genetic risk factor and age.

Structural covariance – described previously (see Chapter 1, Box 1) – is an increasingly used analytical method that is applied to structural MRI data in order to examine co-variation between the morphological features of one brain region with the morphological features of other brain regions (for a review, see Alexander-Bloch, Giedd, & Bullmore, 2013). This analytical

method can be applied to various morphological features, the most common of which are grey matter volume, cortical thickness, and surface area. In this chapter, I focus on grey matter volume, in line with previous investigations (for relevant examples, see DuPre & Spreng, 2017; Spreng & Turner, 2013; Spreng et al., 2019; Nordin et al., 2018; Persson et al., 2014; Stening et al., 2017). By examining the similarity between regional morphology at the population-level, structural covariance analysis can be conceptualised as a method of studying connectivity (Betzal, 2020). Supporting this, a number of studies have reported a relatively large degree of overlap between patterns of structural covariance and fMRI-based functional connectivity (Figure 3.1; for relevant examples, see Clos et al., 2014; Guo et al., 2015; Kelly et al., 2012; Spreng et al., 2019). Overlap between patterns of structural covariance and diffusion MRI-based tractography has likewise been reported (Gong et al., 2012), although the overlap appears weaker than that for fMRI-based functional connectivity (Alexander-Bloch, Giedd, & Bullmore, 2013). There are several different approaches to identify patterns of structural covariance, but the one used here – the most common – is seed-based. Seed-based structural covariance analysis has been used to better understand how connections within and between large-scale networks are affected in variety of psychiatric, neurodevelopmental, and neurological conditions, including AD (Li et al., 2019; Montembeault et al., 2016), stroke (Veldsman et al., 2020), schizophrenia (Spreng et al., 2019), and autism (Sharda et al., 2016; Valk et al., 2015). As such, this method may provide a valuable tool for understanding differential connectivity within the hippocampal and PRC networks, and how this may be modulated across the lifespan and by *APOE*  $\epsilon$ 4.

**Figure 3.1.***Overlap Between Patterns of Structural Covariance and Intrinsic Functional Connectivity*

*Note.* Panel A shows regions demonstrating significant resting-state functional connectivity with a left anterior insula seed, while panel B shows regions demonstrating significant structural covariance with an anterior insula seed. The quite considerable overlap between these two patterns is shown in panel C, underscoring the point that structural covariance in some way reflects connectivity. Adapted from Clos et al. (2014).

Notably, a number of studies have also examined the structural covariance patterns associated with the hippocampus in healthy individuals across the lifespan (Ge et al., 2019; Kharabian Majouleh et al., 2020; Li et al., 2018; Nordin et al., 2018; Persson et al., 2014; Stening et al., 2017; Vogel, La Joie et al., 2020). In one of the earliest examples, Persson et al. (2014) observed common and distinct patterns of grey matter structural covariance associated with the anterior and posterior hippocampus in males and females. The authors found that the anterior and posterior hippocampus were both associated with positive and negative covariance in various cortical regions, including the PCC, in both males and females (Persson et al., 2014). By

contrast, the anterior hippocampus – but not the posterior hippocampus – was found to co-vary with parts of the anterior temporal lobe, including the anterior parahippocampal and fusiform gyri, in females only (Persson et al., 2014). A subsequent study of younger (20-35 years), middle-aged (40-50 years), and older adults (60-70 years) by the same group demonstrated that structural covariance patterns associated with the anterior and posterior hippocampus were differentially linked with associative memory, such that the expression of patterns common to both were associated with better performance whereas the expression of patterns unique to the anterior hippocampus were related to poorer performance (Nordin et al., 2018). Stening et al. (2017) further showed that young adult *APOE*  $\epsilon 4$  carriers and non-carriers differ in terms of hippocampal structural covariance (for non-hippocampal *APOE*-related work, see Cacciaglia et al., 2020; Spreng & Turner, 2013), with differences according to sex and anterior/posterior portion evident. Viewed collectively, it appears that sex, age, and *APOE*  $\epsilon 4$  are all relevant variables in the context of hippocampal structural covariance. While the studies mentioned often compared anterior and posterior portions of the hippocampus, no study to date has compared the hippocampus with the PRC. In fact, no study has yet examined the structural covariance of the PRC, with or without the hippocampus. If structural covariance in some way reflects connectivity, as suggested here and in Chapter 1 (Box 1; see also Alexander-Bloch, Giedd, & Bullmore, 2013), then this method may provide novel insights into the common and/or distinct connections associated with these key nodes within the extended hippocampal navigation network and the ventral feature network (Murray et al., 2017), which may (or may not) correspond with the patterns of intrinsic functional connectivity reported across numerous fMRI studies (e.g. Kahn et al., 2008; Libby et al., 2012; Maass et al., 2015; Wang et al., 2016).

Due to the exclusive focus on female participants in Chapter 2, there remains an open question about the impact of sex on the aforementioned neurocognitive networks, in particular whether sex interacts with *APOE*  $\epsilon 4$  carrier status. This allele has long been linked with a stronger effect on AD risk in females than males (Farrer et al., 1997; Payami et al., 1994, 1996).

Recent evidence indicates that higher levels of AD-related pathology, especially tau, may be driving this increase in risk (Babapour Mofrad et al., 2020; Buckley et al., 2019; Hohman et al., 2018; Wang et al., 2021). This raises the possibility that  $\epsilon 4$ -related alterations in these networks may be particularly evident in females. Offering some support for the notion that female  $\epsilon 4$  carriers exhibit specific alterations in these networks, prior research – discussed above – has shown that sex influences the structural covariance of the hippocampus and, in addition, that sex interacts with *APOE*  $\epsilon 4$ . For example, Stening et al. (2017) observed a specific pattern of covariance associated with the anterior hippocampus in female  $\epsilon 4$  carriers only. This finding is somewhat consistent with studies using DTI and resting-state fMRI, which have reported that older female  $\epsilon 4$  carriers exhibit reduced structural and functional connectivity within the extended hippocampal navigation network (Damoiseaux et al., 2012; Heise et al., 2014). Despite this, little is currently known about the impact of sex and *APOE*  $\epsilon 4$  on the connectivity of the PRC, thereby making it difficult to draw firm conclusions about the role of these factors on its broader network. One of the aims of this chapter is to address this question more directly using structural covariance.

Aside from the interaction between *APOE*  $\epsilon 4$  and sex, it is unclear how the impact of this allele plays out across the adult lifespan. According to lifespan systems vulnerability accounts (Bero et al., 2011; Buckner et al., 2005, 2009; Jagust & Mormino, 2011), *APOE*  $\epsilon 4$  reduces neural efficiency – sometimes conceptualised as “reserve” – in a way that leads to hyper-activation/hyper-metabolism early in life, which in turn increases susceptibility to  $A\beta$ . Over time, the growing burden of  $A\beta$  then leads to network dysfunction, ultimately giving rise to hypo-activation/hypo-metabolism and cognitive decline (see Section 1.3). In line with this, scene-related hyper-activation in the PCC has been observed in young *APOE*  $\epsilon 4$  carriers relative to non-carriers (Shine et al., 2015). Interestingly, a subsequent study related this hyper-activation to the microstructural properties of the PHCB (Hodgetts et al., 2019), which represents the primary white matter tract in the extended hippocampal navigation network. Young, predominantly female *APOE*  $\epsilon 4$  carriers were also found to show higher FA and lower MD – often considered an index of



higher structural connectivity (see Chapter 1, Box 1) – in the PHCB but not the ILF (Hodgetts et al., 2019). This study therefore adds weight to lifespan systems vulnerability accounts, as well as suggesting that early-life  $\epsilon 4$ -related functional alterations (i.e. hyper-activation) in the PCC may be underpinned by concomitant alterations in structural connectivity (i.e. hyper-connectivity; for further discussion, see Chapter 4). However, the results of Chapter 2 imply that *APOE*  $\epsilon 4$  impacts both the extended hippocampal navigation network and the ventral component of the feature network with advancing age, at least when focusing on middle-aged and older individuals. One possible explanation is that the preferential effects of the  $\epsilon 4$  allele on allocentric navigation/scene-based cognition and, by extension, activity and connectivity within the extended hippocampal navigation network may be confined to earlier stages in the lifespan, where significant A $\beta$  burden is unlikely. To test the possibility, even indirectly, it is necessary to include participants from across the adult lifespan, rather than mid-life alone as done in Chapter 2. This represents one of the aims of the current chapter.

Given that the hippocampus and PRC are proposed to be key nodes within different large-scale neurocognitive networks (Murray et al., 2017), it stands to reason that the resulting pattern(s) of structural covariance may be related to different aspects of function. In the current chapter, the cognitive/behavioural correlates of the observed structural covariance patterns were assessed in two ways: using the NeuroSynth decoder (<https://neurosynth.org/decode/>) and via performance on relevant cognitive tasks. NeuroSynth is a large-scale, web-based platform that can be used to meta-analytically “decode” the terms (e.g. episodic memory, anxiety, fear) associated with the observed patterns of covariance (Yarkoni et al., 2011). Many studies have used this to better understand the functional role that patterns of structural covariance, functional activation, and functional connectivity may have (for examples, see Lanzoni et al., 2020; Mckeown et al., 2020; Mwilambwe-Tshilobo & Spreng, 2021; Wang et al., 2018). Regarding cognitive performance, the study reported in the current chapter focused on one particular measure of visual recognition memory: the CANTAB (Cambridge Cognition, Cambridge, UK) delayed match-to-sample

(DMTS) task. The inclusion of this task was primarily motivated by prior research showing that DMTS performance is sensitive to dementia (Fowler et al., 1995, 1997; Swainson et al., 2001). More specifically, it has been reported that patients with AD, but not patients with semantic dementia or frontotemporal dementia, exhibit a selective impairment in DMTS accuracy (Lee et al., 2003). Performance on this task has also been shown to distinguish patients with amnesic MCI from healthy controls (Juncos-Rabadán et al., 2013). Consequently, the DMTS task appears to be sensitive to pathological ageing and AD. In monkeys, it is well established that lesions to the PRC impair no-delay object recognition, as assessed using a variation of the DMTS task (Eacott et al., 1994). However, even after PRC lesions, monkeys can learn repeating-items DMTS (Eacott et al., 1994). To account for this, Cowell et al. (2006) argued that an alternative brain structure – the hippocampus – is recruited when items are not trial unique. According to this view, the use of repeating-items induces a further degree of ambiguity, which must be resolved by more advanced, conjunctive representations housed by the hippocampus (Cowell et al., 2006; see also Lee et al., 2012). There is therefore an interesting question as to whether common/distinct structural covariance associated with the hippocampus and PRC is related to performance, particularly accuracy, on the DMTS task. Performance on a comparison task, the Wechsler Adult Intelligence Scale-III (WAIS-III; Wechsler, 1997) digit symbol-coding task, was also assessed to ensure that any relationship between the expression covariance patterns and DMTS performance is specific to this task and not related to processing speed (Salthouse, 1996, 2003).

To briefly summarise, here I report a study that aimed to examine the impact of *APOE*  $\epsilon$ 4, sex, and age on common and/or distinct patterns of structural covariance associated with the hippocampus and the PRC. These structures were selected as they are considered to be key nodes within the extended hippocampal navigation and (ventral) feature networks, respectively (Murray et al., 2017). Structural covariance was assessed in a relatively large sample ( $N = 353$ ) of participants from the Dallas Lifespan Brain Study (DLBS). This sample included both male and female participants, as well participants from

across the adult lifespan (20-88 years). The cognitive/behavioural correlates of the resulting covariance patterns were assessed via two separate methods, providing insight into the functional implications of the observed covariance.

## 3.2. Methods

### 3.2.1. Participants

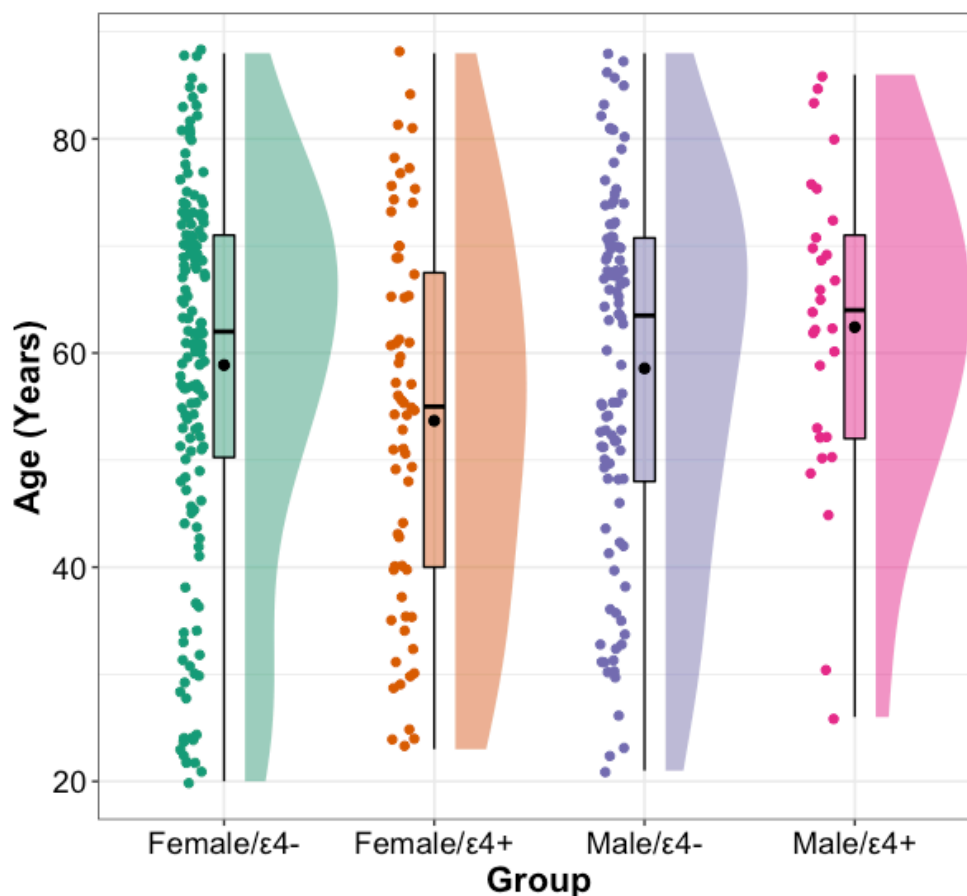
Data used in the current chapter were obtained from the DLBS open-access database (<https://dlbsdata.utdallas.edu>). The DLBS is an on-going longitudinal study designed to investigate the effects of healthy ageing on the brain and cognition. For present purposes, data of sufficient quality and completeness were available for 382 participants from Wave 1 of the DLBS, all of whom were initially recruited from the Dallas-Fort Worth community and provided informed consent prior to participation. All participants were right-handed, fluent in English, and scored 26 or higher on the Mini Mental State Examination (Folstein et al., 1975). Moreover, participants were screened for major neurological and psychiatric disorders, history of central nervous system disease or brain injury, and standard MRI contraindications. Additional details of the DLBS sample, including the inclusion/exclusion criteria, can be found elsewhere (e.g. Chan et al., 2018; Kennedy et al., 2012; Park et al., 2013). Institutional Review Boards at The University of Texas at Dallas and The University of Texas Southwestern Medical Centre approved all DLBS procedures, and The Cardiff University School of Psychology Research Ethics Committee approved the analysis of secondary data.

Following quality control procedures, which are described in the sections below, the final sample comprised 353 participants aged between 20 and 88 years ( $M = 58.1$ ,  $SD = 17.2$ ). While participants were asked to report their gender, which is a social construct, responses were given as male ( $n = 131$ ) or female ( $n = 222$ ), which are terms used to refer to sex (i.e. a biological construct). In this regard, the current chapter conflates sex and gender, a

practice that remains common in psychology, neuroscience, and allied disciplines (for relevant discussions, see Cameron & Stinson, 2019; Clayton & Tannenbaum, 2016; Hyde et al., 2019). For clarity and consistency, I use the terms provided by participants (i.e. male/female) but henceforth refer to any associations as a result of gender/sex (Rippon et al., 2014), highlighting the inability of the current analysis to differentiate between these two constructs. This differs relative to the approach adopted in Chapters 2 and 4, where chromosomal sex was determined as part of genetic quality control procedures. An overview of the age distribution separated by *APOE*  $\epsilon$ 4 carrier status (see Section 3.2.2) and gender/sex is shown in Figure 3.2.

**Figure 3.2.**

*Age Distribution of the Sample Separated by APOE  $\epsilon$ 4 Carrier Status and Gender/Sex*



*Note.* Participant ages are shown for each of the four groups (female/ $\epsilon$ 4-, female/ $\epsilon$ 4+, male/ $\epsilon$ 4-, male/ $\epsilon$ 4+). Individual data points, each representing a single participant, are shown alongside boxplots and density plots. A small amount of jitter has been added to each point for clarity. To facilitate interpretation, the mean value (black circle) and median value (a black line) for each group are both shown. Abbreviations: APOE  $\epsilon$ 4+ = APOE  $\epsilon$ 4 carrier, APOE  $\epsilon$ 4- = APOE  $\epsilon$ 4 non-carrier.

### 3.2.2. APOE genotype

APOE genotype was determined directly by real-time PCR using TaqMan single nucleotide polymorphism (SNP) genotyping assays (Applied Biosystems, Inc., Forster City, CA) corresponding to APOE SNPs rs429358

and rs7412, respectively (for more information, see Rodrigue et al., 2012). Participants were removed from analysis if *APOE* genotype was unavailable or ambiguous. Contrary to the approach adopted in Chapter 2, the current sample was split into  $\epsilon 4$  carrier ( $\epsilon 2/\epsilon 4$ ,  $\epsilon 3/\epsilon 4$ ,  $\epsilon 4/\epsilon 4$ ) and non-carrier ( $\epsilon 2/\epsilon 2$ ,  $\epsilon 2/\epsilon 3$ ,  $\epsilon 3/\epsilon 3$ ) groups. The reason for this discrepancy was the lower number of participants and, in particular, the lower number of *APOE*  $\epsilon 2$  carriers. As such, it was not possible to form an *APOE*  $\epsilon 2$  genotype group of sufficient size, especially when separating out the groups by gender/sex. While some studies adopting this  $\epsilon 4$  carrier vs. non-carrier approach opt to exclude participants who possess the  $\epsilon 2\epsilon 4$  genotype (e.g. Westlye et al., 2011, 2012), I do not do so here because the  $\epsilon 2\epsilon 4$  genotype has been associated with higher levels of AD pathology and overall AD risk (Farrer et al., 1997; Goldberg et al., 2020; Jansen et al., 2015; Oveisgharan et al., 2018; Reiman et al., 2020). This suggests that the effects of the  $\epsilon 4$  allele outweigh the effects of the  $\epsilon 2$  allele, meaning that these participants should be considered part of the risk-enhancing  $\epsilon 4$  carrier group. Indeed, a number of studies relevant to this thesis (Hodgetts et al., 2019; Shine et al., 2015) and this chapter in particular (Stening et al., 2017) have likewise included participants with the  $\epsilon 2\epsilon 4$  genotype as part of the *APOE*  $\epsilon 4$  carrier group. The genotypic distribution of the available sample was as follows: 93  $\epsilon 4$  carriers (13  $\epsilon 2/\epsilon 4$ , 72  $\epsilon 3/\epsilon 4$ , 8  $\epsilon 4/\epsilon 4$ ) and 260 non- $\epsilon 4$  carriers (2  $\epsilon 2/\epsilon 2$ , 35  $\epsilon 2/\epsilon 3$ , 223  $\epsilon 3/\epsilon 3$ ).

### 3.2.3. MRI acquisition

Scanning was conducted as part of the DLBS using a Philips Achieva 3T MRI system (Philips Medical Systems, Best, The Netherlands) equipped with an eight-channel head coil. T1-weighted structural images were acquired using an MPRAGE sequence (TR = 8.1ms; TE = 3.7ms; flip angle = 12°; FOV = 204 x 256 x 260mm; voxel size = 1 x 1 x 1mm; 166 sagittal slices). One participant was removed from the current study, as their T1 scan did not cover the whole brain.

#### 3.2.4. MRI pre-processing

Pre-processing was completed using the Computational Anatomy Toolbox (CAT12.7-RC1 [r1653]; <http://www.neuro.uni-jena.de/cat>) for SPM12 (version 7771; <https://www.fil.ion.ucl.ac.uk/spm/software/spm12/>), as implemented in MATLAB (R2015a; MathWorks Inc, Natick, Massachusetts, USA). First, images were manually reoriented along the anterior commissure/posterior commissure line with the mid-point of the anterior commissure set to the origin ( $x = 0, y = 0, z = 0$ ). Next, images were spatially registered to SPM12 tissue probability maps and segmented into grey matter, white matter, and cerebrospinal fluid. Segmented images were then normalised to Montreal Neurological Institute (MNI) space using a geodesic shooting procedure (Ashburner & Friston, 2011). Nonlinear-only modulation was applied to ensure that the absolute amount of tissue (i.e. volume) in a voxel was corrected for head size. This form of modulation is commonly used in studies that are methodologically similar to the one reported here (DuPre & Spreng, 2017; Spreng et al., 2019; Spreng & Turner, 2013). Finally, the segmented, modulated, and normalised images were smoothed using a 8mm full width at half-maximum Gaussian kernel. Prior work indicates that a kernel of this size is optimal for detecting morphometric differences in both large and small structures (Honea et al., 2005). The resulting voxel size of the pre-processed images was 1.5 x 1.5 x 1.5mm. Following these pre-processing steps, the CAT12 retrospective quality assurance framework was used to evaluate image quality. Only images identified as having a weighted image quality rating of “C” or above were carried forward for analysis (for a similar approach, see Li et al., 2019).

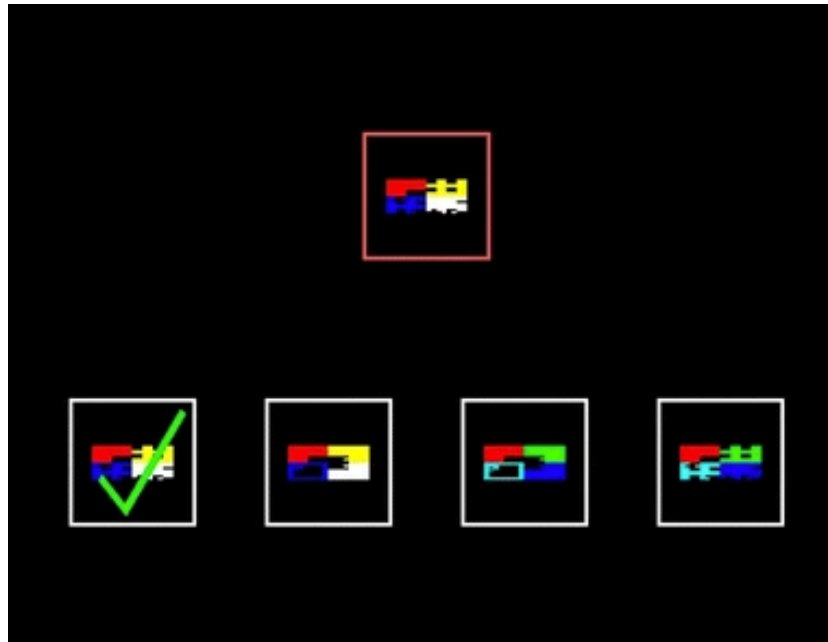
#### 3.2.5. Cognitive tasks

Participants completed an array of cognitive tasks as part of the DLBS. However, regarding an association between structural covariance and task performance, I focus on one task in particular: the CANTAB (Cambridge Cognition, Cambridge, UK) DMTS task. In this task, participants are shown a sample item that is comprised of four “building blocks”, each defined by a

particular pattern, colour, and spatial location within the overall item. Following this, participants are then shown an array of four additional items, three of which are unique distractors or foils and one of which is the same as the sample item. The goal of the task is to select the item that matches the sample – hence, match-to-sample (Figure 3.3). In some trials, the four additional items are shown alongside the sample item (i.e. simultaneous trials), but in others they are shown after a delay of 0, 4, or 12 seconds (i.e. delay trials). Performance was measured here as the proportion of correct responses across all delay trials.

To ensure that any association between structural covariance and DMTS performance was specific to this task, I also focus on an additional task: the WAIS-III (Wechsler, 1997) digit symbol-coding task. In this task, participants are shown nine geometric symbols, each of which is assigned to a number from 1-9 (Figure 3.4). They are then shown a series of randomised digits and asked to draw the corresponding symbol below each digit as quickly as possible. Performance is measured as the total number of items correctly matched in 90 seconds. This task is sensitive to impairments and improvements in processing speed (Jaeger, 2018), which declines with advancing age (Salthouse, 1996, 2003).



**Figure 3.3.***DMTS Items*

*Note.* An example simultaneous match-to-sample trial is shown. The sample item is located in the red box, whereas the target and distractor items are located in white boxes. A green tick identifies the target item – that is, the item that matches the sample. In delay trials, the sample item is not shown alongside the four additional items. Reprinted from Torgersen et al. (2010).

**Figure 3.4.***WAIS-III Digit Symbol Coding Items*

1	2	3	4	5	6	7	8	9
—	⊥	⊏	L	∪	○	^	X	=

*Note.* Geometric symbols and their corresponding numbers, as used in the WAIS-III digit symbol-coding task, are shown. Materials provided by the DLBS (<https://dlbsdata.utdallas.edu/>).

### 3.2.6. Statistical analyses

#### 3.2.6.1. Sample characteristics

Differences in basic sample characteristics were examined using R (version 3.6.0; R Core Team, 2019) in RStudio (version 1.3.1093; RStudio Team, 2020). This was performed to ensure that the four groups (male  $\epsilon 4$  carriers, female  $\epsilon 4$  carriers, male non-carriers, female non-carriers), which were carried forward for structural covariance analysis (see Section 3.2.6.2), did not differ in ways that might themselves affect the observed patterns of covariance. To examine whether this was the case, chi-square tests of independence and robust one-way ANOVAs were conducted. In the case of chi-square tests, Cramer's  $V$  was calculated as a measure of effect size, where relevant, using the *effectsize* package (version 0.4.4-1; Ben-Shachar et al., 2020). Robust one-way ANOVAs based on trimmed means (20% trimming level) were conducted using the *t1way* function from the *WRS2* package (version 1.1-1; Mair & Wilcox, 2020). A robust explanatory measure of effect size,  $\xi$ , was also reported (Wilcox & Tian, 2011). As mentioned in Chapter 2, values of  $\xi$  equal to 0.1, 0.3, and 0.5 roughly correspond to small, medium, and large effect sizes (Mair & Wilcox, 2020). Robust post-hoc tests on trimmed means were conducted using the *lincon* function (Mair & Wilcox, 2020).

#### 3.2.6.2. Structural covariance analysis

Whole-brain structural covariance patterns were analysed using seed-based partial least squares (PLS) analysis, as implemented using the PLSgui (version 6.13; <https://www.rotman-baycrest.on.ca/index.php?section=84>) in MATLAB (R2015a; MathWorks Inc, Natick, Massachusetts, USA). Seed-based PLS is a data-driven multivariate statistical technique that can be used to identify patterns of grey matter volume throughout the brain that co-vary with grey matter volume in one or more seed regions across participants (for a review, see Krishnan et al., 2011; see also McIntosh et al., 1996; McIntosh

& Lobaugh, 2004). I describe this method briefly here using the same nomenclature as Krishnan et al. (2011).

In seed-based PLS, whole-brain imaging data are stored in matrix  $X$ , while data from one or more seed regions are stored in matrix  $Y$ . These matrices can incorporate sub-matrices, each of which corresponds to a particular condition or group. Both  $X$  and  $Y$  are centred and normalised within condition or group. A cross-product matrix, referred to as  $R$ , is then computed between  $X$  and  $Y$ . Thereafter, singular value decomposition is applied, decomposing  $R$  into three matrices:  $U$ ,  $\Delta$ , and  $V$ . The two singular vectors (a.k.a. saliences),  $U$  and  $V$ , represent the seed values and whole-brain spatial patterns that best characterise  $R$ , respectively. By contrast,  $\Delta$  is a diagonal matrix of singular values. Together, the singular vectors and singular values form a set of orthogonal latent variables (LVs) – linear combinations of the original variables that capture the largest amount of information common to  $X$  and  $Y$  (Krishnan et al., 2011). The statistical significance of LVs is evaluated via non-parametric permutation testing, whereby rows (i.e. observations) in  $X$  but not  $Y$  are randomly re-ordered. By repeating this procedure many times over, a sampling distribution of the singular values under the null hypothesis can be obtained and, in turn, used to perform null hypothesis significance testing (NHST). If a particular LV is deemed significant ( $p < .05$ ), the reliability of the elements (i.e. voxels) comprising the singular vectors, or saliences, is assessed. To do so, each element is divided by its standard error, the latter of which is estimated by generating bootstrap samples with replacement. Reliability is thus expressed as a bootstrap ratio (BSR), which is roughly equivalent to a z-score. In brain imaging analysis, voxels are sometimes deemed reliable if they exceed a given BSR cut-off (e.g. Stening et al., 2017) or are thresholded to include only the most reliable voxels (e.g. Spreng & Turner, 2013). For any given LV of interest, a “brain score” can also be calculated for each participant, representing the degree to which the spatial pattern captured by the LV is expressed in that individual. Mathematically, these brain scores are calculated by multiplying the original matrix,  $X$ , by the singular vector,  $V$ , and summing across all elements for each participant. The resulting brain scores can then be used as a

dependent variable in further analyses, as has been done previously (DuPre & Spreng, 2017; Nordin et al., 2018; Persson et al., 2014; Spreng et al., 2019; Spreng & Turner, 2013; Veldsman et al., 2020).

In this chapter, I focus on two regions that anchor large-scale MTL neurocognitive networks: the hippocampus and the PRC. For both seeds, grey matter volume was extracted from peak MNI coordinates with a neighbourhood of six voxels. Functionally defined seeds, as opposed to structurally defined seeds, were used to maintain consistency with relevant structural covariance studies (e.g. DuPre & Spreng, 2017; Spreng & Turner, 2013). The peak MNI coordinates for the hippocampus were obtained from a group-level scene > object functional contrast ( $x = 22$ ,  $y = -16$ ,  $z = -22$ ), as reported by Hodgetts et al. (2016). These coordinates were specifically centred on the anteromedial portion of the hippocampus. This particular portion of the hippocampus has been shown across several reports to be highly responsive to scenes (Baldassano et al., 2016; Dalton et al., 2018; Hodgetts, Voets et al., 2017; McCormick et al., 2021; Zeidman & Maguire, 2016). The peak MNI coordinates for the left PRC seed were obtained from the same dataset, albeit from an unpublished group-level object > scene functional contrast ( $x = -32$ ,  $y = -4$ ,  $z = -40$ ). The coordinates used for the PRC align well with a previously published probabilistic map of this structure (Devlin & Price, 2007).

Seed-based PLS was then used to identify patterns of grey matter volume throughout the brain that co-vary with grey matter volume in the hippocampus and PRC; that is, patterns of whole-brain structural covariance. As in prior research (Stening et al., 2017), four groups were entered into the analysis: male *APOE*  $\epsilon 4$  carriers, male *APOE*  $\epsilon 4$  non-carriers, female *APOE*  $\epsilon 4$  carriers, and female *APOE*  $\epsilon 4$  non-carriers. This group organisation was maintained throughout the PLS analyses, thereby making it possible to directly compare the covariance patterns obtained across groups. Significance of the LVs was determined using 2000 non-parametric permutations without replacement, while reliability was determined using 1000 bootstraps with replacement. Consistent with prior studies (DuPre &

Spreng, 2017; Spreng et al., 2019; Spreng & Turner, 2013), the BSR was thresholded to include only the top 5% of reliable voxels (LV1 BSR  $\pm 6.47$ ). As an additional step, the unthresholded BSR maps were uploaded to NeuroVault (<https://identifiers.org/neurovault.collection:9571>) and decoded using NeuroSynth (<https://neurosynth.org/decode/>). From the resulting maps, it was possible to obtain a list of cognitive/behavioural terms that were associated with the observed spatial patterns. These lists were then plotted as word clouds, with the 15 most strongly associated terms shown. Anatomical terms such as “temporal lobe” or “MTL” were removed from consideration, as were duplicate terms (e.g. “fear”, “fearful”).

Brain scores derived from the PLS analysis were then extracted and analysed separately using R (version 3.6.0; R Core Team, 2019) in RStudio (version 1.3.1093; Rstudio Team, 2020). The aim was to investigate how *APOE*  $\epsilon 4$  carrier status, gender/sex, age, and their interactions influenced the expression of identified LVs. A robust multiple linear regression analysis was conducted using the *lmrob* function from the *robustbase* package (version 0.93-7; Maechler et al., 2021). This method fits a robust variant of the model – described below – based on an M-estimator (Koller & Stahel, 2011; Yohai, 1987) using iteratively re-weighted least squares estimation (for an example of its utility, see Field & Wilcox, 2017). The fitted model was as follows:

$$\text{Brain score} \sim \text{APOE } \epsilon 4 \text{ carrier status} \times \text{age} \times \text{gender/sex}$$

Age was centred and scaled. *APOE*  $\epsilon 4$  carrier status and gender/sex were treated as categorical variables and coded using deviation coding. Results were deemed to be statistically significant if the *p*-value was smaller than, or equal to, the nominal  $\alpha$  level of 0.05.

### 3.2.6.3. Cognitive correlates of the structural covariance patterns

Subsequently, brain scores were correlated with cognitive task performance. More specifically, brain scores derived from the PLS analysis were correlated

with DMTS accuracy across all delay trials (0s, 4s, 12s) and WAIS-III digit symbol coding accuracy. In the former, accuracy was measured as proportion correct. In the latter, accuracy was measured as total correct. Pearson's  $r$  was used for these analyses. A Steiger  $z$ -test (Steiger, 1980) was then conducted to statistically compare the correlations using the *cocor* package (version 1.1-3; Diedenhofen & Musch, 2015). Finally, exploratory mediation (path) analyses (Hayes, 2013) were conducted to better understand these relationships using the *med* function from the *medmod* package (version 1.0.0; Selker, 2017). All of these analyses were performed on a subset of participants ( $n = 348$ ), as the requisite cognitive data were unavailable for 5 participants (1 female  $\epsilon 4+$ , 3 female  $\epsilon 4-$ , 1 male  $\epsilon 4-$ ).

### 3.3. Results

#### 3.3.1. Sample characteristics

As discussed in Section 3.2.1, the final sample included 353 participants aged between 20 and 88 years ( $M = 58.1$ ,  $SD = 17.2$ ). Table 3.1 provides an overview of the basic sample characteristics separated by *APOE*  $\epsilon 4$  carrier status and gender/sex. There was no significant group difference in terms of age ( $F(3, 68.24) = 2.491$ ,  $p = .067$ ,  $\xi = 0.27$ , 95% CI [0.12, 0.49]), years of education ( $F(3, 73.42) = 1.203$ ,  $p = .315$ ,  $\xi = 0.2$ , 95% CI [0.07, 0.43]), or multilingualism ( $\chi^2(3, N = 353) = 2.276$ ,  $p = .517$ , Cramer's  $V = 0.08$ , 95% CI [0, 0.16]). For post-menopausal status, a variable specific to the female groups, there was also no significant group difference ( $\chi^2(1, N = 210) = 3.257$ ,  $p = .071$ , Cramer's  $V = 0.12$ , 95% CI [0, 0.26]). Together, these results show that the four groups did not differ significantly in terms of basic demographics, suggesting that any group-level alterations in structural covariance cannot easily be explained by differences in these variables.

**Table 3.1.**

*Basic Sample Characteristics Separated by APOE ε4 Carrier Status and Gender/Sex*

	Males		Females	
	<i>APOE</i> ε4+ ( <i>n</i> = 29)	<i>APOE</i> ε4- ( <i>n</i> = 102)	<i>APOE</i> ε4+ ( <i>n</i> = 64)	<i>APOE</i> ε4- ( <i>n</i> = 158)
Age (years)	62.4 (14.6)	58.6 (17.2)	53.7 (17.4)	58.9 (17.4)
Education (years)	16.1 (2.3)	16.7 (2.9)	16.4 (2.9)	16.0 (2.8)
Multilingual (% yes)	13.79%	27.45%	25.0%	24.68%
Post-menopausal (% yes)	NA	NA	59.32%	72.19%

*Note.* Values represent the mean and standard deviation (in parentheses) or percentage (%) of participants. Abbreviations: *APOE* ε4+ = *APOE* ε4 carriers, *APOE* ε4- = *APOE* ε4 non-carriers.

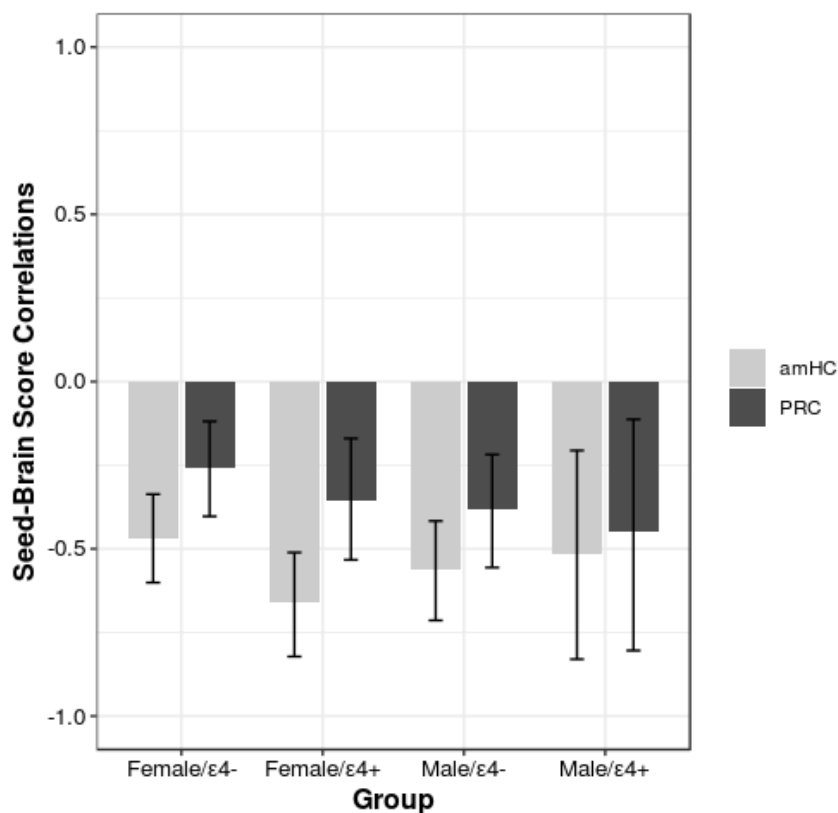
<sup>a</sup> The highest level of education reported was converted into estimated years of education based on typical completion times (for equivalent approaches using this dataset, see Chan et al., 2018; Festini et al., 2016, 2019).

<sup>b</sup> Data regarding post-menopausal status was unavailable for 12 participants (5 ε4+, 7 ε4-).

\*  $p < .05$ , \*\*  $p < .01$ , \*\*\*  $p < .001$  (highlighted in bold, described in text).

### 3.3.2. Structural covariance analysis

The seed PLS analysis identified eight LVs, although only one – LV1 – was significant ( $p < .0005$ ; accounting for 76.58% of the cross-correlation covariance). As shown in Figure 3.5, LV1 captured a pattern of structural covariance common to both the hippocampus and PRC across male and female *APOE* ε4 carriers and non-carriers. The seed-brain score correlation was stronger for the hippocampus than the PRC across all groups, but this difference was not statistically significant and should not be over-interpreted. While the seed-brain score correlations appear negative, the sign is not meaningful per se; rather, PLS creates a series of contrasts, so positive and negative simply constitute ways of differentiating between different sides of a contrast.

**Figure 3.5.***Seed-Brain Score Correlations for LV1 Across Groups*

*Note.* Bars represent the correlation between grey matter values in the seed regions (hippocampus, PRC) and thresholded brain scores derived from LV1, as a function of group. Error bars represent the bootstrapped 95% CI. Abbreviations: ε4+ = APOE ε4 carrier, ε4- = APOE ε4 non-carrier, amHC = anteromedial hippocampus, PRC = perirhinal cortex.

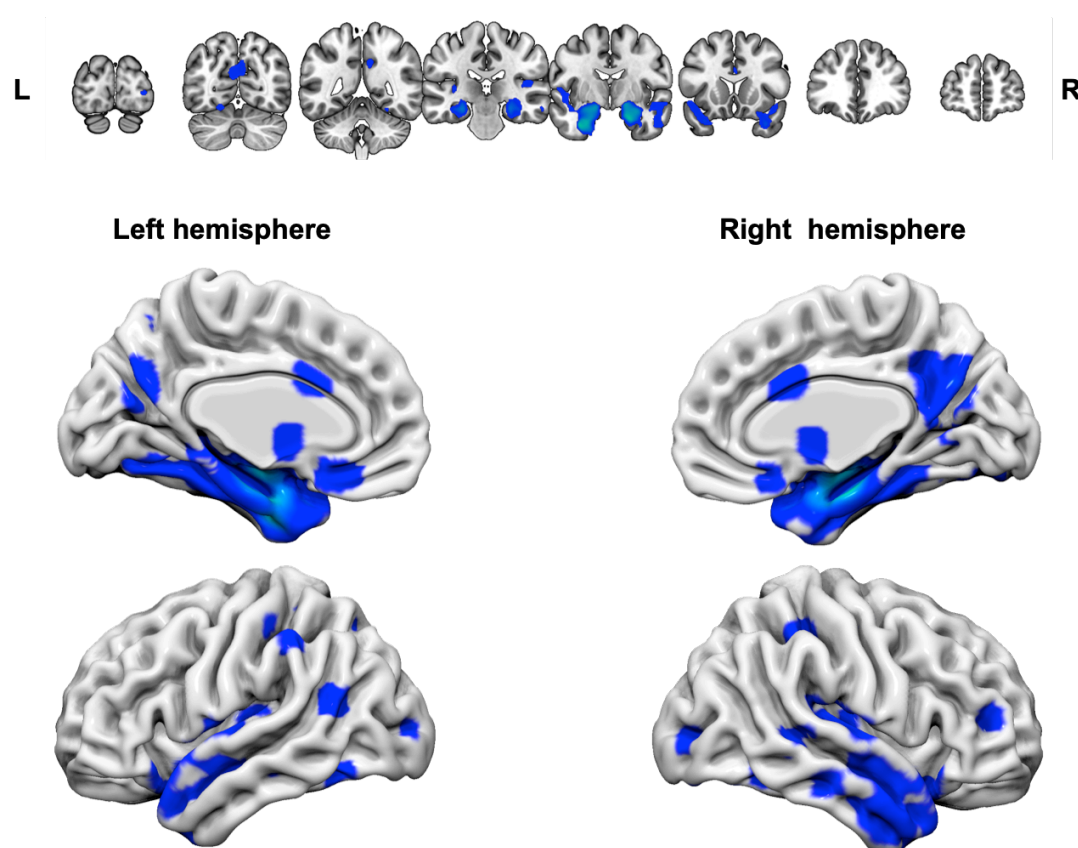
The covariance pattern captured by LV1 is shown visually in Figure 3.6 and a cluster report is provided in Table 3.2. Significant clusters of structural covariance were evident in and around the seed regions, as expected (for similar examples, see Nordin et al., 2018; Persson et al., 2014; Stening et al., 2017), but also in other regions within the frontal, temporal, parietal, and occipital lobes. Notably, this included regions commonly activated during episodic memory retrieval, such as the ventromedial prefrontal cortex, precuneus, and angular gyrus (Benoit & Schacter, 2015; Ferguson et al., 2019; Kim, 2010; Rugg & Vilberg, 2013; Spaniol et al., 2009). In addition, the fusiform gyrus – a region implicated in face processing and object



recognition (Weiner & Zilles, 2016) – was further found to co-vary with the hippocampus and PRC. To identify the cognitive/behavioural terms associated with the observed spatial pattern, the unthresholded BSR map for LV1 was uploaded to the NeuroSynth decoder. The word cloud generated from the decoder, shown in Figure 3.7, revealed a variety of terms associated with LV1. These terms were primarily related to episodic memory and face/emotion processing.

**Figure 3.6.**

*Whole-Brain Structural Covariance Pattern Captured by LV1*



*Note.* The covariance pattern captured by LV1 is shown, thresholded to the top 5% of reliable voxels ( $BSR \pm 6.47$ ). For visualisation purposes, the resulting map was projected onto the standard MNI152 template (top) in MRICroGL (<https://www.nitrc.org/projects/microgl/>) and the standard ICBM-152 template (bottom) in Surfice (<https://www.nitrc.org/projects/surfire/>).

**Table 3.2**

*Location of Peak Voxels From Clusters of Structural Covariance Associated with LV1*

Peak Location	MNI Coordinates			Voxels	BSR
	x	y	z		
Hippocampus (R)	22.5	-13.5	-22.5	8298	-13.85
Perirhinal cortex (L)	-34.5	-3	-33	8785	-12.71
Precuneus (R)	3	-64.5	28.5	1202	-8.65
Ventromedial prefrontal cortex (L)	-7.5	24	-16.5	235	-8.08
Angular gyrus (L)	-48	-58.5	18	123	-7.95
Planum temporale (R)	43.5	-36	13.5	700	-7.85
Auditory cortex (L)	-37.5	-22.5	6	151	-7.84
Temporal occipital fusiform gyrus (L)	-21	-63	-15	476	-7.71
WM fornix	3	3	1.5	93	-7.47
Occipital fusiform gyrus (R)	30	-79.5	-18	98	-7.46
Anterior cingulate gyrus (R)	1.5	12	28.5	77	-7.13

*Note.* The BSR threshold was set include the top 5% of reliable voxels (BSR  $\pm 6.47$ ). The cluster extent threshold was to set to 50 voxels, with a 10mm minimum gap between clusters.

**Figure 3.7.**

*Word Cloud of Terms Decoded from the Unthresholded BSR Map for LV1*

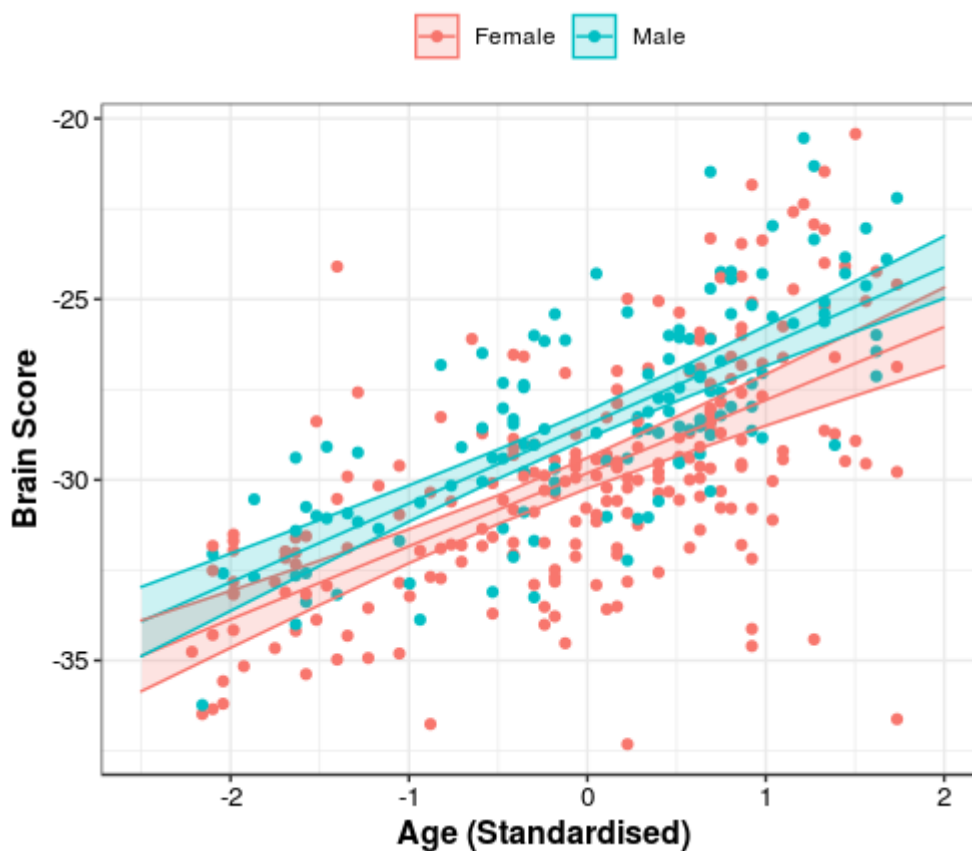


*Note.* Word cloud shows the top 15 cognitive/behavioural terms associated with the unthresholded BSR map, as determined by NeuroSynth. Text colour and size corresponds to the strength of the association (darker colour and larger text = stronger association). Correlations ranged from -0.168 (valence) to -0.230 (neutral). For an alternative way of visualising this data, see the appendix (Section 6.5).

Following the PLS analysis, brain scores were extracted for LV1 and used as dependent variables in a robust multiple regression analysis. Results revealed that gender/sex ( $b = -1.434$ ,  $p < .001$ ) and age ( $b = 2.139$ ,  $p < .001$ ) were significantly associated with the brain scores, such that the covariance pattern captured by LV1 was less strongly expressed with advancing age and in males relative to females (Figure 3.8). *APOE*  $\epsilon 4$  carrier status, by contrast, was not associated with the brain scores derived from LV1 ( $b = 0.068$ ,  $p = .821$ ). In addition, none of the interaction terms included in the model were found to be associated with the brain scores (all  $p \geq .39$ ).

**Figure 3.8.**

*Relationship between Gender/Sex, Age, and Brain Scores Derived from LV1*



*Note.* The fitted lines and 95% confidence intervals are based on predicted values from the robust multiple regression model. Individual data points represent the values for each participant. A small amount of jitter has been added to each point for clarity. As discussed in text, more negative brain scores represent stronger expression of the covariance pattern.

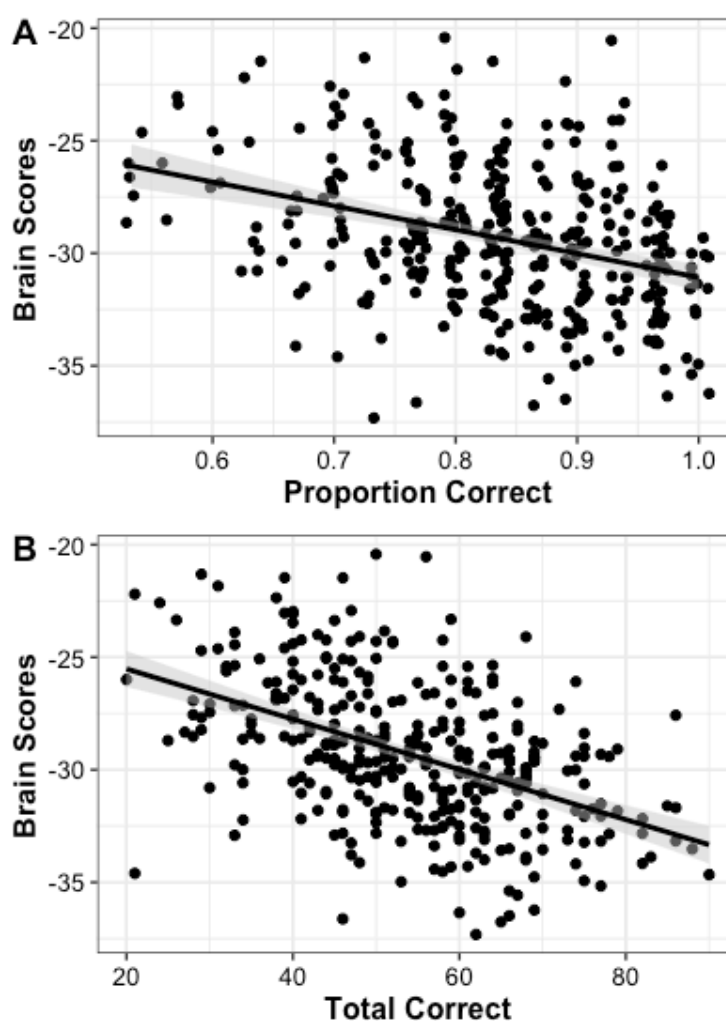
### 3.3.3. Cognitive correlates of the structural covariance pattern

Brain scores were further correlated with proportion correct on the DMTS task (all delay trials) and total correct on the WAIS-III digit symbol-coding task. Analysis revealed that brain scores were significantly correlated with accuracy on both tasks (DMTS:  $r(346) = -0.35$ ,  $p < .001$ ; digit symbol-coding:  $r(346) = -.478$ ,  $p < .001$ ), such that performance was higher in those who more strongly expressed the covariance pattern captured by LV1 (i.e. more negative brain scores). Interestingly, performance on the two tasks was also highly correlated ( $r(346) = .529$ ,  $p < .001$ ), despite purporting to measure

different aspects of cognition. Comparing the task-brain score correlations, a Steiger z-test demonstrated that there was a significant difference between the two ( $z = 2.759$ ,  $p = .006$ ). This was driven by a stronger correlation between brain scores and accuracy on the digit symbol-coding task than the DMTS task (Figure 3.9).

**Figure 3.9.**

*Relationship Between Brain Scores Derived from LV1 and Cognitive Task Performance*

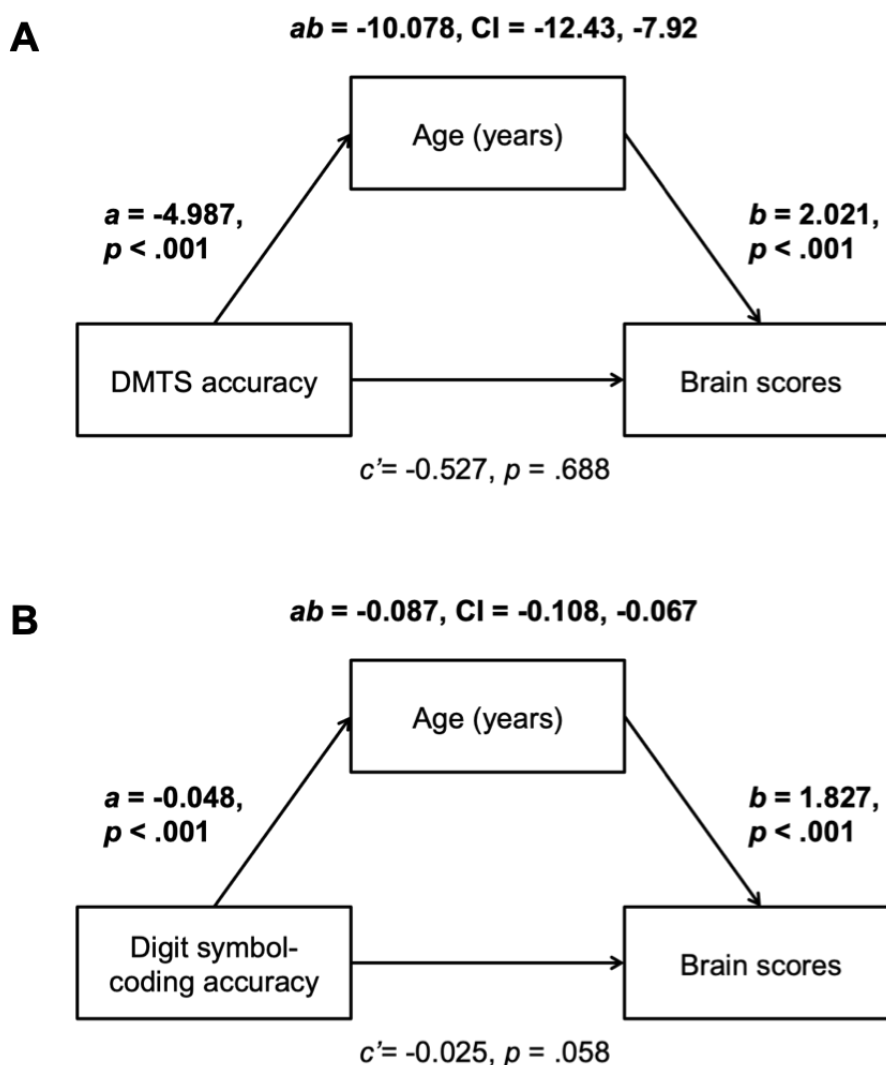


*Note.* The relationship between brain scores and performance on the DMTS task (A) and the WAIS-III digit symbol-coding task (B) are shown. Performance was assessed as proportion correct (0-1) on the DMTS (all delayed trials) and total correct on the digit symbol-coding task. A small amount of jitter has been added to each point for clarity.

Given that age was strongly associated with brain scores, it remained possible that the observed task-related correlations were mediated by age. To test this, exploratory mediation analyses were carried out using ordinary least squares path analysis. Figure 3.10A provides a visual overview of the relationship between DMTS accuracy – measured as proportion correct (all delay trials) – and brain scores with age as a mediator. As shown, participants with higher proportion correct scores on the DMTS were older in age ( $a = -4.987$ ), and participants who were older in age had more positive (i.e. less negative) brain scores ( $b = 2.021$ ). A bootstrap 95% CI (based on 1000 bootstrapped samples) for the indirect effect ( $ab = -10.078$ ) was entirely above zero ( $-12.43$  to  $-7.92$ ). In addition, there was no evidence that DMTS accuracy was related to brain scores independent of age ( $c' = -0.527$ ). This analysis thus provides evidence that the relationship between DMTS accuracy and brain scores was accounted for by age. Turning to the digit symbol-coding task, Figure 3.10B provides a visual overview of the relationship with brain scores mediated by age. Participants with higher total scores on this task were older in age ( $a = -0.048$ ), and participants who were older in age had more positive (i.e. less negative) brain scores ( $b = 1.827$ ). Consistent with the DMTS analysis, the bootstrap 95% CI (based on 1000 bootstrapped samples) for the indirect effect ( $ab = -0.087$ ) was entirely above zero ( $-0.108$  to  $-0.067$ ). There was also no evidence that digit symbol-coding accuracy was related to brain scores independent of age ( $c' = -0.025$ ). Therefore, the analysis indicated that any relationship between performance on this task and brain scores from LV1 was accounted for by age.

**Figure 3.10.**

*Mediation Analysis Examining the Three-Way Relationship between DMTS Accuracy, Age, and LV1 Brain Scores*



*Note.* Panel A shows the mediation model for DMTS accuracy (i.e. proportion correct) across delay trials, whereas panel B shows the mediation model for WAIS-III digit symbol-coding accuracy (i.e. total correct). The lower-left box represents the independent variable (IV), upper-middle box represents the mediator (M), and the lower-right box represents the dependent variable (DV). Unstandardised coefficients and  $p$ -values are shown next to the path of interest ( $a$ ,  $b$ ,  $ab$ ,  $c$ ). In simple mediation models such as those shown here, path  $a$  corresponds to the effect of the IV on the M, path  $b$  corresponds to the causal effect of the M on the DV, and path  $c'$  corresponds to the direct effect of the IV on the DV independent of M. Significant terms are highlighted in bold. The 95% CI is shown for the indirect effects ( $ab$ ).

### 3.4. Discussion

In the study reported in this chapter, the primary aim was to examine the impact of *APOE*  $\epsilon$ 4, gender/sex, and age on the shared and/or unique structural covariance patterns associated with two key nodes in large-scale neurocognitive networks: the hippocampus and the PRC (Murray et al., 2017). Structural covariance – a technique that is thought to index certain aspects of connectivity (Betzel, 2020) – was assessed in a relatively large sample ( $N = 353$ ) of adults from across the lifespan (18-88 years). This sample also included both male and female participants, thereby addressing one of the limitations from Chapter 2. Moreover, to assess the cognitive/behavioural correlates of the observed structural covariance patterns, additional analyses were performed. The aim of these analyses was to provide further insight into the functional role that this observed pattern of structural covariance may have.

Results of the seed-based PLS analysis revealed a single significant LV, capturing patterns of structural covariance common to both the anteromedial hippocampus and PRC. Specifically, grey matter volume in both structures co-varied with grey matter volume in a range of brain regions across the frontal, temporal, parietal, and occipital lobes. These regions included the ventromedial prefrontal cortex, precuneus, and angular gyrus, as well as the fusiform gyrus and anterior cingulate cortex (Figure 3.6, Table 3.2). Given that the hippocampus and the PRC are proposed to represent key nodes within distinct (but interacting) neurocognitive networks (Murray et al., 2017), it is somewhat surprising that shared but not unique patterns of covariance – assumed to represent aspects of connectivity – were observed.

The selection of an anterior hippocampal seed in the current chapter may partially account for this result. Studies using resting-state fMRI provide evidence that the anterior hippocampus and PRC exhibit similar patterns of intrinsic functional connectivity in the human brain. In a relatively large-scale imaging study, Kahn et al. (2008) sought to identify cortical regions linked to structures within the MTL. The authors identified two distinct cortical



networks, one preferentially connected to the body of the hippocampus and posterior PHC, the other preferentially connected to the anterior hippocampus and PRC (Kahn et al., 2008). Building on this, a subsequent study by Libby et al. (2012) investigated whether the PRC and PHC exhibit distinct patterns of intrinsic functional connectivity not only with cortical regions but also with regions of the hippocampus. In addition to showing PRC/PHC cortical connectivity similar to that reported by Kahn et al. (2008; for relevant animal evidence, see Suzuki & Amaral, 1994), their analysis further demonstrated that the PRC was preferentially connected with the anterior hippocampus, whereas the PHC was preferentially connected with the posterior hippocampus (Libby et al., 2012). Although such a clear-cut anterior-posterior split in resting-state fMRI-based functional connectivity is not always observed (e.g. Barnett et al., 2021; Wang et al., 2016), equivalent patterns of task-related functional connectivity have further been observed in the anterior hippocampus and PRC during complex object discrimination (McLelland et al., 2014). These findings therefore suggest that the anterior hippocampus and PRC exhibit comparable patterns of intrinsic functional connectivity, which has led to the proposal that the anterior hippocampus and PRC form part of a so-called “anterotemporal network” (for more on the PMAT framework, see Inhoff & Ranganath, 2017; Ranganath & Ritchey, 2012; Ritchey et al., 2015). This network is hypothesised to have an important role in representing object information (Inhoff & Ranganath, 2015), as well as semantic and perceptual information (Inhoff & Ranganath, 2017). Given that patterns of structural covariance and intrinsic functional connectivity have been shown to overlap (Figure 3.1; see also Clos et al., 2014; Guo et al., 2015; Kelly et al., 2012; Spreng et al., 2019), it is plausible that this may offer an explanation as to why only shared patterns of covariance were observed here.

However, it is important to recognise that hippocampal connectivity (and function) does not differ solely along its anterior-posterior (i.e. longitudinal) axis (Plachti et al., 2019). Studies in rats (van Strien et al., 2009) and monkeys (Aggleton, 2012) provide convincing evidence that anatomical connectivity differs along the transverse (medial-lateral) axis of the

hippocampus (a.k.a. the proximal-distal axis). For example, in rats, it has been shown that distal CA1/proximal subiculum is preferentially interconnected with the lateral EC, whereas proximal CA1/distal subiculum – corresponding to anteromedial hippocampus – is preferentially interconnected with the medial EC (Naber et al., 2001; Witter et al., 2000; for equivalent results in monkeys, see Witter & Amaral, 1991). This pathway through the medial EC has, in turn, been linked with stronger spatial modulation in rats (Henriksen et al., 2010). Such findings are consistent with more recent research in humans showing that the anteromedial portion of the hippocampus – in addition to the posterior PHC and RSC – responds to preferentially to scenes (Hodgetts et al., 2016; see also Hodgetts, Voets et al., 2017; McCormick et al., 2021; Zeidman & Maguire, 2016). In terms of functional connectivity, one high-resolution (7T) fMRI study found that the human distal (medial) subiculum is preferentially connected with the posteromedial EC, as well as the PHC, in line with the animal findings (Maass et al., 2015; see also Baldassano et al., 2016). As such, it appears unlikely that the anteromedial hippocampal seed used here can simply be viewed as part of the so-called anterotemporal network, as suggested above. In the absence of high-resolution MRI data, it is challenging to reconcile these competing narratives in a coherent manner.

Returning to the impact of *APOE*  $\epsilon 4$ , gender/sex, and age, the study reported in this chapter did not identify any differences between the four groups (female  $\epsilon 4+$ , male  $\epsilon 4+$ , female  $\epsilon 4-$ , male  $\epsilon 4-$ ) in the expression of the identified covariance pattern (Figure 3.5). This finding runs counter to one prior structural covariance study to examine the effect of *APOE*  $\epsilon 4$  and gender/sex (Stening et al., 2017), as well as reports that older female  $\epsilon 4$  carriers show structural and functional connectivity alterations within the extended hippocampal navigation network (Damoiseaux et al., 2012; Heise et al., 2014). Robust regression analysis was conducted to further determine whether *APOE*  $\epsilon 4$ , gender/sex, and age influence brain scores derived from the one significant LV. These scores represent the extent to which the covariance pattern was expressed in individuals, lending themselves to individual differences rather than group-level analysis (see Chapter 1, Box

1). Results revealed that age and gender/sex independently impacted the expression of these brain scores, with the covariance pattern less strongly expressed with advancing age and in males relative to females (Figure 3.8). In contrast, *APOE*  $\epsilon$ 4 carrier status did not influence the expression of the covariance pattern associated with both the hippocampus and PRC. The lack of a difference between *APOE*  $\epsilon$ 4 carriers and non-carriers appears inconsistent with the results reported in Chapter 2, namely that female  $\epsilon$ 4 carriers and  $\epsilon$ 2 carriers exhibited different age trends in odd-one-out perceptual discrimination accuracy independent of condition. However, it might be the case that the approach here – that is, comparing  $\epsilon$ 4 carriers relative to non-carriers – masked similar effects. Indeed, the non-carrier group studied as part of the current chapter was predominantly comprised of  $\epsilon$ 3 homozygotes ( $n = 223$ , 89.62%), and Chapter 2 did not observe differences between this genotype group and the *APOE*  $\epsilon$ 4 group in terms of odd-one-out perceptual discrimination. As a counter-point, it is noteworthy that Stening et al. (2017) adopted the same approach as used in the current chapter but nonetheless found *APOE*  $\epsilon$ 4-related differences in structural covariance (see also Spreng & Turner, 2013). Other studies comparing  $\epsilon$ 4 carriers and non-carriers have likewise found differences between the two groups (e.g. Dennis et al., 2010; Filippini et al., 2009; Hodgetts et al., 2019; Shine et al., 2015). There is thus an open question as to whether the lack of an effect represents a true negative, or whether more subtle genotype effects can account for the inconsistency between this study and related studies.

It is interesting that the observed covariance pattern was less strongly expressed with advancing age. One might expect that lifespan changes in structural covariance might be driven, at least in part, by atrophy – that is, regions degenerating together (Manuello et al., 2017; Plachti et al., 2020). It follows that the expression of the covariance pattern might thus become stronger with advancing age. In the current study, by contrast, the covariance pattern was *less* strongly expressed with advancing age. This is consistent with prior work showing that the expression of structural covariance within large-scale neurocognitive networks declines with advancing age (DuPre & Spreng, 2017; Li et al., 2013; Montembeault et al., 2012; Spreng & Turner,

2013), potentially reflecting reductions in connectivity (Betzel, 2020). The current finding adds to this, showing that this age-related pattern extends to covariance associated with MTL structures. Given that the impact of age was not specific to covariance associated with either the hippocampus or PRC, it could be argued that age impacts the connectivity of both structures, in line with some studies examining fMRI-based functional connectivity within their respective networks (Berron et al., 2020; Das et al., 2015; although for a different pattern of results, see Dautricourt et al., 2021). Future research, ideally using multi-modal imaging methods, should seek to determine whether this in fact the case, as it has potential implications for our collective understanding of the role of these networks in ageing and neurodegenerative disease. Regarding the effect of gender/sex, it is somewhat surprising that the covariance pattern was less strongly expressed in males relative to females, especially independent of *APOE*  $\epsilon$ 4. The results of Chapter 2, alongside the broader literature showing that the effect of this allele is stronger in females (Gamache et al., 2020; Riedel et al., 2016; Ungar et al., 2014), indicates that connectivity – indexed by structural covariance – might be more heavily impacted in female  $\epsilon$ 4 carriers. Previous studies examining fMRI-based functional connectivity provide some support for this prediction (Damoiseaux et al., 2012; Heise et al., 2014). However, the current results provide evidence that the covariance of the hippocampus and PRC is impacted by gender/sex alone (for a related study on gender/sex differences, see Persson et al., 2014), rather than its interaction with *APOE*  $\epsilon$ 4. Owing to the complex and controversial nature of gender/sex effects on the brain and cognition (for interesting discussions, see Rippon et al., 2014, 2021), I avoid post-hoc interpretation of this effect (Figure 3.8). It would be useful to examine the impact of gender/sex on the structural covariance of these two key network nodes in a large-scale replication study, ensuring that the results observed here represent true effects.

Turning to the cognitive correlates of the covariance pattern, it was initially shown that accuracy on both the DMTS task and digit symbol-coding task was negatively associated with brain scores. More specifically, higher accuracy was associated with stronger expression of the covariance pattern

(i.e. more negative brain scores). Mediation analyses, however, revealed that the effect of age accounted for these associations. In this regard, it was not the case that task performance was directly related to brain scores. Rather, task performance was related to brain scores through age. This again underscores the importance of age in the context of the observed pattern of structural covariance.

Despite being the first to compare the structural covariance of the hippocampus and PRC, the current study had a number of limitations that should be considered when interpreting the results. First, it is possible that the seed regions were not small enough to pick up on subtle variation in grey matter volume between the hippocampus and PRC. Indeed, the total volume of the seed regions in this study (total volume =  $23.625\text{mm}^3$ ) was more than twice as large (total volume =  $10.5\text{mm}^3$ ) as that used in a few methodologically similar studies (DuPre & Spreng, 2017; Spreng et al., 2019; Spreng & Turner, 2013). This might explain why the structural covariance analysis only picked up on covariance common to these nearby structures, while also providing support for the idea that the hippocampal seed may have included different regions. That being said, other studies have used masks spanning parts of specific brain structures (e.g. Nordin et al. 2018; Persson et al., 2014; Stening et al., 2017), which are likely much larger than the seeds included here. Second, the current study was unable to correct for head motion beyond simply removing poor quality scans identified through visual inspection. Head motion can introduce systematic and regional biases in anatomical estimation (Alexander-Bloch et al., 2016; Madan, 2018), leading to lower values for grey matter volume and cortical thickness (Reuter et al., 2015). Crucially, head motion is also known to be a particular problem in studies including older adults (Pardoe et al., 2016; Savalia et al., 2017). It is possible, therefore, that the age results observed here are somewhat influenced by motion-related biases. Third, as with Chapter 2, it was not possible to distinguish between healthy and pathological ageing. Without access to A $\beta$  and/or tau PET, it remains extremely difficult – if not impossible – to be certain as to whether the results are due to age-related neurodegenerative disease or more “pure” age-related decline (for relevant

discussions, see Fjell et al., 2014; Jagust, 2013; Walhovd et al., 2014). This remains an issue in most research on age and ageing. Future research incorporating A $\beta$  and/or tau PET would thus be greatly beneficial, providing unique insight into effects that can (and cannot) be attributed to underlying pathology. Fourth, the current study utilised a cross-sectional design. Although convenient, these designs can be influenced by cohort effects (Hedden & Gabrieli, 2004; Ganguili, 2017; Grady, 2012), which means that results may not be due to age per se but rather due to characteristics that vary to year or era of birth. To refine our understanding of how age impacts these large-scale neurocognitive networks and their corresponding representations, longitudinal research using sensitive cognitive tasks and/or high-resolution neuroimaging will be needed.

In addition to the above, it is important to consider the challenges associated with interpreting the observed patterns of structural covariance. It is commonly assumed – including here – that structural covariance reflects some form of connectivity, whether anatomical (e.g. white matter tracts) and/or functional (for relevant discussions, see Alexander-Bloch, Giedd, & Bullmore, 2013; Evans, 2013). Support for this notion comes from studies showing that patterns of structural covariance overlap with connectivity estimates derived from fMRI-based functional connectivity (Clos et al., 2014; Guo et al., 2015; Kelly et al., 2012; Spreng et al., 2019) and diffusion MRI-based tractography (Gong et al., 2012). However, the reported correspondence is far from perfect (Reid et al., 2016), and the biological mechanism underpinning structural covariance remains controversial (Alexander-Bloch, Giedd, & Bullmore, 2013). In a relatively recent attempt to provide insight into the biological basis of structural covariance, Yee et al. (2018) examined the influence of distance, transcriptomic similarity, and anatomical connectivity (i.e. neural tract-tracing) on seed-based structural covariance in the mouse brain. Transcriptomics broadly refers to the analysis of all RNA present in a particular cell, often referred to as the transcriptome (Lowe et al., 2017). Each of these three factors was able to account for variation in structural covariance, although the exact amount varied by brain region (Yee et al., 2018). For example, anatomical connectivity explained the

largest amount of structural covariance in parts of the hindbrain, midbrain, and cortex (Yee et al., 2018). This study highlights a critical point: structural covariance does indeed reflect aspects of connectivity but it likewise reflects other biological factors (Alexander-Bloch, Giedd, & Bullmore, 2013). As such, although I have interpreted the results of the current chapter in the context of connectivity, it is important to recognise that this may not necessarily represent the whole picture. I address this somewhat in the next chapter by utilising a different method for studying connectivity: diffusion MRI-based tractography (see Chapter 1, Box 1).

### 3.5. Summary

To briefly summarise, this chapter identified a pattern of structural covariance common to the hippocampus and PRC but did not identify any patterns unique to either structure. This shared pattern was evident in and around the seed regions, as anticipated, but further included regions in the frontal, temporal, parietal, and occipital lobes. Interestingly, these regions included those previously linked to episodic memory and face/emotion processing, consistent with the findings derived from the NeuroSynth decoder. The four groups (males  $\epsilon 4+$ , female  $\epsilon 4+$ , male  $\epsilon 4-$ , female  $\epsilon 4-$ ) entered into the seed PLS analysis did not differ in the expression of this pattern. When brain scores were extracted and analysed, however, age and gender/sex – but not *APOE*  $\epsilon 4$  – were found to have an impact. Specifically, this analysis revealed that the expression of the covariance pattern was less strongly expressed with advancing age and in males relative to females. Given that structural covariance is argued to in some way index connectivity (Chapter 1, Box 1; see also Alexander-Bloch, Giedd, & Bullmore, 2013; Betzel, 2020), this finding implies that *APOE*  $\epsilon 4$  does not impact the connections of the hippocampus and PRC. Despite this, it is important to note that structural covariance can be influenced by multiple biological factors, not just connectivity, and the study reported in this chapter also had a number of other limitations. This included the size of the seed regions and the inability to correct for head motion, both of which may have increased the likelihood

that the analysis seemed to pick-up on age-related decline in the expression of structural covariance.

In the next chapter, I turn to the question of whether *APOE*  $\epsilon 4$  related alterations in network connectivity are evident early in the adult lifespan, prior to  $A\beta$  accumulation. As discussed in Chapter 1 (see Section 1.3), lifespan systems vulnerability accounts (Bero et al., 2011; Buckner et al., 2005, 2009; Jagust & Mormino, 2011) propose that the  $\epsilon 4$  allele reduces neural efficiency (or “reserve”) in a way that leads to hyper-activation and hyper-metabolism early in life, leading to later susceptibility to  $A\beta$ . One relatively recent small-scale study using diffusion MRI-based tractography extended this, showing that young *APOE*  $\epsilon 4$  carrier exhibit higher levels of FA and lower levels of MD (interpreted as higher structural connectivity) in the PHCB but not the ILF (Hodgetts et al., 2019). I attempt to replicate this finding, owing to its relevance to lifespan vulnerability accounts, while further extending the original work.



## Chapter 4: Impact of *APOE* $\epsilon 4$ on parahippocampal cingulum bundle microstructure in healthy young adults

### 4.1. Introduction

Chapters 2 and 3 sought to investigate the impact of *APOE* genotype and age, as well as sex, on two large-scale neurocognitive MTL networks: the so-called extended hippocampal navigation and feature networks (Murray et al., 2017). As outlined in Chapter 1, this research was motivated in part by lifespan systems vulnerability accounts of cognitive decline and AD (Bero et al., 2011; Buckner et al., 2005, 2009; Jagust & Mormino, 2011). According to this view, the *APOE*  $\epsilon 4$  allele reduces “neural efficiency” in a way that leads to heightened levels of brain activation (i.e. hyper-activation) and metabolism (i.e. hyper-metabolism) early in life, which in turn increases susceptibility to  $A\beta$  accumulation. As the burden of  $A\beta$  increases over time, network dysfunction becomes evident, leading to hypo-activation/hypo-metabolism and ultimately cognitive decline (Busche et al., 2008; Busche & Konnerth, 2016; Palop & Mucke, 2010). Given that structures comprising the extended hippocampal navigation network, such as the PCC/RSC, are among the earliest sites of  $A\beta$  accumulation (Oh et al., 2016; Mattsson et al., 2019; Palmqvist et al., 2017; Villeneuve et al., 2015), one might expect early-life *APOE*  $\epsilon 4$ -related hyper-activation and hyper-metabolism to be evident in this network, increasing later susceptibility to  $A\beta$  (Mishra et al., 2018). Such a suggestion would also be somewhat consistent with reports of deficits in navigation and spatial memory among *APOE*  $\epsilon 4$  carriers (Bierbrauer et al., 2020; Coughlan et al., 2019; Gellersen, Coughlan et al., 2021; Laczó et al., 2011), as this network is thought to support complex conjunctive representations of scenes (Murray et al., 2017).

Support for this prediction and the lifespan systems vulnerability account more broadly comes from functional neuroimaging studies (for a more detailed discussion, see Section 1.3). As outlined previously (see Chapter 2), young *APOE*  $\epsilon 4$  carriers relative to non-carriers have been shown to exhibit

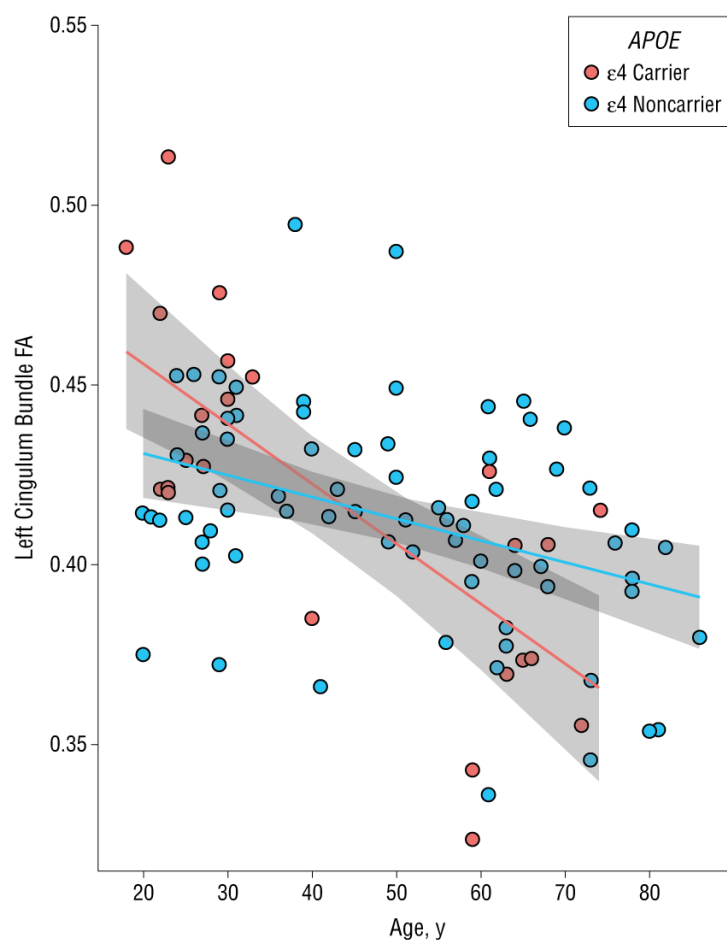
greater task-related activation in the PCC during odd-one-out perceptual discrimination for scenes but not faces/objects (Shine et al., 2015). This mirrors reports of A $\beta$ -related hyper-activation in posteromedial regions (Huijbers et al., 2012; Mormino et al., 2012; Sperling et al., 2009; Vannini et al., 2013), as well as scene-related impairments observed in patients with AD (Lee et al., 2006; see also Lee et al., 2007). Moreover, higher fMRI-based functional connectivity (i.e. hyper-connectivity) between the hippocampus and PCC/RSC has been observed in young *APOE*  $\epsilon$ 4 carriers compared to non-carriers (Filippini et al., 2009; see also Dennis et al., 2010; Zheng et al., 2021). Although there are open questions about the replicability of this finding (Mentink et al., 2021), hippocampal-PCC hyper-connectivity – sometimes referred to as increased synchronisation – has been reported in middle-aged and older *APOE*  $\epsilon$ 4 carriers relative to non-carriers, which in turn was linked to poorer memory performance (Westlye et al., 2011). In this regard, hyper-connectivity within the extended hippocampal navigation network appears to be related to decreased neural efficiency rather than some compensatory mechanism (Elman et al., 2014). Inspired by this line of research, in addition to relevant animal evidence (e.g. Nuriel et al., 2017), it has been proposed that hyper-connectivity precedes hypo-connectivity in the course of AD (Schultz et al., 2017), which is in line with the lifespan systems vulnerability view. A recent MEG study in young adults adds weight to this, observing patterns of hyper-connectivity in young *APOE*  $\epsilon$ 4 carriers and hypo-connectivity in patients with AD (Koelewijn et al., 2019). Together, these findings indicate that *APOE*  $\epsilon$ 4 carriers demonstrate early-life alterations in functional activation, metabolic activity, and functional connectivity within this key neurocognitive network.

A somewhat underexplored question, however, is whether *APOE*  $\epsilon$ 4-related alterations in functional activity and connectivity are associated with concomitant alterations in structural connectivity. Given the close but imperfect correspondence between structural and functional connectivity in the brain (for a discussion, see Suárez et al., 2020), it is plausible that healthy young *APOE*  $\epsilon$ 4 carriers show heightened levels of structural connectivity, which in turn is related to heightened levels of functional

activation and connectivity. In humans, structural connectivity is often assessed at the macro-scale – that is, at the level of large-scale white matter tracts (Betzel, 2020) – via diffusion MRI (for more detail, see Box 1). This method makes it possible to examine the microstructural properties of white matter tracts in vivo, whether at the voxel-level or averaged across reconstructed tracts. As discussed in Chapter 1, higher levels of FA and lower levels of MD – two measures of microstructure – are commonly interpreted as indexing increased myelination and axon density (Beaulieu, 2002), thereby representing “higher” levels of structural connectivity. These measures are also related to functional connectivity (Mollink et al., 2019). In this regard, if the previous prediction were correct, one would expect healthy young *APOE*  $\epsilon$ 4 carriers to demonstrate higher FA and lower MD than non-carriers in relevant white matter tracts, as well as the reverse in older *APOE*  $\epsilon$ 4 carriers. Perhaps the most relevant tract in this context is the PHCB – the primary structural connection between the MTL and PCC/RSC (Jones, Christiansen et al., 2013; Heilbronner & Haber, 2014). In one study using diffusion MRI, lower FA and higher MD were observed in the PHCB of healthy older *APOE*  $\epsilon$ 4 carriers relative to non-carriers (Heise et al., 2014). An additional diffusion MRI study reported an *APOE*  $\epsilon$ 4 by age interaction (Figure 4.1), such that cingulum bundle FA was higher in younger carriers relative to non-carriers but lower in older carriers relative to non-carriers (Felsky & Voineskos, 2013; see also Brown et al., 2011). It should be noted that this particular finding was not specific to the PHCB but rather the cingulum bundle as a whole. Nevertheless, as lower FA and higher MD are often interpreted as lower structural connectivity (although see Box 1), these findings are broadly consistent with the lifespan systems vulnerability view of cognitive decline and AD, and further implicate the extended hippocampal navigation network.

**Figure 4.1.**

*Cingulum Bundle Microstructure as a Function of APOE  $\epsilon$ 4 Carrier Status and Age*



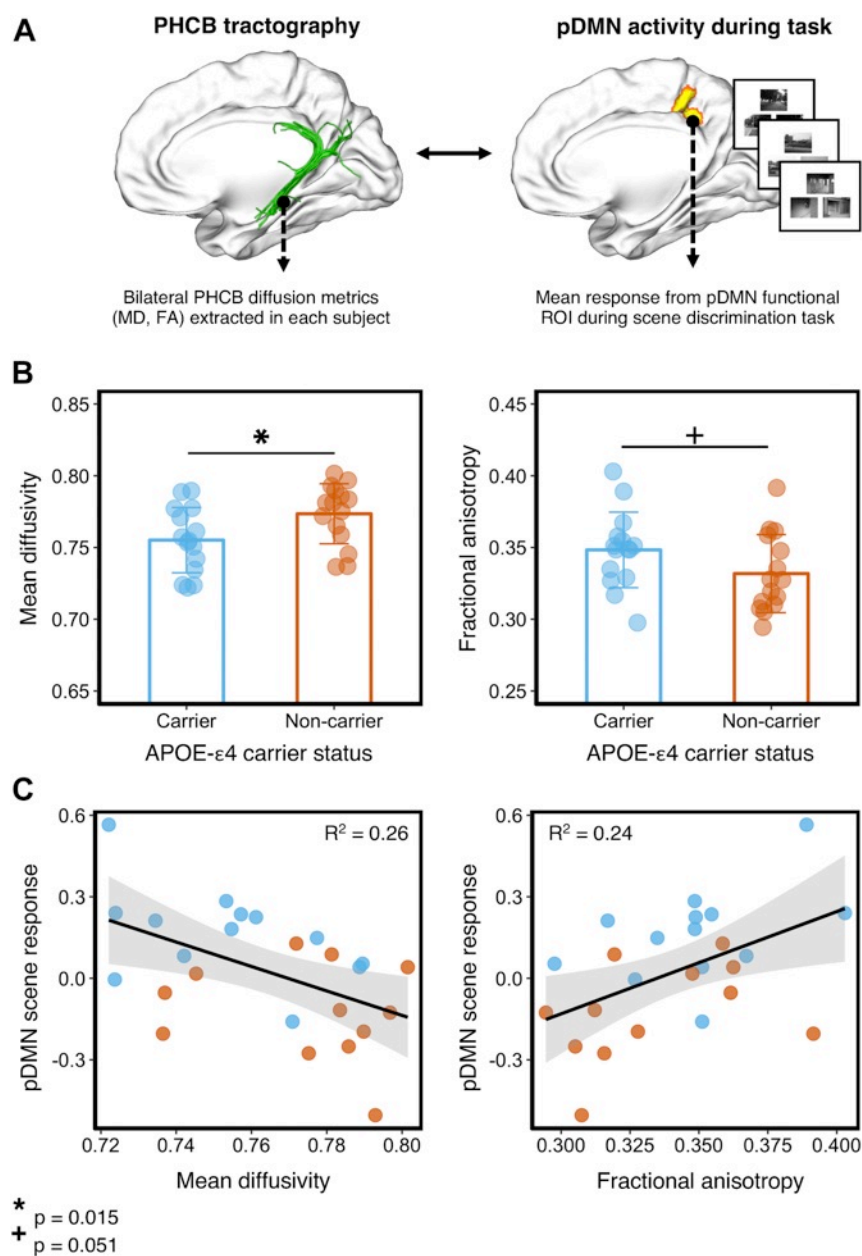
*Note.* FA values for the left cingulum bundle are shown as a function of APOE  $\epsilon$ 4 carrier status and age. Abbreviations: FA = fractional anisotropy. Reprinted from Felsky and Voineskos (2013).

While the above findings indicate that older APOE  $\epsilon$ 4 carriers demonstrate lower FA and higher MD than non-carriers in the PHCB, they do not directly address the question of whether the reverse pattern is true in young APOE  $\epsilon$ 4 carriers. Such an observation would provide evidence that hyper-connectivity is evident in the structural as well as functional connections of the extended hippocampal navigation network, bolstering lifespan systems vulnerability accounts (Bero et al., 2011; Buckner et al., 2005, 2009; Jagust & Mormino, 2011). To investigate this, Hodgetts et al. (2019) used diffusion

MRI-based tractography to examine the impact of *APOE*  $\epsilon 4$  on PHCB microstructure in a sample of young adult participants. The authors reported that *APOE*  $\epsilon 4$  carriers showed higher FA and lower MD than  $\epsilon 4$  non-carriers in the PHCB but not the ILF (Figure 4.2; although for less tract-specific results, see Goltermann et al., 2021). As mentioned in Chapter 1, the ILF is a large association tract that runs from the occipital lobe to the anterior temporal lobe (Catani et al., 2003; Herbet et al., 2018) and is thus proposed to support ventral components of the feature network. This effect was more pronounced when males were removed from the analysis, which is consistent with previous reports of stronger effects in females (e.g. Heise et al., 2014). Crucially, Hodgetts et al. (2019) also found that PHCB microstructure was correlated with increased scene oddity-related activation in the hippocampus, PHC, and PCC (see also Shine et al., 2015). Based on these results and others (e.g. Felsky & Voineskos, 2013), Hodgetts et al. (2019) speculated that the *APOE*  $\epsilon 4$  allele might alter white matter maturation of the late-maturing cingulum bundle (Lebel & Beaulieu, 2011; Lebel et al., 2012), giving rise to an early-life “overshoot” in PHCB microstructure. Subsequently, this overshoot leads to an increase in functional activation (i.e. hyper-activation) and functional connectivity (i.e. hyper-connectivity) within the extended hippocampal navigation network, ultimately increasing network-specific vulnerability to A $\beta$  (Mishra et al., 2018).

**Figure 4.2.**

*APOE  $\epsilon$ 4-Related Differences in PHCB Microstructure and Relationship with Functional Activation During Scene Oddity Performance*



*Note.* Results from Hodgetts et al. (2019). In panel A, a tractography-based reconstruction of the PHCB is shown alongside a scene oddity ROI (Shine et al., 2015). In panel B, differences in PHCB microstructure (FA, MD) between APOE  $\epsilon$ 4 carriers and non-carriers are shown. Finally, in panel C, the relationship between PHCB microstructure and PCC activation is highlighted. Abbreviations: FA = fractional anisotropy, MD = mean diffusivity, pDMN = posterior default mode network, PHCB = parahippocampal cingulum bundle. Reprinted from Hodgetts et al. (2019).

While Hodgetts et al.'s (2019) findings provide support for the presence of early-life *APOE*  $\epsilon 4$ -related alterations in the microstructure of a key white matter tract, the PHCB, it should be noted that the study is not without its limitations. Perhaps the most notable is the modest sample size. With only 15 participants in the  $\epsilon 4$  carrier and non-carrier groups, the study design had 80% power to detect effect sizes as large as Cohen's  $d_s = 0.93$ <sup>1</sup>. In frequentist inference, statistical power refers to the probability of observing an effect of a given size, if an effect exists. There are two often-unappreciated consequences of low statistical power (Button et al., 2013): 1) the probability that an observed effect represents a true effect is reduced, and 2) the magnitude of the observed effect is typically exaggerated (i.e. the "winner's curse"; Ioannidis, 2008). For these reasons, among others, there are growing calls in the field of imaging genetics to increase sample sizes and make replication common practice (e.g. Mitchell, 2017). The original authors themselves acknowledge this, writing "a replication of these effects in a larger independent sample will be required" (Hodgetts et al., 2019, p. 89). It is imperative, therefore, that the replicability of these findings be assessed, especially in light of recent failed replications in this field of research (e.g. Mentink et al., 2021).

Extending this work further, there are additional questions worth exploring. For one, it remains to be seen whether *APOE*  $\epsilon 4$ -related differences in PHCB microstructure are better captured by measures other than FA and MD, which are sensitive to a number of aspects of white matter microstructure without being specific to any one (Jones, Knösche, & Turner, 2013). As discussed previously (see Chapter 1, Box 1), spherical deconvolution approaches attempt to model the diffusion signal as a spherical function with rounded lobes, referred to as the fODF (Tournier et al., 2004). Notably, the fODF not only provides information about the orientation of each fibre component in a given voxel, it also provides information about the fibre population itself (Dell'Acqua & Tournier, 2019). The fODF thus can be

---

<sup>1</sup> Calculated using the *pwr* package (version 1.2-2; Champely, 2018) in R ( $n_1 = 15$ ,  $n_2 = 15$ ,  $\alpha = 0.05$ ,  $1-\beta = 0.8$ , directional hypothesis).

<sup>2</sup> Calculated using the *pwr* package (version 1.2-2; Champely, 2018) in R ( $n_1$

leveraged to derive metrics of diffusion that are more tract-specific than those derived from the diffusion tensor. One such measure is the hindrance modulated orientational anisotropy (HMOA) index, which is defined as the absolute amplitude of each fODF lobe (for a detailed discussion, see Dell'Acqua et al., 2013). This is normalised using a reference amplitude in order to create an index bound between zero and one. A value of zero reflects the absence of a fibre, whereas a value of 1 reflects the highest fODF signal that can realistically be detected in biological tissue (Dell'Acqua et al., 2013). Given that HMOA can describe properties of microstructure specific to a given fibre population, it is argued to be more sensitive to alterations in anisotropy than either FA or MD – that is, metrics derived from DTI (Dell'Acqua et al., 2013). Adding to this, HMOA has been used previously to provide unique insights into the microstructural properties of other tracts, including the pre- and post-commissural fornix (Christiansen et al., 2016), underscoring its potential utility.

Furthermore, while the literature on hemispheric asymmetry of cingulum bundle microstructure in healthy adults is mixed (e.g. Gong et al., 2005; Lebel et al., 2012; Metzler-Baddeley, Jones et al., 2012; Park et al., 2004; Powell et al., 2012; Takao et al., 2010; Thiebaut de Schotten et al., 2011), no study to date has yet examined the extent to which *APOE*  $\epsilon$ 4 carrier status influences hemispheric asymmetry in this tract or its parahippocampal component. Possessing of the  $\epsilon$ 4 allele is relevant here, as prior research has linked AD-related cingulum bundle disruption to right temporoparietal hypo-metabolism, potentially via an indirect route involving the PCC (Villain et al., 2008). An increased rightward asymmetry in white matter networks from healthy controls to MCI to AD has also been observed (Yang et al., 2017). Nevertheless, leftward asymmetry in EC thickness has been reported in middle-aged and older *APOE*  $\epsilon$ 4 carriers (Donix et al., 2012), thereby presenting a mixed picture. This raises an intriguing question: do healthy young *APOE*  $\epsilon$ 4 carriers (relative to non-carriers) show a difference in the asymmetry of tract microstructure? Considering prior research observing higher FA and lower MD in the cingulum bundle of males relative to females (e.g. Lebel & Beaulieu, 2011; Lebel et al., 2012), as well as the proposed



interaction between sex and *APOE*  $\epsilon$ 4 in the context of AD risk (Riedel et al., 2016; Ungar et al., 2014), there is also an interesting question as to whether sex moderates any potential *APOE*  $\epsilon$ 4-related association with hemispheric asymmetry. To address this here, lateralisation indices (LIs) were calculated for the PHCB (and a comparison tract: the ILF), providing per-participant scores that express the degree to which a given metric (FA, MD, HMOA) is higher or lower in a given hemisphere (e.g. Thiebaut de Schotten et al., 2011; Zhao et al., 2016). These LIs were subsequently analysed as a function of *APOE*  $\epsilon$ 4 carrier status, sex, and their interaction.

In the current chapter, I report a study that aimed to replicate Hodgetts et al.'s (2019) finding that healthy young adult *APOE*  $\epsilon$ 4 carriers demonstrate alterations in PHCB microstructure – higher FA, lower MD – relative to non-carriers. To this end, a near-identical experimental procedure was adopted. For example, the same comparison tract used by Hodgetts et al. (2019) – the ILF – was examined to ensure that any effect of *APOE*  $\epsilon$ 4 was tract-specific. A complementary voxel-based approach – TBSS – was also adopted. This replication attempt serves as a robustness check on the original findings, with important implications for lifespan systems vulnerability accounts of cognitive decline and AD (Bero et al., 2011; Buckner et al., 2005, 2009; Jagust & Mormino, 2011). I also report additional analyses that seek to move beyond the original, to-be-replicated findings of Hodgetts et al. (2019). These analyses were designed to address the following aims: 1) whether *APOE*  $\epsilon$ 4 carriers exhibit differences in PHCB HMOA relative to non-carriers, and 2) whether hemispheric asymmetry in tract microstructure is affected by *APOE*  $\epsilon$ 4, as well as sex.

## **4.2. Methods**

### *4.2.1. Participants*

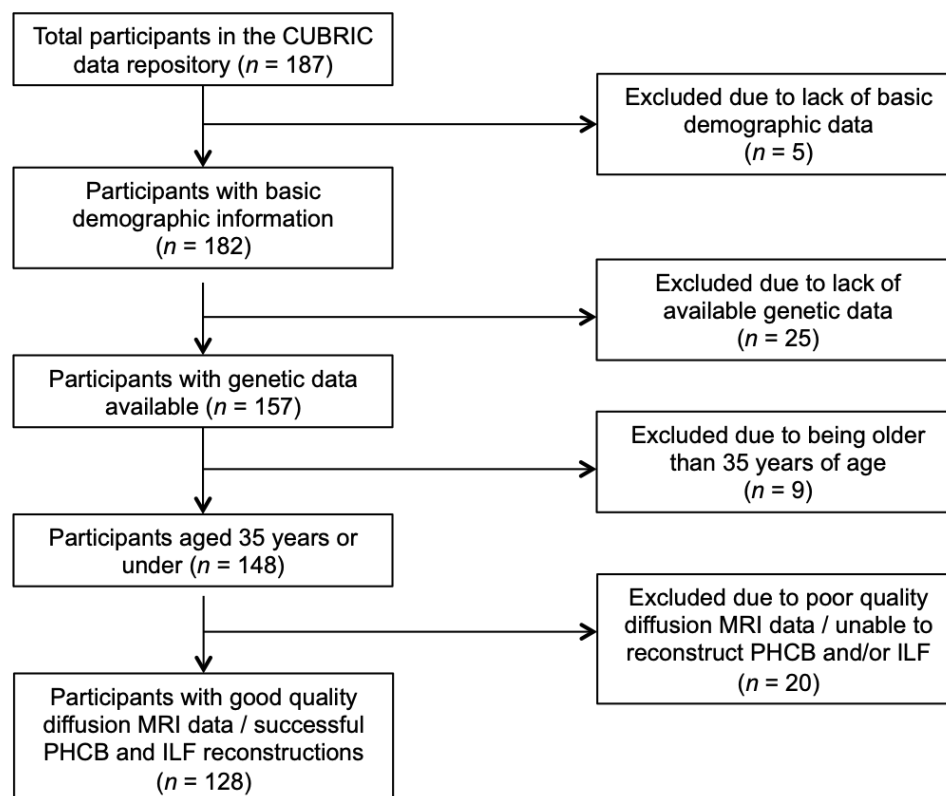
Data used in this chapter were acquired from a repository at the Cardiff University Brain Research Imaging Centre (CUBRIC). Sections of this data have been published elsewhere (e.g. Foley et al., 2017; Koelewijn et al.,

2019). Participants were healthy adults, who were screened via interview or questionnaire for the presence of neuropsychiatric disorders. All were right-handed, had normal or corrected-to-normal vision, and provided consent for their data to be used in genetic-imaging analyses. All procedures were reviewed and approved by the Cardiff University School of Psychology Research Ethics Committee.

Given the focus of the current chapter, I only include participants who completed the necessary diffusion MRI scans, had *APOE* genotype information available, were aged 35 years or under, and passed further quality control procedures (described below). The age cut-off mirrors that used by various other neuroimaging studies examining the impact of the *APOE* genotype on some aspect of brain structure and/or function in young adults (Filippini et al., 2009, 2011; Heise et al., 2011; Persson et al., 2014; Nordin et al., 2018; Stening et al., 2017). A detailed diagram capturing the flow of participants into the final analysis is provided in Figure 4.3. As shown, the final sample comprised 128 participants (86 females, 42 males) aged between 19 and 33 years ( $M = 23.8$ ,  $SD = 3.6$ ). This is more than four times larger than the total sample recruited by Hodgetts et al. (2019) and is comparable to other published studies specifically examining the impact of *APOE*  $\epsilon 4$  on white matter in older participants (e.g. Heise et al., 2014; Westlye et al., 2012). Consistent with Chapter 2 (but not Chapter 3), sex was determined as part of genetic quality control procedures.

**Figure 4.3.**

*Flowchart Capturing the Exclusion Criteria Used and the Number of Participants Removed*



*Note.* Of the total number of participants in the CUBRIC data repository, approximately two-thirds (68.45%) were included in the final sample reported here. Abbreviations: PHCB = parahippocampal cingulum bundle, ILF = inferior longitudinal fasciculus.

#### 4.2.2. *APOE* genotype

*APOE* genotype was inferred from imputed (1000G phase 1, version 3) genome-wide genetic data (for more detail, see Foley et al., 2017). Although *APOE* is often directly genotyped, as in Chapter 3 of this thesis, previous research has demonstrated that it is possible to accurately infer *APOE* genotypes from imputed genetic data (Lupton et al., 2018; Oldmeadow et al., 2014; Radmanesh et al., 2014; Vuoksimaa et al., 2020). Indeed, this is the approach adopted in Chapter 2 of this thesis. Following Hodgetts et al.'s (2019) example, the sample was subsequently split into carrier and non-

carrier groups based on the presence/absence of an *APOE*  $\epsilon 4$  allele. Consistent with the approach adopted in Chapter 3, individuals with the  $\epsilon 2/\epsilon 4$  genotype were included as part of the  $\epsilon 4$  carrier group. This decision was driven by prior research showing that the  $\epsilon 2\epsilon 4$  genotype is associated with higher levels of AD pathology and overall AD risk (Farrer et al., 1997; Goldberg et al., 2020; Jansen et al., 2015; Oveisgharan et al., 2018; Reiman et al., 2020). Overall, the *APOE* genotypic distribution of the available sample was: 40  $\epsilon 4$  carriers (4  $\epsilon 2/\epsilon 4$ , 33  $\epsilon 3/\epsilon 4$ , 3  $\epsilon 4/\epsilon 4$ ) and 82 non- $\epsilon 4$  carriers (4  $\epsilon 2/\epsilon 2$ , 14  $\epsilon 2/\epsilon 3$ , 70  $\epsilon 3/\epsilon 3$ ). Table 4.1 provides a direct comparison of the *APOE* genotypic distribution across studies. Meaningful statistical comparison of the observed frequencies relative to the expected frequencies, as determined by Hodgetts et al. (2019), is challenging as two of the expected cells contain zeros. Consequently, the chi-square goodness of fit test produces a value of infinity when used on the data in Table 4.1 ( $\chi^2(5, N = 128) = \infty, p < .001$ ). While this is not particularly informative, it is clear from the values presented that discrepancies are evident. For instance, the current chapter included a higher proportion of individuals with the  $\epsilon 3/\epsilon 3$  genotype and a lower proportion of individuals with the  $\epsilon 3/\epsilon 4$  genotype relative to Hodgetts et al.'s (2019) sample.

**Table 4.1.**  
*APOE Genotypic Distribution Across Studies*

	<i>APOE</i> $\epsilon 4+$			<i>APOE</i> $\epsilon 4-$		
	$\epsilon 2/\epsilon 4$	$\epsilon 3/\epsilon 4$	$\epsilon 4/\epsilon 4$	$\epsilon 2/\epsilon 2$	$\epsilon 2/\epsilon 3$	$\epsilon 3/\epsilon 3$
Current chapter	4 (3.28%)	33 (27.05%)	3 (2.46%)	4 (3.28%)	14 (11.48%)	70 (57.38%)
Hodgetts et al. (2019)	1 (3.33%)	14 (46.67%)	0 (0%)	0 (0%)	5 (16.67%)	10 (33.33%)

*Note.* Values represent the total number of participants and percentage (%) of the total sample (in parentheses) with each *APOE* genotype. Values are presented for the current chapter and for Hodgetts et al.'s (2019) study. Abbreviations: *APOE*  $\epsilon 4+$  = *APOE*  $\epsilon 4$  carriers, *APOE*  $\epsilon 4-$  = *APOE*  $\epsilon 4$  non-carriers.

#### 4.2.3. MRI acquisition

Scanning was conducted at CUBRIC on a GE SIGNA HDx 3T MRI system (General Electric Healthcare, Milwaukee, WI) with an eight-channel receive-only head coil. Whole-brain high angular resolution diffusion imaging (HARDI) data (Tuch et al., 2002) were acquired using a diffusion-weighted single-shot EPI sequence (TE = 89ms; voxel dimensions = 2.4 x 2.4 x 2.4mm; FOV = 23 x 23cm<sup>2</sup>; acquisition matrix = 96 x 96; 60 slices aligned AC/PC with 2.4mm thickness and no gap). Gradients were applied along 30 isotropic directions (Jones et al., 1999) with  $b = 1200$  s/mm<sup>2</sup>. Three non-diffusion-weighted images were acquired with  $b = 0$  s/mm<sup>2</sup>. Acquisitions were cardiac-gated using a peripheral pulse oximeter. High-resolution T1-weighted anatomical images were acquired using a three-dimensional FSPGR sequence (TR/TE = 7.8/3s; voxel dimensions = 1mm isotropic; FOV ranging from 256 x 256 x 168mm to 256 x 256 x 180mm; acquisition matrix ranging from 256 x 256 x 168 to 256 x 256 x 180; flip angle = 20°). These sequences were near identical to those used by Hodgetts et al. (2019) and,

in addition, both studies acquired data using the same system in the same research centre.

#### *4.2.4. Diffusion MRI*

##### *4.2.4.1. Pre-processing*

The diffusion-weighted data were corrected for motion- and eddy current-induced distortions in ExploreDTI (version 4.8.6; Leemans et al., 2009), which implements an appropriate reorientation of the b-matrix (Leemans & Jones, 2009). Images were registered to down-sampled T1-weighted images (1.5mm isotropic resolution) to correct for EPI/susceptibility deformations (Irfanoglu et al., 2012). Data were visually checked as part of quality assurance procedures, leading to the removal of two participants from analysis. As an additional step, the two-compartment free water elimination (FWE) procedure (Pasternak et al., 2009) was applied post-hoc to correct for voxel-wise partial volume artefacts. Free water – defined as water molecules that are unrestricted but do not experience flow – is found as cerebrospinal fluid in the ventricles and around the parenchyma of the human brain. This becomes problematic when voxels contain both brain tissue and cerebrospinal fluid, as the resulting voxel-wise diffusion measures will reflect the weighted average of both tissue types (Alexander et al., 2001; Pfefferbaum & Sullivan, 2003; Vos et al., 2011). This particular partial volume artefact, often referred to as cerebrospinal fluid contamination, can negatively impact the ability to delineate white matter tracts located near to the ventricles, including the cingulum (Metzler-Baddeley, O’Sullivan et al., 2012). The FWE procedure proposed by Pasternak et al. (2009) addresses this by fitting a bi-tensor model with two compartments – one isotropic, one anisotropic – to the diffusion signal, thereby making it possible to differentiate between the diffusion characteristics of cerebrospinal fluid and tissue. Its application has been shown to improve tract delineation, as well as the sensitivity and specificity of measures traditionally derived from DTI (Albi et al., 2017; Edde et al., 2020; Metzler-Baddeley, O’Sullivan et al., 2012; Salminen et al., 2016).

#### 4.2.4.2. *Tractography*

Deterministic tractography was based on the modified damped Richardson Lucy (dRL) spherical deconvolution algorithm (Dell'Acqua et al., 2010). Spherical deconvolution approaches are capable of extracting multiple peaks in the white matter fODF within a given voxel, making it possible to model complex fibre arrangements such as crossing fibres (Dell'Acqua & Tournier, 2019; see also Box 1). The current study and the original study by Hodgetts et al. (2019) both used spherical deconvolution approaches, although Hodgetts et al. (2019) used constrained spherical deconvolution. While this might feasibly lead to differences between the two studies (Parker et al., 2013), it is worth noting that, relative to the standard constrained algorithm, the dRL algorithm reduces spurious fibre orientations that can negatively impact tracking (Dell'Acqua et al., 2010). An additional advantage of dRL is that it can also be used to calculate the HMOA index. To minimise any further discrepancies between the studies, tracts were reconstructed using the same parameters used by Hodgetts et al. (2019) (fODF amplitude threshold = 0.1; step size = 0.5mm; angle threshold = 60°).

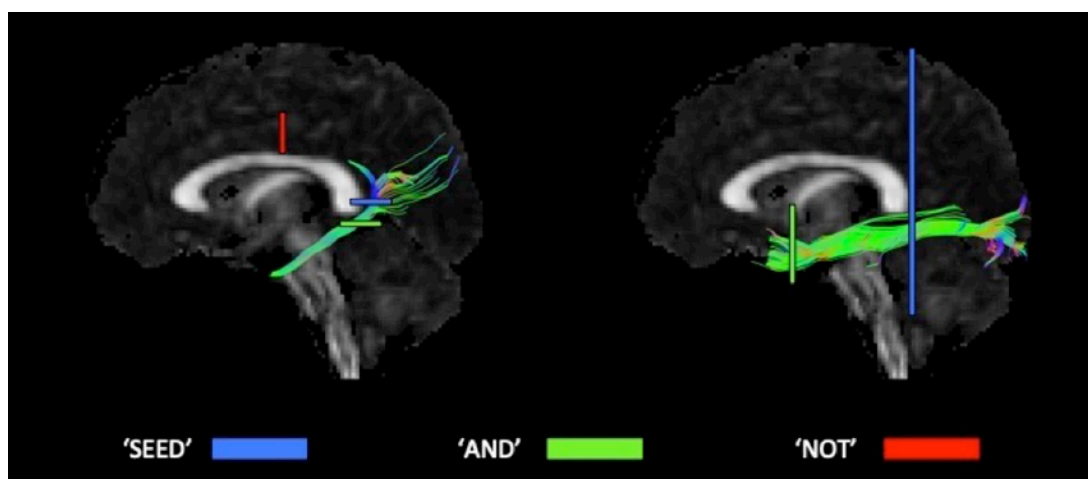
#### 4.2.4.3. *Automated tract reconstruction*

Automated tractography software (Parker et al., 2012) was used to generate three-dimensional reconstructions of the PHCB and ILF in both hemispheres. The software was trained on manual reconstructions ( $n = 18$ ) generated using a waypoint ROI approach in ExploreDTI (version 4.8.6; Leemans et al., 2009), where "SEED", "AND", and "NOT" ROIs were used to isolate tract-specific streamlines. For consistency, ROIs were placed in the same regions as described by Hodgetts et al. (2019). Placement was therefore guided by established protocols for the PHCB (Jones, Christiansen et al., 2013) and ILF (Wakana et al., 2007), respectively (Figure 4.4). All reconstructions generated by the automated software were visually inspected and, where required, manually edited post hoc to remove erroneous, anatomically implausible fibres. Participants for whom the PHCB and ILF could not be reconstructed in both hemispheres were removed from analysis. Thereafter,

tract-specific measures of microstructure (FA, MD, HMOA) were obtained. Although the (semi-)automated approach used here differs to that used by Hodgetts et al. (2019), the number of participants included made an exclusively manual approach impractical.

**Figure 4.4.**

*ROI Placement Used to Manually Reconstruct White Matter Tracts*



*Note.* ROI placement used to manually reconstruct the PHCB (left) and ILF (right). To ensure the reconstructions were accurate, additional “NOT” ROIs were added where necessary. The resulting tract reconstructions were then used to train the automated tractography software (Parker et al., 2012).

#### 4.2.4.4. TBSS

Voxel-wise statistical analysis of the FA and MD data was conducted using TBSS (Smith et al., 2006). Each participant’s FWE-corrected FA and MD maps were first aligned in standard MNI space using nonlinear registration (Andersson et al., 2007a, 2007b). Next, the mean FA images were created and subsequently thinned (threshold = 0.2) to generate the mean FA skeleton, which represents the centre of all tracts common to the group. Each participant’s aligned FA and MD data were then projected onto the skeleton and the resulting data carried forward for voxel-wise cross-subject analysis. These analyses were performed using *randomise*, a permutation-



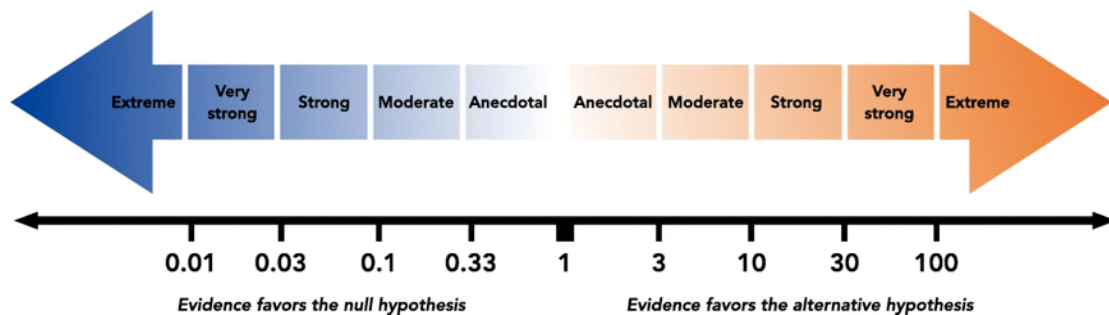
based inference tool. For both FA and MD, a general linear model contrasting *APOE*  $\epsilon 4$  carriers and non-carriers was applied using this tool ( $n$  permutations = 1000). Mirroring Hodgetts et al.'s (2019) example, analyses were restricted to the PHCB using an ROI mask [labelled “cingulum (hippocampus)"] from the John Hopkins University ICBM-DTI-81 white-matter tractography atlas. Statistically significant clusters were extracted using threshold-free cluster enhancement (TFCE; Smith and Nichols, 2009) with a corrected  $\alpha$  level of 0.05.

#### 4.2.5. Statistical analyses

With the exception of TBSS, all statistical analyses were conducted using R (version 3.6.0; R Core Team, 2019) in RStudio (version 1.3.1093; RStudio Team, 2020). In line with Hodgetts et al.'s (2019) study, both frequentist and Bayesian hypothesis testing approaches were adopted (for an overview of these approaches, see Ortega & Navarette, 2017). In frequentist NHST, a  $p$ -value is calculated denoting the conditional probability of observing the data, or more extreme data, assuming the null hypothesis is true. If the observed  $p$ -value falls below a pre-determined  $\alpha$  level, the result is typically declared “statistically significant” and the null hypothesis is rejected (see Chapters 2 and 3). Consistent with Hodgetts et al.'s (2019) study, here the nominal  $\alpha$  level was set at 0.05 (although see Lakens et al., 2018). Following Hodgetts et al.'s (2019) example further, a standardised measure of effect size – Cohen's  $d_s$  for between-subjects comparisons, Cohen's  $d_z$  for within-subjects comparisons (Lakens, 2013) – was calculated to facilitate interpretation. Inspired by a recent proposal, an additional measure of effect size – Hedges'  $g_s^*$  – was likewise calculated for between-subjects comparisons (Delacre et al., 2021). This was performed via the following Shiny app: <https://effectsize.shinyapps.io/deffsize/>.

Despite its near-universal adoption in many fields of scientific inquiry, frequentist NHST has been widely criticised on numerous grounds, including the inability to provide evidence in favour of the null (for an example, see Szucs & Ioannidis, 2017b). While a thorough discussion of these criticisms is

beyond the scope of this thesis, it is worth briefly discussing one in the context of this chapter: the (in)ability to evaluate replication success. In frequentist NHST, the outcome of a replication attempt is evaluated by examining  $p$ -values across studies. That is, replication is deemed successful only if the effect is associated with a  $p$ -value less than a given  $\alpha$  level in both the original and replication study. However, as a difference in statistical significance does not necessarily indicate that the difference itself is statistically significant (Gelman & Stern, 2006), and because statistical power can differ across studies, this approach can lead to erroneous conclusions (for various discussions of this problem, see Asendorpf et al., 2013; Cumming, 2008; Dienes, 2014; Szucs & Ioannidis, 2017b; Simonsohn, 2015; Verhagen & Wagenmakers, 2014). For this reason, Bayes factors (BFs) were calculated as part of a complementary Bayesian hypothesis testing approach. BFs quantify the degree to which the observed data favours predictions made by two models, typically the null hypothesis and the alternative hypothesis (Morey et al., 2014). In this regard, unlike frequentist NHST, BFs are capable of providing evidence in support of the null (Mulder & Wagenmakers, 2016). BFs can be calculated for many different designs, including  $t$ -tests and ANOVAs. In accordance with the evidence categories outlined by Lee & Wagenmakers (2013), a  $BF_{+0}$  ( $BF_{10}$  for two-sided tests) greater than 3 was considered to represent at least moderate evidence for the alternative hypothesis, whereas a  $BF_{+0}$  less than 0.33 was considered to represent at least moderate evidence for the null hypothesis (Figure 4.5).

**Figure 4.5.***Proposed BF Evidence Categories*

*Note.* Lee and Wagenmakers's (2013) proposed BF ( $BF_{+0}$  or  $BF_{10}$ ) evidence categories. While strict adherence to this classification in all research contexts is ill advised, it nevertheless provides a useful frame of reference. Reprinted from Quintana and Williams (2018).

#### 4.2.5.1. Primary (replication) analyses

To test whether *APOE*  $\epsilon 4$  carriers showed higher FA and lower MD in the bilateral PHCB and ILF compared to non-carriers, one-sided Welch's *t*-tests were conducted. This test has been recommended as the default method of comparing groups of unequal size, as is the case in the current chapter (Delacre et al., 2017). Mirroring Hodgett's et al.'s (2019) example, all tests were repeated again, once with male participants removed and once with  $\epsilon 2$  carriers removed. These steps were performed independently of one another. To ensure that the probability of falsely rejecting the null – the Type I error rate – was not inflated, a Bonferroni correction was applied to the  $\alpha$  level ( $.05 / 3 = .016$ ). Two BFs were also calculated in the current chapter: a default JZS BF and a replication BF. The default JZS BF, which uses a default prior distribution and was computed using the *BayesFactor* package (version 0.9.12-4.2; Morey & Rouder, 2018), examines whether an effect is present or absent in the data collected in the replication study, regardless of the original effect. Here, one-sided (directional) default JZS BFs were used (Morey & Wagenmakers, 2014). The replication BF, by contrast, uses the posterior distribution of the original study as the prior distribution in the

replication study, thereby examining whether the original effect is present or absent in the data collected in the replication study. This BF was computed using previously published R code (Verhagen & Wagenmakers, 2014).

#### 4.2.5.2. Secondary (extension) analyses

##### 4.2.5.2.1. HMOA

Given the lack of a directional hypothesis relating to bilateral HMOA, two-sided Welch's *t*-tests and two-sided default JZS BFs were used to identify any differences between *APOE*  $\epsilon 4$  carriers and non-carriers. In line with the primary (replication) analyses described above, these tests were repeated with males removed and then with  $\epsilon 2$  carriers removed. These analytical steps were performed independently. As part of the frequentist NHST analysis, a Bonferroni correction was applied to the  $\alpha$  level ( $.05 / 3 = .016$ ).

##### 4.2.5.2.2. Hemispheric asymmetry in PHCB and ILF microstructure: Impact of *APOE* $\epsilon 4$ and sex

Inspired by the mixed findings regarding the hemispheric asymmetry of FA and to a lesser degree MD in the cingulum bundle as a whole (e.g. Gong et al., 2005; Lebel et al., 2012; Park et al., 2004; Powell et al., 2012; Takao et al., 2010; Thiebaut de Schotten et al., 2011), as well as reports of grey matter and white matter asymmetry related to AD (e.g. Donix et al., 2012; Villain et al., 2008; Yang et al., 2017), microstructural measures were first compared across hemispheres, irrespective of *APOE*  $\epsilon 4$  carrier status (i.e. across all participants). This analysis – conducted using two-sided paired-samples *t*-tests and equivalent default JZS BFs – aimed to provide insight into whether hemispheric asymmetry is evident in a specific portion of the cingulum bundle, the PHCB, and further extends the existing literature by examining HMOA. As with the analyses described previously, the ILF was included as a comparison tract. Thereafter, LIs were calculated for FA, MD, and HMOA in both the PHCB and ILF [ $LI = (\text{left} - \text{right}) / (\text{left} + \text{right})$ ]. For any given participant, a negative LI score indicates that a particular

microstructural measure is higher in the right hemisphere, whereas a positive LI score indicates that a particular microstructural measure is higher in the left hemisphere. These LI scores were subsequently analysed using robust multiple linear regression, which was carried out via the *lmrob* function from the *robustbase* package (version 0.93-7; Maechler et al., 2021; see also Chapter 3). The fitted models were as follows:

$$LI \sim APOE \epsilon 4 \text{ carrier status} \times \text{sex} + \text{age}$$

LIs were entered as dependent variables. *APOE*  $\epsilon 4$  carrier status and sex were treated as categorical variables and coded using deviation coding. Age – the only continuous variable – was centred and scaled. The interaction between *APOE*  $\epsilon 4$  carrier status and sex was included in the model, as outlined in Section 4.1. Results were deemed statistically significant if the observed *p*-value was smaller than, or equal to, the nominal  $\alpha$  level of 0.05.

### 4.3. Results

#### 4.3.1. Sample characteristics

As outlined in Section 4.2.1, the final sample included 128 participants (86 females, 42 males) aged between 19 and 33 ( $M = 23.8$  years;  $SD = 3.6$ ). A sensitivity analysis revealed that, for the primary (replication) analysis, the current study was sufficiently powered ( $1 - \beta = .80$ ) to detect an effect as large as Cohen's  $d_s = 0.48^2$ . Table 4.2 provides a summary of the basic sample characteristics separated by *APOE*  $\epsilon 4$  carrier status. To examine whether carrier and non-carrier groups differed in terms of these basic characteristics, which may therefore impact interpretation of the results, preliminary frequentist NHST (Welch's *t*-test, chi-square test of independence) and BF analyses were conducted. No significant differences were observed between carriers and non-carriers in terms of age ( $t(84.84) = -0.226$ ,  $p = .822$ ,

---

<sup>2</sup> Calculated using the *pwr* package (version 1.2-2; Champely, 2018) in R ( $n_1 = 40$ ,  $n_2 = 88$ ,  $\alpha = 0.05$ ,  $1 - \beta = 0.8$ , directional hypothesis).

Cohen's  $d_s = -0.042$ , Hedges'  $g_s^* = -0.042$ ) or sex ( $\chi^2(1, N = 128) = 0.209, p = .648, \phi = 0.04$ ). In addition, complementary BF analyses provided moderate evidence in favour of the null for  $\epsilon 4$ -related differences in both age ( $BF_{10} = 0.206$ ) and sex ( $BF_{10} = 0.241$ ).

**Table 4.2.**

*Basic Sample Characteristics Separated By APOE  $\epsilon 4$  Carrier Status.*

	<i>APOE <math>\epsilon 4+</math></i> ( $n = 40$ )	<i>APOE <math>\epsilon 4-</math></i> ( $n = 88$ )
Age (years)	23.9 (3.3)	23.7 (3.7)
Sex (M/F)	12 / 28	30 / 58

*Note.* Values represent the mean and standard deviation (in parentheses) or the number of participants. Although sex was self-reported, it was checked against chromosomal sex as part of genetic quality control procedures (see Section 4.2.1). Abbreviations: *APOE  $\epsilon 4+$*  = *APOE  $\epsilon 4$  carrier*, *APOE  $\epsilon 4-$*  = *APOE  $\epsilon 4$  non-carrier*, M = male, F = female.

#### 4.3.2. Primary (replication) analyses

##### 4.3.2.1. Impact of APOE $\epsilon 4$ on bilateral PHCB FA and MD

FA values for the PHCB – separated by *APOE  $\epsilon 4$  carrier status* – are shown in Figure 4.6A. Contrary to expectations, PHCB FA was not significantly higher for *APOE  $\epsilon 4$  carriers* than non-carriers ( $t(87.559) = -0.606, p = .727$ , Cohen's  $d_s = -0.112$ , Hedges'  $g_s^* = -0.111$ ). Supporting this, BF analysis produced moderate evidence in favour of the null (default JZS  $BF_{+0} = 0.138$ , replication  $BF_{10} = 0.141$ ). Removing males from the analysis did not alter the results in any meaningful way ( $t(57.685) = 0.045, p = .482$ , Cohen's  $d_s = 0.01$ , Hedges'  $g_s^* = 0.01$ , default JZS  $BF_{+0} = 0.246$ , replication  $BF_{10} = 0.169$ ), nor did removing  $\epsilon 2$  carriers ( $t(84.459) = -0.923, p = .821$ , Cohen's  $d_s = -0.183$ , Hedges'  $g_s^* = -0.182$ , default JZS  $BF_{+0} = 0.125$ , replication  $BF_{10} = 0.271$ ).

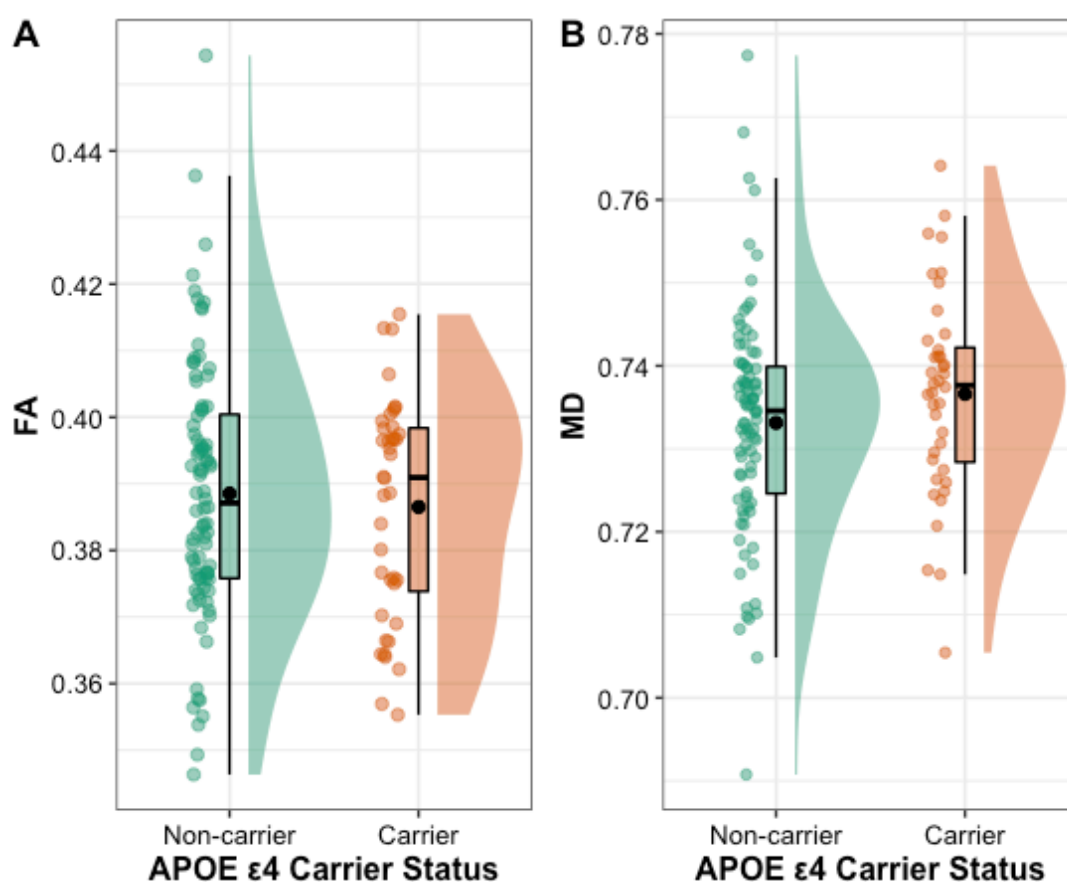
MD values for the PHCB – separated by *APOE*  $\epsilon 4$  carrier status – are shown in Figure 4.6B. Again, contrary to expectations, PHCB MD was not significantly lower for *APOE*  $\epsilon 4$  carriers than non-carriers ( $t(83.625) = 1.429$ ,  $p = .922$ , Cohen's  $d_s = 0.265$ , Hedges'  $g_s^* = 0.265$ ). In accordance with this frequentist analysis, BF analysis revealed strong evidence in favour of the null (default JZS  $BF_{+0} = 0.092$ , replication  $BF_{10} = 0.057$ ). As with FA, the results for MD did not change substantively after removing males ( $t(59.729) = 1.515$ ,  $p = .933$ , Cohen's  $d_s = 0.341$ , Hedges'  $g_s^* = 0.338$ , default JZS  $BF_{+0} = 0.106$ , replication  $BF_{10} = 0.054$ ) or after removing  $\epsilon 2$  carriers ( $t(79.581) = 1.328$ ,  $p = .906$ , Cohen's  $d_s = 0.267$ , Hedges'  $g_s^* = 0.264$ , default JZS  $BF_{+0} = 0.103$ , replication  $BF_{10} = 0.1$ ).

Although these findings clearly differ to those reported by Hodgetts et al. (2019), it is noteworthy that their study included participants that were, on average, younger ( $\epsilon 4+$ :  $M = 19.7$ ,  $SD = 0.8$ ;  $\epsilon 4-$ :  $M = 19.7$ ,  $SD = 0.9$ ) than those included in this study ( $\epsilon 4+$ :  $M = 23.9$ ,  $SD = 3.3$ ;  $\epsilon 4-$ :  $M = 23.7$ ,  $SD = 3.7$ ). Recent research provides evidence of maturational changes in the white matter microstructure of the PHCB over this age range (Tsuchida et al., 2021; see the appendix, Section 6.6). As such, one possibility is that *APOE*  $\epsilon 4$ -related early-life differences in PHCB microstructure are only evident in late adolescence/very early adulthood rather than in early adulthood more generally. An exploratory analysis was conducted to explore this possibility with participants aged 22 years or above removed. This produced a sample of 41 participants (34 females, 7 males) aged between 19 and 21 ( $M = 20.3$ ,  $SD = 0.7$ ). Of these participants, 13 were *APOE*  $\epsilon 4$  carriers (1  $\epsilon 2/\epsilon 4$ , 11  $\epsilon 3/\epsilon 4$ , 1  $\epsilon 4/\epsilon 4$ ) and 28 were *APOE*  $\epsilon 4$  non-carriers (2  $\epsilon 2/\epsilon 2$ , 4  $\epsilon 2/\epsilon 3$ , 22  $\epsilon 3/\epsilon 3$ ). Even in this younger sample, however, analysis revealed that PHCB FA was not significantly higher in carriers than non-carriers ( $t(24.602) = -0.001$ ,  $p = .5$ , Cohen's  $d_s < 0.001$ , Hedges'  $g_s^* < 0.001$ ). BF analysis added to this, providing moderate-anecdotal evidence in support of the null (default JZS  $BF_{+0} = 0.323$ , replication  $BF_{10} = 0.379$ ). In addition, analysis also revealed that PHCB MD was not significantly lower in carriers than non-carriers ( $t(17.685) = -0.033$ ,  $p = .513$ , Cohen's  $d_s = 0.012$ , Hedges'  $g_s^* = 0.012$ ). As with FA, the BF analysis provided moderate evidence in favour of

the null (default JZS  $BF_{+0} = 0.315$ , replication  $BF_{10} = 0.237$ ). This exploratory analysis thus casts doubt on the notion that age differences across studies can account for the results.

**Figure 4.6.**

*Differences in PHCB Microstructure Between APOE  $\epsilon 4$  Carriers and Non-Carriers*



*Note.* Differences in PHCB FA (A) and MD (B) between APOE  $\epsilon 4$  carriers and non-carriers are shown. Individual data points, each representing a single participant, are shown alongside boxplots and density plots. A small amount of jitter has been added to each point for clarity. To facilitate interpretation, the mean value (black circle) and median value (a black line) for each group are both shown. The equivalent result in Hodgetts et al.'s (2019) study is shown in Figure 4.2. Abbreviations: FA = fractional anisotropy, MD = mean diffusivity.



#### 4.3.2.2. Impact of APOE $\epsilon 4$ on bilateral ILF FA and MD

Matching Hodgetts et al.'s (2019) study, the same analysis was conducted on the microstructure (FA, MD) of a comparison tract: the ILF. FA values for the ILF – separated by APOE  $\epsilon 4$  carrier status – are shown in Figure 4.7A. Analysis revealed that ILF FA was not significantly higher for APOE  $\epsilon 4$  carriers than non-carriers ( $t(86.143) = -0.864$ ,  $p = .805$ , Cohen's  $d_s = -0.16$ , Hedges'  $g_s^* = 0.159$ ). BF analysis provided moderate-to-strong evidence favouring the absence of an effect (default JZS  $BF_{+0} = 0.12$ ), as well as anecdotal-to-moderate evidence favouring the absence of the effect reported by Hodgetts et al. (2019) (replication  $BF_{10} = 0.308$ ). This slight discrepancy between BFs is likely due to the fact that the original to-be-replicated effect was also small (n.b. and non-significant in the frequentist NHST analysis), meaning that the informed prior used was already more “sceptical” than the default prior. Results remained largely unchanged when males were removed ( $t(49.129) = -0.069$ ,  $p = .527$ , Cohen's  $d_s = -0.016$ , Hedges'  $g_s^* = -0.016$ , default JZS  $BF_{+0} = 0.226$ , replication  $BF_{10} = 0.308$ ) and when  $\epsilon 2$  carriers were removed<sup>3</sup> ( $t(79.5) = -0.893$ ,  $p = .813$ , Cohen's  $d_s = -0.179$ , Hedges'  $g_s^* = -0.178$ , default JZS  $BF_{+0} = 0.126$ ).

MD values for the ILF – separated by APOE  $\epsilon 4$  carrier status – are shown in Figure 4.7B. Analysis showed that ILF MD was not significantly lower for APOE  $\epsilon 4$  carriers than non-carriers ( $t(81.941) = 0.54$ ,  $p = .705$ , Cohen's  $d_s = 0.101$ , Hedges'  $g_s^* = 0.101$ , default JZS  $BF_{+0} = 0.142$ , replication  $BF_{10} = 0.446$ ). Removing males had no notable impact on the results ( $t(55.856) = 0.818$ ,  $p = .792$ , Cohen's  $d_s = 0.187$ , Hedges'  $g_s^* = 0.185$ , default JZS  $BF_{+0} = 0.144$ , replication  $BF_{10} = 0.613$ ) nor did removing APOE  $\epsilon 2$  carriers<sup>4</sup> ( $t(75.242) = 0.713$ ,  $p = .761$ , Cohen's  $d_s = 0.145$ , Hedges'  $g_s^* = 0.144$ , default JZS  $BF_{+0} = 0.137$ ).

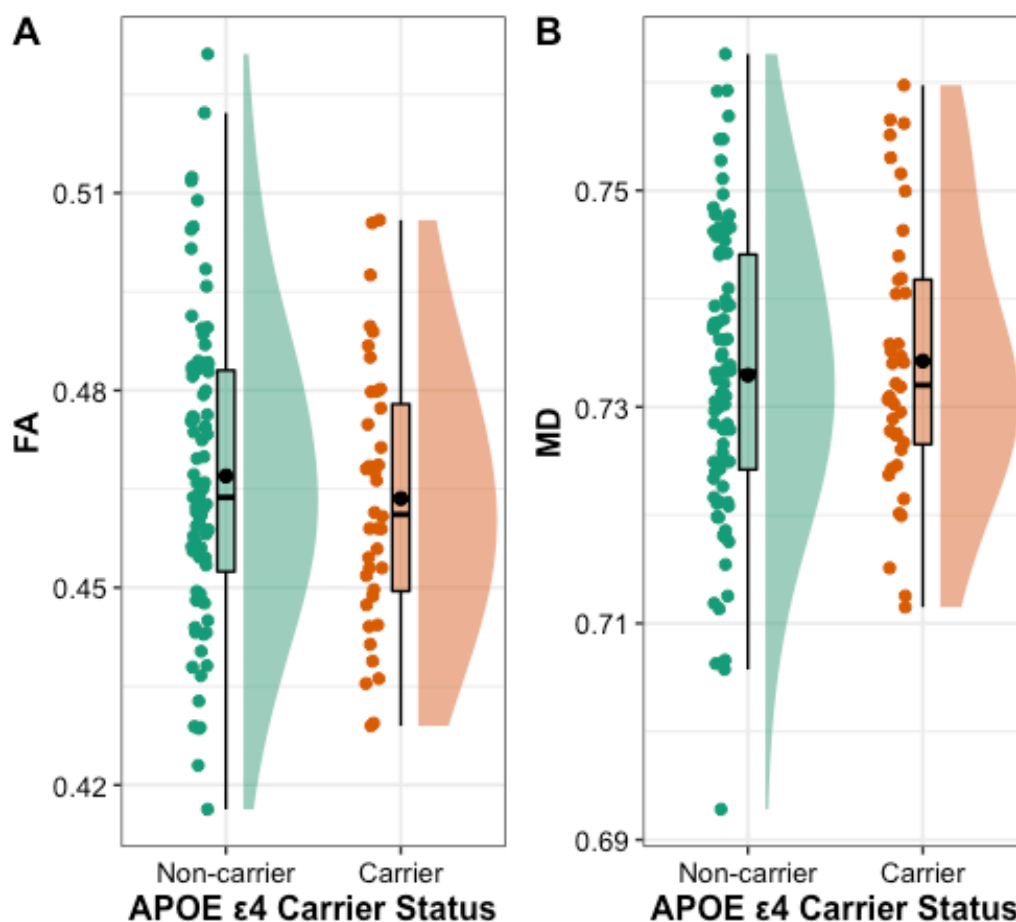
---

<sup>3</sup> A replication BF could not be conducted for this particular analysis, as Hodgetts et al. (2019) did not report the required test statistics.

<sup>4</sup> A replication BF could not be conducted for this particular analysis, as Hodgetts et al. (2019) did not report the required test statistics.

**Figure 4.7.**

*Differences in ILF Microstructure Between APOE  $\epsilon$ 4 Carriers and Non-Carriers*



*Note.* Differences in ILF FA (A) and MD (B) between APOE  $\epsilon$ 4 carriers and non-carriers are shown. Individual data points, each representing a single participant, are shown alongside boxplots and density plots. A small amount of jitter has been added to each point for clarity. To facilitate interpretation, the mean value (black circle) and median value (a black line) for each group are both shown. Abbreviations: FA = fractional anisotropy, MD = mean diffusivity.

#### 4.3.2.3. TBSS

Consistent with the tractography analysis, no TFCE-corrected clusters were observed for FA or MD in the PHCB. This differed from Hodgetts et al.'s (2019) study, which reported a significant TFCE-corrected cluster in the right

posterior portion of the PHCB for FA. Adopting an uncorrected  $\alpha$  level of  $p = .005$ , as has been done previously (e.g. Hodgetts et al., 2019; Postans et al., 2014), did not alter the results.

#### 4.3.3. Secondary (extension) analyses

##### 4.3.3.1. Impact of *APOE* $\epsilon 4$ on bilateral PHCB and ILF HMOA

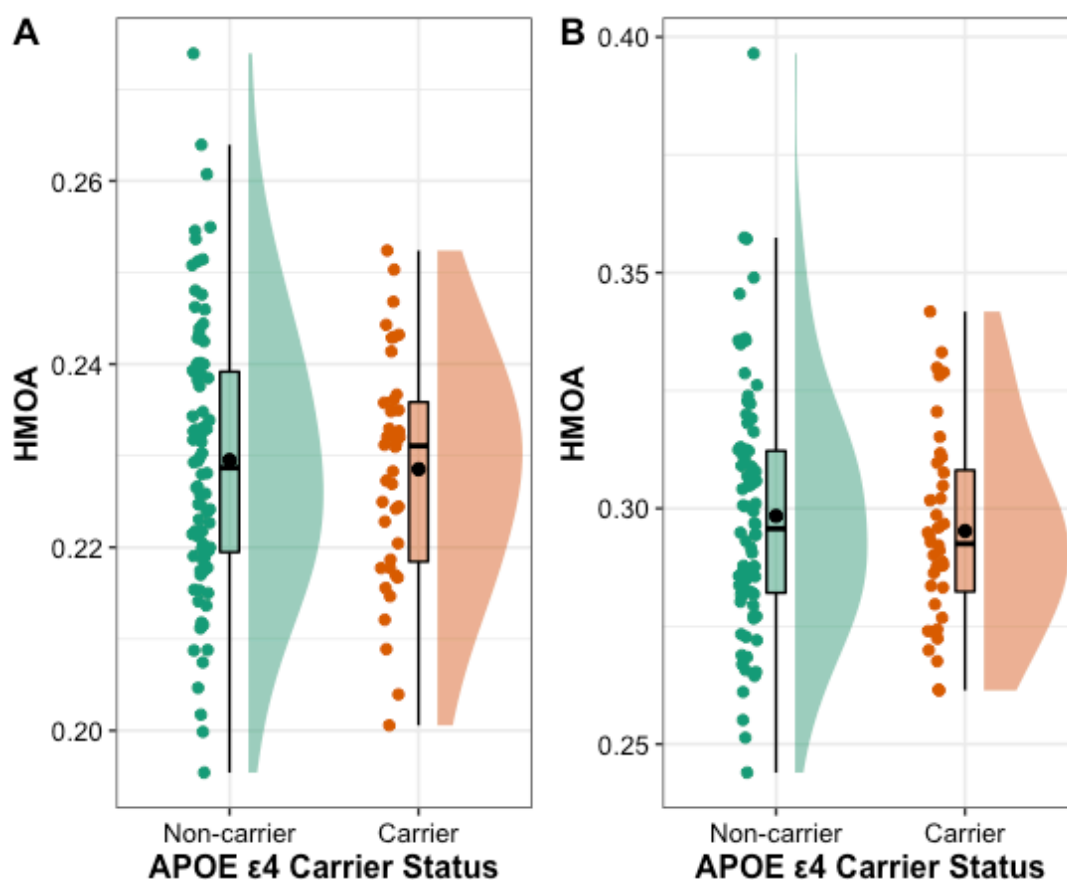
Although the primary analyses did not replicate Hodgetts et al.'s (2019) findings regarding *APOE*  $\epsilon 4$ -related differences in PHCB FA and MD, it remained possible that differences were evident in PHCB HMOA. Indeed, it has previously been proposed that HMOA is more sensitive to alterations in diffusion than either FA or MD (Dell'Acqua et al., 2013), thereby adding weight to this argument. However, as shown in Figure 4.8A, HMOA values for the PHCB did not visibly differ by *APOE*  $\epsilon 4$  carrier status. Subsequent frequentist NHST analysis revealed no significant difference between  $\epsilon 4$  carriers and non-carriers in terms of PHCB HMOA ( $t(90.357) = -0.399$ ,  $p = .691$ , Cohen's  $d_s = -0.073$ , Hedges'  $g_s^* = 0.144$ ). BF analysis also provided moderate evidence in favour of the null (default JZS  $BF_{10} = 0.215$ ). These results were largely unaffected by the removal of males ( $t(58.33) = 0.445$ ,  $p = .658$ , Cohen's  $d_s = 0.101$ , Hedges'  $g_s^* = 0.1$ , default JZS  $BF_{10} = 0.258$ ) or the removal of  $\epsilon 2$  carriers ( $t(85.926) = -0.844$ ,  $p = .401$ , Cohen's  $d_s = -0.167$ , Hedges'  $g_s^* = -0.166$ , default JZS  $BF_{10} = 0.283$ ). These analyses further bolster the results from Section 4.3.2, suggesting that young *APOE*  $\epsilon 4$  carriers and non-carriers did not differ in terms of PHCB microstructure.

For completeness, the same analysis was conducted for ILF HMOA. Figure 4.8B provides an overview of these values separated by *APOE*  $\epsilon 4$  carrier status. Analysis showed that *APOE*  $\epsilon 4$  carriers and non-carriers did not differ significantly in terms of ILF HMOA ( $t(94.682) = -0.762$ ,  $p = .448$ , Cohen's  $d_s = -0.139$ , Hedges'  $g_s^* = -0.138$ ). BF analysis provided complementary evidence, largely favouring the null (default JZS  $BF_{10} = 0.251$ ). This remained true when males were removed ( $t(48.941) = 0.394$ ,  $p = .696$ , Cohen's  $d_s = 0.092$ , Hedges'  $g_s^* = 0.091$ , default JZS  $BF_{10} = 0.256$ ) and

when individuals possessing the  $\epsilon 2$  allele were removed ( $t(84.914) = -0.819$ ,  $p = .415$ , Cohen's  $d_s = -0.162$ , Hedges'  $g_s^* = -0.161$ , default JZS  $BF_{10} = 0.279$ ).

**Figure 4.8.**

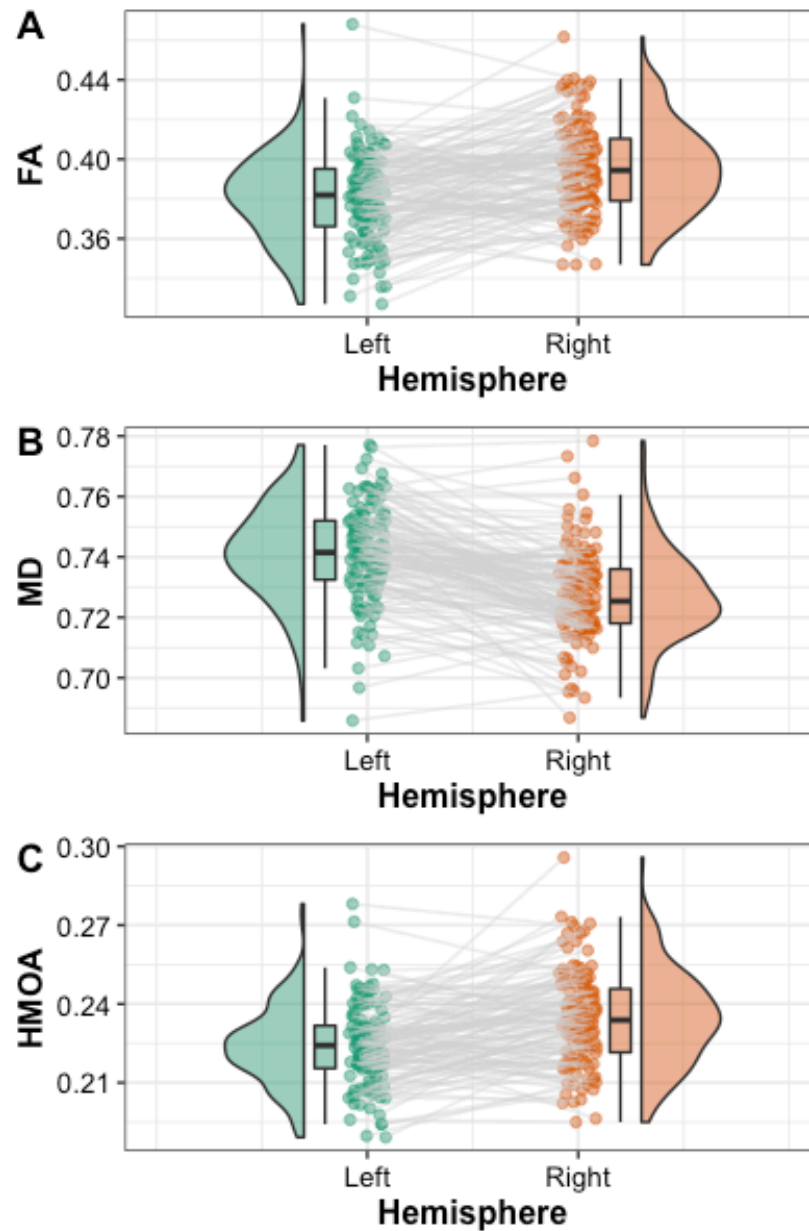
*Differences in PHCB and ILF HMOA Between APOE  $\epsilon 4$  carriers and non-carriers*



*Note.* Differences in PHCB HMOA (A) and ILF HMOA (B) between APOE  $\epsilon 4$  carriers and non-carriers are shown. Individual data points, each representing a single participant, are shown alongside boxplots and density plots. A small amount of jitter has been added to each point for clarity. To facilitate interpretation, the mean value (black circle) and median value (a black line) for each group are both shown. The y-axis differs between the two plots, reflecting the fact that HMOA was generally higher and more variable in the ILF than the PHCB. Abbreviations: HMOA = hindrance modulated orientational anisotropy.

#### 4.3.3.2. Hemispheric asymmetry in PHCB and ILF microstructure: Impact of *APOE* $\epsilon 4$ and sex

Hemispheric differences in PHCB FA, MD, and HMOA – collapsed across groups – are shown in Figure 4.9. FA was higher in the right than the left PHCB ( $t(127) = -6.978$ ,  $p < .001$ , Cohen's  $d_z = -0.617$ , default JZS  $BF_{10} > 100$ ), whereas MD was lower in the right than the left PHCB ( $t(127) = 9.683$ ,  $p < .001$ , Cohen's  $d_z = 0.856$ , default JZS  $BF_{10} > 100$ ). HMOA was higher in the right than the left PHCB ( $t(127) = -6.631$ ,  $p < .001$ , Cohen's  $d_z = -0.586$ , default JZS  $BF_{10} > 100$ ), largely mirroring the results for FA. Together, these findings provide striking evidence of hemispheric asymmetry in PHCB microstructure across the sample. This finding is consistent with prior reports of FA rightward asymmetry in the posterior portion of the cingulum in younger adults (Powell et al., 2012) and in the PHCB in older adults (Metzler-Baddeley, Jones et al., 2012). Given that cingulum bundle disruption has been linked to right temporoparietal hypo-metabolism (Villain et al., 2008) and a rightward asymmetry has been observed in the white matter networks of patients with MCI and AD (Yang et al., 2017), an interesting question is whether *APOE*  $\epsilon 4$  carriers show greater rightward asymmetry than non-carriers (although see Donix et al., 2012). To address this question, as well as the question of whether sex moderates the association between *APOE*  $\epsilon 4$  and hemispheric asymmetry, LIs were calculated for PHCB FA, MD, and HMOA, and robust multiple linear regression analyses were subsequently performed. Age was included as covariate in these analyses, thereby controlling for its effect(s). For PHCB  $LI_{FA}$ ,  $LI_{MD}$ , and  $LI_{HMOA}$ , there was no significant association with *APOE*  $\epsilon 4$  carrier status (all  $ps > .437$ ), sex (all  $ps > .155$ ), or their interaction (all  $ps = .524$ ). Consequently, this analysis indicates that neither *APOE*  $\epsilon 4$  nor sex influences hemispheric asymmetry in PHCB microstructure.

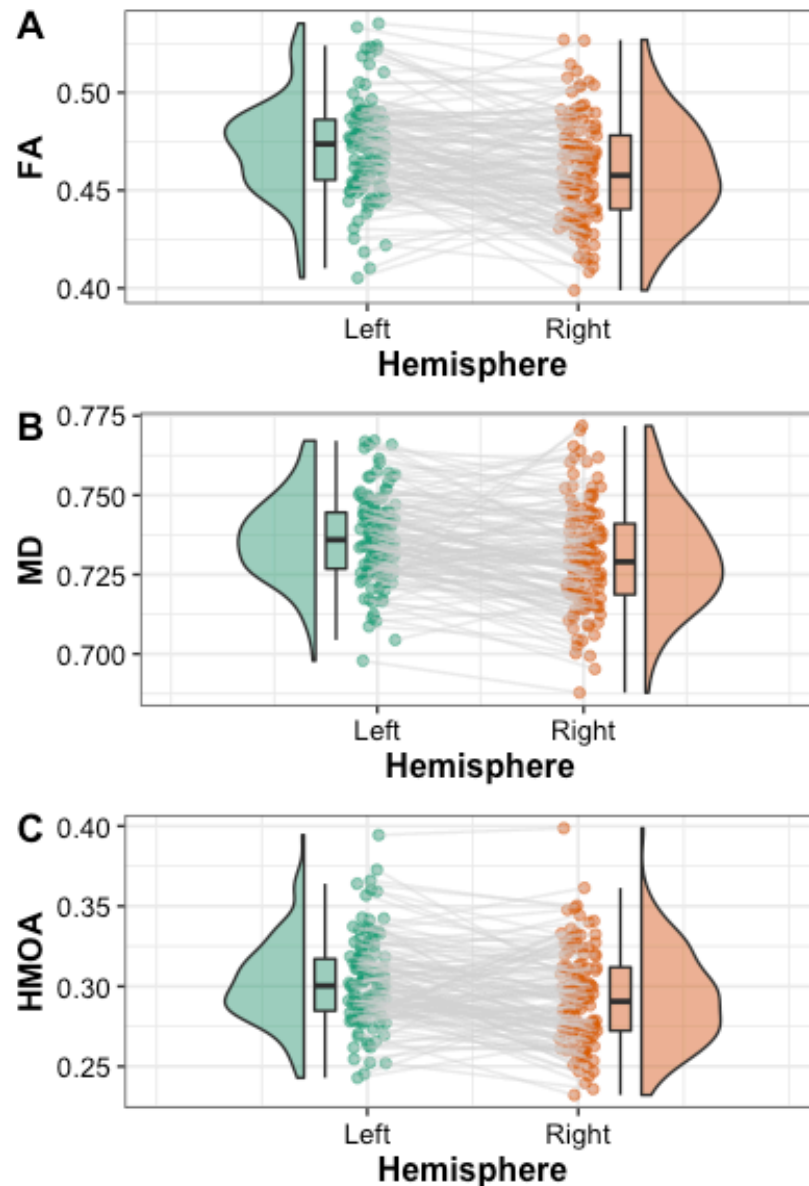
**Figure 4.9.***Hemispheric Differences in PHCB Microstructure*

*Note.* Hemispheric differences in PHCB FA (A), MD (B), and HMOA (C) are shown. Individual data points, each representing a single participant, are shown alongside boxplots and density plots. A small amount of jitter has been added to each point for clarity. Grey lines connect data points for each participant. Abbreviations: FA = fractional anisotropy, HMOA = hindrance modulated orientational anisotropy, MD = mean diffusivity.

The same analysis was conducted on ILF microstructure. Hemispheric differences in ILF FA, MD, and HMOA – collapsed across groups – are shown in Figure 4.10. FA ( $t(127) = 5.865$ ,  $p < .001$ , Cohen's  $d_z = 0.518$ , default JZS  $BF_{10} > 100$ ), MD ( $t(127) = 4.78$ ,  $p < .001$ , Cohen's  $d_z = 0.422$ , default JZS  $BF_{10} > 100$ ), and HMOA ( $t(127) = 3.778$ ,  $p < .001$ , Cohen's  $d_z = 0.334$ , default JZS  $BF_{10} = 74.09$ ) were all higher in the left than the right ILF. This finding might seem surprising as higher FA is usually observed alongside lower MD and vice versa (Soares et al., 2013). However, it is important to note that this relationship holds *within* a given tract rather than *between* tracts. Indeed, it is perfectly plausible for both FA and MD to be higher in one hemisphere than the other, as this is a between tract comparison rather than a within tract comparison (for a similar result, see Table 1, Wahl et al., 2010, p.534). Reassuringly, moderate negative relationships between FA and MD in the left ILF ( $r(126) = -0.391$ ,  $p < .001$ ) and right ILF ( $r(126) = -0.417$ ,  $p < .001$ ) were observed in the current chapter. Moreover, the left lateralisation of ILF microstructure – notably FA – has been observed in prior reports (Banfi et al., 2019; Panesar et al., 2018; Song et al., 2015; Thiebaut de Schotten et al., 2011). Examining whether this hemispheric asymmetry was influenced by *APOE*  $\epsilon 4$  carrier status, sex, or their interaction, LIs were again calculated and analysed. In the case of ILF  $LI_{FA}$ , there was a significant association with *APOE*  $\epsilon 4$  carrier status ( $b = 0.013$ ,  $p = .015$ ) but not with sex ( $b = -0.006$ ,  $p = .274$ ) or their interaction ( $b < 0.001$ ,  $p = .982$ ). Inspection of the estimated marginal means revealed that ILF  $LI_{FA}$  values were higher in  $\epsilon 4$  non-carriers ( $M = 0.02$ , 95% CI [0.013, 0.027]) than  $\epsilon 4$  carriers ( $M = 0.008$ , 95% CI [-0.004, 0.019]), indicating that ILF FA is characterised by a greater leftward asymmetry in non-carriers. In the case of ILF  $LI_{MD}$ , there was no significant association with *APOE*  $\epsilon 4$  carrier status ( $b = 0.004$ ,  $p = .065$ ), sex ( $b < 0.001$ ,  $p = .961$ ) or their interaction ( $b = -0.003$ ,  $p = .524$ ). Finally, in the case of ILF  $LI_{HMOA}$ , there was again a significant association with *APOE*  $\epsilon 4$  carrier status ( $b = -0.027$ ,  $p = .005$ ) but not with sex ( $b = -0.014$ ,  $p = .156$ ) or their interaction ( $b = 0.008$ ,  $p = .674$ ). Inspection of the estimated marginal means revealed that ILF  $LI_{HMOA}$  values were higher in  $\epsilon 4$  non-carriers ( $M = 0.029$ , 95% CI [0.016, 0.041]) than  $\epsilon 4$  carriers ( $M = 0.006$ , 95% CI [-0.017, 0.029]), indicating that ILF

HMOA is characterised by a greater leftward asymmetry in non-carriers. In sum, this particular analysis revealed that while all microstructural measures were higher in the left ILF than the right ILF, *APOE*  $\epsilon$ 4 carriers exhibited a reduced leftward asymmetry than *APOE*  $\epsilon$ 4 non-carriers. The distribution of ILF  $LI_{FA}$  and ILF  $LI_{HMOA}$  are shown in Figure 4.11, separated by *APOE*  $\epsilon$ 4 carrier status.

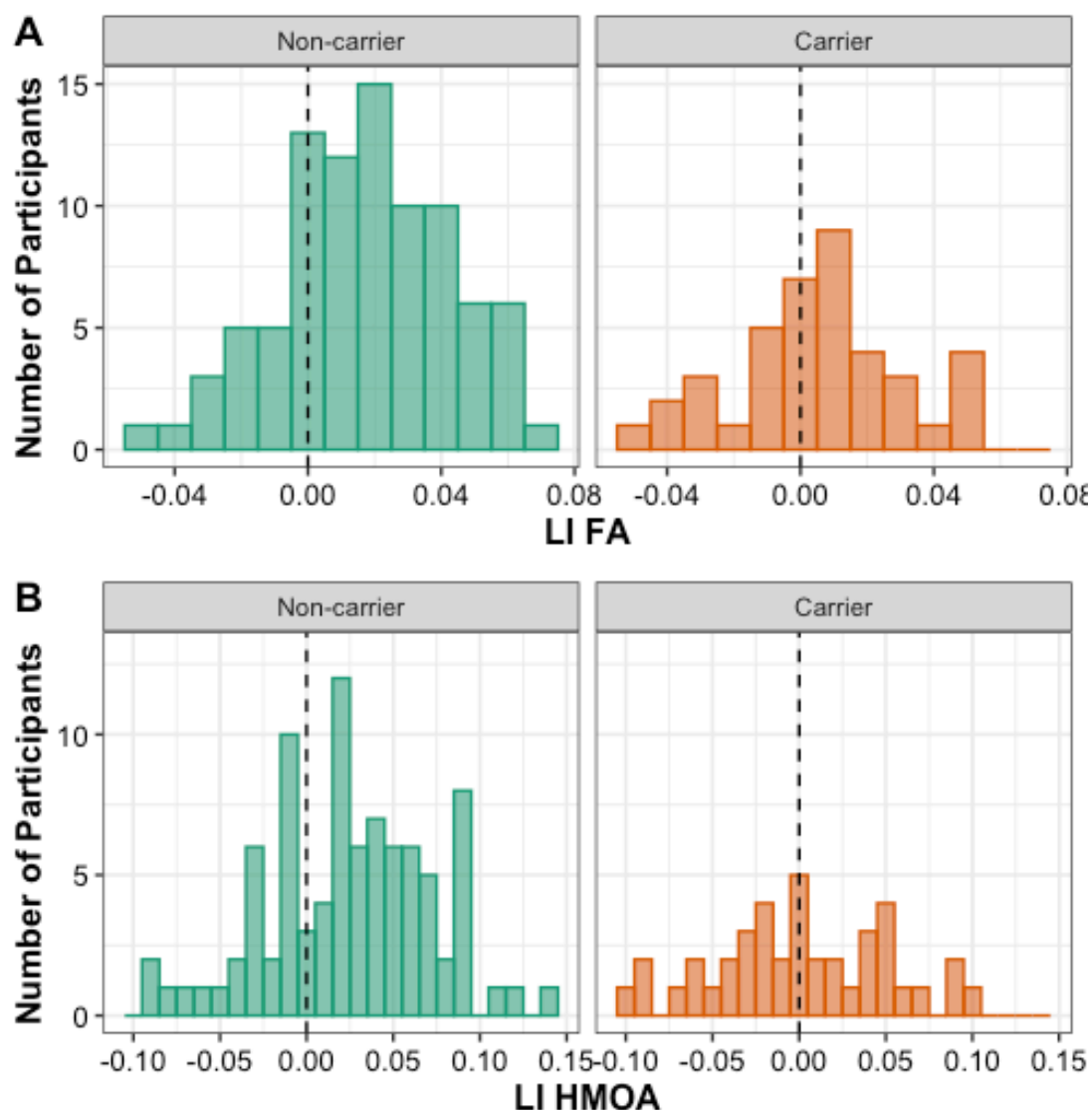


**Figure 4.10.***Hemispheric Differences in ILF Microstructure*

*Note.* Hemispheric differences in ILF FA (A), MD (B), and HMOA (C) are shown. Individual data points, each representing a single participant, are shown alongside boxplots and density plots. A small amount of jitter has been added to each point for clarity. Grey lines connect data points for each participant. Abbreviations: FA = fractional anisotropy, HMOA = hindrance modulated orientational anisotropy, MD = mean diffusivity.

Figure 4.11.

*Distribution of ILF LIs for APOE  $\epsilon 4$  carriers and non-carriers*



*Note.* The distribution of LI<sub>FA</sub> (A) and LI<sub>HMOA</sub> (B) in APOE  $\epsilon 4$  carriers and non-carriers are shown. The dashed line identifies the value for 0 (i.e. no asymmetry). Negative LIs represent rightward asymmetry (i.e. higher values in the right hemisphere than the left), whereas positive LIs represent leftward asymmetry (i.e. higher values in the left hemisphere than the right). Abbreviations: FA = fractional anisotropy, HMOA = hindrance modulated orientational anisotropy, LI = lateralisation index.

#### 4.4. Discussion

The primary aim of the study reported in this chapter was to replicate Hodgetts et al.'s (2019) finding that healthy young *APOE*  $\epsilon$ 4 carriers show higher FA and lower MD in the PHCB (but not the ILF) relative to non-carriers. Higher FA and lower MD have been linked to increased myelination and axon density (Beaulieu, 2002), thereby representing higher structural connectivity (although for a cautionary note, see Jones, Knösche, & Turner, 2013). As part of the replication, a near-identical experimental procedure was employed in a larger, independent sample. This analysis constitutes an important test of the idea that variation in tract microstructure leads to enhanced task-related activation and intrinsic functional connectivity within the extended hippocampal navigation network. The secondary aims of the study were: 1) to determine whether *APOE*  $\epsilon$ 4 carriers exhibit differences in PHCB (and ILF) HMOA relative to non-carriers, and 2) to examine whether hemispheric asymmetry is evident in PHCB (and ILF) microstructure and, in addition, whether this is affected by *APOE*  $\epsilon$ 4 carrier status and sex. Given the relevance of the primary aim – the attempted replication – to the overall goals of this thesis, I interpret and discuss these findings first.

The results of the primary analyses reported here showed no differences between *APOE*  $\epsilon$ 4 carriers and non-carriers in terms of PHCB (and ILF) FA or MD. This remained the case when analyses were restricted to females or when *APOE*  $\epsilon$ 2 carriers were removed. These results stand in direct contrast to those reported by Hodgetts et al. (2019), raising questions about the robustness of the original findings. One could argue that this is unsurprising. Hodgetts et al.'s (2019) study included a total sample size of just 15 participants in the carrier and non-carrier groups, and their analysis therefore did not have the requisite statistical power (~80%) to reliably detect small (Cohen's  $d_s = 0.2$ ), medium (Cohen's  $d_s = 0.5$ ), or even relatively large (Cohen's  $d_s = 0.8$ ) effect sizes (Cohen, 1988; although see Lakens, 2013). As discussed previously, when statistical power is low, the probability that an observed effect ( $p < .05$ ) represents a true effect – the positive predictive value – is reduced (Button et al., 2013). This is especially relevant in imaging

genetics, as effect sizes associated with common genetic variants are typically quite small (Mitchell, 2017). Underscoring this point, a recent large-scale imaging study (Mentink et al., 2021) failed to replicate the findings reported by Filippini et al. (2009), observing no difference between *APOE*  $\epsilon$ 4 carriers and non-carriers in terms of hippocampal task-related activation or functional connectivity within regions of the extended hippocampal navigation network. In this regard, it is plausible that Hodgetts et al.'s (2019) findings relating to the PHCB constitute false positives. BF analyses conducted in this chapter provide complementary support for this assertion, demonstrating moderate-to-strong evidence in support of the null (i.e. the absence of an effect).

An alternative explanation is that the original study by Hodgetts et al. (2019) observed a true effect but its magnitude was exaggerated. Often referred to as the winner's curse (Ioannidis, 2008), effect size inflation is most likely to occur in studies with small sample sizes (Button et al., 2013). To illustrate this point, take the following example. Imagine that the true (population) effect of *APOE*  $\epsilon$ 4 carrier status on PHCB FA or MD is equivalent to Cohen's  $d_s = 0.6$ . Owing to sampling variation and random error, any given study may observe an effect size that is smaller (e.g. Cohen's  $d_s = 0.3$ ) or larger (e.g. Cohen's  $d_s = 0.9$ ) than the true effect size. If these studies are underpowered (e.g.  $1-\beta = 0.2$ ), however, only those studies that detect a sufficiently large effect size – due to variation and error – will reach the threshold for “statistical significance” (e.g.  $p < .05$ ). Hence, the reported effect size will be inflated. This is particularly relevant here, as it is possible that Hodgetts et al. (2019) detected a true effect but over-estimated its magnitude. As the true (population) effect size is unknown, the analysis reported in this chapter might likewise be underpowered to detect it, thereby constituting a Type II error or false negative. While this explanation cannot be completely ruled out, it is worth noting that a sensitivity analysis revealed that the primary analyses were sufficiently powered to detect an effect size of Cohen's  $d_s = 0.48$ . BF analyses also demonstrated that the relative weight of the observed evidence supported the null.

Discrepancies between Hodgetts et al.'s (2019) study and the study reported here might also offer an explanation for the failure to replicate. Most notably, as discussed in Section 4.3.2.1, Hodgetts et al.'s (2019) study included participants that were, on average, younger than those included in this study. Previous cross-sectional studies of tract microstructure (FA, MD) indicate that the cingulum bundle undergoes a prolonged and delayed period of maturation (Lebel et al., 2008, 2011; see also Tamnes et al., 2018). Substantiating this, one longitudinal study reported that more than 40% of participants scanned at least twice between the ages of 22 and 32 years exhibited increasing FA in the cingulum (Lebel et al., 2012). While these studies did not specifically examine the PHCB, it nevertheless stands to reason that the inclusion of slightly older participants in the current study may have masked *APOE*  $\epsilon$ 4-related differences that are restricted to earlier parts of the lifespan. Indeed, Hodgetts et al. (2019) themselves speculate that *APOE*  $\epsilon$ 4 carriers and non-carriers undergo different patterns of white matter maturation, perhaps via reduced or delayed axonal pruning (Chung et al., 2016), leading to an initial “overshoot” in PHCB microstructure. It is plausible that this overshoot might only be evident in childhood, adolescence or very early adulthood (i.e. the second decade of life). Such a perspective would still be consistent with lifespan vulnerability accounts. As shown in the exploratory analyses reported previously, however, restricting the analysis to participants aged 21 years or below did not alter the findings. That is, higher FA and lower MD were still not evident in the PHCB of *APOE*  $\epsilon$ 4 carriers relative to non-carriers. Nonetheless, given the points raised about sample size and statistical power in this chapter (in the context of frequentist NHST), it should be noted that this analysis was itself likely underpowered, limiting the ability to draw definitive conclusions.

Differences in the way tractography was performed in the two studies could further explain the failure to replicate. In Hodgetts et al.'s (2019) study, for example, three-dimensional reconstructions of the PHCB and ILF were generated manually. By contrast, in this chapter, reconstructions were generated using automated software trained on a sample of manual reconstructions. If the manual reconstructions used to train the software were

notably different to those used by Hodgetts et al. (2019) – whether due to error, researcher decisions, or random chance – it is possible that this led to differences in the tract reconstructions, ultimately influencing the microstructural measures derived thereafter. Indeed, concerns have been raised about the reproducibility of diffusion MRI-based tractography more generally (Maier-Hein et al., 2017; Rheault et al., 2020; Schilling et al., 2020). One might counter that large differences are unlikely as both studies used the same established protocols for the PHCB and ILF (Jones, Christiansen et al., 2013; Wakana et al., 2007). These protocols were also applied to data collected from the same imaging centre using near-identical sequences and methods – a notable and somewhat unique advantage of the current chapter. Nevertheless, even if one accepts the argument that differences in tractography reconstruction method could account for the results, it is important to recognise that an entirely manual approach is simply not feasible with the sort of sample size reported here. It is for this reason that other studies recruiting samples of equivalent size have adopted an automated or semi-automated approach (for a relevant example, see Foley et al., 2017). Addressing this issue – that is, the scalability of diffusion MRI tractography – while ensuring results are reproducible is an important goal for future methodological research.

Another potential explanation is that the *APOE*  $\epsilon$ 4 carriers included in this chapter and in Hodgetts et al.'s (2019) study differed in some unobserved factors: so-called “hidden moderators”. It is well known, for instance, that while *APOE*  $\epsilon$ 4 carriers are at increased risk of developing AD relative to non-carriers, not all go on to develop the disease (Liu et al., 2013). In fact, only around ~40-50% of individuals with AD possess one or more copies of the  $\epsilon$ 4 allele (Karch et al., 2014), suggesting other factors – genetic and/or environmental – have an important role in disease pathophysiology. At various points throughout this thesis, and in Chapter 1 in particular, I outlined how sex potentially moderates the link between *APOE*  $\epsilon$ 4 and AD, but other factors such as ancestral background are also relevant (Belloy et al., 2019). This underscores the point here that other factors may be relevant to the current discussion. Following this line of reasoning, it is possible that – due to

sampling variation – studies of *APOE*  $\epsilon 4$  may end up with groups that differ in terms of unobserved, AD-relevant factors (i.e. hidden moderators), thereby including different proportions of individuals who are likely to later develop the disease. While this possibility cannot be ruled out here, it is important to point out that relying on hidden moderators as an argument for failed replications, especially in areas of psychology (e.g. Zwaan et al., 2018) and biology (e.g. Dirnagl, 2019), is controversial.

Moving on to the secondary aims of the study reported in this chapter, it is intriguing that no *APOE*  $\epsilon 4$ -related differences were evident in PHCB or ILF HMOA. Given that HMOA is less affected by crossing fibres and is therefore argued to be more sensitive to alterations in diffusion than either FA or MD (Dell'Acqua et al., 2013), this further suggests that no such differences exist in the PHCB of young adults. This runs counter to the notion that *APOE*  $\epsilon 4$  carriers exhibit early-life increases in structural connectivity, which may or may not underpin concomitant increases in functional activation and connectivity (Dennis et al., 2010; Filippini et al., 2009, 2011; Shine et al., 2015). Nevertheless, as with FA and MD, it remains possible that the impact of *APOE*  $\epsilon 4$  on HMOA is real but notably smaller than previously suggested. The recent failed replication of Filippini et al.'s (2009) study (Mentink et al., 2021), however, casts some doubt on this argument, instead pointing to the absence of an *APOE*  $\epsilon 4$ -related effect large enough to have a meaningful impact on the function and connectivity of the extended hippocampal navigation network in young adults. Such a suggestion has important implications for lifespan systems vulnerability accounts of AD. Taken at face value, for instance, one might argue that the effects of *APOE*  $\epsilon 4$  on the extended hippocampal navigation network are restricted to later stages in the lifespan, which stands in contrast to the view espoused by lifespan systems vulnerability accounts. This idea, something referred to as the so-called “prodromal hypothesis” (for a discussion, see O'Donoghue et al., 2018), posits that  $\epsilon 4$ -related effects become apparent in individuals aged 60 years or above, and that these effects are driven by AD pathology (Foster et al., 2013). Alternatively, it could be the case that *APOE*  $\epsilon 4$  does impact the brain early in the lifespan but that this is restricted to other structural and/or

functional measures, such as hippocampal volume. Indeed, reduced hippocampal volumes have been reported in young *APOE*  $\epsilon 4$  carriers relative to non-carriers (Alexopoulos et al., 2011; O'Dwyer et al., 2012), though this is by no means universally observed (Khan et al., 2014; Lupton et al., 2016). In addition, an early-life reduction in the volume of specific brain structures is not necessarily predicted by lifespan systems vulnerability accounts. Additional research on the impact of *APOE*  $\epsilon 4$  on the brain in young adults would greatly benefit from the inclusion of multiple imaging modalities.

Regarding the asymmetry of PHCB microstructure, the current study observed an interesting pattern. Prior studies present a mixed picture on cingulum FA asymmetry, with reports of rightward asymmetry (Metzler-Baddeley, Jones et al., 2012; Powell et al., 2012), leftward asymmetry (Gong et al., 2005; Park et al., 2004; Takao et al., 2010), and no asymmetry (Arrigo et al., 2014; Lebel et al., 2012; Thiebaut de Schotten et al., 2011). The variability in outcomes is likely due to a number of factors, ranging from the nature and size of the sample to the method and type of analysis used (e.g. TBSS vs. tractography). Moreover, these studies typically examine the cingulum bundle in its entirety, or anterior and posterior components, rather than the PHCB specifically (for an exception, see Metzler-Baddeley, Jones et al., 2012). There is also a tendency within this literature to focus on FA and ignore other microstructural measures such as MD and HMOA (for relevant exceptions, see Honnedevassthana Arun et al., 2021; Ioannucci et al., 2020; Lebel et al., 2012; Metzler-Baddeley, Jones et al., 2012; Zhao et al., 2016). In this regard, the current study adds to this literature, showing that PHCB FA and HMOA are characterised by a rightward asymmetry whereas PHCB MD is characterised by a leftward asymmetry, at least in healthy young adults. In addition, despite prior reports of rightward asymmetries in MCI and AD (Villain et al., 2008; Yang et al., 2017), *APOE*  $\epsilon 4$  carriers and non-carriers did not differ in the degree of PHCB asymmetry. No association with sex was observed either, which is perhaps surprising given previous studies reporting higher FA and lower MD in the cingulum bundle of males relative to females (e.g. Lebel & Beaulieu, 2011; Lebel et al., 2012). That said, evidence of sex effects on white matter development is mixed and inconclusive (for a



discussion, see Lebel & Deoni, 2018). As such, the current chapter provides evidence of PHCB asymmetry in young adults but casts doubt on the notion that *APOE*  $\epsilon 4$  and/or sex influences this.

By contrast, a different pattern emerged in the analysis of ILF microstructure. In the present sample, ILF FA, MD, and HMOA were all characterised by leftward asymmetry – that is, they were all higher in the left hemisphere than the right hemisphere. The finding for FA is consistent with a number of studies examining the ILF (Banfi et al., 2019; Panesar et al., 2018; Song et al., 2015; Thiebaut de Schotten et al., 2011), although certainly not all such studies (for counter-examples, see Arrigo et al., 2014; Latini et al., 2017; Lebel et al., 2012; Park et al., 2004). Interestingly, leftward asymmetry in structural connectivity (Bouhali et al., 2014) and functional connectivity (Hurley et al., 2015) has been observed between regions implicated in language/semantic processing. Perhaps most striking, however, was the observation that the degree of asymmetry in this tract was associated with *APOE*  $\epsilon 4$  carrier status, such that the degree of asymmetry was lower in carriers relative to non-carriers. The ILF connects regions in the occipital lobe with regions in the anterior temporal lobe (Herbet et al., 2018), including the PRC, and has been implicated in face perception (Hodgetts et al., 2015) and semantic memory (Hodgetts, Postans et al., 2017), thus constituting part of the so-called feature network (Murray et al., 2017). This suggests that the *APOE*  $\epsilon 4$  allele may initially alter the asymmetry that exists within this network, potentially impacting object and language/semantic processing. Reports of preclinical impairment in object naming and language/semantic processing in *APOE*  $\epsilon 4$  carriers provide some support for this (Biundo et al., 2011; Ford et al., 2020; Miller et al., 2005; Rosen et al., 2005; Vonk et al., 2019). Moving forward, it would be beneficial to further investigate the impact of *APOE*  $\epsilon 4$  on hemispheric asymmetry within the feature network and to determine what impact – if any – this has aspects of cognition thought to be supported by the specialised representations of the PRC and its broader network (Graham et al., 2010; Murray et al., 2017; Saksida & Bussey, 2010).

Although diffusion MRI-based tractography is presently the only in vivo method capable of reconstructing white matter tracts in the human brain, it is important to acknowledge that this method has a number of limitations. Of particular relevance in the context of this study, diffusion MRI does not currently possess the spatial resolution necessary to examine individual projections (Jones, Knösche, & Turner, 2013), as done in neural tract tracing studies (Saleeba et al., 2019). Voxel dimensions in studies using diffusion MRI are typically around 2-2.5mm<sup>3</sup> (Jeurissen et al., 2019). As such, there are approximately 10<sup>5</sup> axons per voxel, meaning that it is not possible to reconstruct individual projections using this method (Campbell & Pike, 2014). Relatedly, diffusion MRI-based tractography cannot distinguish between afferent and efferent projections – that is, it cannot provide information about polarity (Jbabdi & Johansen-Berg, 2011). For these reasons, our collective knowledge about these projections – whether afferent or efferent projections – is primarily derived from animal research (for a relevant review, see Aggleton, 2012). Moreover, while validation studies comparing tractography with neural tract tracing in mice (Calabrese et al., 2015), ferrets (Delettre et al., 2019), and monkeys (van den Heuvel et al., 2015) provide evidence that diffusion MRI-based tractography can provide reasonably accurate reconstructions, false positives and false negatives remain a problem (Maier-Hein et al., 2017; Schilling et al., 2019; Thomas et al., 2014). Similar results have been observed in comparisons between diffusion MRI-based tractography and neural tract tracing in post-mortem human tissue (Seehaus et al., 2013). While this issue can be partially addressed by incorporating anatomical rules or constraints (Schilling et al., 2020), there are limits to what can be achieved. Indeed, some researchers have argued that these issues stem from an inherent limitation of diffusion MRI-based tractography, namely that inferring fibre orientation from the displacement of water diffusion is an incredibly complex inverse problem that cannot be entirely solved (Thomas et al., 2014). Adding to this, recent research has raised concerns about the replicability and reproducibility of tractography results (Rheault et al., 2020; Schilling et al., 2020, 2021). These limitations do not mean that diffusion MRI-based tractography is not a useful method, or that it cannot provide valuable insight into the human brain. However, given the focus of the

current chapter, it is important to caveat the above interpretations of the observed findings.

#### 4.5. Summary

In summary, this chapter failed to replicate the finding that, relative to non-carriers, young adult *APOE*  $\epsilon$ 4 carriers show higher FA and lower MD in the PHCB (Hodgetts et al., 2019). This was also true of a comparison tract: the ILF. Furthermore, there were no *APOE*  $\epsilon$ 4-related differences in PHCB (or ILF) HMOA, a tract-specific index of diffusion (Dell'Acqua et al., 2013). Together, these findings fail to support the idea that the *APOE*  $\epsilon$ 4 alters PHCB microstructure in healthy young adults. On the surface, this constitutes a challenge the notion that this allele produces alterations in structural connectivity that in turn lead to an increase in functional activation (i.e. hyper-activation), metabolic activity (i.e. hyper-metabolism) and functional connectivity (i.e. hyper-connectivity) within the extended hippocampal navigation network. However, alternative explanations for this discrepancy exist, as highlighted above; those would need to be further investigated to be confident of the outcomes from the analysis reported here. Intriguingly, marked patterns of hemispheric asymmetry were evident in PHCB and ILF microstructure, although only the latter was associated with *APOE*  $\epsilon$ 4 carrier status. This is surprising, not least because this tract forms part of the ventral feature network, and additional large-scale research is therefore warranted to confirm its replicability and to understand its implications for typical cognitive function and AD risk.

In the next chapter, I provide an overview of the findings from this thesis, and then discuss how they contribute to our understanding of *APOE*  $\epsilon$ 4, age, and sex effects on these two large-scale MTL neurocognitive networks and their corresponding representations. Limitations of the research conducted are also discussed. I then present some outstanding questions and outline how future research may address them.

## Chapter 5: General discussion

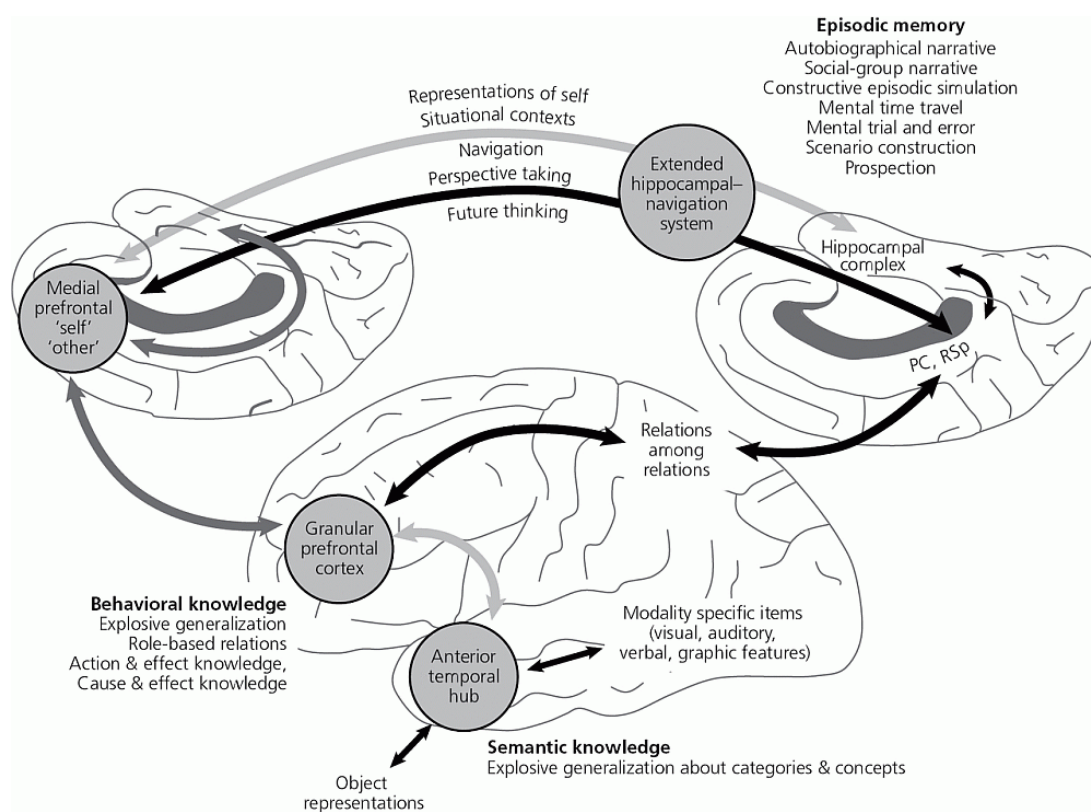
In Chapter 1, I introduced a contemporary representational account of perception, memory, and cognition: the evolutionary accretion model (Murray et al., 2017). According to this account, human memory depends on the function and connectivity of several large-scale neurocognitive networks in the human brain (Figure 5.1). Throughout this thesis, I focused on two such networks in particular: the so-called extended hippocampal navigation network and the ventral component of the so-called feature network. The former is proposed to enrich and elaborate on the complex conjunctive scene representations housed by the hippocampus, supporting the generation of mental views of spatial scenes (for a related account, see Ranganath & Ritchey, 2012; Ritchey et al., 2015). The latter is proposed to represent object-level features, in addition to semantic concepts and categories (Murray et al., 2017; see also Lambon Ralph et al., 2017).

Given global increases in longevity (UN, 2020), there is a pressing need to understand how these two networks and their corresponding representations are impacted by age and age-related neurodegenerative disease, as well as risk factors for such disease (e.g. *APOE*  $\epsilon$ 4). To date, however, findings have been mixed and inconclusive (see Chapter 1, Sections 1.2), underscoring the need for additional research. Moreover, as outlined in Chapter 1 (Section 1.3), early-life alterations in the extended hippocampal navigation network have been observed in young *APOE*  $\epsilon$ 4 carriers relative to non-carriers (e.g. Dennis et al., 2010; Filippini et al., 2009; Hodgetts et al., 2019; Shine et al., 2015). These  $\epsilon$ 4-related alterations have in turn been linked to increased vulnerability to AD-related pathology (i.e.  $A\beta$  accumulation) and ultimately network dysfunction (Bero et al., 2011; Buckner et al., 2005, 2009; Jagust & Mormino, 2011). Nevertheless, not all studies observe these effects (for a failed replication, see Mentink et al., 2021), and it remains challenging to reconcile such findings with the growing number of reports indicating that age and AD risk – defined by MCI or a positive family history of AD – preferentially impact complex object discrimination (Fidalgo et al., 2016;

Güsten et al., 2021; Mason et al., 2017; Reagh et al., 2016; Stark & Stark, 2017) and the function of the feature network (Berron et al., 2018; Reagh et al., 2018; Ryan et al., 2012). As such, there remains a need to examine the impact of *APOE*  $\epsilon$ 4, and *APOE* genotype more broadly, at various points across the adult lifespan.

**Figure 5.1.**

*Interactions Among Large-Scale Neurocognitive Networks as Proposed by the Evolutionary Accretion Model*



*Note.* Interactions among the extended hippocampal navigation network (or system), the ventral component of the feature system (including the anterior temporal hub), and parts of the prefrontal cortex are shown, as proposed by the evolutionary accretion model. The representations and functions supported by the networks and their components are provided alongside the relevant labels. Abbreviations: PC = posterior cingulate cortex, RSp = retrosplenial cortex. Reprinted from Murray et al. (2017)

The aim of this thesis was to examine the impact of *APOE* genotype – especially the *APOE*  $\epsilon$ 4 allele – and age on the extended hippocampal navigation network and the ventral component of the feature network, as well as their corresponding representations. The impact of sex (or gender/sex in the case of Chapter 3) was also examined, either directly or indirectly, as prior research provides strong evidence that the association between *APOE*  $\epsilon$ 4 and AD is stronger in females than in males (Gamache et al., 2020; Riedel et al., 2016; Ungar et al., 2014). The reported studies used a combination of large-scale web-based cognitive testing (Chapter 2), MRI structural covariance analysis (Chapter 3), and diffusion MRI-based tractography (Chapter 4). All analyses were centred on healthy adult participants prior to the onset of any overt clinical symptoms.

In this final chapter, I first summarise the main findings of each study included in this thesis. I then consider the broader theoretical implications, particularly with regard to lifespan systems vulnerability accounts. Thereafter, I discuss the limitations of the research conducted, drawing on established literature. Finally, I present a selection of outstanding questions and outline ways in which future studies can address them, adding to our collective understanding of how *APOE* genotype and age impact these large-scale neurocognitive networks and their corresponding representations.

## **5.1. Summary of main findings**

### *5.1.1. Odd-one-out perceptual discrimination accuracy differs as a function of *APOE* genotype and age in middle-aged and older females*

A number of studies have suggested that the *APOE*  $\epsilon$ 4 allele – the best-established genetic risk factor for AD (Serrano-Pozo et al., 2021) – detrimentally impacts allocentric navigation and scene-based processing prior to overt AD. For example, *APOE*  $\epsilon$ 4 carriers (relative to non-carriers) have been shown to demonstrate reduced grid-cell-like representations and altered navigation behaviour (Kunz et al., 2015). Impairments in path integration (Bierbrauer et al., 2020), wayfinding (Coughlan et al., 2019), and

spatial memory (Laczó et al., 2011) have further been observed in *APOE*  $\epsilon$ 4 carriers relative to non-carriers. In addition, young adult *APOE*  $\epsilon$ 4 carriers have been shown to exhibit hyper-activation in the PCC – part of the extended hippocampal navigation network – during odd-one-out discrimination for scenes but not complex objects/faces (Shine et al., 2015), mirroring the scene oddity-related deficits observed in patients with AD (Lee et al., 2006; see also Lee et al., 2007). Taken together, these findings indicate that allocentric navigation and scene-based processing is impacted by *APOE*  $\epsilon$ 4, perhaps even prior to episodic memory impairments (Coughlan et al., 2018). Despite this, several studies have observed that complex object (including face) discrimination is more prominently impacted by age (Güsten et al., 2021; Reagh et al., 2016, 2018; Ryan et al., 2012; Stark & Stark, 2017). Deficits in object-related discrimination and recognition memory have further been reported in individuals with a positive family history of AD (Mason et al., 2017) and in individuals with amnesic MCI (Fidalgo et al., 2016). This raises an interesting question: to what extent does the *APOE*  $\epsilon$ 4 allele and age impact scene and complex object (including face) perceptual discrimination? Another unanswered question is whether the *APOE*  $\epsilon$ 2 allele impacts scene and object/face perceptual discrimination. It has long been known that this allele is protective against AD (Chartier-Harlin et al., 1994; Corder et al., 1994; Farrer et al., 1997), yet the lack of research on its effect(s) on the brain and cognition has resulted in it being dubbed the “forgotten *APOE* allele” (Suri et al., 2013, p.2879). Of those studies that have directly examined *APOE*  $\epsilon$ 2, there is no clear pattern of results. Indeed, it has been reported that middle-aged participants demonstrate superior cognitive performance (Sinclair et al., 2017), impaired cognitive performance (Lancaster, Forster et al., 2017), and no difference in cognitive performance (Trachtenberg, Filippini, Cheeseman et al., 2012). Nevertheless, these studies have tended to use cognitive tasks that are sensitive to clinical impairment rather than individual differences in performance.

In Chapter 2, I thus reported a study that aimed to address these questions. A web-based version of the odd-one-out perceptual discrimination task was developed in collaboration with Ounce Technology ([www.ouncetech.co.uk](http://www.ouncetech.co.uk)),

facilitating the recruitment of a large sample of female participants from ALSPAC (final  $N = 524$ ). The focus on this sample of middle-aged and older female participants was driven in part by their availability and the amount of genetic data already collected, which made it possible to examine the effect of *APOE* genotype ( $\epsilon 2$ ,  $\epsilon 3$ ,  $\epsilon 4$ ) and age on performance. However, there were also good theoretical reasons for this (Gamache et al., 2020; Riedel et al., 2016; Ungar et al., 2014). In particular, it has long been known that female *APOE*  $\epsilon 4$  carriers are more at risk of AD than male *APOE*  $\epsilon 4$  carriers (Farrer et al., 1997; Payami et al., 1994, 1996), while conversion to MCI and AD is highest in this group (Altmann et al., 2014). Moreover, it is notable that higher levels of AD pathology, especially tau, have been observed in female *APOE*  $\epsilon 4$  carriers (Babapour Mofrad et al., 2020; Buckley et al., 2019; Hohman et al., 2018; Wang et al., 2021). Such findings provided a good rationale for focusing on female participants.

Results revealed an interaction between *APOE* genotype and age on odd-one-out perceptual discrimination accuracy. More specifically, it was found that carriers of the  $\epsilon 4$  ( $\epsilon 3/\epsilon 4$ ,  $\epsilon 4/\epsilon 4$ ) and  $\epsilon 2$  ( $\epsilon 2/\epsilon 2$ ,  $\epsilon 2/\epsilon 3$ ) alleles exhibited opposite age trends, such that the former showed lower accuracy with advancing age and the latter showed higher accuracy with advancing age. This interaction was independent of condition – that is, it was not specific to the different-view scene or different-view face condition. This finding runs counter to prior reports of preferential *APOE*  $\epsilon 4$ -related impairment in allocentric navigation and scene-based processing, as well as preferential age-related decline in complex object (including face) discrimination. That being said, the observation that the  $\epsilon 2$  carriers performed better than the  $\epsilon 4$  carriers is somewhat consistent with the results reported by Sinclair et al. (2017) and more general longevity effects associated with this allele (Sebastiani et al., 2019; Shinohara et al., 2020; Wolters et al., 2019; for a relevant discussion, see Li et al., 2020). It is currently unclear why the *APOE*  $\epsilon 2$  group exhibited *higher* levels of accuracy with advancing age, although bias due to selective attrition might explain this.



### 5.1.2. Gender/sex and age but not *APOE* $\epsilon 4$ impact the shared structural covariance of the anteromedial hippocampus and PRC

As already discussed in this chapter, the evolutionary accretion model (Murray et al., 2017) posits that the extended hippocampal navigation network and the ventral component of the feature network support the specialised representations necessary to perform scene and complex object (including face) discrimination, respectively (for relevant evidence, see Barense et al., 2007, 2010; Behrmann et al., 2016; Erez et al., 2013; Hodgetts, Voets et al., 2017; Lee, Buckley et al., 2005; Lee et al., 2008; Mundy et al., 2013). As such, the results of Chapter 2 could be interpreted as showing that *APOE*  $\epsilon 4$  and age together impact both of these networks, at least in middle-aged and older adults. While this could in theory be influenced by a global effect of age on the brain, a recent study using diffusion MRI-based tractography provides evidence that the effect of age on fornix and ILF microstructure mediates scene and face processing, respectively (Bourbon-Teles et al., 2021). Although this study did not include the cingulum, or its parahippocampal component, it serves to demonstrate that the effect of age on scene and face discrimination is not necessarily a global one. Nonetheless, it is important to note the participants included in Chapter 2 were all female and the age span was largely restricted between the 5<sup>th</sup> and 7<sup>th</sup> decade of life. There were thus open questions as to whether the impact of *APOE*  $\epsilon 4$  and age on these networks would extend to males as well as females, and how the impact of this allele plays out across the entire adult lifespan. The latter is particularly important here, as lifespan systems vulnerability accounts of cognitive decline and AD (Bero et al., 2011; Buckner et al., 2005, 2009; Jagust & Mormino, 2011) propose that *APOE*  $\epsilon 4$  reduces neural efficiency in a way that leads to early-life hyper-activation/hyper-metabolism, which in turn increases later susceptibility to A $\beta$  (Mishra et al., 2018) and ultimately network dysfunction (Seeley, 2017). It is possible, therefore, that the preferential effects of the  $\epsilon 4$  allele on allocentric navigation/scene-based processing and, by extension, the extended hippocampal navigation network may be confined to earlier stages in the lifespan when significant A $\beta$  burden is unlikely.

To address this in Chapter 3, I reported a study that aimed to examine the impact of *APOE*  $\epsilon 4$ , gender/sex, and age on the unique and/or shared structural covariance associated with the anteromedial hippocampus and PRC. These seeds regions were selected based on a prior study showing that these structures respond preferentially to scene and object stimuli (Hodgetts et al., 2016), in line with their proposed status as key nodes within the extended hippocampal navigation and feature networks (Murray et al., 2017). Structural covariance is a now widely used analytical method applied to structural MRI data in order to identify co-variation between the morphological features (e.g. grey matter volume) of a priori selected seed regions with the same features of other brain regions (Alexander-Bloch Giedd, & Bullmore, 2013). Given this, as well as the overlap with fMRI-based functional connectivity (Clos et al., 2014; Guo et al., 2015; Kelly et al., 2012; Spreng et al., 2019), diffusion MRI-based tractography (Gong et al., 2012), and neural tract tracing (Yee et al., 2018), structural covariance analysis can be conceptualised as a method of studying connectivity. In this particular study, I investigated structural covariance of the anteromedial hippocampus and PRC in a relatively large sample of participants from the DLBS (total  $N = 353$ ) using a multivariate method: seed PLS (Krishnan et al., 2011). In addition to its advantages over univariate methods, seed PLS facilitates the extraction of brain scores, which represent the extent to which the observed covariance pattern is expressed in a given individual. These scores were subsequently used as dependent variables as part of further analyses (for relevant examples, see DuPre & Spreng, 2017; Nordin et al., 2018; Persson et al., 2014; Spreng et al., 2019; Spreng & Turner, 2013; Veldsman et al., 2020).

Contrary to expectations, seed PLS identified only one significant LV, which captured a pattern of structural covariance common to both the anteromedial hippocampus and PRC across male and female *APOE*  $\epsilon 4$  carriers and non-carriers. This LV incorporated significant clusters of covariance in the frontal, temporal, parietal, and occipital lobes, notably including the ventromedial prefrontal cortex, precuneus, angular gyrus, and fusiform gyrus. Brain scores were subsequently extracted and analysed using robust linear regression.

Analysis revealed that these scores varied as a function of gender/sex and age, such that the covariance pattern was less strongly expressed with advancing age and in males relative to females. *APOE*  $\epsilon 4$  carrier status was not related to these scores. Interestingly, the association between age and brain scores accounted for all associations between cognitive task performance and brain scores, underscoring the role of age. These findings provide evidence that age and gender/sex – but not *APOE*  $\epsilon 4$  – impact the shared connectivity of the anteromedial hippocampus and PRC. Alternative explanations exist for the lack of an *APOE*-related effect, however, including the fact that the non-carrier group ( $\epsilon 2/\epsilon 2$ ,  $\epsilon 2/\epsilon 3$ ,  $\epsilon 3/\epsilon 3$ ) was primarily comprised of  $\epsilon 3$  homozygotes (89.62%), and the carrier group ( $\epsilon 2/\epsilon 4$ ,  $\epsilon 3/\epsilon 4$ ,  $\epsilon 4/\epsilon 4$ ) included those with the  $\epsilon 2/\epsilon 4$  genotype. Owing to the fact that age impacted the shared covariance of the anteromedial hippocampus and PRC, it appears that age impacts the connectivity of both structures, assuming that covariance reflects connectivity. Consistent with this, prior studies of fMRI-based functional connectivity have shown age effects on the broader hippocampal and PRC networks (Berron et al., 2020; Das et al., 2015; although for a different pattern of results, see Dautricourt et al., 2021). It should be recognised, however, that structural covariance reflects anatomical connectivity *and* other biological factors (Yee et al., 2018). Accordingly, it is important to assess the impact of *APOE* genotype and age on other measures that claim to assess connectivity.

### *5.1.3. APOE $\epsilon 4$ does not impact PHCB microstructure in young adults but does impact ILF lateralisation*

Lifespan systems vulnerability accounts of cognitive decline and AD (Bero et al., 2011; Buckner et al., 2005, 2009; Jagust & Mormino, 2011) predict that young *APOE*  $\epsilon 4$  will exhibit hyper-activation and hyper-metabolism in regions that are later characterised by high levels of  $A\beta$ . The observation that *APOE*  $\epsilon 4$  carriers exhibit hyper-activation within the PCC during scene discrimination in early adulthood provides support for this (Shine et al., 2015; see also Koelewijn et al., 2019), as this region is among the earliest sites of  $A\beta$  accumulation (Oh et al., 2016; Mattsson et al., 2019; Palmqvist et al.,

2017; Villeneuve et al., 2015). Moreover, higher levels of intrinsic functional connectivity (.e. hyper-connectivity) between the hippocampus and PCC/RSC has been reported in young *APOE*  $\epsilon$ 4 carriers relative to non-carriers (Dennis et al., 2010; Filippini et al., 2009; Koelewijn et al., 2019; Zheng et al., 2021). An interesting question, therefore, is whether *APOE*  $\epsilon$ 4-related alterations in functional activation, metabolism, and functional connectivity are associated with concomitant alterations in structural connectivity. Hodgetts et al. (2019) previously provided evidence that this is in fact the case, with PHCB microstructure underpinning scene-related activation in the PCC, as well as the hippocampus and PHC. Hodgetts et al. (2019) further reported that young *APOE*  $\epsilon$ 4 carriers show higher FA and lower MD – argued to reflect higher connectivity (for a discussion, see Chapter 1, Box 1) – in the PHCB relative to non-carriers, while no such differences were evident in a comparison tract (i.e. the ILF). The authors speculated that the *APOE*  $\epsilon$ 4 allele might alter white matter maturation of the cingulum bundle (Lebel & Beaulieu, 2011; Lebel et al., 2012), which in turn gives rise to an early-life “overshoot” in PHCB microstructure and a corresponding reduction in neural efficiency, thereby producing an increase in functional activation (i.e. hyper-activation) and functional connectivity (i.e. hyper-connectivity) within the extended hippocampal navigation network (Hodgetts et al., 2019).

Although interesting, Hodgetts et al.’s (2019) study included a modest sample size ( $N = 30$ ) and was consequently underpowered to detect even relatively large effect sizes. This raises the possibility that their results may be false positives, something that is a particular concern in this area of research (Mitchell, 2017), especially in light of recent failed replications (Mentink et al., 2021). In Chapter 4, I attempted to replicate Hodgetts et al.’s (2019) finding that young adult *APOE*  $\epsilon$ 4 carriers exhibit higher FA and lower MD in the PHCB (but not the ILF) relative to young *APOE*  $\epsilon$ 4 non-carriers. To this end, a near-identical procedure was used albeit in a larger sample of participants ( $N = 128$ ). Moving beyond Hodgetts et al.’s (2019) original study, however, additional analyses were included. First, an alternative microstructural measure – HMOA – was analysed, which is argued to be

more sensitive to subtle alterations in diffusion than either FA or MD (Dell'Acqua et al., 2013). Second, I examined how *APOE*  $\epsilon$ 4 and sex impact the hemispheric asymmetry of PHCB and ILF microstructure. Motivating this analysis, prior research on hemispheric asymmetry in cingulum bundle and ILF microstructure provides a mixed picture, both in healthy adults and in relation to MCI and AD (see Section 4.1).

In contrast to the results reported by Hodgetts et al. (2019), the study reported in Chapter 4 did not observe higher FA or lower MD in the PHCB (or ILF) of young *APOE*  $\epsilon$ 4 carriers relative to non-carriers. This remained the case when analyses were repeated with males removed or with carriers of the  $\epsilon$ 2 allele removed, as well as when the analysis was restricted to younger participants only. No *APOE*  $\epsilon$ 4-related differences were evident in PHCB HMOA either, adding to the results for FA and MD. Collectively, these findings question the robustness of the Hodgetts et al.'s (2019) results, and indicate that early-life alterations in functional activation and connectivity may not be underpinned by concomitant alterations in structural connectivity, assuming that such functional alterations are themselves not false positives (Mentink et al., 2021). Somewhat surprisingly, *APOE*  $\epsilon$ 4 did have an effect on the asymmetry of ILF microstructure, with the degree of asymmetry being lower in carriers relative to non-carriers. This early-life alteration in the ILF might be related to reports of preclinical impairment in object naming and language/semantic processing in *APOE*  $\epsilon$ 4 carriers (Biundo et al., 2011; Ford et al., 2020; Miller et al., 2005; Rosen et al., 2005; Vonk et al., 2019), but further research is required to determine whether this is the case.

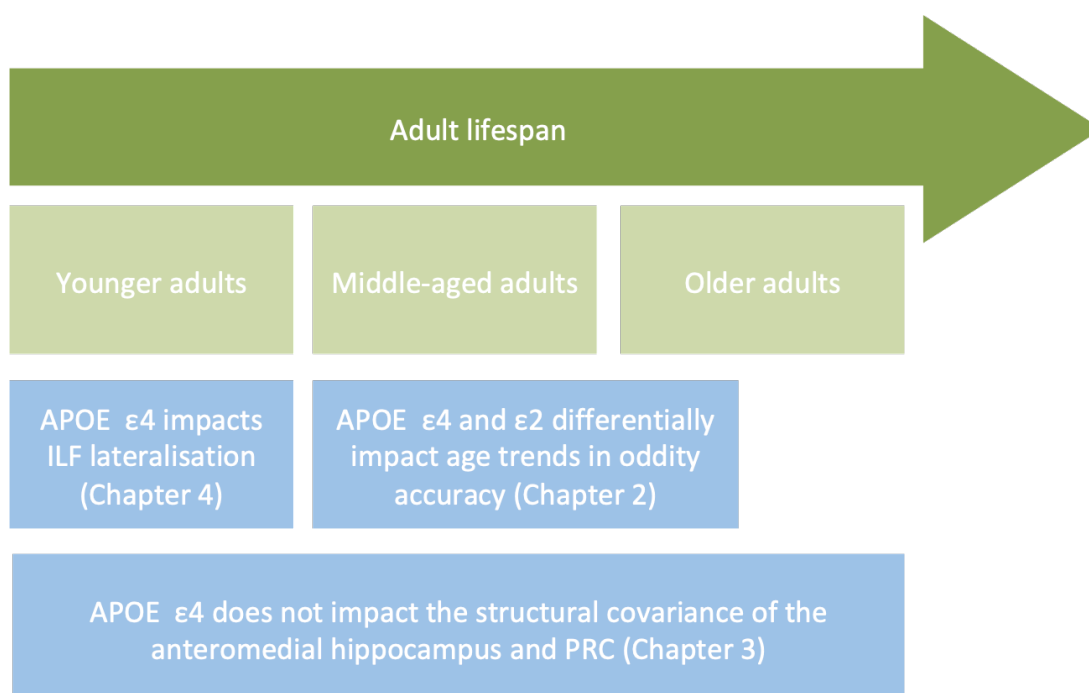
## **5.2. Theoretical implications**

The research in this thesis was motivated in part by the mixed evidence regarding the impact of age and age-related neurodegenerative disease on tasks tapping scene/spatial context and object representations (Chapter 1, Section 1.2), but also – crucially – lifespan vulnerability accounts of cognitive decline and AD (Chapter 1, Section 1.3). In this next section, I focus on the theoretical implications of the reported findings (Figure 5.2) for lifespan

systems vulnerability accounts, as well as their relation to the evolutionary accretion model (Murray et al., 2017). I start by focusing on younger adults before then moving on to middle-aged and older adults. I draw on relevant literature and highlight discrepancies where relevant.

**Figure 5.2.**

*Main Findings of the Thesis in Relation to APOE Genotype at Different Time Points in the Adult Lifespan*



*Note.* The main *APOE*-related finding of each chapter (blue) is shown according to the time point in the adult lifespan (green) that it was focused on. For example, Chapter 4 appears below younger adults, as the study reported in that particular chapter was centred on adults aged 35 years or under.

The results of Chapter 4, which focused specifically on healthy younger adults, have important implications for lifespan systems vulnerability accounts. Taken at face value, the failure to replicate one of Hodgetts et al.'s (2019) key findings – higher FA and lower MD in the PHCB of ε4 carriers verses non-carriers – challenges the notion that the *APOE* ε4 allele impacts

this key white matter tract in early adulthood. While this does not necessarily run counter to lifespan vulnerability systems accounts (Bero et al., 2011; Buckner et al., 2005, 2009; Jagust & Mormino, 2011), as they do not focus on structural connectivity per se, it does raise the question of what exactly underpins the previously reported early-life  $\epsilon 4$ -related alterations in functional activation and intrinsic functional connectivity (Dennis et al., 2010; Filippini et al., 2009; Shine et al., 2015; Zheng et al., 2021), assuming they reflect true effects (Mentink et al., 2021). One possibility is that these functional alterations arise as a compensatory response to damage or pathology. For example, it could be the case that the *APOE*  $\epsilon 4$  allele is associated with damage or pathology to the hippocampus, leading to the compensatory recruitment of other structures within its extended network (e.g. PCC/RSC) and ultimately increased nodal stress and network breakdown (Jones et al., 2016). Indeed, a couple of small-scale studies have previously reported that young  $\epsilon 4$  carriers exhibited lower hippocampal grey matter volume compared to non-carriers (Alexopoulos et al., 2011; O'Dwyer et al., 2012). This could, in theory, lead to hyper-activation within the PCC/RSC, as seen in Shine et al.'s (2015) study. More recent large-scale analyses cast doubt on this proposal (Khan et al., 2014; Lupton et al., 2016), however, suggesting that early-life hippocampal volume reduction (i.e. atrophy) in *APOE*  $\epsilon 4$  carriers is unlikely to account for the functional results discussed previously.

Despite this, damage or pathology affecting structures other than the hippocampus could likewise lead to an  $\epsilon 4$ -related compensatory response within the extended hippocampal navigation network. Kunz et al.'s (2015) study provides some support for this view. The authors found that young  $\epsilon 4$  carriers (relative to non-carriers) displayed reduced grid-cell-like representations in the EC, which itself was related to increased hippocampal task activation (Kunz et al., 2015). This increased activation (i.e. hyper-activation) within the hippocampus was proposed to reflect a compensatory response that enabled  $\epsilon 4$  carriers to maintain spatial memory performance at the level of non-carriers, despite apparent EC dysfunction (Kunz et al., 2015). Adding further weight to this view, a subsequent study by the same group showed that *APOE*  $\epsilon 4$  carriers demonstrated impaired path integration

performance – linked to grid-cell function in the EC (Hafting et al., 2005; Stangl et al., 2018) – when the use of compensatory strategies was restricted (Bierbrauer et al., 2020). Interestingly, the recruitment of compensatory navigational strategies was also found to involve the PCC and RSC (Bierbrauer et al., 2020). Although speculative, it is possible that this might be related to the scene-specific pattern of PCC hyper-activation observed by Shine et al. (2015). Regardless, these studies collectively provide support for the view that  $\epsilon 4$ -related alterations in functional activation and functional connectivity within the extended hippocampal navigation network may reflect a compensatory response to dysfunction, particularly of the EC. Although this does little to challenge the notion that heightened functional activation and connectivity is related to increased  $A\beta$  susceptibility, it does not align with the idea that prior results in young adults are due to reduced neural efficiency or “reserve” in *APOE*  $\epsilon 4$  carriers (Jagust & Mormino, 2011). In this regard, the findings of Chapter 4 are not entirely consistent with lifespan systems vulnerability accounts.

If *APOE*  $\epsilon 4$ -related alterations in early adulthood are a product of a compensatory response to EC dysfunction, rather than reduced neural efficiency, this raises a further question: what exactly is causing the dysfunction? One plausible answer is the growing burden of tau pathology in the EC. Post-mortem data suggest that tau pathology is sometimes present in young adults (Braak & Del Tredici, 2011) and that the extent of this pathology is exacerbated by possession of the  $\epsilon 4$  allele (Ghebremedhin et al., 1998). Given that the transentorhinal region – comprised of the lateral portion of the EC and the PRC – is among the earliest sites of tau accumulation (for recent PET evidence, see Berron et al., 2021; Yushkevich et al., 2021), it could well be the case that young *APOE*  $\epsilon 4$  carriers possess higher levels of tau in the EC than non-carriers (for relevant evidence in older adults, see Therriault et al., 2020), leading to a compensatory functional response during tasks that are directly or even indirectly EC-dependent. In Chapter 1, however, I suggested that the anterolateral EC and PRC form part of the feature network, which is proposed to support complex object (including face) representations (Murray et al., 2017). Why then would tau-



related dysfunction of the feature network in early adulthood lead to scene oddity-specific hyper-activation within the extended hippocampal navigation network, as observed by Shine et al. (2015)? It is currently challenging to reconcile these findings, especially in accordance with the evolutionary accretion model.

Alternatively, it could be the case that the *APOE*  $\epsilon$ 4 allele has no impact on these large-scale neurocognitive networks in early adulthood. According to this interpretation, the previously reported results, including those of Hodgetts et al. (2019), represent false positives. This is plausible as many studies reporting significant differences between young  $\epsilon$ 4 carriers and non-carriers involve relatively small samples (~30 per group; for relevant examples, see Alexopoulos et al., 2011; Dennis et al., 2010; Filippini et al., 2009; Heise et al., 2014; Hodgetts et al., 2019; Shine et al., 2015), and the resulting analyses are thus underpowered to detect realistic effect sizes (Mitchell, 2017). As highlighted in Chapters 1 and 4, when analyses are underpowered, the probability that an observed effect represents a true effect is reduced (Button et al., 2013). Supporting this point, large-scale attempts to identify  $\epsilon$ 4-related effects on brain structure and function in young adults have largely failed to identify any significant differences between carriers and non-carriers (Dell'Acqua et al., 2015; Khan et al., 2014; Lupton et al., 2016; Mentink et al., 2021), whether focused on the neurocognitive networks of interest or not. This interpretation of Chapter 4 has greater implications for lifespan systems vulnerability accounts than the compensatory hypothesis outlined previously. If *APOE*  $\epsilon$ 4 has no effect on the brain in early adulthood, this would directly contradict the notion that low reserve – as indexed by this allele – leads to early-life alterations within the extended hippocampal navigation network, thereby increasing susceptibility to A $\beta$  and ultimately leading to network deterioration (Bero et al., 2011; Buckner et al., 2005, 2009; Jagust & Mormino, 2011). That being said, such a suggestion is consistent with the so-called prodromal hypothesis (for a discussion, see O'Donoghue et al., 2018), which claims that the impact of  $\epsilon$ 4 only becomes apparent in individuals age 60 years or older, and that this is driven solely by the indirect effects of AD pathology (Foster et al., 2013).

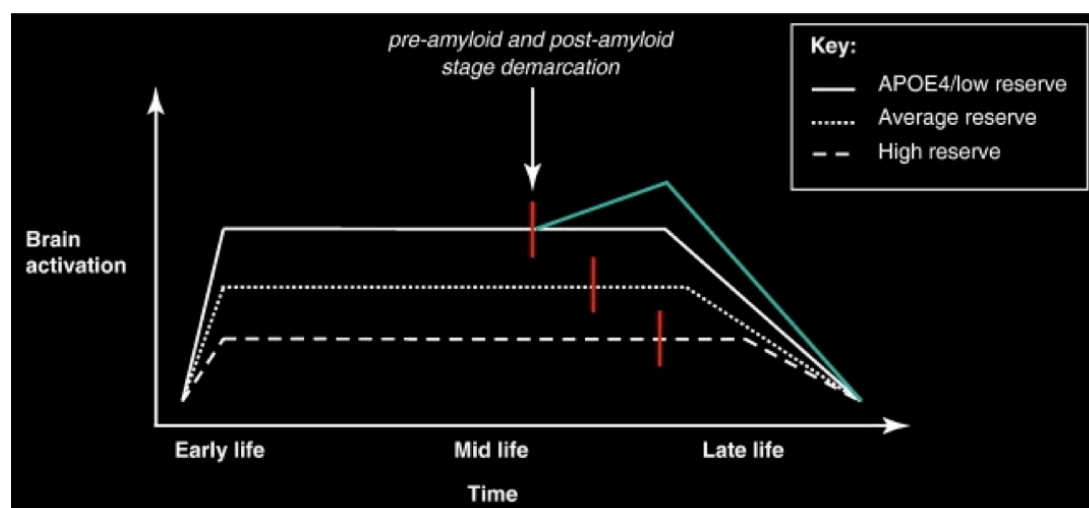
Despite this, it should be noted that Chapter 4 did find that *APOE*  $\epsilon 4$  carriers (compared to non-carriers) exhibited reduced leftward asymmetry in ILF FA and HMOA. Large-scale replication is required to determine whether this finding represents a true positive, and it is unclear how this relates to lifespan systems vulnerability accounts. Nevertheless, the lateralisation finding suggests that it may be premature to simply dismiss all early-life *APOE*  $\epsilon 4$  effects as false positives.

Turning to the research conducted on middle-aged and older adults (Chapters 2), there are further implications for theoretical accounts of *APOE*. Lifespan systems vulnerability accounts do not make firm predictions about cognitive performance in mid-life, instead focusing on functional activation/connectivity and the accumulation of A $\beta$  (Bero et al., 2011; Buckner et al., 2005, 2009; Jagust & Mormino, 2011). As shown in Figure 5.3, hyper-activation early in the adult lifespan is proposed to precipitate A $\beta$  accumulation, which in turn leads to earlier network decline. Given the recent link between A $\beta$  burden in posteromedial regions (e.g. PCC/RSC) and poorer scene mnemonic discrimination (Maass et al., 2019), as well as reports of preferential *APOE*  $\epsilon 4$  effects on allocentric navigation and scene-based deficits in young adults (Hodgetts et al., 2019; Kunz et al., 2015; Shine et al., 2015; although see Chapter 4), one might expect to observe poorer scene oddity performance in middle-aged  $\epsilon 4$  carriers relative to non-carriers. In Chapter 2, however,  $\epsilon 4$  carriers showed lower accuracy with advancing age independent of condition (i.e. not specific to the scene or face condition), and only when compared to  $\epsilon 2$  carriers (i.e. not when compared to  $\epsilon 3$  carriers). Although this does not necessarily rule out the possibility that the  $\epsilon 4$  allele is associated with increased A $\beta$  in key nodes of the extended hippocampal navigation network, which is in turn linked with scene discrimination impairment, it does indicate that the ventral component of the feature network may likewise be impacted by this allele in mid-life. Several possible explanations exist (see Chapter 2, Section 2.4), ranging from more advanced and widespread A $\beta$  accumulation in  $\epsilon 4$  carriers compared with  $\epsilon 3$  and particularly  $\epsilon 2$  carriers (Mishra et al., 2018) to the co-existence of A $\beta$  and tau pathology in selective networks (Maass et al., 2019). Irrespective of the

underlying explanation, it isn't clear how lifespan systems vulnerability accounts can explain the pattern of results observed, especially given that they focus more heavily on regions comprising the extended hippocampal navigation network (e.g. PCC). Moreover, if early-life  $\epsilon 4$ -related functional alterations within this particular network constitute false positives (see above), it is even harder for lifespan systems vulnerability accounts to explain this finding.

### Figure 5.3.

*Lifespan Changes in Functional Brain Activation and their Relation to A $\beta$  Accumulation*



*Note.* Hypothetical patterns of functional brain activation across the lifespan are shown for individuals with low, average, and high reserve. In this context, carriers of the *APOE*  $\epsilon 4$  allele are considered to have low reserve. Red vertical lines indicate the stage at which notable A $\beta$  is thought to be evident in each group. Reprinted from Jagust and Mormino (2011).

However, the presence of age-related differences in oddity accuracy between  $\epsilon 4$  and  $\epsilon 2$  carriers does not necessarily align with other theories regarding *APOE*'s impact on the brain and cognition either. Briefly mentioned above, the prodromal hypothesis states that the impact of *APOE*  $\epsilon 4$  on cognition is an indirect reflection of AD pathology, emerging around age 60

(Foster et al., 2013). This account differs from lifespan systems vulnerability accounts in that it does not consider early-life effects of the  $\epsilon 4$  allele. Endorsing this account, a number of studies have reported that cognitive differences among healthy older  $\epsilon 4$  carriers and non-carriers are reduced or disappear entirely when individuals who later develop AD are removed (e.g. Bondi et al., 1999; Hayden et al., 2009; Knight et al., 2014; for a discussion, see O'Donoghue et al., 2018). It is difficult to rule this out without longitudinal follow-up, or at least  $A\beta$  and tau PET imaging, but the majority of participants included in Chapter 2 were below 60 years of age (57.44%). As such, it seems unlikely that these effects are driven entirely by the presence of individuals who will go on to later develop AD. Another theory that cannot readily explain the results of Chapter 2 – not yet discussed in this thesis – is the antagonistic pleiotropy hypothesis (Han & Bondi, 2008; Tuminello & Han, 2011). According to this account, the *APOE*  $\epsilon 4$  allele is proposed to have a beneficial effect on the brain and cognition in early-life, but a disadvantageous effect in late-life. No clear effects are predicted in mid-life, which is consistent with a meta-analysis on *APOE* genotype effects in this age group (Lancaster, Tabet, & Rusted, 2017). Contrary to this prediction, Chapter 2 reported a significant difference in the age trend for  $\epsilon 4$  and  $\epsilon 2$  carriers in mid-life, while Chapter 4 reported only one – yet to be replicated – effect of  $\epsilon 4$  carrier status on the lateralisation of ILF microstructure. In addition, Chapter 3 did not observe any  $\epsilon 4$ -related effects or  $\epsilon 4$  by age interactions in relation to structural covariance. These findings do not correspond well with the antagonistic pleiotropy hypothesis, which is arguably consistent with recent work testing its key predictions (Henson et al., 2020; Weissberger et al., 2018). Taken together, it is clear that the findings from the current thesis do not form a coherent narrative, and they cannot easily be explained by current theories of *APOE* genotype and age, including lifespan systems vulnerability accounts.

### **5.3. Methodological considerations and limitations**

In each chapter in this thesis, I discussed relevant limitations and their implications. Here, I focus on a select number of limitations that are

applicable to all or most of the studies reported. These limitations should be considered when interpreting the findings of the studies, as well as the chapter-specific limitations.

### *5.3.1. Reliance on cross-sectional designs and the treatment of age as an independent variable*

All studies reported in this thesis either examined the impact of *APOE* genotype and age (Chapters 2 and 3) or aimed to determine whether *APOE*  $\epsilon 4$  impacts age-related processes (Chapter 4). To this end, these studies adopted cross-sectional designs, whereby the key variables were measured at the same time point. Cross-sectional studies are, by their nature, convenient and easy to conduct, at least relative to longitudinal studies. A drawback of such designs, however, is the potential influence of cohort effects (Hedden & Gabrieli, 2004; Ganguli, 2017; Grady, 2012). Cohort effects refer to the phenomenon in which individuals born in a particular year or era share characteristics that individuals born in another year or era do not (Dodge et al., 2017). As an example, consider how performance on a web-based cognitive task could be driven by experience with technology, which tends to differ between younger adults and older adults (Olson et al., 2011). More substantively, one prior study on episodic and semantic memory over the lifespan showed that differences between cross-sectional and longitudinal analyses could be explained by cohort differences in educational attainment (Rönnlund et al., 2005). It is clear from these examples that differences in various characteristics may account for age effects observed in cross-sectional research. Given that the independent variable of interest – in this case, age – is measured at the same time as the dependent variable (e.g. cognitive task performance), cross-sectional designs also do not provide insight into *rates* of ageing within individuals (Hofer & Sliwinski, 2001). A study by Nyberg et al. (2010) highlights the importance of this point (see also Argiris et al., 2021), as the authors observed contrasting patterns of frontal cortex activations during a semantic categorisation task in cross-sectional and longitudinal analyses. More specifically, Nyberg et al. (2010) reported that while cross-sectional analyses indicated that age was

associated with the over-recruitment of frontal regions during the task, longitudinal analyses indicated that aging was actually associated with the under-recruitment of frontal regions. This finding demonstrates how cross-sectional designs can, in certain circumstances, produce misleading impressions about the impact of age on the brain and cognition within individuals (for a broader discussion, see Nyberg & Pudas, 2019). It might be the case, for instance, that *APOE*  $\epsilon 2$  and  $\epsilon 4$  carriers display different longitudinal patterns of age-related *decline*, as opposed to the cross-sectional patterns reported in Chapter 2. The same could also be said of the age-related patterns of structural covariance observed in Chapter 3. The adoption of longitudinal designs would, therefore, aid our collective understanding of change over time – specifically, decline.

Despite these limitations, it is important to recognise that the reliance on cross-sectional designs can be somewhat unavoidable. As noted by Jack et al. (2015), most longitudinal data covers a span of a few years rather than 50, 60 or 70 years. If one is interested in age trends covering the adult lifespan, this means that longitudinal data are not always useful, particularly if more recent technology (e.g. fMRI) is of interest. A hybrid approach, such as combining retrospective longitudinal data with modern technology, can help to ameliorate this somewhat. For example, the cognitive data collected in Chapter 2 could be related to relevant phenotypic data, made available via ALSPAC. Notably, longitudinal designs are not without their own drawbacks. In addition to being costly and time intensive, it has been argued that longitudinal studies of cognition can be distorted by the presence of practice effects (Salthouse, 2019). This is not a problem here, as the chapter examining performance on the odd-out-out perceptual discrimination task only tested participants once. In this regard, while longitudinal studies provide important insights into brain and cognitive ageing, they are not a panacea for all challenges in age-related research.

Aside from the cross-sectional nature of the studies reported in this thesis, an additional consideration is the treatment of age in this context. Prior research investigating the impact of age on object and scene/spatial

processing has often compared groups of younger and older adults against each other (e.g. Berron et al., 2018; Reagh et al., 2016, 2018; Ryan et al., 2012; Stark & Stark, 2017). While this has provided some interesting insights, treating age as a categorical variable (i.e. younger adults/older adults) can potentially mask changes that occur across the lifespan (Hedden & Gabrieli, 2004). Indeed, this approach provides relatively limited information about the nature of the age effects, such as whether they are linear or non-linear. The work in Chapters 2 and 3 adopt a different approach, examining age as a continuous variable. This difference in approach could explain why the current thesis did not observe selective impairments in the ventral component of the feature network or its corresponding complex object (including face) representations, as has been observed elsewhere (although for object-specific age impairments using a similar approach, see Güsten et al., 2021). Moving forward, it would be interesting to investigate whether previously reported findings replicate when adopting a more sensitive approach to the treatment of age, as adopted in this thesis.

### *5.3.2. Lack of A $\beta$ and tau PET imaging*

One of the central challenges in studies seeking to understand the impact of *APOE* genotype and age is the difficulty associated with differentiating between “normal” and pathological ageing. Over the last two decades, research conducted using PET has convincingly demonstrated that various forms of neuropathology are present in the ageing brain despite a lack of overt clinical impairment (Jagust, 2018). Illustrating this point, Jansen et al. (2015) estimated that 10.4% of cognitively unimpaired individuals aged 50 years were already deemed to be A $\beta$  positive. Split by *APOE*  $\epsilon$ 4 carriers and non-carriers, the resulting estimates were 14.9% and 5.7%, respectively (Jansen et al., 2015; see also Mishra et al., 2018). This suggests that even by the fifth decade of life, approximately one in ten individuals may possess significant amounts of AD-related pathology, a figure that is even higher among those who possess one or more copies of the  $\epsilon$ 4 allele. Uncertainty exists as to what age tau pathology typically starts, but post-mortem data

indicate that tau may be present as early as the third decade of life (Braak & Del Tredici, 2011). Consequently, despite focusing on healthy individuals without overt clinical impairments, participants in this thesis – especially those in Chapters 2 and 3 – could have had significant levels of both A $\beta$  and tau pathology.

A recent line of evidence, discussed at various points throughout this thesis, indicates that A $\beta$  and tau preferentially accumulate in distinct large-scale neurocognitive networks. In the case of A $\beta$ , PET studies have shown that early accumulation occurs in regions comprising the extended hippocampal navigation network, notably the PCC/RSC (Oh et al., 2016; Mattsson et al., 2019; Palmqvist et al., 2017; Villeneuve et al., 2015). By contrast, evidence from both post-mortem examination (Braak & Braak, 1997) and PET (Berron et al., 2021; Yushkevich et al., 2021) indicate that the transentorhinal region – including the PRC and parts of the EC – is among the earliest sites of pathological tau accumulation. The PRC and the anterolateral EC form part of the ventral component of the feature network, thereby suggesting that tau preferentially impacts this network. The preferential targeting of these networks by distinct forms of AD pathology has subsequently been linked to scene and object discrimination impairment in older adults (Maass et al., 2019), as one might predict based on the proposed functions of these two networks (Murray et al., 2017). These findings highlight the challenge associated with determining whether the impact of age and *APOE* genotype – or *APOE*  $\epsilon$ 4 specifically – are a by-product of neurodegenerative disease or if there is a “pure” form of age-related decline (for relevant discussions, see Fjell et al., 2014; Jagust, 2013; Walhovd et al., 2014). For instance, it remains an open question as to whether effects of age and/or *APOE* observed in this thesis would hold in sub-groups without signs of pathology in key brain structures, such as the hippocampus, EC, or PCC.

### *5.3.3. Inability to account for ethnicity/ancestry*

In Chapters 2 and 4, participants of non-European ancestry were removed from consideration during genetic pre-processing. This was not the case in



Chapter 3, although ethnicity/ancestry was not explicitly examined either. While it is common to remove participants of non-European ancestry in genetic analyses, it is increasingly recognised that the resulting Eurocentric bias limits our understanding of genetic variation and leads to a poorer understanding of disease prediction in individuals of non-European ancestry (Sirugo et al., 2019). Furthermore, regarding *APOE* genotype specifically, there is evidence that the association between the  $\epsilon 4$  allele and AD risk varies as a function of ethnicity/ancestry. In Farrer et al.'s (1997) early meta-analysis, it was observed that the odds ratios for AD were higher for Japanese individuals ( $\epsilon 3/\epsilon 4 = 5.6$ ,  $\epsilon 4/\epsilon 4 = 33.1$ ) than for so-called Caucasian populations ( $\epsilon 3/\epsilon 4 = \sim 4$ ,  $\epsilon 4/\epsilon 4 = \sim 12$ ). This same meta-analysis likewise reported that the odds ratios for AD among African Americans were lower ( $\epsilon 3/\epsilon 4 = 1.1$ ,  $\epsilon 4/\epsilon 4 = 5.7$ ) than those observed for European and Japanese individuals. More recent work has largely substantiated these ethnicity-/ancestry-specific associations between *APOE*  $\epsilon 4$  and AD risk (e.g. Hendrie et al., 2014; Lui et al., 2014; Zheng et al., 2016), although variability exists (Alzheimer's Association, 2020). Such findings suggest that the link between *APOE* genotype and AD may not be equivalent across populations that differ in their ethnic and ancestral backgrounds (for a discussion, see Belloy et al., 2019). This raises an important and intriguing question: do the reported effects of *APOE*  $\epsilon 4$  on the brain and cognition likewise vary according to ethnicity/ancestry? There is some evidence to indicate that is indeed the case. For example, Turney et al. (2020) reported that older *APOE*  $\epsilon 4$  carriers relative to non-carriers exhibited lower intrinsic functional connectivity between temporal regions of the so-called default mode network, albeit only in non-Hispanic white individuals. The same effect was not seen in Hispanic or non-Hispanic black individuals (Turney et al., 2020). The authors interpret their results in the context of ancestral differences. Although far from conclusive, the above findings highlight the importance of considering ethnicity/ancestry in studies related to *APOE* genotype, and further indicate that the findings reported throughout this thesis may not generalise to populations with different ancestral backgrounds to those studied.

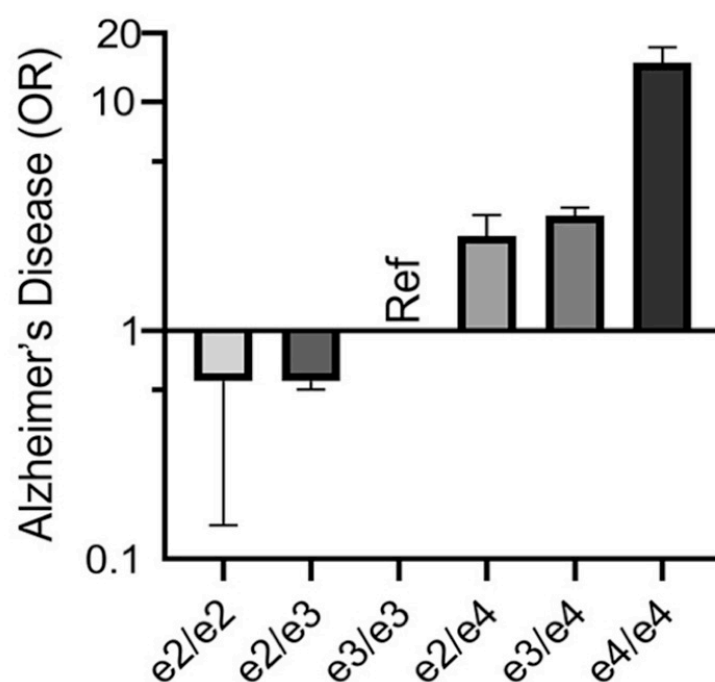
#### 5.3.4. *Lack of statistical power to investigate the impact of all APOE allele combinations*

Throughout this thesis, I adopted two approaches to studying the impact of *APOE* genotype and *APOE*  $\epsilon 4$  in particular. In Chapter 2, I compared  $\epsilon 2$  ( $\epsilon 2/\epsilon 2$ ,  $\epsilon 2/\epsilon 3$ ),  $\epsilon 3$  ( $\epsilon 3/\epsilon 3$ ), and  $\epsilon 4$  ( $\epsilon 3/\epsilon 4$ ,  $\epsilon 4/\epsilon 4$ ) groups against each other, while excluding those with the  $\epsilon 2/\epsilon 4$  genotype. In Chapters 3 and 4, I compared  $\epsilon 4$  carriers ( $\epsilon 2/\epsilon 4$ ,  $\epsilon 3/\epsilon 4$ ,  $\epsilon 4/\epsilon 4$ ) against non-carriers ( $\epsilon 2/\epsilon 2$ ,  $\epsilon 2/\epsilon 3$ ,  $\epsilon 3/\epsilon 3$ ). While the latter approach is common in the literature (e.g. Hodgetts et al., 2019; Shine et al., 2015; Stening et al., 2017), the former approach remains relatively rare (for exceptions, see Lancaster, Forster et al., 2017; Suri et al., 2015). In fact, the ability to examine the impact of *APOE*  $\epsilon 2$  in Chapter 2 was a notable advantage of that particular study (Suri et al., 2013). However, it is important to acknowledge that there are six possible combinations of the two *APOE* alleles:  $\epsilon 2/\epsilon 2$ ,  $\epsilon 2/\epsilon 3$ ,  $\epsilon 3/\epsilon 3$ ,  $\epsilon 2/\epsilon 4$ ,  $\epsilon 3/\epsilon 4$ , and  $\epsilon 4/\epsilon 4$ . By combining individuals with different allelic combinations into distinct groups, whether  $\epsilon 4$  carrier/non-carriers or  $\epsilon 2/\epsilon 3/\epsilon 4$  groups, the studies reported here may have masked subtle yet interesting effects. It is relatively well established, for example, that  $\epsilon 4$  homozygotes are at much higher risk of developing AD than  $\epsilon 4$  heterozygotes (Figure 5.4). It follows, therefore, that similar effects on the brain and cognition may be evident prior to overt clinical symptoms. Supporting this notion, a relatively recent study observed that older  $\epsilon 4$  homozygotes exhibited a dissociable pattern of short-term and long-term object location memory compared to  $\epsilon 4$  heterozygotes ( $\epsilon 3/\epsilon 4$ ) and  $\epsilon 3$  homozygotes, such that they were superior on the former but impaired on the latter (Zokaei et al., 2019). This same group further reported that  $\epsilon 2$  heterozygotes ( $\epsilon 2/\epsilon 3$ ) outperformed  $\epsilon 3$  homozygotes on sensitive measures of short-term memory, independent of age (Zokaei et al., 2021). Collectively, these studies highlight how grouping individuals with different genotypes together may potentially lead to inconsistencies within the literature. Unfortunately, the studies included in this thesis did not include large enough numbers of participants with each allelic combination to adequately power genotype-specific analyses. The availability of large-scale, population-level studies such as UK Biobank now makes such analyses feasible (for a

relevant example, see Lumsden et al., 2020), and future research would benefit from examining genotype-specific effects on the brain and cognition in these studies.

**Figure 5.4.**

*Risk of Developing AD According to APOE Genotype*



*Note.* Odds ratios and 95% confidence intervals for AD are shown for five different *APOE* allelic combinations relative to the most common allelic combination ( $\epsilon 3/\epsilon 3$ ). Data shown are from the meta-analysis conducted by Farrer et al. (1997). Abbreviations: OR = odds ratio, Ref = reference. Reprinted from Belloy et al. (2019).

### 5.3.5. Inability to examine polygenic effects

To fully understand the effect of *APOE* on the brain and cognition, it is necessary to explore the effects of other AD risk factors, elucidating precisely which effects can be attributed to *APOE*. In recent years, GWAS have identified a number of genetic loci that are associated with AD (Jansen et al., 2019; Lambert et al., 2013; Marioni et al., 2018). Although each of these

common variants confers relatively little risk, polygenic risk scores (PRS) based on their summated effects have demonstrable predictive utility for AD (Escott-Price et al., 2015; Escott-Price, Myers et al., 2017; Escott-Price, Shoai, et al., 2017). In addition, AD PRS – excluding or accounting for *APOE*  $\epsilon 4$  – have been associated with hippocampal volume (Foley et al., 2017; Ge et al., 2018; Lupton et al., 2016; Mormino et al., 2016), and the volume/cortical thickness of posteromedial structures (Li et al., 2018; Sabuncu et al., 2012) in cognitively normal individuals (for a review, see Harrison & Bookheimer, 2016). These brain regions form part of the extended hippocampal navigation network (Murray et al., 2017) and are affected early in the course of AD (Braak & Braak, 1991, 2006; Chetelat et al., 2003; Greicius et al., 2004; Minoshima et al., 1997; Pengas, Hodges et al., 2010). More recently, a relatively large study of healthy young adults further observed that AD PRS – but not *APOE*  $\epsilon 4$  – was associated with scene-related activation in the hippocampus (Chandler et al., 2020). Given that *APOE*  $\epsilon 4$  is linked with  $A\beta$  deposition in posteromedial regions, as discussed, it could be the case that *APOE*  $\epsilon 4$  and AD PRS (excluding *APOE*  $\epsilon 4$ ) impact different components of the extended hippocampal navigation network, potentially via  $A\beta$  and non- $A\beta$  pathways, respectively. Such a suggestion could help reconcile the findings of both Chandler et al. (2020) and Shine et al. (2015). An related question, therefore, is whether AD PRS – independent of the  $\epsilon 4$  allele – differentially impact perceptual scene and object/face discrimination in mid-life.

#### **5.4. Outstanding questions and future directions**

The limitations discussed above, as well as those mentioned in individual chapters (e.g. the limitations of tractography), provide a foundation for future work to build on that conducted as part of this thesis. However, there are broader questions pertaining to network models of cognition, such as the evolutionary accretion model (Murray et al., 2017), and lifespan systems vulnerability accounts of cognitive decline and AD. In this section, I highlight a small selection of outstanding questions – inspired by the current thesis –

and outline ways in which these questions could be addressed, providing avenues for future research.

#### *5.4.1. How does the APOE $\epsilon$ 2 allele fit into lifespan systems vulnerability accounts?*

As mentioned at various points throughout this thesis, lifespan systems vulnerability accounts propose that the *APOE*  $\epsilon$ 4 allele impacts neural efficiency or reserve in early-life, leading to heightened functional activation in and connectivity between key brain regions, which in turn result in increased A $\beta$  accumulation (Bero et al., 2011; Buckner et al., 2005, 2009; Jagust & Mormino, 2011). However, despite explicitly linking  $\epsilon$ 4 with low reserve (Figure 5.3), these accounts do not directly address the role of  $\epsilon$ 2. It has long been known that the *APOE*  $\epsilon$ 2 allele has a protective role against AD (Chartier-Harlin et al., 1994; Corder et al., 1994; Farrer et al., 1997). Moreover, contemporary research provides convincing evidence that the protection conferred by this allele is largely driven by a reduction in A $\beta$  (Goldberg et al., 2020; Reiman et al., 2020; Salvadó et al., 2021). In the context of lifespan systems vulnerability accounts, therefore, one might expect young *APOE*  $\epsilon$ 2 carriers to demonstrate *reduced* functional activation/connectivity in regions such as the PCC, thereby following the pattern of a “high reserve” factor (Figure 5.3). This would potentially explain why the  $\epsilon$ 2 allele is associated with lower levels of A $\beta$  burden and, in addition, AD risk. However, few studies to date have examined the impact of this allele on brain function and connectivity in young adults (although for an exception, see Suri et al., 2015), owing in part to its relatively low prevalence in the population (O’Donoghue et al., 2018). Nonetheless, in two separate studies involving both younger and middle-aged participants,  $\epsilon$ 2 and  $\epsilon$ 4 carriers showed increased encoding-related activation (Trachtenberg, Filippini, Cheeseman et al., 2012) and similar patterns of increased/decreased intrinsic functional connectivity (Trachtenberg, Filippini, Ebmeier et al., 2012) when compared to  $\epsilon$ 3 carriers. Although not necessarily focused on the neurocognitive networks of interest in this thesis, these studies point to the possibility that the effects of *APOE*  $\epsilon$ 2 do not necessarily

reflect the inverse of *APOE*  $\epsilon 4$ , as one might predict based on patterns of AD risk. Consequently, it is questionable as to whether this allele is associated with patterns of activation and connectivity that match those of hypothetical individuals with “high reserve”, as predicted by lifespan systems vulnerability accounts. Large-scale fMRI studies involving young  $\epsilon 2$ ,  $\epsilon 3$ , and  $\epsilon 4$  carriers would help to address this gap in the literature, especially if using tasks that are sensitive to the specialised representations supported by the extended hippocampal navigation and feature networks. A replication and extension of Shine et al.’s (2015) study would represent an excellent candidate in this regard.

#### *5.4.2. Do APOE $\epsilon 4$ carriers and non-carriers undergo different patterns of white matter maturation during childhood/adolescence?*

Hodgetts et al. (2019) previously reported that young *APOE*  $\epsilon 4$  carriers relative to non-carriers showed higher structural connectivity (i.e. higher FA, lower MD) in the PHCB but not the ILF. To account for this result, the authors speculated that  $\epsilon 4$  carriers and non-carriers undergo different patterns of white matter maturation, possibly via reduced/delayed axonal pruning during adolescence (Chung et al., 2016), leading to an initial “overshoot” in PHCB microstructure (see also Yeatman et al., 2012) and related increases in functional activation (e.g. Shine et al., 2015). While I observed no such differences in PHCB microstructure between those with and without the  $\epsilon 4$  allele in Chapter 4, the participants included were older than those recruited by Hodgetts et al. (2019). Moreover, while a sub-group analysis focused only on the youngest participants did not reveal any significant effects, the sample was small and the analysis thus underpowered to detect realistic effects (if they exist). The cross-sectional design adopted in both studies further limits what inferences can be drawn about *maturational change*, as white matter microstructure was examined at one time point only. It is challenging, therefore, to draw firm conclusions about the maturation of white matter tracts, such as the PHCB, in  $\epsilon 4$  carriers and non-carriers from this work. To address this, a large-scale longitudinal study of young children incorporating annual or bi-annual diffusion MRI scans would be hugely beneficial, enabling

researchers to track how PHCB (and ILF) microstructure changes over the course of childhood/adolescence and whether this differs according to *APOE*  $\epsilon 4$  carrier status. The Adolescent Brain Cognitive Development (ABCD) study represents an especially intriguing resource in this context (<https://abcdstudy.org/>). This ongoing study involves more than 11,000 children aged 9-10 years from 21 sites across the U.S., who will be followed for approximately 10 years (Karcher & Barch, 2021). Crucially, the protocol for the ABCD study includes diffusion MRI scans (Casey et al., 2018; Hagler et al., 2019), facilitating the sort of longitudinal analysis proposed here. If combined with task-related or resting-state fMRI, such a study could further test whether maturation of PHCB microstructure can account for the early-life  $\epsilon 4$ -related alterations that feature prominently in lifespan systems vulnerability accounts (Bero et al., 2011; Buckner et al., 2005, 2009; Jagust & Mormino, 2011).

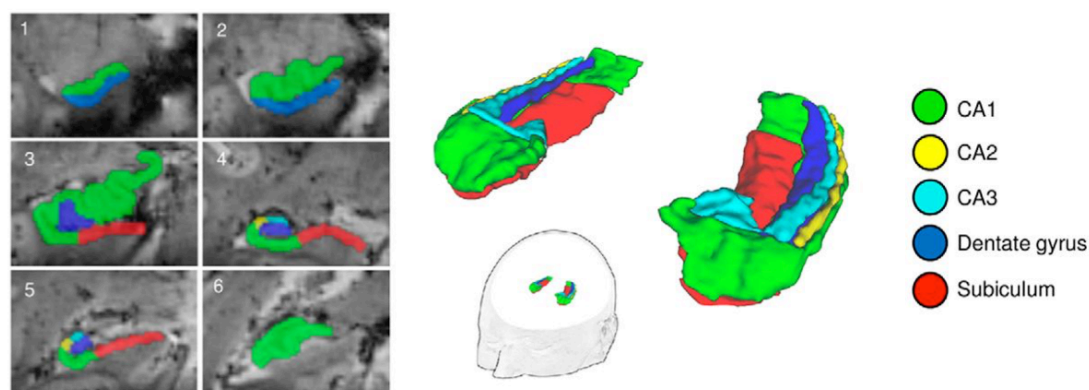
#### *5.4.3. Are hippocampal subfields differentially vulnerable to the impact of *APOE* $\epsilon 4$ and age?*

Prior studies have reported heightened activation (i.e. hyper-activation) in the hippocampus of young *APOE*  $\epsilon 4$  carriers relative to non-carriers during episodic memory tasks (Dennis et al., 2010; Filippini et al., 2009). Moreover, it has further been shown that while younger  $\epsilon 4$  carriers exhibit heightened encoding-related activation in the hippocampus compared to younger  $\epsilon 4$  non-carriers, older  $\epsilon 4$  carriers demonstrate reduced encoding-related activation in the hippocampus compared to older  $\epsilon 4$  non-carriers (Filippini et al., 2011). This points to an age interaction, whereby the *APOE*  $\epsilon 4$  allele is associated with hyper-activation in early adulthood but hypo-activation in late adulthood (see also Busche & Konnerth, 2015). However, while the hippocampus is often treated as a single unitary brain structure, it is actually comprised of several distinct subfields, namely CA1-CA3, the dentate gyrus, and the subiculum (Figure 5.5). Owing to the development of ultra-high resolution (7T) fMRI, it is now possible to segment these subfields and examine their function in the living human brain (Olsen et al., 2019; Wisse et al., 2017; Yushkevich et al., 2015). For example, Hodgetts, Voets et al.

(2017) used 7T fMRI to investigate which hippocampal subfields support scene oddity discrimination. The authors found that activation in the subiculum, especially the anteromedial subiculum, was greater for scenes relative to objects and faces (Hodgetts, Voets et al., 2017). Given that patients with AD are selectively impaired on scene oddity (Lee et al., 2006), this raises the possibility that the subiculum – a subfield of the hippocampus – may show early scene-related functional changes in individuals at-risk of developing AD, including *APOE*  $\epsilon$ 4 carriers. This would be consistent with histological work in AD, which has shown that the subiculum appears particularly vulnerable early in the course of the disease (Carlesimo et al., 2015). To confirm this possibility, future research should seek to conduct a 7T fMRI study in which participants complete the odd-one-out task. In addition, the inclusion of large number of participants from across the adult lifespan (18-90) would help address the question of whether the impact of *APOE*  $\epsilon$ 4 changes over the lifespan. This approach avoids the pitfalls associated with comparisons of younger and older adults (see Section 5.3.1), while ensuring that the potential interaction between this genetic risk factor and age is not ignored.

**Figure 5.5.**

*Hippocampal Subfields Identified using 7T MRI*



*Note.* Manually segmented hippocampal subfields (CA1, CA2, CA3, dentate gyrus, subiculum) are shown on six coronal slices for a single participant (left) and as three-dimensional reconstructions (right). Colours relate to specific subfields. Reprinted from Hodgetts, Voets et al. (2017).



## 5.5. Concluding remarks

The current thesis had two primary aims: 1) to contribute new knowledge regarding the impact of age on the so-called extended hippocampal navigation and feature networks (Murray et al., 2017), and 2) to further characterise the impact of *APOE* genotype – specifically *APOE*  $\epsilon 4$  – on these same networks at various points in the adult lifespan. To achieve these aims, the studies reported here used a unique combination of large-scale web-based cognitive testing and MRI-based methods to examine healthy participants prior to the onset of clinical symptoms. All three studies included relatively large sample sizes (min  $N = 128$ , max  $N = 524$ ), at least by current standards in cognitive neuroscience (Szucs & Ioannidis, 2017a) and neuroimaging (Szucs & Ioannidis, 2020). This made it possible to compare individuals with both risk enhancing ( $\epsilon 4$ ) and risk reducing ( $\epsilon 2$ ) alleles in Chapter 2, addressing a common limitation in the broader *APOE* literature (Suri et al., 2013). Collectively, the findings across studies provided mixed evidence regarding the impact of *APOE* genotype and age on these large-scale neurocognitive networks and their corresponding representations. *APOE*  $\epsilon 4$  carrier status was found to impact the lateralisation of ILF microstructure in young adults (Chapter 4), whereas possession of the  $\epsilon 2$  and  $\epsilon 4$  alleles was found to differentially impact odd-one-out perceptual discrimination accuracy – independent of stimulus type (scene/face) – in middle-aged and older females (Chapter 2). Although these novel findings require further replication, they *prima facie* suggest that *APOE* genotype, especially the  $\epsilon 4$  allele, has distinct effects on these networks at different points in the lifespan. However, it is important to note that while age and gender/sex were associated with the structural covariance pattern common to both the hippocampus and PRC, *APOE*  $\epsilon 4$  was not (Chapter 3). This finding implies that the common connections of these two key network nodes are not impacted by this genetic risk factor, but methodological limitations may account for this finding. Nevertheless, when viewed as a collective, it is clearly challenging to interpret these findings according to any given theoretical viewpoint, including lifespan systems vulnerability accounts (Bero et al., 2011; Buckner et al., 2005, 2009; Jagust & Mormino, 2011). This

thesis, therefore, highlights the need for further research on the impact of *APOE* genotype in large samples, at various points in the lifespan. Through the use of multi-modal imaging methods, including PET, and sensitive cognitive tasks such as the oddity, future studies will generate a clearer picture of how *APOE* genotype and age impact large-scale neurocognitive networks.

## References

- Acosta-Cabronero, J., Patterson, K., Fryer, T. D., Hodges, J. R., Pengas, G., Williams, G. B., & Nestor, P. J. (2011). Atrophy, hypometabolism and white matter abnormalities in semantic dementia tell a coherent story. *Brain*, *134*(7), 2025–2035. <https://doi.org/10.1093/brain/awr119>
- Addis, D. R., Wong, A. T., & Schacter, D. L. (2008). Age-related changes in the episodic simulation of future events. *Psychological Science*, *19*(1), 33–41. <https://doi.org/10.1111/j.1467-9280.2008.02043.x>
- Aggleton, J. P. (2012). Multiple anatomical systems embedded within the primate medial temporal lobe: Implications for hippocampal function. *Neuroscience & Biobehavioral Reviews*, *36*(7), 1579–1596. <https://doi.org/10.1016/j.neubiorev.2011.09.005>
- Aggleton, J. P., & Brown, M. W. (1999). Episodic memory, amnesia, and the hippocampal-anterior thalamic axis. *Behavioral and Brain Sciences*, *22*(3), 425–444. <https://doi.org/10.1017/S0140525X99002034>
- Aggleton, J. P., & Christiansen, K. (2015). The subiculum: The heart of the extended hippocampal system. In S. O'Mara & M. Tsanov (Eds.), *Progress in brain research* (Vol. 219, pp. 65–82). Elsevier. <https://doi.org/10.1016/bs.pbr.2015.03.003>
- Aggleton, J. P., McMackin, D., Carpenter, K., Hornak, J., Kapur, N., Halpin, S., Wiles, C. M., Kamel, H., Brennan, P., Carton, S., & Gaffan, D. (2000). Differential cognitive effects of colloid cysts in the third ventricle that spare or compromise the fornix. *Brain*, *123*(4), 800–815. <https://doi.org/10.1093/brain/123.4.800>
- Ahmed, Z., Cooper, J., Murray, T. K., Garn, K., McNaughton, E., Clarke, H., Parhizkar, S., Ward, M. A., Cavallini, A., Jackson, S., Bose, S., Clavaguera, F., Tolnay, M., Lavenir, I., Goedert, M., Hutton, M. L., & O'Neill, M. J. (2014). A novel in vivo model of tau propagation with rapid and progressive neurofibrillary tangle pathology: The pattern of spread is determined by connectivity, not proximity. *Acta Neuropathologica*, *127*(5), 667–683. <https://doi.org/10.1007/s00401-014-1254-6>
- Albert, M. S., DeKosky, S. T., Dickson, D., Dubois, B., Feldman, H. H., Fox, N. C., Gamst, A., Holtzman, D. M., Jagust, W. J., Petersen, R. C., Snyder, P. J., Carrillo, M. C., Thies, B., & Phelps, C. H. (2011). The diagnosis of mild cognitive impairment due to Alzheimer's disease: Recommendations from

- the National Institute on Aging-Alzheimer's Association workgroups on diagnostic guidelines for Alzheimer's disease. *Alzheimer's & Dementia*, 7(3), 270–279. <https://doi.org/10.1016/j.jalz.2011.03.008>
- Albi, A., Pasternak, O., Minati, L., Marizzoni, M., Bartrés-Faz, D., Bargalló, N., Bosch, B., Rossini, P. M., Marra, C., Müller, B., Fiedler, U., Wiltfang, J., Roccatagliata, L., Picco, A., Nobili, F. M., Blin, O., Sein, J., Ranjeva, J.-P., Didic, M., ... The PharmaCog Consortium. (2017). Free water elimination improves test-retest reproducibility of diffusion tensor imaging indices in the brain: A longitudinal multisite study of healthy elderly subjects. *Human Brain Mapping*, 38(1), 12–26. <https://doi.org/10.1002/hbm.23350>
- Alexander, A. L. (2010). Deterministic white matter tractography. In D. K. Jones (Ed.), *Diffusion MRI: Theory, methods, and applications* (pp. 383–395). Oxford University Press. <https://oxfordmedicine.com/view/10.1093/med/9780195369779.001.0001/med-9780195369779-chapter-022>
- Alexander, A. L., Hasan, K. M., Lazar, M., Tsuruda, J. S., & Parker, D. L. (2001). Analysis of partial volume effects in diffusion-tensor MRI. *Magnetic Resonance in Medicine*, 45(5), 770–780. <https://doi.org/10.1002/mrm.1105>
- Alexander-Bloch, A., Clasen, L., Stockman, M., Ronan, L., Lalonde, F., Giedd, J. N., & Raznahan, A. (2016). Subtle in-scanner motion biases automated measurement of brain anatomy from in vivo MRI. *Human Brain Mapping*, 37(7), 2385–2397. <https://doi.org/10.1002/hbm.23180>
- Alexander-Bloch, A., Giedd, J. N., & Bullmore, E. (2013). Imaging structural covariance between human brain regions. *Nature Reviews Neuroscience*, 14(5), 322–336. <https://doi.org/10.1038/nrn3465>
- Alexander-Bloch, A., Raznahan, A., Bullmore, E., & Giedd, J. N. (2013). The convergence of maturational change and structural covariance in human cortical networks. *Journal of Neuroscience*, 33(7), 2889–2899. <https://doi.org/10.1523/JNEUROSCI.3554-12.2013>
- Alexopoulos, P., Richter-Schmidinger, T., Horn, M., Maus, S., Reichel, M., Sidiropoulos, C., Rhein, C., Lewczuk, P., Doerfler, A., & Kornhuber, J. (2011). Hippocampal volume differences between healthy young apolipoprotein E  $\epsilon$ 2 and  $\epsilon$ 4 carriers. *Journal of Alzheimer's Disease*, 26(2), 207–210. <https://doi.org/10.3233/JAD-2011-110356>

- Allison, S. L., Fagan, A. M., Morris, J. C., & Head, D. (2016). Spatial navigation in preclinical Alzheimer's disease. *Journal of Alzheimer's Disease*, *52*(1), 77–90. <https://doi.org/10.3233/JAD-150855>
- Almgren, H., Van de Steen, F., Razi, A., Friston, K., & Marinazzo, D. (2020). The effect of global signal regression on DCM estimates of noise and effective connectivity from resting state fMRI. *NeuroImage*, *208*, 116435. <https://doi.org/10.1016/j.neuroimage.2019.116435>
- Altmann, A., Tian, L., Henderson, V. W., & Greicius, M. D. (2014). Sex modifies the APOE-related risk of developing Alzheimer disease. *Annals of Neurology*, *75*(4), 563–573. <https://doi.org/10.1002/ana.24135>
- Aly, M., Ranganath, C., & Yonelinas, A. P. (2013). Detecting changes in scenes: The hippocampus is critical for strength-based perception. *Neuron*, *78*(6), 1127–1137. <https://doi.org/10.1016/j.neuron.2013.04.018>
- Alzheimer's Association. (2020). 2020 Alzheimer's disease facts and figures. *Alzheimer's & Dementia*, *16*(3), 391–460. <https://doi.org/10.1002/alz.12068>
- Alzheimer's Society. (2014). *Dementia UK: Update*. [https://www.alzheimers.org.uk/sites/default/files/migrate/downloads/dementia\\_uk\\_update.pdf](https://www.alzheimers.org.uk/sites/default/files/migrate/downloads/dementia_uk_update.pdf)
- Andersson, J. L. R., Jenkinson, M., & Smith, S. M. (2007a). *Non-linear optimisation. FMRIB technical report TR07JA1*. [www.fmrib.ox.ac.uk/analysis/techrep](http://www.fmrib.ox.ac.uk/analysis/techrep)
- Andersson, J. L. R., Jenkinson, M., & Smith, S. M. (2007b). *Non-linear registration, aka spatial normalisation FMRIB technical report TR07JA2*. [www.fmrib.ox.ac.uk/analysis/techrep](http://www.fmrib.ox.ac.uk/analysis/techrep)
- Ankudowich, E., Pasvanis, S., & Rajah, M. N. (2016). Changes in the modulation of brain activity during context encoding vs. context retrieval across the adult lifespan. *NeuroImage*, *139*, 103–113. <https://doi.org/10.1016/j.neuroimage.2016.06.022>
- Ankudowich, E., Pasvanis, S., & Rajah, M. N. (2019). Age-related differences in prefrontal-hippocampal connectivity are associated with reduced spatial context memory. *Psychology and Aging*, *34*(2), 251–261. <https://doi.org/10.1037/pag0000310>
- Annese, J., Schenker-Ahmed, N. M., Bartsch, H., Maechler, P., Sheh, C., Thomas, N., Kayano, J., Ghatan, A., Bresler, N., Frosch, M. P., Klaming, R.,

- & Corkin, S. (2014). Postmortem examination of patient H.M.'s brain based on histological sectioning and digital 3D reconstruction. *Nature Communications*, 5, 3122. <https://doi.org/10.1038/ncomms4122>
- Antonova, D. E., Parslow, D., Brammer, M., Dawson, G. R., Jackson, S. H. D., & Morris, R. G. (2009). Age-related neural activity during allocentric spatial memory. *Memory*, 17(2), 125–143. <https://doi.org/10.1080/09658210802077348>
- Argiris, G., Stern, Y., & Habeck, C. (2021). Quantifying age-related changes in brain and behavior: A longitudinal versus cross-sectional approach. *eNeuro*, 8(4), 1–20. <https://doi.org/10.1523/ENEURO.0273-21.2021>
- Arrigo, A., Mormina, E., Anastasi, G. P., Gaeta, M., Calamuneri, A., Quartarone, A., De Salvo, S., Bruschetta, D., Rizzo, G., Trimarchi, F., & Milardi, D. (2014). Constrained spherical deconvolution analysis of the limbic network in human, with emphasis on a direct cerebello-limbic pathway. *Frontiers in Human Neuroscience*, 8, 987. <https://doi.org/10.3389/fnhum.2014.00987>
- Asendorpf, J. B., Conner, M., Fruyt, F. D., Houwer, J. D., Denissen, J. J. A., Fiedler, K., Fiedler, S., Funder, D. C., Kliegl, R., Nosek, B. A., Perugini, M., Roberts, B. W., Schmitt, M., Aken, M. A. G. van, Weber, H., & Wicherts, J. M. (2013). Recommendations for increasing replicability in psychology. *European Journal of Personality*, 27(2), 108–119. <https://doi.org/10.1002/per.1919>
- Asendorpf, J. B., van de Schoot, R., Denissen, J. J. A., & Hutteman, R. (2014). Reducing bias due to systematic attrition in longitudinal studies: The benefits of multiple imputation. *International Journal of Behavioral Development*, 38(5), 453–460. <https://doi.org/10.1177/0165025414542713>
- Ashburner, J., & Friston, K. J. (2011). Diffeomorphic registration using geodesic shooting and Gauss-Newton optimisation. *NeuroImage*, 55(3), 954–967. <https://doi.org/10.1016/j.neuroimage.2010.12.049>
- Ashford, J. W. (2004). APOE genotype effects on Alzheimer's disease onset and epidemiology. *Journal of Molecular Neuroscience*, 23(3), 157–165. <https://doi.org/10.1385/JMN:23:3:157>
- Assaf, Y., Johansen-Berg, H., & Thiebaut de Schotten, M. (2019). The role of diffusion MRI in neuroscience. *NMR in Biomedicine*, 32(4), e3762. <https://doi.org/10.1002/nbm.3762>

- Baayen, R. H., Davidson, D. J., & Bates, D. M. (2008). Mixed-effects modeling with crossed random effects for subjects and items. *Journal of Memory and Language*, *59*(4), 390–412. <https://doi.org/10.1016/j.jml.2007.12.005>
- Babapour Mofrad, R., Tijms, B. M., Scheltens, P., Barkhof, F., van der Flier, W. M., Sikkes, S. A. M., & Teunissen, C. E. (2020). Sex differences in CSF biomarkers vary by Alzheimer disease stage and APOE  $\epsilon$ 4 genotype. *Neurology*, *95*(17), e2378–e2388. <https://doi.org/10.1212/WNL.00000000000010629>
- Baldassano, C., Esteva, A., Fei-Fei, L., & Beck, D. M. (2016). Two distinct scene-processing networks connecting vision and memory. *eNeuro*, *3*(5), 1–14. <https://doi.org/10.1523/ENEURO.0178-16.2016>
- Banfi, C., Koschutnig, K., Moll, K., Schulte-Körne, G., Fink, A., & Landerl, K. (2019). White matter alterations and tract lateralization in children with dyslexia and isolated spelling deficits. *Human Brain Mapping*, *40*(3), 765–776. <https://doi.org/10.1002/hbm.24410>
- Barense, M. D., Bussey, T. J., Lee, A. C. H., Rogers, T. T., Davies, R. R., Saksida, L. M., Murray, E. A., & Graham, K. S. (2005). Functional specialization in the human medial temporal lobe. *Journal of Neuroscience*, *25*(44), 10239–10246. <https://doi.org/10.1523/JNEUROSCI.2704-05.2005>
- Barense, M. D., Gaffan, D., & Graham, K. S. (2007). The human medial temporal lobe processes online representations of complex objects. *Neuropsychologia*, *45*(13), 2963–2974. <https://doi.org/10.1016/j.neuropsychologia.2007.05.023>
- Barense, M. D., Henson, R. N. A., Lee, A. C. H., & Graham, K. S. (2010). Medial temporal lobe activity during complex discrimination of faces, objects, and scenes: Effects of viewpoint. *Hippocampus*, *20*(3), 389–401. <https://doi.org/10.1002/hipo.20641>
- Barnett, A. J., Reilly, W., Dimsdale-Zucker, H. R., Mizrak, E., Reagh, Z. M., & Ranganath, C. (2021). Intrinsic connectivity reveals functionally distinct cortico-hippocampal networks in the human brain. *PLOS Biology*, *19*(6), e3001275. <https://doi.org/10.1371/journal.pbio.3001275>
- Bastiani, M., & Roebroek, A. (2015). Unraveling the multiscale structural organization and connectivity of the human brain: The role of diffusion MRI. *Frontiers in Neuroanatomy*, *9*, 77. <https://doi.org/10.3389/fnana.2015.00077>

- Bates, D., Mächler, M., Bolker, B., & Walker, S. (2015). Fitting linear mixed-effects models using lme4. *Journal of Statistical Software*, *67*(1), 1–48. <https://doi.org/10.18637/jss.v067.i01>
- Baxter, M. G. (2009). Involvement of medial temporal lobe structures in memory and perception. *Neuron*, *61*(5), 667–677. <https://doi.org/10.1016/j.neuron.2009.02.007>
- Beaulieu, C. (2002). The basis of anisotropic water diffusion in the nervous system—A technical review. *NMR in Biomedicine*, *15*(7–8), 435–455. <https://doi.org/10.1002/nbm.782>
- Behrmann, M., Lee, A. C. H., Geskin, J. Z., Graham, K. S., & Barense, M. D. (2016). Temporal lobe contribution to perceptual function: A tale of three patient groups. *Neuropsychologia*, *90*, 33–45. <https://doi.org/10.1016/j.neuropsychologia.2016.05.002>
- Behrmann, M., & Plaut, D. C. (2013). Distributed circuits, not circumscribed centers, mediate visual recognition. *Trends in Cognitive Sciences*, *17*(5), 210–219. <https://doi.org/10.1016/j.tics.2013.03.007>
- Belloy, M. E., Napolioni, V., & Greicius, M. D. (2019). A quarter century of APOE and Alzheimer’s disease: Progress to date and the path forward. *Neuron*, *101*(5), 820–838. <https://doi.org/10.1016/j.neuron.2019.01.056>
- Benoit, R. G., & Schacter, D. L. (2015). Specifying the core network supporting episodic simulation and episodic memory by activation likelihood estimation. *Neuropsychologia*, *75*, 450–457. <https://doi.org/10.1016/j.neuropsychologia.2015.06.034>
- Ben-Shachar, M. S., Lüdtke, D., & Makowski, D. (2020). effectsize: Estimation of Effect Size Indices and Standardized Parameters. *Journal of Open Source Software*, *5*(56), 2815. <https://doi.org/10.21105/joss.02815>
- Bernhardt, B. C., Hong, S., Bernasconi, A., & Bernasconi, N. (2013). Imaging structural and functional brain networks in temporal lobe epilepsy. *Frontiers in Human Neuroscience*, *7*, 624. <https://doi.org/10.3389/fnhum.2013.00624>
- Bero, A. W., Yan, P., Roh, J. H., Cirrito, J. R., Stewart, F. R., Raichle, M. E., Lee, J.-M., & Holtzman, D. M. (2011). Neuronal activity regulates the regional vulnerability to amyloid- $\beta$  deposition. *Nature Neuroscience*, *14*(6), 750–756. <https://doi.org/10.1038/nn.2801>



- Berron, D., Neumann, K., Maass, A., Schütze, H., Fliessbach, K., Kiven, V., Jessen, F., Sauvage, M., Kumaran, D., & Düzel, E. (2018). Age-related functional changes in domain-specific medial temporal lobe pathways. *Neurobiology of Aging*, *65*, 86–97. <https://doi.org/10.1016/j.neurobiolaging.2017.12.030>
- Berron, D., van Westen, D., Ossenkoppele, R., Strandberg, O., & Hansson, O. (2020). Medial temporal lobe connectivity and its associations with cognition in early Alzheimer's disease. *Brain*, *143*(3), 1233–1248. <https://doi.org/10.1093/brain/awaa068>
- Berron, D., Vogel, J. W., Insel, P. S., Pereira, J. B., Xie, L., Wisse, L. E. M., Yushkevich, P. A., Palmqvist, S., Mattsson-Carlsson, N., Stomrud, E., Smith, R., Strandberg, O., & Hansson, O. (2021). Early stages of tau pathology and its associations with functional connectivity, atrophy and memory. *Brain*, *awab114*. <https://doi.org/10.1093/brain/awab114>
- Betzel, R. (2020). Network neuroscience and the connectomics revolution. *arXiv*. <http://arxiv.org/abs/2010.01591>
- Bierbrauer, A., Kunz, L., Gomes, C. A., Luhmann, M., Deuker, L., Getzmann, S., Wascher, E., Gajewski, P. D., Hengstler, J. G., Fernandez-Alvarez, M., Atienza, M., Cammisuli, D. M., Bonatti, F., Pruneti, C., Percesepe, A., Bellaali, Y., Hanseeuw, B., Strange, B. A., Cantero, J. L., & Axmacher, N. (2020). Unmasking selective path integration deficits in Alzheimer's disease risk carriers. *Science Advances*, *6*(35), eaba1394. <https://doi.org/10.1126/sciadv.aba1394>
- Bird, C. M., Chan, D., Hartley, T., Pijnenburg, Y. A., Rossor, M. N., & Burgess, N. (2010). Topographical short-term memory differentiates Alzheimer's disease from frontotemporal lobar degeneration. *Hippocampus*, *20*(10), 1154–1169. <https://doi.org/10.1002/hipo.20715>
- Biswal, B., Yetkin, F. Z., Haughton, V. M., & Hyde, J. S. (1995). Functional connectivity in the motor cortex of resting human brain using echo-planar mri. *Magnetic Resonance in Medicine*, *34*(4), 537–541. <https://doi.org/10.1002/mrm.1910340409>
- Biundo, R., Gardini, S., Caffarra, P., Concari, L., Martorana, D., Neri, T. M., Shanks, M. F., & Venneri, A. (2011). Influence of APOE status on lexical–semantic skills in Mild Cognitive Impairment. *Journal of the International Neuropsychological Society*, *17*(3), 423–430. <https://doi.org/10.1017/S135561771100021X>

- Blacker, D., Haines, J. L., Rodes, L., Terwedow, H., Go, R. C. P., Harrell, L. E., Perry, R. T., Bassett, S. S., Chase, G., Meyers, D., Albert, M. S., & Tanzi, R. (1997). ApoE-4 and age at onset of Alzheimer's disease: The NIMH Genetics Initiative. *Neurology*, *48*(1), 139–147. <https://doi.org/10.1212/WNL.48.1.139>
- Bondi, M. W., Salmon, D. P., Galasko, D., Thomas, R. G., & Thal, L. J. (1999). Neuropsychological function and apolipoprotein E genotype in the preclinical detection of Alzheimer's disease. *Psychology and Aging*, *14*(2), 295–303. <https://doi.org/10.1037//0882-7974.14.2.295>
- Bouhali, F., Schotten, M. T. de, Pinel, P., Poupon, C., Mangin, J.-F., Dehaene, S., & Cohen, L. (2014). Anatomical connections of the visual word form area. *Journal of Neuroscience*, *34*(46), 15402–15414. <https://doi.org/10.1523/JNEUROSCI.4918-13.2014>
- Bourbon-Teles, J., Jorge, L., Canário, N., & Castelo-Branco, M. (2021). Structural impairments in hippocampal and occipitotemporal networks specifically contribute to decline in place and face category processing but not to other visual object categories in healthy aging. *Brain and Behavior*, e02127. <https://doi.org/10.1002/brb3.2127>
- Boyd, A., Golding, J., Macleod, J., Lawlor, D. A., Fraser, A., Henderson, J., Molloy, L., Ness, A., Ring, S., & Smith, G. D. (2012). Cohort profile: The 'Children of the 90s'—The index offspring of the Avon Longitudinal Study of Parents and Children. *International Journal of Epidemiology*, *42*(1), 111–127. <https://doi.org/10.1093/ije/dys064>
- Boyd, A., Thomas, R., Hansell, A. L., Gulliver, J., Hicks, L. M., Griggs, R., Vande Hey, J., Taylor, C. M., Morris, T., Golding, J., Doerner, R., Fecht, D., Henderson, J., Lawlor, D. A., Timpson, N. J., & Macleod, J. (2019). Data Resource Profile: The ALSPAC birth cohort as a platform to study the relationship of environment and health and social factors. *International Journal of Epidemiology*, *48*(4), 1038–1039k. <https://doi.org/10.1093/ije/dyz063>
- Braak, H., & Braak, E. (1985). On areas of transition between entorhinal allocortex and temporal isocortex in the human brain. Normal morphology and lamina-specific pathology in Alzheimer's disease. *Acta Neuropathologica*, *68*(4), 325–332. <https://doi.org/10.1007/BF00690836>
- Braak, H., & Braak, E. (1997). Frequency of stages of Alzheimer-related lesions in different age categories. *Neurobiology of Aging*, *18*(4), 351–357. [https://doi.org/10.1016/S0197-4580\(97\)00056-0](https://doi.org/10.1016/S0197-4580(97)00056-0)

- Braak, H., & Del Tredici, K. (2011). The pathological process underlying Alzheimer's disease in individuals under thirty. *Acta Neuropathologica*, *121*(2), 171–181. <https://doi.org/10.1007/s00401-010-0789-4>
- Bressler, S. L., & Menon, V. (2010). Large-scale brain networks in cognition: Emerging methods and principles. *Trends in Cognitive Sciences*, *14*(6), 277–290. <https://doi.org/10.1016/j.tics.2010.04.004>
- Brown, J. A., Terashima, K. H., Burggren, A. C., Ercoli, L. M., Miller, K. J., Small, G. W., & Bookheimer, S. Y. (2011). Brain network local interconnectivity loss in aging APOE-4 allele carriers. *Proceedings of the National Academy of Sciences*, *108*(51), 20760–20765. <https://doi.org/10.1073/pnas.1109038108>
- Brown, V. A. (2021). An introduction to linear mixed-effects modeling in R. *Advances in Methods and Practices in Psychological Science*, *4*(1), 1–9. <https://doi.org/10.1177/2515245920960351>
- Browning, P. G. F., Baxter, M. G., & Gaffan, D. (2013). Prefrontal-temporal disconnection impairs recognition memory but not familiarity discrimination. *Journal of Neuroscience*, *33*(23), 9667–9674. <https://doi.org/10.1523/JNEUROSCI.5759-12.2013>
- Browning, P. G. F., Easton, A., Buckley, M. J., & Gaffan, D. (2005). The role of prefrontal cortex in object-in-place learning in monkeys. *European Journal of Neuroscience*, *22*(12), 3281–3291. <https://doi.org/10.1111/j.1460-9568.2005.04477.x>
- Browning, P. G. F., Easton, A., & Gaffan, D. (2007). Frontal–temporal disconnection abolishes object discrimination learning set in macaque monkeys. *Cerebral Cortex*, *17*(4), 859–864. <https://doi.org/10.1093/cercor/bhk039>
- Browning, P. G. F., & Gaffan, D. (2008a). Prefrontal cortex function in the representation of temporally complex events. *Journal of Neuroscience*, *28*(15), 3934–3940. <https://doi.org/10.1523/JNEUROSCI.0633-08.2008>
- Browning, P. G. F., & Gaffan, D. (2008b). Global retrograde amnesia but selective anterograde amnesia after frontal–temporal disconnection in monkeys. *Neuropsychologia*, *46*(10), 2494–2502. <https://doi.org/10.1016/j.neuropsychologia.2008.04.012>
- Bruyer, R., & Brysbaert, M. (2011). Combining speed and accuracy in cognitive psychology: Is the inverse efficiency score (IES) a better dependent variable

- than the mean reaction time (RT) and the percentage of errors (PE)? *Psychologica Belgica*, 51(1), 5–13. <https://doi.org/10.5334/pb-51-1-5>
- Brydges, C. R. (2019). Effect size guidelines, sample size calculations, and statistical power in gerontology. *Innovation in Aging*, 3(4), 1–8. <https://doi.org/10.1093/geroni/igz036>
- Bubb, E. J., Kinnavane, L., & Aggleton, J. P. (2017). Hippocampal–diencephalic–cingulate networks for memory and emotion: An anatomical guide. *Brain and Neuroscience Advances*, 1, 1–20. <https://doi.org/10.1177/2398212817723443>
- Bubb, E. J., Metzler-Baddeley, C., & Aggleton, J. P. (2018). The cingulum bundle: Anatomy, function, and dysfunction. *Neuroscience & Biobehavioral Reviews*, 92, 104–127. <https://doi.org/10.1016/j.neubiorev.2018.05.008>
- Buckley, M. J. (2005). The role of the perirhinal cortex and hippocampus in learning, memory, and perception. *The Quarterly Journal of Experimental Psychology Section B*, 58(3–4b), 246–268. <https://doi.org/10.1080/02724990444000186>
- Buckley, M. J., Booth, M. C. A., Rolls, E. T., & Gaffan, D. (2001). Selective perceptual impairments after perirhinal cortex ablation. *Journal of Neuroscience*, 21(24), 9824–9836. <https://doi.org/10.1523/JNEUROSCI.21-24-09824.2001>
- Buckley, M. J., Charles, D. P., Browning, P. G. F., & Gaffan, D. (2004). Learning and retrieval of concurrently presented spatial discrimination tasks: Role of the fornix. *Behavioral Neuroscience*, 118(1), 138–149. <https://doi.org/10.1037/0735-7044.118.1.138>
- Buckley, M. J., & Gaffan, D. (1997). Impairment of visual object-discrimination learning after perirhinal cortex ablation. *Behavioral Neuroscience*, 111(3), 467–475. <https://doi.org/10.1037//0735-7044.111.3.467>
- Buckley, M. J., & Gaffan, D. (1998). Perirhinal cortex ablation impairs visual object identification. *Journal of Neuroscience*, 18(6), 2268–2275. <https://doi.org/10.1523/JNEUROSCI.18-06-02268.1998>
- Buckley, M. J., & Gaffan, D. (2006). Perirhinal cortical contributions to object perception. *Trends in Cognitive Sciences*, 10(3), 100–107. <https://doi.org/10.1016/j.tics.2006.01.008>

- Buckley, R. F., Mormino, E. C., Rabin, J. S., Hohman, T. J., Landau, S., Hanseeuw, B. J., Jacobs, H. I. L., Papp, K. V., Amariglio, R. E., Properzi, M. J., Schultz, A. P., Kirn, D., Scott, M. R., Hedden, T., Farrell, M., Price, J., Chhatwal, J., Rentz, D. M., Villemagne, V. L., ... Sperling, R. A. (2019). Sex differences in the association of global amyloid and regional tau deposition measured by positron emission tomography in clinically normal older adults. *JAMA Neurology*, *76*(5), 542–551. <https://doi.org/10.1001/jamaneurol.2018.4693>
- Buckner, R. L., & DiNicola, L. M. (2019). The brain's default network: Updated anatomy, physiology and evolving insights. *Nature Reviews Neuroscience*, *20*(10), 593–608. <https://doi.org/10.1038/s41583-019-0212-7>
- Buckner, R. L., Sepulcre, J., Talukdar, T., Krienen, F. M., Liu, H., Hedden, T., Andrews-Hanna, J. R., Sperling, R. A., & Johnson, K. A. (2009). Cortical hubs revealed by intrinsic functional connectivity: Mapping, assessment of stability, and relation to Alzheimer's disease. *Journal of Neuroscience*, *29*(6), 1860–1873. <https://doi.org/10.1523/JNEUROSCI.5062-08.2009>
- Buckner, R. L., Snyder, A. Z., Shannon, B. J., LaRossa, G., Sachs, R., Fotenos, A. F., Sheline, Y. I., Klunk, W. E., Mathis, C. A., Morris, J. C., & Mintun, M. A. (2005). Molecular, structural, and functional characterization of Alzheimer's disease: Evidence for a relationship between default activity, amyloid, and memory. *Journal of Neuroscience*, *25*(34), 7709–7717. <https://doi.org/10.1523/JNEUROSCI.2177-05.2005>
- Burke, S. N., Gaynor, L. S., Barnes, C. A., Bauer, R. M., Bizon, J. L., Roberson, E. D., & Ryan, L. (2018). Shared functions of perirhinal and parahippocampal cortices: Implications for cognitive aging. *Trends in Neurosciences*, *41*(6), 349–359. <https://doi.org/10.1016/j.tins.2018.03.001>
- Burwell, R. D. (2001). Borders and cytoarchitecture of the perirhinal and postrhinal cortices in the rat. *Journal of Comparative Neurology*, *437*(1), 17–41. <https://doi.org/10.1002/cne.1267>
- Burwell, R. D., Witter, M. P., & Amaral, D. G. (1995). Perirhinal and postrhinal cortices of the rat: A review of the neuroanatomical literature and comparison with findings from the monkey brain. *Hippocampus*, *5*(5), 390–408. <https://doi.org/10.1002/hipo.450050503>
- Busche, M. A., Eichhoff, G., Adelsberger, H., Abramowski, D., Wiederhold, K.-H., Haass, C., Staufenbiel, M., Konnerth, A., & Garaschuk, O. (2008). Clusters of hyperactive neurons near amyloid plaques in a mouse model of

- Alzheimer's disease. *Science*, 321(5896), 1686–1689. <https://doi.org/10.1126/science.1162844>
- Busche, M. A., & Konnerth, A. (2015). Neuronal hyperactivity – A key defect in Alzheimer's disease? *BioEssays*, 37(6), 624–632. <https://doi.org/10.1002/bies.201500004>
- Busche, M. A., & Konnerth, A. (2016). Impairments of neural circuit function in Alzheimer's disease. *Philosophical Transactions of the Royal Society B: Biological Sciences*, 371(1700), 20150429. <https://doi.org/10.1098/rstb.2015.0429>
- Bussey, T. J., & Saksida, L. M. (2002). The organization of visual object representations: A connectionist model of effects of lesions in perirhinal cortex. *European Journal of Neuroscience*, 15(2), 355–364. <https://doi.org/10.1046/j.0953-816x.2001.01850.x>
- Bussey, T. J., & Saksida, L. M. (2007). Memory, perception, and the ventral visual-perirhinal-hippocampal stream: Thinking outside of the boxes. *Hippocampus*, 17(9), 898–908. <https://doi.org/10.1002/hipo.20320>
- Button, K. S., Ioannidis, J. P. A., Mokrysz, C., Nosek, B. A., Flint, J., Robinson, E. S. J., & Munafò, M. R. (2013). Power failure: Why small sample size undermines the reliability of neuroscience. *Nature Reviews Neuroscience*, 14(5), 365–376. <https://doi.org/10.1038/nrn3475>
- Byrne, P., Becker, S., & Burgess, N. (2007). Remembering the past and imagining the future: A neural model of spatial memory and imagery. *Psychological Review*, 114(2), 340–375. <https://doi.org/10.1037/0033-295X.114.2.340>
- Cabeza, R., Albert, M., Belleville, S., Craik, F. I. M., Duarte, A., Grady, C. L., Lindenberger, U., Nyberg, L., Park, D. C., Reuter-Lorenz, P. A., Rugg, M. D., Steffener, J., & Rajah, M. N. (2018). Maintenance, reserve and compensation: The cognitive neuroscience of healthy ageing. *Nature Reviews Neuroscience*, 19(11), 701–710. <https://doi.org/10.1038/s41583-018-0068-2>
- Calabrese, E., Badea, A., Cofer, G., Qi, Y., & Johnson, G. A. (2015). A diffusion MRI tractography connectome of the mouse brain and comparison with neuronal tracer data. *Cerebral Cortex*, 25(11), 4628–4637. <https://doi.org/10.1093/cercor/bhv121>

- Cameron, J. J., & Stinson, D. A. (2019). Gender (mis)measurement: Guidelines for respecting gender diversity in psychological research. *Social and Personality Psychology Compass*, *13*(11), e12506. <https://doi.org/10.1111/spc3.12506>
- Campbell, J. S. W., & Pike, G. B. (2014). Potential and limitations of diffusion MRI tractography for the study of language. *Brain and Language*, *131*, 65–73. <https://doi.org/10.1016/j.bandl.2013.06.007>
- Cansino, S. (2009). Episodic memory decay along the adult lifespan: A review of behavioral and neurophysiological evidence. *International Journal of Psychophysiology*, *71*(1), 64–69. <https://doi.org/10.1016/j.ijpsycho.2008.07.005>
- Cansino, S., Estrada-Manilla, C., Trejo-Morales, P., Pasaye-Alcaraz, E. H., Aguilar-Castañeda, E., Salgado-Lujambio, P., & Sosa-Ortiz, A. L. (2015). fMRI subsequent source memory effects in young, middle-aged and old adults. *Behavioural Brain Research*, *280*, 24–35. <https://doi.org/10.1016/j.bbr.2014.11.042>
- Carlesimo, G. A., Piras, F., Orfei, M. D., Iorio, M., Caltagirone, C., & Spalletta, G. (2015). Atrophy of presubiculum and subiculum is the earliest hippocampal anatomical marker of Alzheimer's disease. *Alzheimer's & Dementia: Diagnosis, Assessment and Disease Monitoring*, *1*(1), 24–32. <https://doi.org/10.1016/j.dadm.2014.12.001>
- Carroll, S., & Turkheimer, E. (2018). Midlife risk factors for late-life cognitive decline. *Developmental Review*, *48*, 201–222. <https://doi.org/10.1016/j.dr.2018.01.001>
- Casey, B. J., Cannonier, T., Conley, M. I., Cohen, A. O., Barch, D. M., Heitzeg, M. M., Soules, M. E., Teslovich, T., Dellarco, D. V., Garavan, H., Orr, C. A., Wager, T. D., Banich, M. T., Speer, N. K., Sutherland, M. T., Riedel, M. C., Dick, A. S., Bjork, J. M., Thomas, K. M., ... Dale, A. M. (2018). The Adolescent Brain Cognitive Development (ABCD) study: Imaging acquisition across 21 sites. *Developmental Cognitive Neuroscience*, *32*, 43–54. <https://doi.org/10.1016/j.dcn.2018.03.001>
- Catani, M., Jones, D. K., Donato, R., & Ffytche, D. H. (2003). Occipito-temporal connections in the human brain. *Brain*, *126*(9), 2093–2107. <https://doi.org/10.1093/brain/awg203>
- Champely, S. (2018). *pwr: Basic functions for power analysis* (Version 1.2-2) [Computer software]. <https://CRAN.R-project.org/package=pwr>

- Chan, D., Gallaher, L. M., Moodley, K., Minati, L., Burgess, N., & Hartley, T. (2016). The 4 Mountains Test: A short test of spatial memory with high sensitivity for the diagnosis of pre-dementia Alzheimer's disease. *Journal of Visualized Experiments*, *116*, e54454. <https://doi.org/10.3791/54454>
- Chan, M. Y., Na, J., Agres, P. F., Savalia, N. K., Park, D. C., & Wig, G. S. (2018). Socioeconomic status moderates age-related differences in the brain's functional network organization and anatomy across the adult lifespan. *Proceedings of the National Academy of Sciences*, *115*(22), E5144–E5153. <https://doi.org/10.1073/pnas.1714021115>
- Chandler, H. L., Hodgetts, C. J., Caseras, X., Murphy, K., & Lancaster, T. M. (2020). Polygenic risk for Alzheimer's disease shapes hippocampal scene-selectivity. *Neuropsychopharmacology*, *45*(7), 1171–1178. <https://doi.org/10.1038/s41386-019-0595-1>
- Chartier-Harlin, M. C., Parfitt, M., Legrain, S., Pérez-Tur, J., Brousseau, T., Evans, A., Berr, C., Vidal, O., Roques, P., & Gourlet, V. (1994). Apolipoprotein E, epsilon 4 allele as a major risk factor for sporadic early and late-onset forms of Alzheimer's disease: Analysis of the 19q13.2 chromosomal region. *Human Molecular Genetics*, *3*(4), 569–574. <https://doi.org/10.1093/hmg/3.4.569>
- Chen, X., Cassady, K. E., Adams, J. N., Harrison, T. M., Baker, S. L., & Jagust, W. J. (2021). Regional tau effects on prospective cognitive change in cognitively normal older adults. *Journal of Neuroscience*, *41*(2), 366–375. <https://doi.org/10.1523/JNEUROSCI.2111-20.2020>
- Chetelat, G., Desgranges, B., de la Sayette, V., Viader, F., Berkouk, K., Landeau, B., Lalevée, C., Le Doze, F., Dupuy, B., Hannequin, D., Baron, J.-C., & Eustache, F. (2003). Dissociating atrophy and hypometabolism impact on episodic memory in mild cognitive impairment. *Brain*, *126*(9), 1955–1967. <https://doi.org/10.1093/brain/awg196>
- Christiansen, K., Aggleton, J. P., Parker, G. D., O'Sullivan, M. J., Vann, S. D., & Metzler-Baddeley, C. (2016). The status of the precommissural and postcommissural fornix in normal ageing and mild cognitive impairment: An MRI tractography study. *NeuroImage*, *130*, 35–47. <https://doi.org/10.1016/J.NEUROIMAGE.2015.12.055>
- Chung, W.-S., Verghese, P. B., Chakraborty, C., Joung, J., Hyman, B. T., Ulrich, J. D., Holtzman, D. M., & Barres, B. A. (2016). Novel allele-dependent role for APOE in controlling the rate of synapse pruning by astrocytes.



- Proceedings of the National Academy of Sciences*, 113(36), 10186–10191.  
<https://doi.org/10.1073/pnas.1609896113>
- Cirrito, J. R., Yamada, K. A., Finn, M. B., Sloviter, R. S., Bales, K. R., May, P. C., Schoepp, D. D., Paul, S. M., Mennerick, S., & Holtzman, D. M. (2005). Synaptic activity regulates interstitial fluid amyloid-beta levels in vivo. *Neuron*, 48(6), 913–922. <https://doi.org/10.1016/j.neuron.2005.10.028>
- Clarke, A. (2020). Dynamic activity patterns in the anterior temporal lobe represents object semantics. *Cognitive Neuroscience*, 11(3), 111–121. <https://doi.org/10.1080/17588928.2020.1742678>
- Clarke, A., & Tyler, L. K. (2014). Object-specific semantic coding in human perirhinal cortex. *Journal of Neuroscience*, 34(14), 4766–4775. <https://doi.org/10.1523/JNEUROSCI.2828-13.2014>
- Clarke, A., & Tyler, L. K. (2015). Understanding what we see: How we derive meaning from vision. *Trends in Cognitive Sciences*, 19(11), 677–687. <https://doi.org/10.1016/j.tics.2015.08.008>
- Clayton, J. A., & Tannenbaum, C. (2016). Reporting sex, gender, or both in clinical research? *JAMA*, 316(18), 1863–1864. <https://doi.org/10.1001/jama.2016.16405>
- Clos, M., Rottschy, C., Laird, A. R., Fox, P. T., & Eickhoff, S. B. (2014). Comparison of structural covariance with functional connectivity approaches exemplified by an investigation of the left anterior insula. *NeuroImage*, 99, 269–280. <https://doi.org/10.1016/j.neuroimage.2014.05.030>
- Cohen, J. (1988). *Statistical power analysis for the behavioral sciences*. Routledge Academic.
- Cohen, N. J., & Squire, L. R. (1980). Preserved learning and retention of pattern-analyzing skill in amnesia: Dissociation of knowing how and knowing that. *Science*, 210(4466), 207–210. <https://doi.org/10.1126/science.7414331>
- Colombo, D., Serino, S., Tuena, C., Pedrolì, E., Dakanalis, A., Cipresso, P., & Riva, G. (2017). Egocentric and allocentric spatial reference frames in aging: A systematic review. *Neuroscience & Biobehavioral Reviews*, 80, 605–621. <https://doi.org/10.1016/j.neubiorev.2017.07.012>
- Corder, E. H., Ghebremedhin, E., Taylor, M. G., Thal, D. R., Ohm, T. G., & Braak, H. (2004). The biphasic relationship between regional brain senile plaque and neurofibrillary tangle distributions: Modification by age, sex, and

- APOE polymorphism. *Annals of the New York Academy of Sciences*, 1019(1), 24–28. <https://doi.org/10.1196/annals.1297.005>
- Corder, E. H., Saunders, A. M., Risch, N. J., Strittmatter, W. J., Schmechel, D. E., Gaskell, P. C., Rimmler, J. B., Locke, P. A., Conneally, P. M., Schmechel, K. E., Small, G. W., Roses, A. D., Haines, J. L., & Pericak-Vance, M. A. (1994). Protective effect of apolipoprotein E type 2 allele for late onset Alzheimer disease. *Nature Genetics*, 7(2), 180–184. <https://doi.org/10.1038/ng0694-180>
- Corder, E. H., Saunders, A., Strittmatter, W., Schmechel, D., Gaskell, P., Small, G., Roses, A., Haines, J., & Pericak-Vance, M. (1993). Gene dose of apolipoprotein E type 4 allele and the risk of Alzheimer's disease in late onset families. *Science*, 261(5123), 921–923. <https://doi.org/10.1126/science.8346443>
- Corkin, S., Amaral, D. G., González, R. G., Johnson, K. A., & Hyman, B. T. (1997). H. M.'s medial temporal lobe lesion: Findings from magnetic resonance imaging. *Journal of Neuroscience*, 17(10), 3964–3979. <https://doi.org/10.1523/JNEUROSCI.17-10-03964.1997>
- Costigan, A. G., Umla-Runge, K., Evans, C. J., Hodgetts, C. J., Lawrence, A. D., & Graham, K. S. (2019). Neurochemical correlates of scene processing in the precuneus/posterior cingulate cortex: A multimodal fMRI and 1H-MRS study. *Human Brain Mapping*, 40(10), 2884–2898. <https://doi.org/10.1002/hbm.24566>
- Coughlan, G., Coutrot, A., Khondoker, M., Minihane, A.-M., Spiers, H. J., & Hornberger, M. (2019). Toward personalized cognitive diagnostics of at-genetic-risk Alzheimer's disease. *Proceedings of the National Academy of Sciences*, 116(19), 9285–9292. <https://doi.org/10.1073/pnas.1901600116>
- Coughlan, G., Laczó, J., Hort, J., Minihane, A.-M., & Hornberger, M. (2018). Spatial navigation deficits—Overlooked cognitive marker for preclinical Alzheimer disease? *Nature Reviews Neurology*, 14(8), 496–506. <https://doi.org/10.1038/s41582-018-0031-x>
- Cowell, R. A., Barense, M. D., & Saksida, P. S. (2019). A roadmap for understanding memory: Decomposing cognitive processes into operations and representations. *eNeuro*, 6(4), 1–19. <https://doi.org/10.1523/ENEURO.0122-19.2019>
- Cowell, R. A., Bussey, T. J., & Saksida, L. M. (2006). Why does brain damage impair memory? A connectionist model of object recognition memory in

- perirhinal cortex. *Journal of Neuroscience*, 26(47), 12186–12197. <https://doi.org/10.1523/JNEUROSCI.2818-06.2006>
- Cowell, R. A., Bussey, T. J., & Saksida, L. M. (2010a). Components of recognition memory: Dissociable cognitive processes or just differences in representational complexity? *Hippocampus*, 20(11), 1245–1262. <https://doi.org/10.1002/hipo.20865>
- Cowell, R. A., Bussey, T. J., & Saksida, L. M. (2010b). Functional dissociations within the ventral object processing pathway: Cognitive modules or a hierarchical continuum? *Journal of Cognitive Neuroscience*, 22(11), 2460–2479. <https://doi.org/10.1162/jocn.2009.21373>
- Cox, S. R., Lyall, D. M., Ritchie, S. J., Bastin, M. E., Harris, M. A., Buchanan, C. R., Fawns-Ritchie, C., Barbu, M. C., de Nooij, L., Reus, L. M., Alloza, C., Shen, X., Neilson, E., Alderson, H. L., Hunter, S., Liewald, D. C., Whalley, H. C., McIntosh, A. M., Lawrie, S. M., ... Deary, I. J. (2019). Associations between vascular risk factors and brain MRI indices in UK Biobank. *European Heart Journal*, 40(28), 2290–2300. <https://doi.org/10.1093/eurheartj/ehz100>
- Cumming, G. (2008). Replication and p intervals: P values predict the future only vaguely, but confidence intervals do much better. *Perspectives on Psychological Science*, 3(4), 286–300. <https://doi.org/10.1111/j.1745-6924.2008.00079.x>
- Cushman, L. A., Stein, K., & Duffy, C. J. (2008). Detecting navigational deficits in cognitive aging and Alzheimer disease using virtual reality. *Neurology*, 71(12), 888–895. <https://doi.org/10.1212/01.wnl.0000326262.67613.fe>
- Dalton, M. A., Zeidman, P., McCormick, C., & Maguire, E. A. (2018). Differentiable processing of objects, associations, and scenes within the hippocampus. *Journal of Neuroscience*, 38(38), 8146–8159. <https://doi.org/10.1523/JNEUROSCI.0263-18.2018>
- Damoiseaux, J. S., Seeley, W. W., Zhou, J., Shirer, W. R., Coppola, G., Karydas, A., Rosen, H. J., Miller, B. L., Kramer, J. H., & Greicius, M. D. (2012). Gender modulates the APOE  $\epsilon$ 4 effect in healthy older adults: Convergent evidence from functional brain connectivity and spinal fluid tau levels. *Journal of Neuroscience*, 32(24), 8254–8262. <https://doi.org/10.1523/JNEUROSCI.0305-12.2012>
- Das, S. R., Pluta, J., Mancuso, L., Kliot, D., Yushkevich, P. A., & A. Wolk, D. (2015). Anterior and posterior MTL networks in aging and MCI. *Neurobiology*

- of *Aging*, 36(S1), S141-S150.e1.  
<https://doi.org/10.1016/j.neurobiolaging.2014.03.041>
- Daselaar, S. M., Fleck, M. S., Dobbins, I. G., Madden, D. J., & Cabeza, R. (2006). Effects of healthy aging on hippocampal and rhinal memory functions: An event-related fMRI study. *Cerebral Cortex*, 16(12), 1771–1782. <https://doi.org/10.1093/cercor/bhj112>
- Davies, R. R., Graham, K. S., Xuereb, J. H., Williams, G. B., & Hodges, J. R. (2004). The human perirhinal cortex and semantic memory. *European Journal of Neuroscience*, 20(9), 2441–2446. <https://doi.org/10.1111/j.1460-9568.2004.03710.x>
- Davies, R. R., Halliday, G. M., Xuereb, J. H., Kril, J. J., & Hodges, J. R. (2009). The neural basis of semantic memory: Evidence from semantic dementia. *Neurobiology of Aging*, 30(12), 2043–2052. <https://doi.org/10.1016/j.neurobiolaging.2008.02.005>
- DeBruine, L. M., & Barr, D. J. (2021). Understanding mixed-effects models through data simulation. *Advances in Methods and Practices in Psychological Science*, 4(1), 1–15. <https://doi.org/10.1177/2515245920965119>
- Delacre, M., Lakens, D., Ley, C., Liu, L., & Leys, C. (2021). Why Hedges'  $g$ 's based on the non-pooled standard deviation should be reported with Welch's  $t$ -test. *PsyArXiv*. <https://doi.org/10.31234/osf.io/tu6mp>
- Delacre, M., Lakens, D., & Leys, C. (2017). Why psychologists should by default use Welch's  $t$ -test instead of Student's  $t$ -test. *International Review of Social Psychology*, 30(1), 92–101. <https://doi.org/10.5334/irsp.82>
- Delettre, C., Messé, A., Dell, L.-A., Foubet, O., Heuer, K., Larrat, B., Meriaux, S., Mangin, J.-F., Reillo, I., de Juan Romero, C., Borrell, V., Toro, R., & Hilgetag, C. C. (2019). Comparison between diffusion MRI tractography and histological tract-tracing of cortico-cortical structural connectivity in the ferret brain. *Network Neuroscience*, 3(4), 1038–1050. [https://doi.org/10.1162/netn\\_a\\_00098](https://doi.org/10.1162/netn_a_00098)
- Dell'Acqua, F., Khan, W., Gottlieb, N., Giampietro, V., Ginestet, C., Bouls, D., Newhouse, S., Dobson, R., Banaschewski, T., Barker, G. J., Bokde, A. L. W., Büchel, C., Conrod, P., Flor, H., Frouin, V., Garavan, H., Gowland, P., Heinz, A., Lemaître, H., ... the IMAGEN consortium. (2015). Tract based spatial statistic reveals no differences in white matter microstructural organization between carriers and non-carriers of the APOE  $\epsilon$ 4 and  $\epsilon$ 2 alleles in young

- healthy adolescents. *Journal of Alzheimer's Disease*, 47(4), 977–984. <https://doi.org/10.3233/JAD-140519>
- Dell'Acqua, F., Scifo, P., Rizzo, G., Catani, M., Simmons, A., Scotti, G., & Fazio, F. (2010). A modified damped Richardson–Lucy algorithm to reduce isotropic background effects in spherical deconvolution. *NeuroImage*, 49(2), 1446–1458. <https://doi.org/10.1016/j.neuroimage.2009.09.033>
- Dell'Acqua, F., Simmons, A., Williams, S. C. R., & Catani, M. (2013). Can spherical deconvolution provide more information than fiber orientations? Hindrance modulated orientational anisotropy, a true-tract specific index to characterize white matter diffusion. *Human Brain Mapping*, 34(10), 2464–2483. <https://doi.org/10.1002/hbm.22080>
- Dell'Acqua, F., & Tournier, J.-D. (2019). Modelling white matter with spherical deconvolution: How and why? *NMR in Biomedicine*, 32(4), e3945. <https://doi.org/10.1002/nbm.3945>
- Dennis, N. A., Browndyke, J. N., Stokes, J., Need, A., Burke, J. R., Welsh-Bohmer, K. A., & Cabeza, R. (2010). Temporal lobe functional activity and connectivity in young adult APOE  $\epsilon$ 4 carriers. *Alzheimer's & Dementia*, 6(4), 303–311. <https://doi.org/10.1016/j.jalz.2009.07.003>
- DeTure, M. A., & Dickson, D. W. (2019). The neuropathological diagnosis of Alzheimer's disease. *Molecular Neurodegeneration*, 14, 32. <https://doi.org/10.1186/s13024-019-0333-5>
- Devlin, J. T., & Price, C. J. (2007). Perirhinal contributions to human visual perception. *Current Biology*, 17(17), 1484–1488. <https://doi.org/10.1016/j.cub.2007.07.066>
- D'Hooge, R., & De Deyn, P. P. (2001). Applications of the Morris water maze in the study of learning and memory. *Brain Research Reviews*, 36(1), 60–90. [https://doi.org/10.1016/s0165-0173\(01\)00067-4](https://doi.org/10.1016/s0165-0173(01)00067-4)
- Diamond, N. B., Romero, K., Jeyakumar, N., & Levine, B. (2018). Age-related decline in item but not spatiotemporal associative memory for a real-world event. *Psychology and Aging*, 33(7), 1079–1092. <https://doi.org/10.1037/pag0000303>
- Diedenhofen, B., & Musch, J. (2015). cocor: A comprehensive solution for the statistical comparison of correlations. *PLOS ONE*, 10(4), e0121945. <https://doi.org/10.1371/journal.pone.0121945>

- Dienes, Z. (2014). Using Bayes to get the most out of non-significant results. *Frontiers in Psychology*, 5, 781. <https://doi.org/10.3389/fpsyg.2014.00781>
- Dirnagl, U. (2019). Rethinking research reproducibility. *The EMBO Journal*, 38(2), e101117. <https://doi.org/10.15252/emboj.2018101117>
- Dodge, H. H., Zhu, J., Hughes, T. F., Snitz, B. E., Chang, C.-C. H., Jacobsen, E. P., & Ganguli, M. (2017). Cohort effects in verbal memory function and practice effects: A population-based study. *International Psychogeriatrics*, 29(1), 137–148. <https://doi.org/10.1017/S1041610216001551>
- Doeller, C. F., Barry, C., & Burgess, N. (2010). Evidence for grid cells in a human memory network. *Nature*, 463(7281), 657–661. <https://doi.org/10.1038/nature08704>
- Donix, M., Burggren, A. C., Scharf, M., Marschner, K., Suthana, N. A., Siddarth, P., Krupa, A. K., Jones, M., Martin-Harris, L., Ercoli, L. M., Miller, K. J., Werner, A., von Kummer, R., Sauer, C., Small, G. W., Holthoff, V. A., & Bookheimer, S. Y. (2013). APOE associated hemispheric asymmetry of entorhinal cortical thickness in aging and Alzheimer's disease. *Psychiatry Research: Neuroimaging*, 214(3), 212–220. <https://doi.org/10.1016/j.pscychresns.2013.09.006>
- Dubois, B., Feldman, H. H., Jacova, C., DeKosky, S. T., Barberger-Gateau, P., Cummings, J., Delacourte, A., Galasko, D., Gauthier, S., Jicha, G., Meguro, K., O'Brien, J., Pasquier, F., Robert, P., Rossor, M., Salloway, S., Stern, Y., Visser, P. J., & Scheltens, P. (2007). Research criteria for the diagnosis of Alzheimer's disease: Revising the NINCDS-ADRDA criteria. *The Lancet Neurology*, 6(8), 734–746. [https://doi.org/10.1016/S1474-4422\(07\)70178-3](https://doi.org/10.1016/S1474-4422(07)70178-3)
- Dubois, B., Feldman, H. H., Jacova, C., Hampel, H., Molinuevo, J. L., Blennow, K., DeKosky, S. T., Gauthier, S., Selkoe, D., Bateman, R., Cappa, S., Crutch, S., Engelborghs, S., Frisoni, G. B., Fox, N. C., Galasko, D., Habert, M.-O., Jicha, G. A., Nordberg, A., ... Cummings, J. L. (2014). Advancing research diagnostic criteria for Alzheimer's disease: The IWG-2 criteria. *The Lancet Neurology*, 13(6), 614–629. [https://doi.org/10.1016/S1474-4422\(14\)70090-0](https://doi.org/10.1016/S1474-4422(14)70090-0)
- Dully, J., McGovern, D. P., & O'Connell, R. G. (2018). The impact of natural aging on computational and neural indices of perceptual decision making: A review. *Behavioural Brain Research*, 355, 48–55. <https://doi.org/10.1016/j.bbr.2018.02.001>

- DuPre, E., & Spreng, R. N. (2017). Structural covariance networks across the life span, from 6 to 94 years of age. *Network Neuroscience*, 1(3), 302–323. [https://doi.org/10.1162/NETN\\_a\\_00016](https://doi.org/10.1162/NETN_a_00016)
- Eacott, M. J., Gaffan, D., & Murray, E. A. (1994). Preserved recognition memory for small sets, and impaired stimulus identification for large sets, following rhinal cortex ablations in monkeys. *European Journal of Neuroscience*, 6(9), 1466–1478. <https://doi.org/10.1111/j.1460-9568.1994.tb01008.x>
- Eacott, M. J., & Gaffan, E. A. (2005). The roles of perirhinal cortex, postrhinal cortex, and the fornix in memory for objects, contexts, and events in the rat. *The Quarterly Journal of Experimental Psychology Section B*, 58(3–4), 202–217. <https://doi.org/10.1080/02724990444000203>
- Edde, M., Dilharreguy, B., Theaud, G., Chanraud, S., Helmer, C., Dartigues, J.-F., Amieva, H., Allard, M., Descoteaux, M., & Catheline, G. (2020). Age-related change in episodic memory: Role of functional and structural connectivity between the ventral posterior cingulate and the parietal cortex. *Brain Structure and Function*, 225(7), 2203–2218. <https://doi.org/10.1007/s00429-020-02121-7>
- Eichenbaum, H. (2013). What H.M. taught us. *Journal of Cognitive Neuroscience*, 25(1), 14–21. [https://doi.org/10.1162/jocn\\_a\\_00285](https://doi.org/10.1162/jocn_a_00285)
- Eichenbaum, H., Sauvage, M., Fortin, N., Komorowski, R., & Lipton, P. (2012). Towards a functional organization of episodic memory in the medial temporal lobe. *Neuroscience & Biobehavioral Reviews*, 36(7), 1597–1608. <https://doi.org/10.1016/j.neubiorev.2011.07.006>
- Ekstrom, A. D., Arnold, A. E. G. F., & Iaria, G. (2014). A critical review of the allocentric spatial representation and its neural underpinnings: Toward a network-based perspective. *Frontiers in Human Neuroscience*, 8, 803. <https://doi.org/10.3389/fnhum.2014.00803>
- Ekstrom, A. D., Bohbot, V. D., Spiers, H. J., & Rosenbaum, R. S. (2018). *Human spatial navigation*. Princeton University Press.
- Ekstrom, A. D., Huffman, D. J., & Starrett, M. (2017). Interacting networks of brain regions underlie human spatial navigation: A review and novel synthesis of the literature. *Journal of Neurophysiology*, 118(6), 3328–3344. <https://doi.org/10.1152/jn.00531.2017>

- Eldridge, M. A. G., Hines, B. E., & Murray, E. A. (2021). The visual prefrontal cortex of anthropoids: Interaction with temporal cortex in decision making and its role in the making of 'visual animals'. *Current Opinion in Behavioral Sciences*, *41*, 22–29. <https://doi.org/10.1016/j.cobeha.2021.02.012>
- Eldridge, M. A. G., Matsumoto, N., Wittig, J. H. J., Masseau, E. C., Saunders, R. C., & Richmond, B. J. (2018). Perceptual processing in the ventral visual stream requires area TE but not rhinal cortex. *eLife*, *7*, e36310. <https://doi.org/10.7554/eLife.36310>
- Elman, J. A., Oh, H., Madison, C. M., Baker, S. L., Vogel, J. W., Marks, S. M., Crowley, S., O'Neil, J. P., & Jagust, W. J. (2014). Neural compensation in older people with brain amyloid- $\beta$  deposition. *Nature Neuroscience*, *17*(10), 1316–1318. <https://doi.org/10.1038/nn.3806>
- Emrani, S., Arain, H. A., DeMarshall, C., & Nuriel, T. (2020). APOE4 is associated with cognitive and pathological heterogeneity in patients with Alzheimer's disease: A systematic review. *Alzheimer's Research & Therapy*, *12*(1), 141. <https://doi.org/10.1186/s13195-020-00712-4>
- Erez, J., Lee, A. C. H., & Barense, M. D. (2013). It does not look odd to me: Perceptual impairments and eye movements in amnesic patients with medial temporal lobe damage. *Neuropsychologia*, *51*(1), 168–180. <https://doi.org/10.1016/j.neuropsychologia.2012.11.003>
- Escott-Price, V., Myers, A. J., Huentelman, M., & Hardy, J. (2017). Polygenic risk score analysis of pathologically confirmed Alzheimer disease. *Annals of Neurology*, *82*(2), 311–314. <https://doi.org/10.1002/ana.24999>
- Escott-Price, V., Shoai, M., Pither, R., Williams, J., & Hardy, J. (2017). Polygenic score prediction captures nearly all common genetic risk for Alzheimer's disease. *Neurobiology of Aging*, *49*, 214.e7-214.e11. <https://doi.org/10.1016/j.neurobiolaging.2016.07.018>
- Escott-Price, V., Sims, R., Bannister, C., Harold, D., Vronskaya, M., Majounie, E., Badarinarayan, N., Morgan, K., Passmore, P., Holmes, C., Powell, J., Brayne, C., Gill, M., Mead, S., Goate, A., Cruchaga, C., Lambert, J. C., Van Duijn, C., Maier, W., ... Williams, J. (2015). Common polygenic variation enhances risk prediction for Alzheimer's disease. *Brain*, *138*(12), 3673–3684. <https://doi.org/10.1093/brain/awv268>
- Evans, A. C. (2013). Networks of anatomical covariance. *NeuroImage*, *80*, 489–504. <https://doi.org/10.1016/j.neuroimage.2013.05.054>



- Ezzati, A., Katz, M. J., Lipton, M. L., Zimmerman, M. E., & Lipton, R. B. (2016). Hippocampal volume and cingulum bundle fractional anisotropy are independently associated with verbal memory in older adults. *Brain Imaging and Behavior*, *10*(3), 652–659. <https://doi.org/10.1007/s11682-015-9452-y>
- Farrer, L. A., Cupples, L. A., Haines, J. L., Hyman, B., Kukull, W. A., Mayeux, R., Myers, R. H., Pericak-Vance, M. A., Risch, N., van Duijn, C. M., & for the APOE and Alzheimer's Disease Meta Analysis Consortium. (1997). Effects of age, sex, and ethnicity on the association between apolipoprotein E genotype and Alzheimer disease: A meta-analysis. *JAMA*, *278*(16), 1349–1356. <https://doi.org/10.1001/jama.1997.03550160069041>
- Felsky, D., & Voineskos, A. N. (2013). APOE  $\epsilon$ 4, aging, and effects on white matter across the adult life span. *JAMA Psychiatry*, *70*(6), 646–647. <https://doi.org/10.1001/jamapsychiatry.2013.865>
- Ferguson, M. A., Lim, C., Cooke, D., Darby, R. R., Wu, O., Rost, N. S., Corbetta, M., Grafman, J., & Fox, M. D. (2019). A human memory circuit derived from brain lesions causing amnesia. *Nature Communications*, *10*, 3497. <https://doi.org/10.1038/s41467-019-11353-z>
- Festini, S. B., Hertzog, C., McDonough, I. M., & Park, D. C. (2019). What makes us busy? Predictors of perceived busyness across the adult lifespan. *The Journal of General Psychology*, *146*(2), 111–133. <https://doi.org/10.1080/00221309.2018.1540396>
- Festini, S. B., McDonough, I. M., & Park, D. C. (2016). The busier the better: Greater busyness is associated with better cognition. *Frontiers in Aging Neuroscience*, *8*, 98. <https://doi.org/10.3389/fnagi.2016.00098>
- Fidalgo, C. O., & Martin, C. B. (2016). The hippocampus contributes to allocentric spatial memory through coherent scene representations. *Journal of Neuroscience*, *36*(9), 2555–2557. <https://doi.org/10.1523/JNEUROSCI.4548-15.2016>
- Fidalgo, C. O., Changoor, A. T., Page-Gould, E., Lee, A. C. H., & Barense, M. D. (2016). Early cognitive decline in older adults better predicts object than scene recognition performance. *Hippocampus*, *26*(12), 1579–1592. <https://doi.org/10.1002/hipo.22658>
- Field, A. P., & Wilcox, R. R. (2017). Robust statistical methods: A primer for clinical psychology and experimental psychopathology researchers. *Behaviour Research and Therapy*, *98*, 19–38. <https://doi.org/10.1016/j.brat.2017.05.013>

- Filippini, N., Ebmeier, K. P., MacIntosh, B. J., Trachtenberg, A. J., Frisoni, G. B., Wilcock, G. K., Beckmann, C. F., Smith, S. M., Matthews, P. M., & Mackay, C. E. (2011). Differential effects of the APOE genotype on brain function across the lifespan. *NeuroImage*, *54*(1), 602–610. <https://doi.org/10.1016/j.neuroimage.2010.08.009>
- Filippini, N., MacIntosh, B. J., Hough, M. G., Goodwin, G. M., Frisoni, G. B., Smith, S. M., Matthews, P. M., Beckmann, C. F., & Mackay, C. E. (2009). Distinct patterns of brain activity in young carriers of the APOE-ε4 allele. *Proceedings of the National Academy of Sciences*, *106*(17), 7209–7214. <https://doi.org/10.1073/pnas.0811879106>
- Fjell, A. M., McEvoy, L., Holland, D., Dale, A. M., & Walhovd, K. B. (2014). What is normal in normal aging? Effects of aging, amyloid and Alzheimer's disease on the cerebral cortex and the hippocampus. *Progress in Neurobiology*, *117*, 20–40. <https://doi.org/10.1016/j.pneurobio.2014.02.004>
- Fletcher, P. D., & Warren, J. D. (2011). Semantic dementia: A specific network-opathy. *Journal of Molecular Neuroscience*, *45*(3), 629–636. <https://doi.org/10.1007/s12031-011-9586-3>
- Foley, S. F., Tansey, K. E., Caseras, X., Lancaster, T., Bracht, T., Parker, G., Hall, J., Williams, J., & Linden, D. E. J. (2017). Multimodal brain imaging reveals structural differences in Alzheimer's disease polygenic risk carriers: A study in healthy young adults. *Biological Psychiatry*, *81*(2), 154–161. <https://doi.org/10.1016/j.biopsych.2016.02.033>
- Folstein, M. F., Folstein, S. E., & McHugh, P. R. (1975). 'Mini-mental state': A practical method for grading the cognitive state of patients for the clinician. *Journal of Psychiatric Research*, *12*(3), 189–198. [https://doi.org/10.1016/0022-3956\(75\)90026-6](https://doi.org/10.1016/0022-3956(75)90026-6)
- Ford, J., Zheng, B., Hurtado, B., Jager, C. A. de, Udeh-Momoh, C., Middleton, L., & Price, G. (2020). Strategy or symptom: Semantic clustering and risk of Alzheimer's disease-related impairment. *Journal of Clinical and Experimental Neuropsychology*, *42*(8), 849–856. <https://doi.org/10.1080/13803395.2020.1819964>
- Foster, C. M., Kennedy, K. M., Hoagey, D. A., & Rodrigue, K. M. (2019). The role of hippocampal subfield volume and fornix microstructure in episodic memory across the lifespan. *Hippocampus*, *29*(12), 1206–1223. <https://doi.org/10.1002/hipo.23133>

- Foster, J. K., Albrecht, M. A., Savage, G., Lautenschlager, N. T., Ellis, K. A., Maruff, P., Szoek, C., Taddei, K., Martins, R., Masters, C. L., Ames, D., & AIBL Research Group. (2013). Lack of reliable evidence for a distinctive  $\epsilon 4$ -related cognitive phenotype that is independent from clinical diagnostic status: Findings from the Australian Imaging, Biomarkers and Lifestyle Study. *Brain*, *136*(7), 2201–2216. <https://doi.org/10.1093/brain/awt127>
- Fowler, K. S., Saling, M. M., Conway, E. L., & Semple, J. M. (1997). Computerized neuropsychological tests in the early detection of dementia: Prospective findings. *Journal of the International Neuropsychological Society*, *3*(2), 139–146.
- Fowler, K. S., Saling, M. M., Conway, E. L., Semple, J. M., & Louis, W. J. (1995). Computerized delayed matching to sample and paired associate performance in the early detection of dementia. *Applied Neuropsychology*, *2*(2), 72–78. [https://doi.org/10.1207/s15324826an0202\\_4](https://doi.org/10.1207/s15324826an0202_4)
- Fraser, A., Macdonald-Wallis, C., Tilling, K., Boyd, A., Golding, J., Davey Smith, G., Henderson, J., Macleod, J., Molloy, L., Ness, A., Ring, S., Nelson, S. M., & Lawlor, D. A. (2013). Cohort Profile: The Avon Longitudinal Study of Parents and Children: ALSPAC mothers cohort. *International Journal of Epidemiology*, *42*(1), 97–110. <https://doi.org/10.1093/ije/dys066>
- Friston, K. J., Kahan, J., Biswal, B., & Razi, A. (2014). A DCM for resting state fMRI. *NeuroImage*, *94*, 396–407. <https://doi.org/10.1016/j.neuroimage.2013.12.009>
- Fullerton, S. M., Clark, A. G., Weiss, K. M., Nickerson, D. A., Taylor, S. L., Stengård, J. H., Salomaa, V., Vartiainen, E., Perola, M., Boerwinkle, E., & Sing, C. F. (2000). Apolipoprotein E variation at the sequence haplotype level: Implications for the origin and maintenance of a major human polymorphism. *American Journal of Human Genetics*, *67*(4), 881–900. <https://doi.org/10.1086/303070>
- Gaesser, B., Sacchetti, D. C., Addis, D. R., & Schacter, D. L. (2011). Characterizing age-related changes in remembering the past and imagining the future. *Psychology and Aging*, *26*(1), 80–84. <https://doi.org/10.1037/a0021054>
- Gaffan, D. (1991). Spatial organization of episodic memory. *Hippocampus*, *1*(3), 262–264. <https://doi.org/10.1002/hipo.450010311>

- Gaffan, D. (1994). Scene-specific memory for objects: A model of episodic memory impairment in monkeys with fornix transection. *Journal of Cognitive Neuroscience*, *6*(4), 305–320. <https://doi.org/10.1162/jocn.1994.6.4.305>
- Gaffan, D. (2002). Against memory systems. *Philosophical Transactions of the Royal Society B: Biological Sciences*, *357*(1424), 1111–1121. <https://doi.org/10.1098/rstb.2002.1110>
- Gaffan, D., & Parker, A. (1996). Interaction of perirhinal cortex with the fornix–fimbria: Memory for objects and “object-in-place” memory. *Journal of Neuroscience*, *16*(18), 5864–5869. <https://doi.org/10.1523/JNEUROSCI.16-18-05864.1996>
- Gaffan, D., Parker, A., & Easton, A. (2001). Dense amnesia in the monkey after transection of fornix, amygdala and anterior temporal stem. *Neuropsychologia*, *39*(1), 51–70. [https://doi.org/10.1016/s0028-3932\(00\)00097-x](https://doi.org/10.1016/s0028-3932(00)00097-x)
- Gaffan, D., & Wilson, C. R. E. (2008). Medial temporal and prefrontal function: Recent behavioural disconnection studies in the macaque monkey. *Cortex*, *44*(8), 928–935. <https://doi.org/10.1016/j.cortex.2008.03.005>
- Gallagher, M., Burwell, R., & Burchinal, M. (1993). Severity of spatial learning impairment in aging: Development of a learning index for performance in the Morris water maze. *Behavioral Neuroscience*, *107*(4), 618–626. <https://doi.org/10.1037//0735-7044.107.4.618>
- Gallagher, M., & Rapp, P. R. (1997). The use of animal models to study the effects of aging on cognition. *Annual Review of Psychology*, *48*, 339–370. <https://doi.org/10.1146/annurev.psych.48.1.339>
- Gamache, J., Yun, Y., & Chiba-Falek, O. (2020). Sex-dependent effect of APOE on Alzheimer’s disease and other age-related neurodegenerative disorders. *Disease Models & Mechanisms*, *13*(8), dmm045211. <https://doi.org/10.1242/dmm.045211>
- Ganguli, M. (2017). The times they are a-changin’: Cohort effects in aging, cognition, and dementia. *International Psychogeriatrics*, *29*(3), 353–355. <https://doi.org/10.1017/S1041610216001927>
- Gauthier, I., & Tarr, M. J. (1997). Becoming a ‘Greeble’ expert: Exploring mechanisms for face recognition. *Vision Research*, *37*(12), 1673–1682. [https://doi.org/10.1016/s0042-6989\(96\)00286-6](https://doi.org/10.1016/s0042-6989(96)00286-6)

- Gaynor, L. S., Curiel, R. E., Penate, A., Rosselli, M., Burke, S. N., Wicklund, M., Loewenstein, D. A., & Bauer, R. M. (2019). Visual object discrimination impairment as an early predictor of Mild Cognitive Impairment and Alzheimer's disease. *Journal of the International Neuropsychological Society*, *25*(7), 688–698. <https://doi.org/10.1017/S1355617719000316>
- Gazova, I., Laczó, J., Rubinova, E., Mokrisova, I., Hyncicova, E., Anđel, R., Vyhnaek, M., Sheardova, K., Coulson, E. J., & Hort, J. (2013). Spatial navigation in young versus older adults. *Frontiers in Aging Neuroscience*, *5*(94). <https://doi.org/10.3389/fnagi.2013.00094>
- Ge, R., Kot, P., Liu, X., Lang, D. J., Wang, J. Z., Honer, W. G., & Vila-Rodriguez, F. (2019). Parcellation of the human hippocampus based on gray matter volume covariance: Replicable results on healthy young adults. *Human Brain Mapping*, *40*(13), 3738–3752. <https://doi.org/10.1002/hbm.24628>
- Ge, T., Sabuncu, M. R., Smoller, J. W., Sperling, R. A., Mormino, E. C., & for the Alzheimer's Disease Neuroimaging Initiative. (2018). Dissociable influences of APOE  $\epsilon$ 4 and polygenic risk of AD dementia on amyloid and cognition. *Neurology*, *90*(18), e1605–e1612. <https://doi.org/10.1212/WNL.00000000000005415>
- Gellersen, H. M., Coughlan, G., Hornberger, M., & Simons, J. S. (2021). Memory precision of object-location binding is unimpaired in APOE  $\epsilon$ 4-carriers with spatial navigation deficits. *Brain Communications*, *3*(2), fcab087. <https://doi.org/10.1093/braincomms/fcab087>
- Gellersen, H. M., Trelle, A. N., Henson, R. N. A., & Simons, J. S. (2021). Executive function and high ambiguity perceptual discrimination contribute to individual differences in mnemonic discrimination in older adults. *Cognition*, *209*, 104556. <https://doi.org/10.1016/j.cognition.2020.104556>
- Gelman, A., & Stern, H. (2006). The difference between “significant” and “not significant” is not itself statistically significant. *The American Statistician*, *60*(4), 328–331. <https://doi.org/10.1198/000313006X152649>
- Genin, E., Hannequin, D., Wallon, D., Sleegers, K., Hiltunen, M., Combarros, O., Bullido, M. J., Engelborghs, S., De Deyn, P., Berr, C., Pasquier, F., Dubois, B., Tognoni, G., Fiévet, N., Brouwers, N., Bettens, K., Arosio, B., Coto, E., Del Zompo, M., ... Campion, D. (2011). APOE and Alzheimer disease: A major gene with semi-dominant inheritance. *Molecular Psychiatry*, *16*(9), 903–907. <https://doi.org/10.1038/mp.2011.52>

- Germine, L., Nakayama, K., Duchaine, B. C., Chabris, C. F., Chatterjee, G., & Wilmer, J. B. (2012). Is the web as good as the lab? Comparable performance from web and lab in cognitive/perceptual experiments. *Psychonomic Bulletin & Review*, *19*(5), 847–857. <https://doi.org/10.3758/s13423-012-0296-9>
- Germine, L., Reinecke, K., & Chaytor, N. S. (2019). Digital neuropsychology: Challenges and opportunities at the intersection of science and software. *The Clinical Neuropsychologist*, *33*(2), 271–286. <https://doi.org/10.1080/13854046.2018.1535662>
- Ghebremedhin, E., Schultz, C., Braak, E., & Braak, H. (1998). High frequency of apolipoprotein E epsilon4 allele in young individuals with very mild Alzheimer's disease-related neurofibrillary changes. *Experimental Neurology*, *153*(1), 152–155. <https://doi.org/10.1006/exnr.1998.6860>
- Goldberg, T. E., Huey, E. D., & Devanand, D. P. (2020). Association of APOE e2 genotype with Alzheimer's and non-Alzheimer's neurodegenerative pathologies. *Nature Communications*, *11*, 4727. <https://doi.org/10.1038/s41467-020-18198-x>
- Goltermann, J., Repple, J., Redlich, R., Dohm, K., Flint, C., Grotegerd, D., Waltemate, L., Lemke, H., Fingas, S. M., Meinert, S., Enneking, V., Hahn, T., Bauer, J., Schmitt, S., Meller, T., Stein, F., Brosch, K., Steinträger, O., Jansen, A., ... Opel, N. (2021). Apolipoprotein E homozygous ε4 allele status: Effects on cortical structure and white matter integrity in a young to mid-age sample. *European Neuropsychopharmacology*, *46*, 93–104. <https://doi.org/10.1016/j.euroneuro.2021.02.006>
- Gomez, J., Pestilli, F., Witthoft, N., Golarai, G., Liberman, A., Poltoratski, S., Yoon, J., & Grill-Spector, K. (2015). Functionally defined white matter reveals segregated pathways in human ventral temporal cortex associated with category-specific processing. *Neuron*, *85*(1), 216–227. <https://doi.org/10.1016/j.neuron.2014.12.027>
- Gong, G., He, Y., Chen, Z. J., & Evans, A. C. (2012). Convergence and divergence of thickness correlations with diffusion connections across the human cerebral cortex. *NeuroImage*, *59*(2), 1239–1248. <https://doi.org/10.1016/j.neuroimage.2011.08.017>
- Gong, G., Jiang, T., Zhu, C., Zang, Y., Wang, F., Xie, S., Xiao, J., & Guo, X. (2005). Asymmetry analysis of cingulum based on scale-invariant parameterization by diffusion tensor imaging. *Human Brain Mapping*, *24*(2), 92–98. <https://doi.org/10.1002/hbm.20072>

- Grady, C. (2012). The cognitive neuroscience of ageing. *Nature Reviews Neuroscience*, *13*(7), 491–505. <https://doi.org/10.1038/nrn3256>
- Graham, K. S., Barense, M. D., & Lee, A. C. H. (2010). Going beyond LTM in the MTL: A synthesis of neuropsychological and neuroimaging findings on the role of the medial temporal lobe in memory and perception. *Neuropsychologia*, *48*(4), 831–853. <https://doi.org/10.1016/j.neuropsychologia.2010.01.001>
- Greicius, M. D., Srivastava, G., Reiss, A. L., & Menon, V. (2004). Default-mode network activity distinguishes Alzheimer's disease from healthy aging: Evidence from functional MRI. *Proceedings of the National Academy of Sciences*, *101*(13), 4637–4642. <https://doi.org/10.1073/pnas.0308627101>
- Greicius, M. D., Supekar, K., Menon, V., & Dougherty, R. F. (2009). Resting-state functional connectivity reflects structural connectivity in the default mode network. *Cerebral Cortex*, *19*(1), 72–78. <https://doi.org/10.1093/cercor/bhn059>
- Grilli, M. D., Wank, A. A., Bercl, J. J., & Ryan, L. (2018). Evidence for reduced autobiographical memory episodic specificity in cognitively normal middle-aged and older individuals at increased risk for Alzheimer's disease dementia. *Journal of the International Neuropsychological Society*, *24*(10), 1073–1083. <https://doi.org/10.1017/S1355617718000577>
- Grossi, D., Soricelli, A., Ponari, M., Salvatore, E., Quarantelli, M., Prinster, A., & Trojano, L. (2014). Structural connectivity in a single case of progressive prosopagnosia: The role of the right inferior longitudinal fasciculus. *Cortex*, *56*, 111–120. <https://doi.org/10.1016/j.cortex.2012.09.010>
- Grothe, M. J., Barthel, H., Sepulcre, J., Dyrba, M., Sabri, O., & Teipel, S. J. (2017). In vivo staging of regional amyloid deposition. *Neurology*, *89*(20), 2031–2038. <https://doi.org/10.1212/WNL.0000000000004643>
- Guo, X., Wang, Y., Guo, T., Chen, K., Zhang, J., Li, K., Jin, Z., & Yao, L. (2015). Structural covariance networks across healthy young adults and their consistency. *Journal of Magnetic Resonance Imaging*, *42*(2), 261–268. <https://doi.org/10.1002/jmri.24780>
- Güsten, J., Ziegler, G., Düzel, E., & Berron, D. (2021). Age impairs mnemonic discrimination of objects more than scenes: A web-based, large-scale approach across the lifespan. *Cortex*, *137*, 138–148. <https://doi.org/10.1016/j.cortex.2020.12.017>

- Hafting, T., Fyhn, M., Molden, S., Moser, M.-B., & Moser, E. I. (2005). Microstructure of a spatial map in the entorhinal cortex. *Nature*, *436*(7052), 801–806. <https://doi.org/10.1038/nature03721>
- Hagler, D. J., Hatton, S. N., Cornejo, M. D., Makowski, C., Fair, D. A., Dick, A. S., Sutherland, M. T., Casey, B., Barch, D. M., Harms, M. P., Watts, R., Bjork, J. M., Garavan, H. P., Hilmer, L., Pung, C. J., Sicut, C. S., Kuperman, J., Bartsch, H., Xue, F., ... Dale, A. M. (2019). Image processing and analysis methods for the Adolescent Brain Cognitive Development Study. *NeuroImage*, *202*, 116091. <https://doi.org/10.1016/j.neuroimage.2019.116091>
- Hampton, R. R. (2005). Monkey perirhinal cortex is critical for visual memory, but not for visual perception: Reexamination of the behavioural evidence from monkeys. *The Quarterly Journal of Experimental Psychology Section B*, *58*(3–4), 283–299. <https://doi.org/10.1080/02724990444000195>
- Han, S. D., & Bondi, M. W. (2008). Revision of the apolipoprotein E compensatory mechanism recruitment hypothesis. *Alzheimer's & Dementia*, *4*(4), 251–254. <https://doi.org/10.1016/j.jalz.2008.02.006>
- Hardy, J. A., & Higgins, G. A. (1992). Alzheimer's disease: The amyloid cascade hypothesis. *Science*, *256*(5054), 184–185. <https://doi.org/10.1126/science.1566067>
- Hardy, J., & Allsop, D. (1991). Amyloid deposition as the central event in the aetiology of Alzheimer's disease. *Trends in Pharmacological Sciences*, *12*, 383–388. [https://doi.org/10.1016/0165-6147\(91\)90609-V](https://doi.org/10.1016/0165-6147(91)90609-V)
- Harris, M. A., & Wolbers, T. (2014). How age-related strategy switching deficits affect wayfinding in complex environments. *Neurobiology of Aging*, *35*(5), 1095–1102. <https://doi.org/10.1016/j.neurobiolaging.2013.10.086>
- Harris, M. A., Wolbers, T., & Wiener, J. M. (2012). Aging specifically impairs switching to an allocentric navigational strategy. *Frontiers in Aging Neuroscience*, *4*, 29. <https://doi.org/10.3389/fnagi.2012.00029>
- Harrison, T. M., & Bookheimer, S. Y. (2016). Neuroimaging genetic risk for Alzheimer's disease in preclinical individuals: From candidate genes to polygenic approaches. *Biological Psychiatry: Cognitive Neuroscience and Neuroimaging*, *1*(1), 14–23. <https://doi.org/10.1016/j.bpsc.2015.09.003>
- Hartley, T., Bird, C. M., Chan, D., Cipolotti, L., Husain, M., Vargha-Khadem, F., & Burgess, N. (2007). The hippocampus is required for short-term



- topographical memory in humans. *Hippocampus*, 17(1), 34–48. <https://doi.org/10.1002/hipo.20240>
- Hassabis, D., & Maguire, E. A. (2007). Deconstructing episodic memory with construction. *Trends in Cognitive Sciences*, 11(7), 299–306. <https://doi.org/10.1016/j.tics.2007.05.001>
- Hassabis, D., & Maguire, E. A. (2009). The construction system of the brain. *Philosophical Transactions of the Royal Society B: Biological Sciences*, 364(1521), 1263–1271. <https://doi.org/10.1098/rstb.2008.0296>
- Hayden, K. M., Zandi, P. P., West, N. A., Tschanz, J. T., Norton, M. C., Corcoran, C., Breitner, J. C. S., Welsh-Bohmer, K. A., & Cache County Study Group. (2009). Effects of family history and apolipoprotein E epsilon4 status on cognitive decline in the absence of Alzheimer dementia: The Cache County Study. *Archives of Neurology*, 66(11), 1378–1383. <https://doi.org/10.1001/archneurol.2009.237>
- He, Z., Guo, J. L., McBride, J. D., Narasimhan, S., Kim, H., Changolkar, L., Zhang, B., Gathagan, R. J., Yue, C., Dengler, C., Stieber, A., Nitla, M., Coulter, D. A., Abel, T., Brunden, K. R., Trojanowski, J. Q., & Lee, V. M.-Y. (2018). Amyloid- $\beta$  plaques enhance Alzheimer's brain tau-seeded pathologies by facilitating neuritic plaque tau aggregation. *Nature Medicine*, 24(1), 29–38. <https://doi.org/10.1038/nm.4443>
- Hedden, T., & Gabrieli, J. D. E. (2004). Insights into the ageing mind: A view from cognitive neuroscience. *Nature Reviews Neuroscience*, 5(2), 87–96. <https://doi.org/10.1038/nrn1323>
- Hedge, C., Powell, G., & Sumner, P. (2018). The mapping between transformed reaction time costs and models of processing in aging and cognition. *Psychology and Aging*, 33(7), 1093–1104. <https://doi.org/10.1037/pag0000298>
- Heilbronner, S. R., & Haber, S. N. (2014). Frontal cortical and subcortical projections provide a basis for segmenting the cingulum bundle: Implications for neuroimaging and psychiatric disorders. *Journal of Neuroscience*, 34(30), 10041–10054. <https://doi.org/10.1523/JNEUROSCI.5459-13.2014>
- Heise, V., Filippini, N., Ebmeier, K. P., & MacKay, C. E. (2011). The APOE  $\epsilon$ 4 allele modulates brain white matter integrity in healthy adults. *Molecular Psychiatry*, 16(9), 908–916. <https://doi.org/10.1038/mp.2010.90>

- Heise, V., Filippini, N., Trachtenberg, A. J., Suri, S., Ebmeier, K. P., & Mackay, C. E. (2014). Apolipoprotein E genotype, gender and age modulate connectivity of the hippocampus in healthy adults. *NeuroImage*, *98*, 23–30. <https://doi.org/10.1016/j.neuroimage.2014.04.081>
- Heitz, R. P. (2014). The speed-accuracy tradeoff: History, physiology, methodology, and behavior. *Frontiers in Neuroscience*, *8*, 150. <https://doi.org/10.3389/fnins.2014.00150>
- Hendrie, H. C., Murrell, J., Baiyewu, O., Lane, K. A., Purnell, C., Ogunniyi, A., Unverzagt, F. W., Hall, K., Callahan, C. M., Saykin, A. J., Gureje, O., Hake, A., Foroud, T., & Gao, S. (2014). APOE  $\epsilon$ 4 and the risk for Alzheimer disease and cognitive decline in African Americans and Yoruba. *International Psychogeriatrics*, *26*(6), 977–985. <https://doi.org/10.1017/S1041610214000167>
- Henriksen, E. J., Colgin, L. L., Barnes, C. A., Witter, M. P., Moser, M.-B., & Moser, E. I. (2010). Spatial representation along the proximodistal axis of CA1. *Neuron*, *68*(1), 127–137. <https://doi.org/10.1016/j.neuron.2010.08.042>
- Henson, R. N. A., Suri, S., Knights, E., Rowe, J. B., Kievit, R. A., Lyall, D. M., Chan, D., Eising, E., & Fisher, S. E. (2020). Effect of apolipoprotein E polymorphism on cognition and brain in the Cambridge Centre for Ageing and Neuroscience cohort. *Brain and Neuroscience Advances*, *4*, 1–12. <https://doi.org/10.1177/2398212820961704>
- Herbet, G., Zemmoura, I., & Duffau, H. (2018). Functional anatomy of the inferior longitudinal fasciculus: From historical reports to current hypotheses. *Frontiers in Neuroanatomy*, *12*, 77. <https://doi.org/10.3389/fnana.2018.00077>
- Herrup, K. (2015). The case for rejecting the amyloid cascade hypothesis. *Nature Neuroscience*, *18*(6), 794–799. <https://doi.org/10.1038/nn.4017>
- Hodges, J. R., Mitchell, J., Dawson, K., Spillantini, M. G., Xuereb, J. H., McMonagle, P., Nestor, P. J., & Patterson, K. (2010). Semantic dementia: Demography, familial factors and survival in a consecutive series of 100 cases. *Brain*, *133*(1), 300–306. <https://doi.org/10.1093/brain/awp248>
- Hodges, J. R., & Patterson, K. (2007). Semantic dementia: A unique clinicopathological syndrome. *The Lancet Neurology*, *6*(11), 1004–1014. [https://doi.org/10.1016/S1474-4422\(07\)70266-1](https://doi.org/10.1016/S1474-4422(07)70266-1)
- Hodgetts, C. J., Postans, M., Shine, J. P., Jones, D. K., Lawrence, A. D., & Graham, K. S. (2015). Dissociable roles of the inferior longitudinal fasciculus

- and fornix in face and place perception. *eLife*, 4, e07902. <https://doi.org/10.7554/eLife.07902>
- Hodgetts, C. J., Postans, M., Warne, N., Varnava, A., Lawrence, A. D., & Graham, K. S. (2017). Distinct contributions of the fornix and inferior longitudinal fasciculus to episodic and semantic autobiographical memory. *Cortex*, 94, 1–14. <https://doi.org/10.1016/J.CORTEX.2017.05.010>
- Hodgetts, C. J., Shine, J. P., Lawrence, A. D., Downing, P. E., & Graham, K. S. (2016). Evidencing a place for the hippocampus within the core scene processing network. *Human Brain Mapping*, 37(11), 3779–3794. <https://doi.org/10.1002/hbm.23275>
- Hodgetts, C. J., Shine, J. P., Williams, H., Postans, M., Sims, R., Williams, J., Lawrence, A. D., & Graham, K. S. (2019). Increased posterior default mode network activity and structural connectivity in young adult APOE- $\epsilon$ 4 carriers: A multimodal imaging investigation. *Neurobiology of Aging*, 73, 82–91. <https://doi.org/10.1016/j.neurobiolaging.2018.08.026>
- Hodgetts, C. J., Voets, N. L., Thomas, A. G., Clare, S., Lawrence, A. D., & Graham, K. S. (2017). Ultra-high-field fMRI reveals a role for the subiculum in scene perceptual discrimination. *Journal of Neuroscience*, 37(12), 3150–3159. <https://doi.org/10.1523/JNEUROSCI.3225-16.2017>
- Hofer, S. M., & Sliwinski, M. J. (2001). Understanding ageing. *Gerontology*, 47(6), 341–352. <https://doi.org/10.1159/000052825>
- Hohman, T. J., Dumitrescu, L., Barnes, L. L., Thambisetty, M., Beecham, G., Kunkle, B., Gifford, K. A., Bush, W. S., Chibnik, L. B., Mukherjee, S., De Jager, P. L., Kukull, W., Crane, P. K., Resnick, S. M., Keene, C. D., Montine, T. J., Schellenberg, G. D., Haines, J. L., Zetterberg, H., ... for the Alzheimer's Disease Genetics Consortium and the Alzheimer's Disease Neuroimaging Initiative. (2018). Sex-specific association of apolipoprotein E with cerebrospinal fluid levels of tau. *JAMA Neurology*, 75(8), 989–998. <https://doi.org/10.1001/jamaneurol.2018.0821>
- Honea, R., Crow, T. J., Passingham, D., & Mackay, C. E. (2005). Regional deficits in brain volume in schizophrenia: A meta-analysis of voxel-based morphometry studies. *The American Journal of Psychiatry*, 162(12), 2233–2245. <https://doi.org/10.1176/appi.ajp.162.12.2233>
- Honnedevassthana Arun, A., Connelly, A., Smith, R. E., & Calamante, F. (2021). Characterisation of white matter asymmetries in the healthy human brain

- using diffusion MRI fixel-based analysis. *NeuroImage*, 225, 117505. <https://doi.org/10.1016/j.neuroimage.2020.117505>
- Hort, J., Laczó, J., Vyhnálek, M., Bojar, M., Bureš, J., & Vlček, K. (2007). Spatial navigation deficit in amnesic mild cognitive impairment. *Proceedings of the National Academy of Sciences*, 104(10), 4042–4047. <https://doi.org/10.1073/pnas.0611314104>
- Huang, Y., & Mahley, R. W. (2014). Apolipoprotein E: Structure and function in lipid metabolism, neurobiology, and Alzheimer's diseases. *Neurobiology of Disease*, 72, 3–12. <https://doi.org/10.1016/j.nbd.2014.08.025>
- Huentelman, M. J., Talboom, J. S., Lewis, C. R., Chen, Z., & Barnes, C. A. (2020). Reinventing neuroaging research in the digital age. *Trends in Neurosciences*, 43(1), 17–23. <https://doi.org/10.1016/j.tins.2019.11.004>
- Huijbers, W., Mormino, E. C., Wigman, S. E., Ward, A. M., Vannini, P., McLaren, D. G., Becker, J. A., Schultz, A. P., Hedden, T., Johnson, K. A., & Sperling, R. A. (2014). Amyloid deposition is linked to aberrant entorhinal activity among cognitively normal older adults. *Journal of Neuroscience*, 34(15), 5200–5210. <https://doi.org/10.1523/JNEUROSCI.3579-13.2014>
- Huijbers, W., Vannini, P., Sperling, R. A., Pennartz, C. M. A., Cabeza, R., & Daselaar, S. M. (2012). Explaining the encoding/retrieval flip: Memory-related deactivations and activations in the posteromedial cortex. *Neuropsychologia*, 50(14), 3764–3774. <https://doi.org/10.1016/j.neuropsychologia.2012.08.021>
- Hurley, R. S., Bonakdarpour, B., Wang, X., & Mesulam, M.-M. (2015). Asymmetric connectivity between the anterior temporal lobe and the language network. *Journal of Cognitive Neuroscience*, 27(3), 464–473. [https://doi.org/10.1162/jocn\\_a\\_00722](https://doi.org/10.1162/jocn_a_00722)
- Hurtado, D. E., Molina-Porcel, L., Iba, M., Aboagye, A. K., Paul, S. M., Trojanowski, J. Q., & Lee, V. M.-Y. (2010). A $\beta$  accelerates the spatiotemporal progression of tau pathology and augments tau amyloidosis in an Alzheimer mouse model. *The American Journal of Pathology*, 177(4), 1977–1988. <https://doi.org/10.2353/ajpath.2010.100346>
- Hyde, J. S., Bigler, R. S., Joel, D., Tate, C. C., & van Anders, S. M. (2019). The future of sex and gender in psychology: Five challenges to the gender binary. *American Psychologist*, 74(2), 171–193. <https://doi.org/10.1037/amp0000307>

- Iaccarino, L., La Joie, R., Edwards, L., Strom, A., Schonhaut, D. R., Ossenkoppele, R., Pham, J., Mellinger, T., Janabi, M., Baker, S. L., Soleimani-Meigooni, D., Rosen, H. J., Miller, B. L., Jagust, W. J., & Rabinovici, G. D. (2021). Spatial relationships between molecular pathology and neurodegeneration in the Alzheimer's disease continuum. *Cerebral Cortex*, *31*(1), 1–14. <https://doi.org/10.1093/cercor/bhaa184>
- Iaccarino, L., Tammewar, G., Ayakta, N., Baker, S. L., Bejanin, A., Boxer, A. L., Gorno-Tempini, M. L., Janabi, M., Kramer, J. H., Lazaris, A., Lockhart, S. N., Miller, B. L., Miller, Z. A., O'Neil, J. P., Ossenkoppele, R., Rosen, H. J., Schonhaut, D. R., Jagust, W. J., & Rabinovici, G. D. (2018). Local and distant relationships between amyloid, tau and neurodegeneration in Alzheimer's Disease. *NeuroImage: Clinical*, *17*, 452–464. <https://doi.org/10.1016/j.nicl.2017.09.016>
- Inhoff, M. C., & Ranganath, C. (2015). Significance of objects in the perirhinal cortex. *Trends in Cognitive Sciences*, *19*(6), 302–303. <https://doi.org/10.1016/j.tics.2015.04.008>
- Inhoff, M. C., & Ranganath, C. (2017). Dynamic cortico-hippocampal networks underlying memory and cognition: The PMAT framework. In D. E. Hannula & M. C. Duff (Eds.), *The hippocampus from cells to systems: Structure, connectivity, and functional contributions to memory and flexible cognition* (pp. 559–589). Springer International Publishing. [https://doi.org/10.1007/978-3-319-50406-3\\_18](https://doi.org/10.1007/978-3-319-50406-3_18)
- Ioannidis, J. P. A. (2008). Why most discovered true associations are inflated. *Epidemiology*, *19*(5), 640–648. <https://doi.org/10.1097/EDE.0b013e31818131e7>
- Ioannucci, S., George, N., Friedrich, P., Cerliani, L., & Thiebaut de Schotten, M. (2020). White matter correlates of hemi-face dominance in happy and sad expression. *Brain Structure and Function*, *225*(4), 1379–1388. <https://doi.org/10.1007/s00429-020-02040-7>
- Irfanoglu, M. O., Walker, L., Sarlls, J., Marengo, S., & Pierpaoli, C. (2012). Effects of image distortions originating from susceptibility variations and concomitant fields on diffusion MRI tractography results. *NeuroImage*, *61*(1), 275–288. <https://doi.org/10.1016/j.neuroimage.2012.02.054>
- Irish, M., Lawlor, B. A., Coen, R. F., & O'Mara, S. M. (2011). Everyday episodic memory in amnesic mild cognitive impairment: A preliminary investigation. *BMC Neuroscience*, *12*, 80. <https://doi.org/10.1186/1471-2202-12-80>

- Irish, M., & Vatansever, D. (2020). Rethinking the episodic-semantic distinction from a gradient perspective. *Current Opinion in Behavioral Sciences*, 32, 43–49. <https://doi.org/10.1016/j.cobeha.2020.01.016>
- Jack, C. R., Bennett, D. A., Blennow, K., Carrillo, M. C., Dunn, B., Haeberlein, S. B., Holtzman, D. M., Jagust, W. J., Jessen, F., Karlawish, J., Liu, E., Molinuevo, J. L., Montine, T., Phelps, C., Rankin, K. P., Rowe, C. C., Scheltens, P., Siemers, E., Snyder, H. M., & Sperling, R. (2018). NIA-AA Research Framework: Toward a biological definition of Alzheimer's disease. *Alzheimer's & Dementia*, 14(4), 535–562. <https://doi.org/10.1016/j.jalz.2018.02.018>
- Jack, C. R., Bennett, D. A., Blennow, K., Carrillo, M. C., Feldman, H. H., Frisoni, G. B., Hampel, H., Jagust, W. J., Johnson, K. A., Knopman, D. S., Petersen, R. C., Scheltens, P., Sperling, R. A., & Dubois, B. (2016). A/T/N: An unbiased descriptive classification scheme for Alzheimer disease biomarkers. *Neurology*, 87(5), 539–547. <https://doi.org/10.1212/WNL.0000000000002923>
- Jack, C. R., Wiste, H. J., Weigand, S. D., Knopman, D. S., Vemuri, P., Mielke, M. M., Lowe, V., Senjem, M. L., Gunter, J. L., Machulda, M. M., Gregg, B. E., Pankratz, V. S., Rocca, W. A., & Petersen, R. C. (2015). Age, sex, and APOE  $\epsilon$ 4 effects on memory, brain structure, and  $\beta$ -amyloid across the adult life span. *JAMA Neurology*, 72(5), 511–519. <https://doi.org/10.1001/jamaneurol.2014.4821>
- Jacobs, H. I. L., Hedden, T., Schultz, A. P., Sepulcre, J., Perea, R. D., Amariglio, R. E., Papp, K. V., Rentz, D. M., Sperling, R. A., & Johnson, K. A. (2018). Structural tract alterations predict downstream tau accumulation in amyloid-positive older individuals. *Nature Neuroscience*, 21(3), 424–431. <https://doi.org/10.1038/s41593-018-0070-z>
- Jaeger, J. (2018). Digit symbol substitution test. *Journal of Clinical Psychopharmacology*, 38(5), 513–519. <https://doi.org/10.1097/JCP.0000000000000941>
- Jagust, W. J. (2013). Vulnerable neural systems and the borderland of brain aging and neurodegeneration. *Neuron*, 77(2), 219–234. <https://doi.org/10.1016/j.neuron.2013.01.002>
- Jagust, W. J. (2018). Imaging the evolution and pathophysiology of Alzheimer disease. *Nature Reviews Neuroscience*, 19(11), 687–700. <https://doi.org/10.1038/s41583-018-0067-3>

- Jagust, W. J. (2021). Integrating events in the disintegration of Alzheimer's disease. *Brain*, *144*(1), 11–14. <https://doi.org/10.1093/brain/awaa402>
- Jagust, W. J., & Mormino, E. C. (2011). Lifespan brain activity,  $\beta$ -amyloid, and Alzheimer's disease. *Trends in Cognitive Sciences*, *15*(11), 520–526. <https://doi.org/10.1016/j.tics.2011.09.004>
- Jansen, I. E., Savage, J. E., Watanabe, K., Bryois, J., Williams, D. M., Steinberg, S., Sealock, J., Karlsson, I. K., Hägg, S., Athanasiu, L., Voyle, N., Proitsi, P., Witoelar, A., Stringer, S., Aarsland, D., Almdahl, I. S., Andersen, F., Bergh, S., Bettella, F., ... Posthuma, D. (2019). Genome-wide meta-analysis identifies new loci and functional pathways influencing Alzheimer's disease risk. *Nature Genetics*, *51*(3), 404–413. <https://doi.org/10.1038/s41588-018-0311-9>
- Jansen, W. J., Ossenkuppele, R., Knol, D. L., Tijms, B. M., Scheltens, P., Verhey, F. R. J., Visser, P. J., Aalten, P., Aarsland, D., Alcolea, D., Alexander, M., Almdahl, I. S., Arnold, S. E., Baldeiras, I., Barthel, H., Berckel, B. N. M. van, Bibeau, K., Blennow, K., Brooks, D. J., ... Zetterberg, H. (2015). Prevalence of cerebral amyloid pathology in persons without dementia: A meta-analysis. *JAMA*, *313*(19), 1924–1938. <https://doi.org/10.1001/jama.2015.4668>
- Jansen, W. J., Ossenkuppele, R., Tijms, B. M., Fagan, A. M., Hansson, O., Klunk, W. E., van der Flier, W. M., Villemagne, V. L., Frisoni, G. B., Fleisher, A. S., Lleó, A., Mintun, M. A., Wallin, A., Engelborghs, S., Na, D. L., Chételat, G., Molinuevo, J. L., Landau, S. M., Mattsson, N., ... Zetterberg, H. (2018). Association of cerebral amyloid- $\beta$  aggregation with cognitive functioning in persons without dementia. *JAMA Psychiatry*, *75*(1), 84–95. <https://doi.org/10.1001/jamapsychiatry.2017.3391>
- Jaroudi, W., Garami, J., Garrido, S., Hornberger, M., Keri, S., & Moustafa, A. A. (2017). Factors underlying cognitive decline in old age and Alzheimer's disease: The role of the hippocampus. *Reviews in the Neurosciences*, *28*(7), 705–714. <https://doi.org/10.1515/revneuro-2016-0086>
- Jbabdi, S., & Behrens, T. E. (2013). Long-range connectomics. *Annals of the New York Academy of Sciences*, *1305*(1), 83–93. <https://doi.org/10.1111/nyas.12271>
- Jbabdi, S., & Johansen-Berg, H. (2011). Tractography: Where do we go from here? *Brain Connectivity*, *1*(3), 169–183. <https://doi.org/10.1089/brain.2011.0033>

- Jeurissen, B., Descoteaux, M., Mori, S., & Leemans, A. (2019). Diffusion MRI fiber tractography of the brain. *NMR in Biomedicine*, 32(4), e3785. <https://doi.org/10.1002/nbm.3785>
- Jones, D. K. (2008). Studying connections in the living human brain with diffusion MRI. *Cortex*, 44(8), 936–952. <https://doi.org/10.1016/j.cortex.2008.05.002>
- Jones, D. K., Christiansen, K. F., Chapman, R. J., & Aggleton, J. P. (2013). Distinct subdivisions of the cingulum bundle revealed by diffusion MRI fibre tracking: Implications for neuropsychological investigations. *Neuropsychologia*, 51(1), 67–78. <https://doi.org/10.1016/J.NEUROPSYCHOLOGIA.2012.11.018>
- Jones, D. K., Horsfield, M. A., & Simmons, A. (1999). Optimal strategies for measuring diffusion in anisotropic systems by magnetic resonance imaging. *Magnetic Resonance in Medicine*, 42(3), 515–525. [https://doi-org.abc.cardiff.ac.uk/10.1002/\(SICI\)1522-2594\(199909\)42:3<515::AID-MRM14>3.0.CO;2-Q](https://doi.org/abc.cardiff.ac.uk/10.1002/(SICI)1522-2594(199909)42:3<515::AID-MRM14>3.0.CO;2-Q)
- Jones, D. K., Knösche, T. R., & Turner, R. (2013). White matter integrity, fiber count, and other fallacies: The do's and don'ts of diffusion MRI. *NeuroImage*, 73, 239–254. <https://doi.org/10.1016/j.neuroimage.2012.06.081>
- Jones, D. T., Knopman, D. S., Gunter, J. L., Graff-Radford, J., Vemuri, P., Boeve, B. F., Petersen, R. C., Weiner, M. W., & Jack, C. R. (2016). Cascading network failure across the Alzheimer's disease spectrum. *Brain*, 139(2), 547–562. <https://doi.org/10.1093/brain/awv338>
- Juncos-Rabadán, O., Pereiro, A. X., Facal, D., Reboredo, A., & Lojo-Seoane, C. (2014). Do the Cambridge Neuropsychological Test Automated Battery episodic memory measures discriminate amnesic mild cognitive impairment? *International Journal of Geriatric Psychiatry*, 29(6), 602–609. <https://doi.org/10.1002/gps.4042>
- Kaas, J. H. (2013). The evolution of brains from early mammals to humans. *Wiley Interdisciplinary Reviews: Cognitive Science*, 4(1), 33–45. <https://doi.org/10.1002/wcs.1206>
- Kafkas, A., Migo, E. M., Morris, R. G., Kopelman, M. D., Montaldi, D., & Mayes, A. R. (2017). Material specificity drives medial temporal lobe familiarity but not hippocampal recollection. *Hippocampus*, 27(2), 194–209. <https://doi.org/10.1002/hipo.22683>



- Kahn, I., Andrews-Hanna, J. R., Vincent, J. L., Snyder, A. Z., & Buckner, R. L. (2008). Distinct cortical anatomy linked to subregions of the medial temporal lobe revealed by intrinsic functional connectivity. *Journal of Neurophysiology*, *100*(1), 129–139. <https://doi.org/10.1152/jn.00077.2008>
- Kamenetz, F., Tomita, T., Hsieh, H., Seabrook, G., Borchelt, D., Iwatsubo, T., Sisodia, S., & Malinow, R. (2003). APP processing and synaptic function. *Neuron*, *37*(6), 925–937. [https://doi.org/10.1016/s0896-6273\(03\)00124-7](https://doi.org/10.1016/s0896-6273(03)00124-7)
- Kanwisher, N. (2017). The quest for the FFA and where it led. *Journal of Neuroscience*, *37*(5), 1056–1061. <https://doi.org/10.1523/JNEUROSCI.1706-16.2016>
- Karch, C. M., Cruchaga, C., & Goate, A. M. (2014). Alzheimer's disease genetics: From the bench to the clinic. *Neuron*, *83*(1), 11–26. <https://doi.org/10.1016/j.neuron.2014.05.041>
- Karcher, N. R., & Barch, D. M. (2021). The ABCD study: Understanding the development of risk for mental and physical health outcomes. *Neuropsychopharmacology*, *46*(1), 131–142. <https://doi.org/10.1038/s41386-020-0736-6>
- Kelly, C., Toro, R., Di Martino, A., Cox, C. L., Bellec, P., Castellanos, F. X., & Milham, M. P. (2012). A convergent functional architecture of the insula emerges across imaging modalities. *NeuroImage*, *61*(4), 1129–1142. <https://doi.org/10.1016/j.neuroimage.2012.03.021>
- Kennedy, K. M., Rodrigue, K. M., Devous, M. D., Hebrank, A. C., Bischof, G. N., & Park, D. C. (2012). Effects of beta-amyloid accumulation on neural function during encoding across the adult lifespan. *NeuroImage*, *62*(1), 1–8. <https://doi.org/10.1016/j.neuroimage.2012.03.077>
- Kent, B. A., Hvoslef-Eide, M., Saksida, L. M., & Bussey, T. J. (2016). The representational–hierarchical view of pattern separation: Not just hippocampus, not just space, not just memory? *Neurobiology of Learning and Memory*, *129*, 99–106. <https://doi.org/10.1016/j.nlm.2016.01.006>
- Kessels, R. P. C., Hobbel, D., & Postma, A. (2007). Aging, context memory and binding: A comparison of “what, where and when” in young and older adults. *International Journal of Neuroscience*, *117*(6), 795–810. <https://doi.org/10.1080/00207450600910218>

- Khan, W., Giampietro, V., Ginestet, C., Dell'Acqua, F., Bouls, D., Newhouse, S., Dobson, R., Banaschewski, T., Barker, G. J., Bokde, A. L. W., Büchel, C., Conrod, P., Flor, H., Frouin, V., Garavan, H., Gowland, P., Heinz, A., Ittermann, B., Lemaître, H., ... the IMAGEN Consortium. (2014). No differences in hippocampal volume between carriers and non-carriers of the ApoE  $\epsilon$ 4 and  $\epsilon$ 2 alleles in young healthy adolescents. *Journal of Alzheimer's Disease*, *40*(1), 37–43. <https://doi.org/10.3233/JAD-131841>
- Kharabian Masouleh, S., Plachti, A., Hoffstaedter, F., Eickhoff, S., & Genon, S. (2020). Characterizing the gradients of structural covariance in the human hippocampus. *NeuroImage*, *218*, 116972. <https://doi.org/10.1016/j.neuroimage.2020.116972>
- Kim, H. (2010). Dissociating the roles of the default-mode, dorsal, and ventral networks in episodic memory retrieval. *NeuroImage*, *50*(4), 1648–1657. <https://doi.org/10.1016/j.neuroimage.2010.01.051>
- Kim, J., Park, S., Yoo, H., Jang, H., Kim, Y., Kim, K. W., Jang, Y. K., Lee, J. S., Kim, S. T., Kim, S., Lee, J. M., Ki, C.-S., Na, D. L., Seo, S. W., & Kim, H. J. (2018). The impact of APOE  $\epsilon$ 4 in Alzheimer's disease differs according to age. *Journal of Alzheimer's Disease*, *61*(4), 1377–1385. <https://doi.org/10.3233/JAD-170556>
- Kim, S., Jeneson, A., van der Horst, A. S., Frascino, J. C., Hopkins, R. O., & Squire, L. R. (2011). Memory, visual discrimination performance, and the human hippocampus. *Journal of Neuroscience*, *31*(7), 2624–2629. <https://doi.org/10.1523/JNEUROSCI.5954-10.2011>
- King, D. R., Chastelaine, M. de, Elward, R. L., Wang, T. H., & Rugg, M. D. (2015). Recollection-related increases in functional connectivity predict individual differences in memory accuracy. *Journal of Neuroscience*, *35*(4), 1763–1772. <https://doi.org/10.1523/JNEUROSCI.3219-14.2015>
- Klein, D. A., Steinberg, M., Galik, E., Steele, C., Sheppard, J. M., Warren, A., Rosenblatt, A., & Lyketsos, C. G. (1999). Wandering behaviour in community-residing persons with dementia. *International Journal of Geriatric Psychiatry*, *14*(4), 272–279. [https://doi.org/10.1002/\(sici\)1099-1166\(199904\)14:4<272::aid-gps896>3.0.co;2-p](https://doi.org/10.1002/(sici)1099-1166(199904)14:4<272::aid-gps896>3.0.co;2-p)
- Knight, R. G., Tsui, H. S. L., Abraham, W. C., Skeaff, C. M., McMahon, J. A., & Cutfield, N. J. (2014). Lack of effect of the apolipoprotein E  $\epsilon$ 4 genotype on cognition during healthy aging. *Journal of Clinical and Experimental Neuropsychology*, *36*(7), 742–750. <https://doi.org/10.1080/13803395.2014.935706>

- Koelewijn, L., Lancaster, T. M., Linden, D., Dima, D. C., Routley, B. C., Magazzini, L., Barawi, K., Brindley, L., Adams, R., Tansey, K. E., Bompas, A., Tales, A., Bayer, A., & Singh, K. (2019). Oscillatory hyperactivity and hyperconnectivity in young APOE- $\epsilon$ 4 carriers and hypoconnectivity in Alzheimer's disease. *eLife*, *8*, e36011. <https://doi.org/10.7554/eLife.36011>
- Koller, M., & Stahel, W. A. (2011). Sharpening Wald-type inference in robust regression for small samples. *Computational Statistics & Data Analysis*, *55*(8), 2504–2515. <https://doi.org/10.1016/j.csda.2011.02.014>
- Krishnan, A., Williams, L. J., McIntosh, A. R., & Abdi, H. (2011). Partial Least Squares (PLS) methods for neuroimaging: A tutorial and review. *NeuroImage*, *56*(2), 455–475. <https://doi.org/10.1016/j.neuroimage.2010.07.034>
- Kunz, L., Schröder, T. N., Lee, H., Montag, C., Lachmann, B., Sariyska, R., Reuter, M., Stirnberg, R., Stöcker, T., Messing-Floeter, P. C., Fell, J., Doeller, C. F., & Axmacher, N. (2015). Reduced grid-cell-like representations in adults at genetic risk for Alzheimer's disease. *Science*, *350*(6259), 430–433. <https://doi.org/10.1126/science.aac8128>
- Kuo, C.-L., Pilling, L. C., Atkins, J. L., Kuchel, G. A., & Melzer, D. (2020). ApoE e2 and aging-related outcomes in 379,000 UK Biobank participants. *Aging*, *12*(12), 12222–12233. <https://doi.org/10.18632/aging.103405>
- Kuznetsova, A., Brockhoff, P. B., & Christensen, R. H. B. (2017). lmerTest package: Tests in linear mixed effects models. *Journal of Statistical Software*, *82*(1), 1–26. <https://doi.org/10.18637/jss.v082.i13>
- La Joie, R., Visani, A. V., Baker, S. L., Brown, J. A., Bourakova, V., Cha, J., Chaudhary, K., Edwards, L., Iaccarino, L., Janabi, M., Lesman-Segev, O. H., Miller, Z. A., Perry, D. C., O'Neil, J. P., Pham, J., Rojas, J. C., Rosen, H. J., Seeley, W. W., Tsai, R. M., ... Rabinovici, G. D. (2020). Prospective longitudinal atrophy in Alzheimer's disease correlates with the intensity and topography of baseline tau-PET. *Science Translational Medicine*, *12*(524), eaau5732. <https://doi.org/10.1126/scitranslmed.aau5732>
- Laczó, J., Andel, R., Vlček, K., Macoška, V., Vyhnálek, M., Tolar, M., Bojar, M., & Hort, J. (2011). Spatial navigation and APOE in amnesic mild cognitive impairment. *Neurodegenerative Diseases*, *8*(4), 169–177. <https://doi.org/10.1159/000321581>
- La Joie, R., Landeau, B., Perrotin, A., Bejanin, A., Egret, S., Pélerin, A., Mézenge, F., Belliard, S., de La Sayette, V., Eustache, F., Desgranges, B., &

- Chételat, G. (2014). Intrinsic connectivity identifies the hippocampus as a main crossroad between Alzheimer's and semantic dementia-targeted networks. *Neuron*, 81(6), 1417–1428. <https://doi.org/10.1016/j.neuron.2014.01.026>
- Lakens, D. (2013). Calculating and reporting effect sizes to facilitate cumulative science: A practical primer for t-tests and ANOVAs. *Frontiers in Psychology*, 4, 863. <https://doi.org/10.3389/fpsyg.2013.00863>
- Lakens, D., Adolphi, F. G., Albers, C. J., Anvari, F., Apps, M. A. J., Argamon, S. E., Baguley, T., Becker, R. B., Benning, S. D., Bradford, D. E., Buchanan, E. M., Caldwell, A. R., Van Calster, B., Carlsson, R., Chen, S.-C., Chung, B., Colling, L. J., Collins, G. S., Crook, Z., ... Zwaan, R. A. (2018). Justify your alpha. *Nature Human Behaviour*, 2(3), 168–171. <https://doi.org/10.1038/s41562-018-0311-x>
- Lalla, A., Robin, J., & Moscovitch, M. (2020). The contributions of spatial context and imagery to the recollection of single words. *Hippocampus*, 30(8), 865–878. <https://doi.org/10.1002/hipo.23181>
- Lambert, J.-C., Ibrahim-Verbaas, C. A., Harold, D., Naj, A. C., Sims, R., Bellenguez, C., Jun, G., DeStefano, A. L., Bis, J. C., Beecham, G. W., Grenier-Boley, B., Russo, G., Thornton-Wells, T. A., Jones, N., Smith, A. V., Chouraki, V., Thomas, C., Ikram, M. A., Zelenika, D., ... Amouyel, P. (2013). Meta-analysis of 74,046 individuals identifies 11 new susceptibility loci for Alzheimer's disease. *Nature Genetics*, 45(12), 1452–1458. <https://doi.org/10.1038/ng.2802>
- Lambon Ralph, M. A., Jefferies, E., Patterson, K., & Rogers, T. T. (2017). The neural and computational bases of semantic cognition. *Nature Reviews Neuroscience*, 18(1), 42–55. <https://doi.org/10.1038/nrn.2016.150>
- Lancaster, C., Forster, S., Tabet, N., & Rusted, J. (2017). Putting attention in the spotlight: The influence of APOE genotype on visual search in mid adulthood. *Behavioural Brain Research*, 334, 97–104. <https://doi.org/10.1016/j.bbr.2017.07.015>
- Lancaster, C., Tabet, N., & Rusted, J. (2017). The elusive nature of APOE  $\epsilon$ 4 in mid-adulthood: Understanding the cognitive profile. *Journal of the International Neuropsychological Society*, 23(3), 239–253. <https://doi.org/10.1017/S1355617716000990>
- Lanzoni, L., Ravasio, D., Thompson, H., Vatansever, D., Margulies, D., Smallwood, J., & Jefferies, E. (2020). The role of default mode network in

- semantic cue integration. *NeuroImage*, 219, 117019. <https://doi.org/10.1016/j.neuroimage.2020.117019>
- Latini, F., Mårtensson, J., Larsson, E.-M., Fredrikson, M., Åhs, F., Hjortberg, M., Aldskogius, H., & Ryttefors, M. (2017). Segmentation of the inferior longitudinal fasciculus in the human brain: A white matter dissection and diffusion tensor tractography study. *Brain Research*, 1675, 102–115. <https://doi.org/10.1016/j.brainres.2017.09.005>
- Leal, S. L., Landau, S. M., Bell, R. K., & Jagust, W. J. (2017). Hippocampal activation is associated with longitudinal amyloid accumulation and cognitive decline. *eLife*, 6, e22978. <https://doi.org/10.7554/eLife.22978>
- Lebel, C., & Beaulieu, C. (2011). Longitudinal development of human brain wiring continues from childhood into adulthood. *Journal of Neuroscience*, 31(30), 10937–10947. <https://doi.org/10.1523/JNEUROSCI.5302-10.2011>
- Lebel, C., & Deoni, S. (2018). The development of brain white matter microstructure. *NeuroImage*, 182, 207–218. <https://doi.org/10.1016/j.neuroimage.2017.12.097>
- Lebel, C., Gee, M., Camicioli, R., Wieler, M., Martin, W., & Beaulieu, C. (2012). Diffusion tensor imaging of white matter tract evolution over the lifespan. *NeuroImage*, 60(1), 340–352. <https://doi.org/10.1016/j.neuroimage.2011.11.094>
- Lebel, C., Walker, L., Leemans, A., Phillips, L., & Beaulieu, C. (2008). Microstructural maturation of the human brain from childhood to adulthood. *NeuroImage*, 40(3), 1044–1055. <https://doi.org/10.1016/j.neuroimage.2007.12.053>
- Lee, A. C. H., Barense, M. D., & Graham, K. S. (2005). The contribution of the human medial temporal lobe to perception: Bridging the gap between animal and human studies. *The Quarterly Journal of Experimental Psychology Section B*, 58(3–4), 300–325. <https://doi.org/10.1080/02724990444000168>
- Lee, A. C. H., Brodersen, K. H., & Rudebeck, S. R. (2013). Disentangling spatial perception and spatial memory in the hippocampus: A univariate and multivariate pattern analysis fMRI study. *Journal of Cognitive Neuroscience*, 25(4), 534–546. [https://doi.org/10.1162/jocn\\_a\\_00301](https://doi.org/10.1162/jocn_a_00301)
- Lee, A. C. H., Buckley, M. J., Gaffan, David., Emery, Tina., Hodges, J. R., & Graham, K. S. (2006). Differentiating the roles of the hippocampus and perirhinal cortex in processes beyond long-term declarative memory: A

- double dissociation in dementia. *Journal of Neuroscience*, 26(19), 5198–5203. <https://doi.org/10.1523/JNEUROSCI.3157-05.2006>
- Lee, A. C. H., Buckley, M. J., Pegman, S. J., Spiers, H. J., Scahill, V. L., Gaffan, D., Bussey, T. J., Davies, R. R., Kapur, N., Hodges, J. R., & Graham, K. S. (2005). Specialization in the medial temporal lobe for processing of objects and scenes. *Hippocampus*, 15(6), 782–797. <https://doi.org/10.1002/hipo.20101>
- Lee, A. C. H., Bussey, T. J., Murray, E. A., Saksida, L. M., Epstein, R. A., Kapur, N., Hodges, J. R., & Graham, K. S. (2005). Perceptual deficits in amnesia: Challenging the medial temporal lobe ‘mnemonic’ view. *Neuropsychologia*, 43(1), 1–11. <https://doi.org/10.1016/j.neuropsychologia.2004.07.017>
- Lee, A. C. H., Levi, N., Davies, R. R., Hodges, J. R., & Graham, K. S. (2007). Differing profiles of face and scene discrimination deficits in semantic dementia and Alzheimer’s disease. *Neuropsychologia*, 45(9), 2135–2146. <https://doi.org/10.1016/j.neuropsychologia.2007.01.010>
- Lee, A. C. H., Rahman, S., Hodges, J. R., Sahakian, B. J., & Graham, K. S. (2003). Associative and recognition memory for novel objects in dementia: Implications for diagnosis. *European Journal of Neuroscience*, 18(6), 1660–1670. <https://doi.org/10.1046/j.1460-9568.2003.02883.x>
- Lee, A. C. H., & Rudebeck, S. R. (2010). Investigating the interaction between spatial perception and working memory in the human medial temporal lobe. *Journal of Cognitive Neuroscience*, 22(12), 2823–2835. <https://doi.org/10.1162/jocn.2009.21396>. Investigating
- Lee, A. C. H., Scahill, V. L., & Graham, K. S. (2008). Activating the medial temporal lobe during oddity judgment for faces and scenes. *Cerebral Cortex*, 18(3), 683–696. <https://doi.org/10.1093/cercor/bhm104>
- Lee, A. C. H., Yeung, L.-K., & Barense, M. D. (2012). The hippocampus and visual perception. *Frontiers in Human Neuroscience*, 6, 91. <https://doi.org/10.3389/fnhum.2012.00091>
- Lee, M. D., & Wagenmakers, E.-J. (2013). *Bayesian cognitive modeling: A practical course*. Cambridge University Press. <https://doi.org/10.1017/CBO9781139087759>

- Lee, M. H., Smyser, C. D., & Shimony, J. S. (2013). Resting-state fMRI: A review of methods and clinical applications. *American Journal of Neuroradiology*, *34*(10), 1866–1872. <https://doi.org/10.3174/ajnr.A3263>
- Leemans, A., Jeurissen, B., Sijbers, J., & Jones, D. K. (2009). ExploreDTI: A graphical toolbox for processing, analyzing, and visualizing diffusion MR data. *Proceedings of the 17th Scientific Meeting, International Society for Magnetic Resonance in Medicine*, *17*, 3537.
- Leemans, A., & Jones, D. K. (2009). The B-matrix must be rotated when correcting for subject motion in DTI data. *Magnetic Resonance in Medicine*, *61*(6), 1336–1349. <https://doi.org/10.1002/mrm.21890>
- Lenth, R. (2021). *emmeans: Estimated marginal means, aka least-squares means* (Version 1.5.4) [Computer software]. <https://CRAN.R-project.org/package=emmeans>
- Lester, A. W., Moffat, S. D., Wiener, J. M., Barnes, C. A., & Wolbers, T. (2017). The aging navigational system. *Neuron*, *95*(5), 1019–1035. <https://doi.org/10.1016/j.neuron.2017.06.037>
- Levine, B., Svoboda, E., Hay, J. F., Winocur, G., & Moscovitch, M. (2002). Aging and autobiographical memory: Dissociating episodic from semantic retrieval. *Psychology and Aging*, *17*(4), 677–689. <https://doi.org/10.1037/0882-7974.17.4.677>
- Levine, T. F., Allison, S. L., Stojanovic, M., Fagan, A. M., Morris, J. C., & Head, D. (2020). Spatial navigation ability predicts progression of dementia symptomatology. *Alzheimer's & Dementia*, *16*(3), 491–500. <https://doi.org/10.1002/alz.12031>
- Levy, D. A., Shrager, Y., & Squire, L. R. (2005). Intact visual discrimination of complex and feature-ambiguous stimuli in the absence of perirhinal cortex. *Learning & Memory*, *12*(1), 61–66. <https://doi.org/10.1101/lm.84405>
- Lewis, J., & Dickson, D. W. (2016). Propagation of tau pathology: Hypotheses, discoveries, and yet unresolved questions from experimental and human brain studies. *Acta Neuropathologica*, *131*(1), 27–48. <https://doi.org/10.1007/s00401-015-1507-z>
- Li, A. W. Y., & King, J. (2019). Spatial memory and navigation in ageing: A systematic review of MRI and fMRI studies in healthy participants. *Neuroscience & Biobehavioral Reviews*, *103*, 33–49. <https://doi.org/10.1016/j.neubiorev.2019.05.005>

- Li, J., Zhang, X., Li, A., Liu, S., Qin, W., Yu, C., Liu, Y., Liu, B., & Jiang, T. (2018). Polygenic risk for Alzheimer's disease influences precuneal volume in two independent general populations. *Neurobiology of Aging*, *64*, 116–122. <https://doi.org/10.1016/j.neurobiolaging.2017.12.022>
- Li, K., Luo, X., Zeng, Q., Huang, P., Shen, Z., Xu, X., Xu, J., Wang, C., Zhou, J., & Zhang, M. (2019). Gray matter structural covariance networks changes along the Alzheimer's disease continuum. *NeuroImage: Clinical*, *23*, 101828. <https://doi.org/10.1016/j.nicl.2019.101828>
- Li, X., Li, Q., Wang, X., Li, D., & Li, S. (2018). Differential age-related changes in structural covariance networks of human anterior and posterior hippocampus. *Frontiers in Physiology*, *9*, 518. <https://doi.org/10.3389/fphys.2018.00518>
- Li, X., Pu, F., Fan, Y., Niu, H., Li, S., & Li, D. (2013). Age-related changes in brain structural covariance networks. *Frontiers in Human Neuroscience*, *7*, 98. <https://doi.org/10.3389/fnhum.2013.00098>
- Li, Z., Shue, F., Zhao, N., Shinohara, M., & Bu, G. (2020). APOE2: Protective mechanism and therapeutic implications for Alzheimer's disease. *Molecular Neurodegeneration*, *15*, 63. <https://doi.org/10.1186/s13024-020-00413-4>
- Liang, J. C., Erez, J., Zhang, F., Cusack, R., & Barense, M. D. (2020). Experience transforms conjunctive object representations: Neural evidence for unitization after visual expertise. *Cerebral Cortex*, *30*(5), 2721–2739. <https://doi.org/10.1093/cercor/bhz250>
- Libby, L. A., Ekstrom, A. D., Ragland, J. D., & Ranganath, C. (2012). Differential connectivity of perirhinal and parahippocampal cortices within human hippocampal subregions revealed by high-resolution functional imaging. *Journal of Neuroscience*, *32*(19), 6550–6560. <https://doi.org/10.1523/JNEUROSCI.3711-11.2012>
- Liesefeld, H. R., & Janczyk, M. (2019). Combining speed and accuracy to control for speed-accuracy trade-offs(?). *Behavior Research Methods*, *51*(1), 40–60. <https://doi.org/10.3758/s13428-018-1076-x>
- Lim, Y. Y., Baker, J. E., Mills, A., Bruns, L., Fowler, C., Fripp, J., Rainey-Smith, S. R., Ames, D., Masters, C. L., & Maruff, P. (2021). Learning deficit in cognitively normal APOE  $\epsilon$ 4 carriers with LOW  $\beta$ -amyloid. *Alzheimer's & Dementia: Diagnosis, Assessment & Disease Monitoring*, *13*(1), e12136. <https://doi.org/10.1002/dad2.12136>



- Liu, C.-C., Kanekiyo, T., Xu, H., & Bu, G. (2013). Apolipoprotein E and Alzheimer disease: Risk, mechanisms, and therapy. *Nature Reviews Neurology*, *9*(2), 106–118. <https://doi.org/10.1038/nrneurol.2012.263>
- Liu, M., Bian, C., Zhang, J., & Wen, F. (2014). Apolipoprotein E gene polymorphism and Alzheimer's disease in Chinese population: A meta-analysis. *Scientific Reports*, *4*, 4383. <https://doi.org/10.1038/srep04383>
- Livingston, G., Huntley, J., Sommerlad, A., Ames, D., Ballard, C., Banerjee, S., Brayne, C., Burns, A., Cohen-Mansfield, J., Cooper, C., Costafreda, S. G., Dias, A., Fox, N., Gitlin, L. N., Howard, R., Kales, H. C., Kivimäki, M., Larson, E. B., Ogunniyi, A., ... Mukadam, N. (2020). Dementia prevention, intervention, and care: 2020 report of the Lancet Commission. *The Lancet*, *396*(10248), 413–446. [https://doi.org/10.1016/S0140-6736\(20\)30367-6](https://doi.org/10.1016/S0140-6736(20)30367-6)
- Lowe, R., Shirley, N., Bleackley, M., Dolan, S., & Shafee, T. (2017). Transcriptomics technologies. *PLOS Computational Biology*, *13*(5), e1005457. <https://doi.org/10.1371/journal.pcbi.1005457>
- Luck, T., Roehr, S., Rodriguez, F. S., Schroeter, M. L., Witte, A. V., Hinz, A., Mehnert, A., Engel, C., Loeffler, M., Thiery, J., Villringer, A., & Riedel-Heller, S. G. (2018). Memory-related subjective cognitive symptoms in the adult population: Prevalence and associated factors – Results of the LIFE-Adult-Study. *BMC Psychology*, *6*, 23. <https://doi.org/10.1186/s40359-018-0236-1>
- Luke, S. G. (2017). Evaluating significance in linear mixed-effects models in R. *Behavior Research Methods*, *49*(4), 1494–1502. <https://doi.org/10.3758/s13428-016-0809-y>
- Lumsden, A. L., Mulugeta, A., Zhou, A., & Hyppönen, E. (2020). Apolipoprotein E (APOE) genotype-associated disease risks: A phenome-wide, registry-based, case-control study utilising the UK Biobank. *EBioMedicine*, *59*, 102954. <https://doi.org/10.1016/j.ebiom.2020.102954>
- Lupton, M. K., Medland, S. E., Gordon, S. D., Goncalves, T., MacGregor, S., Mackey, D. A., Young, T. L., Duffy, D. L., Visscher, P. M., Wray, N. R., Nyholt, D. R., Bain, L., Ferreira, M. A., Henders, A. K., Wallace, L., Montgomery, G. W., Wright, M. J., & Martin, N. G. (2018). Accuracy of inferred APOE genotypes for a range of genotyping arrays and imputation reference panels. *Journal of Alzheimer's Disease*, *64*(1), 49–54. <https://doi.org/10.3233/JAD-171104>
- Lupton, M. K., Strike, L., Hansell, N. K., Wen, W., Mather, K. A., Armstrong, N. J., Thalamuthu, A., McMahon, K. L., de Zubicaray, G. I., Assareh, A. A.,

- Simmons, A., Proitsi, P., Powell, J. F., Montgomery, G. W., Hibar, D. P., Westman, E., Tsolaki, M., Kloszewska, I., Soininen, H., ... Wright, M. J. (2016). The effect of increased genetic risk for Alzheimer's disease on hippocampal and amygdala volume. *Neurobiology of Aging*, *40*, 68–77. <https://doi.org/10.1016/j.neurobiolaging.2015.12.023>
- Lv, H., Wang, Z., Tong, E., Williams, L. M., Zaharchuk, G., Zeineh, M., Goldstein-Piekarski, A. N., Ball, T. M., Liao, C., & Wintermark, M. (2018). Resting-state functional MRI: Everything that nonexperts have always wanted to know. *American Journal of Neuroradiology*, *39*(8), 1–10. <https://doi.org/10.3174/ajnr.A5527>
- Lyall, D. M., Harris, S. E., Bastin, M. E., Muñoz Maniega, S., Murray, C., Lutz, M. W., Saunders, A. M., Roses, A. D., Valdés Hernández, M. del C., Royle, N. A., Starr, J. M., Porteous, David. J., Wardlaw, J. M., & Deary, I. J. (2014). Alzheimer's disease susceptibility genes APOE and TOMM40, and brain white matter integrity in the Lothian Birth Cohort 1936. *Neurobiology of Aging*, *35*(6), 1513.e25-1513.e33. <https://doi.org/10.1016/j.neurobiolaging.2014.01.006>
- Ma, Y., Afnakina, O., Steptoe, A., & Cadar, D. (2020). Higher risk of dementia in English older individuals who are overweight or obese. *International Journal of Epidemiology*, *49*(4), 1353–1365. <https://doi.org/10.1093/ije/dyaa099>
- Maass, A., Berron, D., Harrison, T. M., Adams, J. N., La Joie, R., Baker, S., Mellinger, T., Bell, R. K., Swinnerton, K., Inglis, B., Rabinovici, G. D., Düzel, E., & Jagust, W. J. (2019). Alzheimer's pathology targets distinct memory networks in the ageing brain. *Brain*, *142*(8), 2492–2509. <https://doi.org/10.1093/brain/awz154>
- Maass, A., Berron, D., Libby, L. A., Ranganath, C., & Düzel, E. (2015). Functional subregions of the human entorhinal cortex. *eLife*, *4*, e06426. <https://doi.org/10.7554/eLife.06426>
- Maass, A., Landau, S., Baker, S. L., Horng, A., Lockhart, S. N., La Joie, R., Rabinovici, G. D., & Jagust, W. J. (2017). Comparison of multiple tau-PET measures as biomarkers in aging and Alzheimer's disease. *NeuroImage*, *157*, 448–463. <https://doi.org/10.1016/j.neuroimage.2017.05.058>
- Madan, C. R. (2018). Age differences in head motion and estimates of cortical morphology. *PeerJ*, *6*, e5176. <https://doi.org/10.7717/peerj.5176>
- Maechler, M., Rousseeuw, P., Croux, C., Todorov, V., Ruckstuhl, A., Salibian-Barrera, M., Verbeke, T., Koller, M., Conceicao, E. L., & Anna di Palma, M.

- (2021). *robustbase: Basic robust statistics* (Version 0.93-7) [Computer software]. <http://CRAN.R-project.org/package=robustbase>
- Maguire, E. A., Intraub, H., & Mullally, S. L. (2016). Scenes, spaces, and memory traces: What does the hippocampus do? *Neuroscientist*, *22*(5), 432–439. <https://doi.org/10.1177/1073858415600389>
- Maguire, E. A., & Mullally, S. L. (2013). The hippocampus: A manifesto for change. *Journal of Experimental Psychology: General*, *142*(4), 1180–1189. <https://doi.org/10.1037/a0033650>
- Mahley, R. W. (2016). Apolipoprotein E: From cardiovascular disease to neurodegenerative disorders. *Journal of Molecular Medicine*, *94*(7), 739–746. <https://doi.org/10.1007/s00109-016-1427-y>
- Mahley, R. W., & Huang, Y. (2012a). Apolipoprotein E sets the stage: Response to injury triggers neuropathology. *Neuron*, *76*(5), 871–885. <https://doi.org/10.1016/j.neuron.2012.11.020>
- Mahley, R. W., & Huang, Y. (2012b). Small-molecule structure correctors target abnormal protein structure and function: Structure corrector rescue of apolipoprotein E4-associated neuropathology. *Journal of Medicinal Chemistry*, *55*(21), 8997–9008. <https://doi.org/10.1021/jm3008618>
- Maier-Hein, K. H., Neher, P. F., Houde, J.-C., Côté, M.-A., Garyfallidis, E., Zhong, J., Chamberland, M., Yeh, F.-C., Lin, Y.-C., Ji, Q., Reddick, W. E., Glass, J. O., Chen, D. Q., Feng, Y., Gao, C., Wu, Y., Ma, J., He, R., Li, Q., ... Descoteaux, M. (2017). The challenge of mapping the human connectome based on diffusion tractography. *Nature Communications*, *8*, 1349. <https://doi.org/10.1038/s41467-017-01285-x>
- Mair, P., & Wilcox, R. R. (2020). Robust statistical methods in R using the WRS2 package. *Behavior Research Methods*, *52*(2), 464–488. <https://doi.org/10.3758/s13428-019-01246-w>
- Manuello, J., Nani, A., Premi, E., Borroni, B., Costa, T., Tatu, K., Liloia, D., Duca, S., & Cauda, F. (2018). The pathoconnectivity profile of Alzheimer's disease: A morphometric coalteration network analysis. *Frontiers in Neurology*, *8*, 739. <https://doi.org/10.3389/fneur.2017.00739>
- Marioni, R. E., Harris, S. E., Zhang, Q., McRae, A. F., Hagenaars, S. P., Hill, W. D., Davies, G., Ritchie, C. W., Gale, C. R., Starr, J. M., Goate, A. M., Porteous, D. J., Yang, J., Evans, K. L., Deary, I. J., Wray, N. R., & Visscher,

- P. M. (2018). GWAS on family history of Alzheimer's disease. *Translational Psychiatry*, 8(99), 1–7. <https://doi.org/10.1038/s41398-018-0150-6>
- Martin, C. B., Cowell, R. A., Gribble, P. L., Wright, J., & Köhler, S. (2016). Distributed category-specific recognition-memory signals in human perirhinal cortex. *Hippocampus*, 26(4), 423–436. <https://doi.org/10.1002/hipo.22531>
- Martin, C. B., McLean, D. A., O'Neil, E. B., & Köhler, S. (2013). Distinct familiarity-based response patterns for faces and buildings in perirhinal and parahippocampal cortex. *Journal of Neuroscience*, 33(26), 10915–10923. <https://doi.org/10.1523/JNEUROSCI.0126-13.2013>
- Martin, C. B., Sullivan, J. A., Wright, J., & Köhler, S. (2018). How landmark suitability shapes recognition memory signals for objects in the medial temporal lobes. *NeuroImage*, 166, 425–436. <https://doi.org/10.1016/j.neuroimage.2017.11.004>
- Mason, E. J., Hussey, E. P., Molitor, R. J., Ko, P. C., Donahue, M. J., & Ally, B. A. (2017). Family history of Alzheimer's disease is associated with impaired perceptual discrimination of novel objects. *Journal of Alzheimer's Disease*, 57(3), 735–745. <https://doi.org/10.3233/JAD-160772>
- Matthews, F. E., Chatfield, M., Freeman, C., McCracken, C., Brayne, C., & MRC CFAS. (2004). Attrition and bias in the MRC cognitive function and ageing study: An epidemiological investigation. *BMC Public Health*, 4, 12. <https://doi.org/10.1186/1471-2458-4-12>
- Mattsson, N., Palmqvist, S., Stomrud, E., Vogel, J., & Hansson, O. (2019). Staging  $\beta$ -amyloid pathology with amyloid positron emission tomography. *JAMA Neurology*, 76(11), 1319–1329. <https://doi.org/10.1001/jamaneurol.2019.2214>
- Mauguière, F., & Corkin, S. (2015). H.M. never again! An analysis of H.M.'s epilepsy and treatment. *Revue Neurologique*, 171(3), 273–281. <https://doi.org/10.1016/j.neurol.2015.01.002>
- McCormick, C., Dalton, M. A., Zeidman, P., & Maguire, E. A. (2021). Characterising the hippocampal response to perception, construction and complexity. *Cortex*, 1–17. <https://doi.org/10.1016/j.cortex.2020.12.018>
- McIntosh, A. M., Bennett, C., Dickson, D., Anestis, S. F., Watts, D. P., Webster, T. H., Fontenot, M. B., & Bradley, B. J. (2012). The apolipoprotein E (APOE) gene appears functionally monomorphic in chimpanzees (*Pan troglodytes*). *PLOS ONE*, 7(10), e47760. <https://doi.org/10.1371/journal.pone.0047760>

- McIntosh, A. R., & Lobaugh, N. J. (2004). Partial least squares analysis of neuroimaging data: Applications and advances. *NeuroImage*, *23*(S1), S250–263. <https://doi.org/10.1016/j.neuroimage.2004.07.020>
- Mckeown, B., Strawson, W. H., Wang, H.-T., Karapanagiotidis, T., Vos de Wael, R., Benkarim, O., Turnbull, A., Margulies, D., Jefferies, E., McCall, C., Bernhardt, B., & Smallwood, J. (2020). The relationship between individual variation in macroscale functional gradients and distinct aspects of ongoing thought. *NeuroImage*, *220*, 117072. <https://doi.org/10.1016/j.neuroimage.2020.117072>
- McKhann, G. M., Knopman, D. S., Chertkow, H., Hyman, B. T., Jack, C. R., Kawas, C. H., Klunk, W. E., Koroshetz, W. J., Manly, J. J., Mayeux, R., Mohs, R. C., Morris, J. C., Rossor, M. N., Scheltens, P., Carrillo, M. C., Thies, B., Weintraub, S., & Phelps, C. H. (2011). The diagnosis of dementia due to Alzheimer's disease: Recommendations from the National Institute on Aging-Alzheimer's Association workgroups on diagnostic guidelines for Alzheimer's disease. *Alzheimer's & Dementia*, *7*(3), 263–269. <https://doi.org/10.1016/j.jalz.2011.03.005>
- McLelland, V. C., Chan, D., Ferber, S., & Barense, M. D. (2014). Stimulus familiarity modulates functional connectivity of the perirhinal cortex and anterior hippocampus during visual discrimination of faces and objects. *Frontiers in Human Neuroscience*, *8*, 117. <https://doi.org/10.3389/fnhum.2014.00117>
- McNaughton, L., Chen, L. L., & Markus, J. (1991). "Dead Reckoning," landmark learning, and the sense of direction: A neurophysiological and computational hypothesis. *Journal of Cognitive Neuroscience*, *3*(2), 190–202. <https://doi.org.abc.cardiff.ac.uk/10.1162/jocn.1991.3.2.190>
- McTighe, S. M., Mar, A. C., Romberg, C., Bussey, T. J., & Saksida, L. M. (2009). A new touchscreen test of pattern separation: Effect of hippocampal lesions. *NeuroReport*, *20*(9), 881–885. <https://doi.org/10.1097/WNR.0b013e32832c5eb2>
- Mechelli, A., Friston, K. J., Frackowiak, R. S., & Price, C. J. (2005). Structural covariance in the human cortex. *Journal of Neuroscience*, *25*(36), 8303–8310. <https://doi.org/10.1523/JNEUROSCI.0357-05.2005>
- Memel, M., Wank, A. A., Ryan, L., & Grilli, M. D. (2020). The relationship between episodic detail generation and anterotemporal, posteromedial, and hippocampal white matter tracts. *Cortex*, *123*, 124–140. <https://doi.org/10.1016/j.cortex.2019.10.010>

- Mentink, L. J., Guimarães, J. P. O. F. T., Faber, M., Sprooten, E., Rikkert, M. G. M. O., Haak, K. V., & Beckmann, C. F. (2021). Functional co-activation of the default mode network in APOE  $\epsilon$ 4-carriers: A replication study. *NeuroImage*, 118304. <https://doi.org/10.1016/j.neuroimage.2021.118304>
- Mesulam, M.-M. (1990). Large-scale neurocognitive networks and distributed processing for attention, language, and memory. *Annals of Neurology*, 28(5), 597–613. <https://doi.org/10.1002/ana.410280502>
- Mesulam, M.-M. (1994). Distributed locality and large-scale neurocognitive networks. *Behavioral and Brain Sciences*, 17(1), 74–76. <https://doi.org/10.1017/S0140525X0003346X>
- Mesulam, M.-M. (2009). Defining neurocognitive networks in the BOLD new world of computed connectivity. *Neuron*, 62(1), 1–3. <https://doi.org/10.1016/j.neuron.2009.04.001>
- Meteyard, L., & Davies, R. A. I. (2020). Best practice guidance for linear mixed-effects models in psychological science. *Journal of Memory and Language*, 112, 104092. <https://doi.org/10.1016/j.jml.2020.104092>
- Metzler-Baddeley, C., Jones, D. K., Steventon, J., Westacott, L., Aggleton, J. P., & O'Sullivan, M. J. (2012). Cingulum microstructure predicts cognitive control in older age and mild cognitive impairment. *Journal of Neuroscience*, 32(49), 17612–17619. <https://doi.org/10.1523/JNEUROSCI.3299-12.2012>
- Metzler-Baddeley, C., O'Sullivan, M. J., Bells, S., Pasternak, O., & Jones, D. K. (2012). How and how not to correct for CSF-contamination in diffusion MRI. *NeuroImage*, 59(2), 1394–1403. <https://doi.org/10.1016/j.neuroimage.2011.08.043>
- Miller, K. J., Rogers, S. A., Siddarth, P., & Small, G. W. (2005). Object naming and semantic fluency among individuals with genetic risk for Alzheimer's disease. *International Journal of Geriatric Psychiatry*, 20(2), 128–136. <https://doi.org/10.1002/gps.1262>
- Minoshima, S., Giordani, B., Berent, S., Frey, K. A., Foster, N. L., & Kuhl, D. E. (1997). Metabolic reduction in the posterior cingulate cortex in very early Alzheimer's disease. *Annals of Neurology*, 42(1), 85–94. <https://doi.org/10.1002/ana.410420114>
- Mishra, S., Blazey, T. M., Holtzman, D. M., Cruchaga, C., Su, Y., Morris, J. C., Benzinger, T. L. S., & Gordon, B. A. (2018). Longitudinal brain imaging in

- preclinical Alzheimer disease: Impact of APOE  $\epsilon$ 4 genotype. *Brain*, 141(6), 1828–1839. <https://doi.org/10.1093/brain/awy103>
- Mitchell, K. J. (2017). Neurogenomics – Towards a more rigorous science. *European Journal of Neuroscience*, 47(2), 109–114. <https://doi.org/doi:10.1111/ejn.13801>
- Moffat, S. D., & Resnick, S. M. (2002). Effects of age on virtual environment place navigation and allocentric cognitive mapping. *Behavioral Neuroscience*, 116(5), 851–859. <https://doi.org/10.1037/0735-7044.116.5.851>
- Mollink, J., Smith, S. M., Elliott, L. T., Kleinnijenhuis, M., Hiemstra, M., Alfaro-Almagro, F., Marchini, J., van Cappellen van Walsum, A.-M., Jbabdi, S., & Miller, K. L. (2019). The spatial correspondence and genetic influence of interhemispheric connectivity with white matter microstructure. *Nature Neuroscience*, 22(5), 809–819. <https://doi.org/10.1038/s41593-019-0379-2>
- Montembeault, M., Joubert, S., Doyon, J., Carrier, J., Gagnon, J.-F., Monchi, O., Lungu, O., Belleville, S., & Brambati, S. M. (2012). The impact of aging on gray matter structural covariance networks. *NeuroImage*, 63(2), 754–759. <https://doi.org/10.1016/j.neuroimage.2012.06.052>
- Montembeault, M., Rouleau, I., Provost, J.-S., & Brambati, S. M. (2016). Altered gray matter structural covariance networks in early stages of Alzheimer's disease. *Cerebral Cortex*, 26(6), 2650–2662. <https://doi.org/10.1093/cercor/bhv105>
- Moodley, K., Minati, L., Contarino, V., Prioni, S., Wood, R., Cooper, R., D'Incerti, L., Tagliavini, F., & Chan, D. (2015). Diagnostic differentiation of mild cognitive impairment due to Alzheimer's disease using a hippocampus-dependent test of spatial memory. *Hippocampus*, 25(8), 939–951. <https://doi.org/10.1002/hipo.22417>
- Morey, R. D., & Rouder, J. N. (2018). *BayesFactor: Computation of Bayes factors for common designs* (Version 0.9.12-4.2) [Computer software]. <http://CRAN.R-project.org/package=robustbase>
- Morey, R. D., Rouder, J. N., Verhagen, J., & Wagenmakers, E.-J. (2014). Why hypothesis tests are essential for psychological science: A comment on Cumming (2014). *Psychological Science*, 25(6), 1289–1290. <https://doi.org/10.1177/0956797614525969>

- Morey, R. D., & Wagenmakers, E.-J. (2014). Simple relation between Bayesian order-restricted and point-null hypothesis tests. *Statistics & Probability Letters*, *92*, 121–124. <https://doi.org/10.1016/j.spl.2014.05.010>
- Mormino, E. C., Brandel, M. G., Madison, C. M., Marks, S., Baker, S. L., & Jagust, W. J. (2012). A $\beta$  deposition in aging Is associated with increases in brain activation during successful memory encoding. *Cerebral Cortex*, *22*(8), 1813–1823. <https://doi.org/10.1093/cercor/bhr255>
- Mormino, E. C., Sperling, R. A., Holmes, A. J., Buckner, R. L., De Jager, P. L., Smoller, J. W., & Sabuncu, M. R. (2016). Polygenic risk of Alzheimer disease is associated with early- and late-life processes. *Neurology*, *87*(5), 481–488. <https://doi.org/10.1212/WNL.0000000000002922>
- Morris, R. G. M. (1981). Spatial localization does not require the presence of local cues. *Learning and Motivation*, *12*(2), 239–260. [https://doi.org/10.1016/0023-9690\(81\)90020-5](https://doi.org/10.1016/0023-9690(81)90020-5)
- Morris, R. G. M., Garrud, P., Rawlins, J. N. P., & O'Keefe, J. (1982). Place navigation impaired in rats with hippocampal lesions. *Nature*, *297*(5868), 681–683. <https://doi.org/10.1038/297681a0>
- Mulder, J., & Wagenmakers, E.-J. (2016). Editors' introduction to the special issue "Bayes factors for testing hypotheses in psychological research: Practical relevance and new developments". *Journal of Mathematical Psychology*, *72*, 1–5. <https://doi.org/10.1016/j.jmp.2016.01.002>
- Mundy, M. E., Downing, P. E., Dwyer, D. M., Honey, R. C., & Graham, K. S. (2013). A critical role for the hippocampus and perirhinal cortex in perceptual learning of scenes and faces: Complementary findings from amnesia and fMRI. *Journal of Neuroscience*, *33*(25), 10490–10502. <https://doi.org/10.1523/JNEUROSCI.2958-12.2013>
- Murphy, K., Birn, R. M., & Bandettini, P. A. (2013). Resting-state fMRI confounds and cleanup. *NeuroImage*, *80*, 349–359. <https://doi.org/10.1016/J.NEUROIMAGE.2013.04.001>
- Murray, E. A., Bussey, T. J., & Saksida, L. M. (2007). Visual perception and memory: A new view of medial temporal lobe function in primates and rodents. *Annual Review of Neuroscience*, *30*, 99–122. <https://doi.org/10.1146/annurev.neuro.29.051605.113046>
- Murray, E. A., & Wise, S. P. (2004). What, if anything, is the medial temporal lobe, and how can the amygdala be part of it if there is no such thing?



- Neurobiology of Learning and Memory*, 82(3), 178–198.  
<https://doi.org/10.1016/j.nlm.2004.05.005>
- Murray, E. A., & Wise, S. P. (2010). What, if anything, can monkeys tell us about human amnesia when they can't say anything at all? *Neuropsychologia*, 48(8), 2385–2405.  
<https://doi.org/10.1016/j.neuropsychologia.2010.01.011>
- Murray, E. A., & Wise, S. P. (2012). Why is there a special issue on perirhinal cortex in a journal called Hippocampus?: The perirhinal cortex in historical perspective. *Hippocampus*, 22(10), 1941–1951.  
<https://doi.org/10.1002/hipo.22055>
- Murray, E. A., Wise, S. P., & Graham, K. S. (2017). *The evolution of memory systems: Ancestors, anatomy, and adaptations*. Oxford University Press.
- Murray, E. A., Wise, S. P., & Graham, K. S. (2018). Representational specializations of the hippocampus in phylogenetic perspective. *Neuroscience Letters*, 680, 4–12.  
<https://doi.org/10.1016/j.neulet.2017.04.065>.
- Mwilambwe-Tshilobo, L., & Spreng, R. N. (2021). Social exclusion reliably engages the default network: A meta-analysis of Cyberball. *NeuroImage*, 227, 117666. <https://doi.org/10.1016/j.neuroimage.2020.117666>
- Naber, P. A., Caballero-Bleda, M., Jorritsma-Byham, B., & Witter, M. P. (1997). Parallel input to the hippocampal memory system through peri- and postrhinal cortices. *NeuroReport*, 8(11), 2617–2621.  
<https://doi.org/10.1097/00001756-199707280-00039>
- Nadel, L., & Peterson, M. A. (2013). The hippocampus: Part of an interactive posterior representational system spanning perceptual and memorial systems. *Journal of Experimental Psychology: General*, 142(4), 1242–1254.  
<https://doi.org/10.1037/a0033690>
- Navarro Schröder, T. N., Haak, K. V., Zaragoza Jimenez, N. I., Beckmann, C. F., & Doeller, C. F. (2015). Functional topography of the human entorhinal cortex. *eLife*, 4, e06738. <https://doi.org/10.7554/eLife.06738>
- Navlakha, S., Bar-Joseph, Z., & Barth, A. L. (2018). Network design and the brain. *Trends in Cognitive Sciences*, 22(1), 64–78.  
<https://doi.org/10.1016/j.tics.2017.09.012>

- Nestor, P. J., Fryer, T. D., & Hodges, J. R. (2006). Declarative memory impairments in Alzheimer's disease and semantic dementia. *NeuroImage*, *30*(3), 1010–1020. <https://doi.org/10.1016/j.neuroimage.2005.10.008>
- Neu, S. C., Pa, J., Kukull, W., Beekly, D., Kuzma, A., Gangadharan, P., Wang, L. S., Romero, K., Arneric, S. P., Redolfi, A., Orlandi, D., Frisoni, G. B., Au, R., Devine, S., Auerbach, S., Espinosa, A., Boada, M., Ruiz, A., Johnson, S. C., ... Toga, A. W. (2017). Apolipoprotein E genotype and sex risk factors for Alzheimer disease: A meta-analysis. *JAMA Neurology*, *74*(10), 1178–1189. <https://doi.org/10.1001/jamaneurol.2017.2188>
- Noble, S., Scheinost, D., & Constable, R. T. (2019). A decade of test-retest reliability of functional connectivity: A systematic review and meta-analysis. *NeuroImage*, *203*, 116157. <https://doi.org/10.1016/j.neuroimage.2019.116157>
- Nordin, K., Persson, J., Stening, E., Herlitz, A., Larsson, E.-M., & Söderlund, H. (2018). Structural whole-brain covariance of the anterior and posterior hippocampus: Associations with age and memory. *Hippocampus*, *28*(2), 151–163. <https://doi.org/10.1002/hipo.22817>
- Nuriel, T., Angulo, S. L., Khan, U., Ashok, A., Chen, Q., Figueroa, H. Y., Emrani, S., Liu, L., Herman, M., Barrett, G., Savage, V., Buitrago, L., Cepeda-Prado, E., Fung, C., Goldberg, E., Gross, S. S., Hussaini, S. A., Moreno, H., Small, S. A., & Duff, K. E. (2017). Neuronal hyperactivity due to loss of inhibitory tone in APOE4 mice lacking Alzheimer's disease-like pathology. *Nature Communications*, *8*, 1464. <https://doi.org/10.1038/s41467-017-01444-0>
- Nyberg, L. (2017). Functional brain imaging of episodic memory decline in ageing. *Journal of Internal Medicine*, *281*(1), 65–74. <https://doi.org/10.1111/joim.12533>
- Nyberg, L., & Pudas, S. (2019). Successful memory aging. *Annual Review of Psychology*, *70*, 219–243. <https://doi.org/10.1146/annurev-psych-010418-103052>
- Nyberg, L., Salami, A., Andersson, M., Eriksson, J., Kalpouzos, G., Kauppi, K., Lind, J., Pudas, S., Persson, J., & Nilsson, L.-G. (2010). Longitudinal evidence for diminished frontal cortex function in aging. *Proceedings of the National Academy of Sciences*, *107*(52), 22682–22686. <https://doi.org/10.1073/pnas.1012651108>

- O'Donnell, L. J., & Pasternak, O. (2015). Does diffusion MRI tell us anything about the white matter? An overview of methods and pitfalls. *Schizophrenia Research, 161*(1), 133–141. <https://doi.org/10.1016/j.schres.2014.09.007>
- O'Donoghue, M. C., Murphy, S. E., Zamboni, G., Nobre, A. C., & Mackay, C. E. (2018). APOE genotype and cognition in healthy individuals at-risk of Alzheimer's disease: A review. *Cortex, 104*, 103–123. <https://doi.org/10.1016/j.cortex.2018.03.025>
- O'Dwyer, L., Lamberton, F., Matura, S., Tanner, C., Scheibe, M., Miller, J., Rujescu, D., Prvulovic, D., & Hampel, H. (2012). Reduced hippocampal volume in healthy young ApoE4 carriers: An MRI study. *PLOS ONE, 7*(11), e48895. <https://doi.org/10.1371/journal.pone.0048895>
- Oh, H., Madison, C., Baker, S., Rabinovici, G., & Jagust, W. J. (2016). Dynamic relationships between age, amyloid- $\beta$  deposition, and glucose metabolism link to the regional vulnerability to Alzheimer's disease. *Brain, 139*(8), 2275–2289. <https://doi.org/10.1093/brain/aww108>
- Öhman, F., Hassenstab, J., Berron, D., Schöll, M., & Papp, K. V. (2021). Current advances in digital cognitive assessment for preclinical Alzheimer's disease. *Alzheimer's & Dementia: Diagnosis, Assessment & Disease Monitoring, 13*(1), e12217. <https://doi.org/10.1002/dad2.12217>
- O'Keefe, J., & Nadel, L. (1978). *The hippocampus as a cognitive map*. Oxford University Press.
- Olaya, B., Bobak, M., Haro, J. M., & Demakakos, P. (2017). Trajectories of verbal episodic memory in middle-aged and older adults: Evidence from the English Longitudinal Study of Ageing. *Journal of the American Geriatrics Society, 65*(6), 1274–1281. <https://doi.org/10.1111/jgs.14789>
- Old, S. R., & Naveh-Benjamin, M. (2008). Memory for people and their actions: Further evidence for an age-related associative deficit. *Psychology and Aging, 23*(2), 467–472. <https://doi.org/10.1037/0882-7974.23.2.467>
- Oldmeadow, C., Holliday, E. G., McEvoy, M., Scott, R., Kwok, J. B. J., Mather, K., Sachdev, P., Schofield, P., & Attia, J. (2014). Concordance between direct and imputed APOE genotypes using 1000 Genomes data. *Journal of Alzheimer's Disease, 42*(2), 391–393. <https://doi.org/10.3233/JAD-140846>
- Olsen, R. K., Carr, V. A., Daugherty, A. M., La Joie, R., Amaral, R. S. C., Amunts, K., Augustinack, J. C., Bakker, A., Bender, A. R., Berron, D., Boccardi, M., Bocchetta, M., Burggren, A. C., Chakravarty, M. M., Chételat,

- G., de Flores, R., DeKraaker, J., Ding, S.-L., Geerlings, M. I., ... Wisse, L. E. M. (2019). Progress update from the hippocampal subfields group. *Alzheimer's & Dementia: Diagnosis, Assessment & Disease Monitoring*, 11(1), 439–449. <https://doi.org/10.1016/j.dadm.2019.04.001>
- Olson, K. E., O'Brien, M. A., Rogers, W. A., & Charness, N. (2011). Diffusion of technology: Frequency of use for younger and older adults. *Ageing International*, 36(1), 123–145. <https://doi.org/10.1007/s12126-010-9077-9>
- O'Neil, E. B., Cate, A. D., & Köhler, S. (2009). Perirhinal cortex contributes to accuracy in recognition memory and perceptual discriminations. *Journal of Neuroscience*, 29(26), 8329–8334. <https://doi.org/10.1523/JNEUROSCI.0374-09.2009>
- Ortega, A., & Navarrete, G. (2017). Bayesian hypothesis testing: An alternative to null hypothesis significance testing (NHST) in psychology and social sciences. In J. Prieto (Ed.), *Bayesian inference*. IntechOpen. <https://doi.org/10.5772/intechopen.70230>
- Ossenkoppele, R., Jansen, W. J., Rabinovici, G. D., Knol, D. L., van der Flier, W. M., van Berckel, B. N. M., Scheltens, P., Visser, P. J., Amyloid PET Study Group, Verfaillie, S. C. J., Zwan, M. D., Adriaanse, S. M., Lammertsma, A. A., Barkhof, F., Jagust, W. J., Miller, B. L., Rosen, H. J., Landau, S. M., Villemagne, V. L., ... Brooks, D. J. (2015). Prevalence of amyloid PET positivity in dementia syndromes: A meta-analysis. *JAMA*, 313(19), 1939–1949. <https://doi.org/10.1001/jama.2015.4669>
- Oveisgharan, S., Buchman, A. S., Yu, L., Farfel, J., Hachinski, V., Gaiteri, C., De Jager, P. L., Schneider, J. A., & Bennett, D. A. (2018). APOE  $\epsilon 2\epsilon 4$  genotype, incident AD and MCI, cognitive decline, and AD pathology in older adults. *Neurology*, 90(24), e2127–e2134. <https://doi.org/10.1212/WNL.0000000000005677>
- Palmqvist, S., Schöll, M., Strandberg, O., Mattsson, N., Stomrud, E., Zetterberg, H., Blennow, K., Landau, S., Jagust, W., & Hansson, O. (2017). Earliest accumulation of  $\beta$ -amyloid occurs within the default-mode network and concurrently affects brain connectivity. *Nature Communications*, 8, 1214. <https://doi.org/10.1038/s41467-017-01150-x>
- Palop, J. J., & Mucke, L. (2010). Amyloid-beta-induced neuronal dysfunction in Alzheimer's disease: From synapses toward neural networks. *Nature Neuroscience*, 13(7), 812–818. <https://doi.org/10.1038/nn.2583>

- Panesar, S. S., Yeh, F.-C., Jacquesson, T., Hula, W., & Fernandez-Miranda, J. C. (2018). A quantitative tractography study into the connectivity, segmentation and laterality of the human inferior longitudinal fasciculus. *Frontiers in Neuroanatomy*, *12*, 47. <https://doi.org/10.3389/fnana.2018.00047>
- Pardoe, H. R., Kucharsky Hiess, R., & Kuzniecky, R. (2016). Motion and morphometry in clinical and nonclinical populations. *NeuroImage*, *135*, 177–185. <https://doi.org/10.1016/j.neuroimage.2016.05.005>
- Parizkova, M., Kalinova, J., Vyhnalek, M., Hort, J., Wiener, J., & Laczó, J. (2020). Virtual navigation and scene exploration in early Alzheimer's disease. *Alzheimer's & Dementia*, *16*(S6), e043878. <https://doi.org/10.1002/alz.043878>
- Park, D. C., & Reuter-Lorenz, P. (2009). The adaptive brain: Aging and neurocognitive scaffolding. *Annual Review of Psychology*, *60*, 173–196. <https://doi.org/10.1146/annurev.psych.59.103006.093656>
- Park, H., Kennedy, K. M., Rodrigue, K. M., Hebrank, A., & Park, D. C. (2013). An fMRI study of episodic encoding across the lifespan: Changes in subsequent memory effects are evident by middle-age. *Neuropsychologia*, *51*(3), 448–456. <https://doi.org/10.1016/j.neuropsychologia.2012.11.025>
- Park, H.-J., Friston, K. J., Pae, C., Park, B., & Razi, A. (2018). Dynamic effective connectivity in resting state fMRI. *NeuroImage*, *180*, 594–608. <https://doi.org/10.1016/j.neuroimage.2017.11.033>
- Park, H.-J., Westin, C.-F., Kubicki, M., Maier, S. E., Niznikiewicz, M., Baer, A., Frumin, M., Kikinis, R., Jolesz, F. A., McCarley, R. W., & Shenton, M. E. (2004). White matter hemisphere asymmetries in healthy subjects and in schizophrenia: A diffusion tensor MRI study. *NeuroImage*, *23*(1), 213–223. <https://doi.org/10.1016/j.neuroimage.2004.04.036>
- Parker, A., & Gaffan, D. (1997). Mamillary body lesions in monkeys impair object-in-place memory: Functional unity of the fornix-mamillary system. *Journal of Cognitive Neuroscience*, *9*(4), 512–521. <https://doi.org/10.1162/jocn.1997.9.4.512>
- Parker, A., & Gaffan, D. (1998). Interaction of frontal and perirhinal cortices in visual object recognition memory in monkeys. *European Journal of Neuroscience*, *10*(10), 3044–3057. <https://doi.org/10.1046/j.1460-9568.1998.00306.x>

- Parker, G. D., Rosin, P. L., & Marshall, D. (2012). *Automated segmentation of diffusion weighted MRI tractography*. AVA / BMVA Meeting on Biological and Computer Vision, Spring (AGM) Meeting, Cambridge, United Kingdom.
- Parker, G. D., Marshall, D., Rosin, P. L., Drage, N., Richmond, S., & Jones, D. K. (2013). A pitfall in the reconstruction of fibre ODFs using spherical deconvolution of diffusion MRI data. *NeuroImage*, *65*, 433–448. <https://doi.org/10.1016/j.neuroimage.2012.10.022>
- Parker, G. J. M. (2010). Probabilistic fiber tracking. In D. K. Jones (Ed.), *Diffusion MRI: Theory, methods, and applications* (pp. 396–408). Oxford University Press. <https://oxfordmedicine.com/view/10.1093/med/9780195369779.001.0001/med-9780195369779-chapter-023>
- Passell, E., Strong, R. W., Rutter, L. A., Kim, H., Scheuer, L., Martini, P., Grinspoon, L., & Germine, L. (2021). Cognitive test scores vary with choice of personal digital device. *Behavior Research Methods*. <https://doi.org/10.3758/s13428-021-01597-3>
- Passingham, R. E., & Wise, S. P. (2012). *The neurobiology of the prefrontal cortex: Anatomy, evolution, and the origin of insight*. Oxford University Press.
- Pasternak, O., Sochen, N., Gur, Y., Intrator, N., & Assaf, Y. (2009). Free water elimination and mapping from diffusion MRI. *Magnetic Resonance in Medicine*, *62*(3), 717–730. <https://doi.org/10.1002/mrm.22055>
- Payami, H., Montee, K. R., Kaye, J. A., Bird, T. D., Yu, C.-E., Wijsman, E. M., & Schellenberg, G. D. (1994). Alzheimer's disease, apolipoprotein E4, and gender. *JAMA*, *271*(17), 1316–1317. <https://doi.org/10.1001/jama.1994.03510410028015>
- Payami, H., Zarepari, S., Montee, K. R., Sexton, G. J., Kaye, J. A., Bird, T. D., Yu, C. E., Wijsman, E. M., Heston, L. L., Litt, M., & Schellenberg, G. D. (1996). Gender difference in apolipoprotein E-associated risk for familial Alzheimer disease: A possible clue to the higher incidence of Alzheimer disease in women. *American Journal of Human Genetics*, *58*(4), 803–811.
- Pengas, G., Hodges, J. R., Watson, P., & Nestor, P. J. (2010). Focal posterior cingulate atrophy in incipient Alzheimer's disease. *Neurobiology of Aging*, *31*(1), 25–33. <https://doi.org/10.1016/j.neurobiolaging.2008.03.014>
- Pengas, G., Patterson, K., Arnold, R. J., Bird, C. M., Burgess, N., & Nestor, P. J. (2010). Lost and found: Bespoke memory testing for Alzheimer's disease

- and semantic dementia. *Journal of Alzheimer's Disease*, 21(4), 1347–1365. <https://doi.org/10.3233/JAD-2010-100654>
- Pereira, J. B., Janelidze, S., Ossenkoppele, R., Kvartsberg, H., Brinkmalm, A., Mattsson-Carlgen, N., Stomrud, E., Smith, R., Zetterberg, H., Blennow, K., & Hansson, O. (2021). Untangling the association of amyloid- $\beta$  and tau with synaptic and axonal loss in Alzheimer's disease. *Brain*, 144(1), 310–324. <https://doi.org/10.1093/brain/awaa395>
- Persson, J., Pudas, S., Lind, J., Kauppi, K., Nilsson, L.-G., & Nyberg, L. (2012). Longitudinal structure-function correlates in elderly reveal MTL dysfunction with cognitive decline. *Cerebral Cortex*, 22(10), 2297–2304. <https://doi.org/10.1093/cercor/bhr306>
- Persson, J., Spreng, R. N., Turner, G., Herlitz, A., Morell, A., Stening, E., Wahlund, L.-O., Wikström, J., & Söderlund, H. (2014). Sex differences in volume and structural covariance of the anterior and posterior hippocampus. *NeuroImage*, 99, 215–225. <https://doi.org/10.1016/j.neuroimage.2014.05.038>
- Pertesi, S., Coughlan, G., Puthusseryppady, V., Morris, E., & Hornberger, M. (2019). Menopause, cognition and dementia – A review. *Post Reproductive Health*, 25(4), 200–206. <https://doi.org/10.1177/2053369119883485>
- Petersen, S. E., & Sporns, O. (2015). Brain networks and cognitive architectures. *Neuron*, 88(1), 207–219. <https://doi.org/10.1016/j.neuron.2015.09.027>
- Pfefferbaum, A., & Sullivan, E. V. (2003). Increased brain white matter diffusivity in normal adult aging: Relationship to anisotropy and partial voluming. *Magnetic Resonance in Medicine*, 49(5), 953–961. <https://doi.org/10.1002/mrm.10452>
- Plachti, A., Eickhoff, S. B., Hoffstaedter, F., Patil, K. R., Laird, A. R., Fox, P. T., Amunts, K., & Genon, S. (2019). Multimodal parcellations and extensive behavioral profiling tackling the hippocampus gradient. *Cerebral Cortex*, 29(11), 4595–4612. <https://doi.org/10.1093/cercor/bhy336>
- Plachti, A., Kharabian, S., Eickhoff, S. B., Maleki Balajoo, S., Hoffstaedter, F., Varikuti, D. P., Jockwitz, C., Caspers, S., Amunts, K., & Genon, S. (2020). Hippocampus co-atrophy pattern in dementia deviates from covariance patterns across the lifespan. *Brain*, 143(9), 2788–2802. <https://doi.org/10.1093/brain/awaa222>

- Pooler, A. M., Polydoro, M., Maury, E. A., Nicholls, S. B., Reddy, S. M., Wegmann, S., William, C., Saqran, L., Cagsal-Getkin, O., Pitstick, R., Beier, D. R., Carlson, G. A., Spires-Jones, T. L., & Hyman, B. T. (2015). Amyloid accelerates tau propagation and toxicity in a model of early Alzheimer's disease. *Acta Neuropathologica Communications*, 3, 14. <https://doi.org/10.1186/s40478-015-0199-x>
- Postans, M., Hodgetts, C. J., Mundy, M. E., Jones, D. K., Lawrence, A. D., & Graham, K. S. (2014). Interindividual variation in fornix microstructure and macrostructure is related to visual discrimination accuracy for scenes but not faces. *Journal of Neuroscience*, 34(36), 12121–12126. <https://doi.org/10.1523/JNEUROSCI.0026-14.2014>
- Powell, J. L., Parkes, L., Kemp, G. J., Sluming, V., Barrick, T. R., & García-Fiñana, M. (2012). The effect of sex and handedness on white matter anisotropy: A diffusion tensor magnetic resonance imaging study. *Neuroscience*, 207, 227–242. <https://doi.org/10.1016/j.neuroscience.2012.01.016>
- Power, J. D., Cohen, A. L., Nelson, S. M., Wig, G. S., Barnes, K. A., Church, J. A., Vogel, A. C., Laumann, T. O., Miezin, F. M., Schlaggar, B. L., & Petersen, S. E. (2011). Functional network organization of the human brain. *Neuron*, 72(4), 665–678. <https://doi.org/10.1016/j.neuron.2011.09.006>
- Quintana, D. S., & Williams, D. R. (2018). Bayesian alternatives for common null-hypothesis significance tests in psychiatry: A non-technical guide using JASP. *BMC Psychiatry*, 18, 178. <https://doi.org/10.1186/s12888-018-1761-4>
- R Core Team. (2019). *R: A language and environment for statistical computing* (Version 3.6.0) [Computer software]. <https://www.R-project.org/>
- Raamana, P. R., & Strother, S. C. (2018). graynet: Single-subject morphometric networks for neuroscience connectivity applications. *Journal of Open Source Software*, 3(30), 924. <https://doi.org/10.21105/joss.00924>
- Raamana, P. R., & Strother, S. C. (2020). Does size matter? The relationship between predictive power of single-subject morphometric networks to spatial scale and edge weight. *Brain Structure and Function*, 225(8), 2475–2493. <https://doi.org/10.1007/s00429-020-02136-0>
- Radmanesh, F., Devan, W. J., Anderson, C. D., Rosand, J., Falcone, G. J., & for the Alzheimer's Disease Neuroimaging Initiative. (2014). Accuracy of imputation to infer unobserved APOE epsilon alleles in genome-wide



- genotyping data. *European Journal of Human Genetics*, 22(10), 1239–1242. <https://doi.org/10.1038/ejhg.2013.308>
- Raichle, M. E. (2015). The brain's default mode network. *Annual Review of Neuroscience*, 38, 433–447. <https://doi.org/10.1146/annurev-neuro-071013-014030>
- Rall, S. C., Weisgraber, K. H., & Mahley, R. W. (1982). Human apolipoprotein E. The complete amino acid sequence. *Journal of Biological Chemistry*, 257(8), 4171–4178. [https://doi.org/10.1016/S0021-9258\(18\)34702-1](https://doi.org/10.1016/S0021-9258(18)34702-1)
- Ranganath, C. (2019). Time, memory, and the legacy of Howard Eichenbaum. *Hippocampus*, 29(3), 146–161. <https://doi.org/10.1002/hipo.23007>
- Ranganath, C., & Ritchey, M. (2012). Two cortical systems for memory-guided behaviour. *Nature Reviews Neuroscience*, 13(10), 713–726. <https://doi.org/10.1038/nrn3338>
- Razi, A., Kahan, J., Rees, G., & Friston, K. J. (2015). Construct validation of a DCM for resting state fMRI. *NeuroImage*, 106, 1–14. <https://doi.org/10.1016/j.neuroimage.2014.11.027>
- Reagh, Z. M., Ho, H. D., Leal, S. L., Noche, J. A., Chun, A., Murray, E. A., & Yassa, M. A. (2016). Greater loss of object than spatial mnemonic discrimination in aged adults. *Hippocampus*, 26(4), 417–422. <https://doi.org/10.1002/hipo.22562>
- Reagh, Z. M., Noche, J. A., Tustison, N. J., Delisle, D., Murray, E. A., & Yassa, M. A. (2018). Functional imbalance of anterolateral entorhinal cortex and hippocampal dentate/CA3 underlies age-related object pattern separation deficits. *Neuron*, 97(5), 1187–1198.e4. <https://doi.org/10.1016/j.neuron.2018.01.039>
- Reagh, Z. M., Roberts, J. M., Ly, M., DiProspero, N., Murray, E. A., & Yassa, M. A. (2014). Spatial discrimination deficits as a function of mnemonic interference in aged adults with and without memory impairment. *Hippocampus*, 24(3), 303–314. <https://doi.org/10.1002/hipo.22224>
- Reas, E. T., Laughlin, G. A., Bergstrom, J., Kritz-Silverstein, D., Barrett-Connor, E., & McEvoy, L. K. (2019). Effects of APOE on cognitive aging in community-dwelling older adults. *Neuropsychology*, 33(3), 406–416. <https://doi.org/10.1037/neu0000501>

- Reid, A. T., Lewis, J., Bezgin, G., Khundrakpam, B., Eickhoff, S. B., McIntosh, A. R., Bellec, P., & Evans, A. C. (2016). A cross-modal, cross-species comparison of connectivity measures in the primate brain. *NeuroImage*, *125*, 311–331. <https://doi.org/10.1016/j.neuroimage.2015.10.057>
- Reiman, E. M., Arboleda-Velasquez, J. F., Quiroz, Y. T., Huentelman, M. J., Beach, T. G., Caselli, R. J., Chen, Y., Su, Y., Myers, A. J., Hardy, J., Paul Vonsattel, J., Younkin, S. G., Bennett, D. A., De Jager, P. L., Larson, E. B., Crane, P. K., Keene, C. D., Kamboh, M. I., Kofler, J. K., ... Jun, G. R. (2020). Exceptionally low likelihood of Alzheimer's dementia in APOE2 homozygotes from a 5,000-person neuropathological study. *Nature Communications*, *11*, 667. <https://doi.org/10.1038/s41467-019-14279-8>
- Reiman, E. M., Caselli, R. J., Chen, K., Alexander, G. E., Bandy, D., & Frost, J. (2001). Declining brain activity in cognitively normal apolipoprotein E epsilon 4 heterozygotes: A foundation for using positron emission tomography to efficiently test treatments to prevent Alzheimer's disease. *Proceedings of the National Academy of Sciences*, *98*(6), 3334–3339. <https://doi.org/10.1073/pnas.061509598>
- Renoult, L., & Rugg, M. D. (2020). An historical perspective on Endel Tulving's episodic-semantic distinction. *Neuropsychologia*, *139*, 107366. <https://doi.org/10.1016/j.neuropsychologia.2020.107366>
- Reuter, M., Tisdall, M. D., Qureshi, A., Buckner, R. L., van der Kouwe, A. J. W., & Fischl, B. (2015). Head motion during MRI acquisition reduces gray matter volume and thickness estimates. *NeuroImage*, *107*, 107–115. <https://doi.org/10.1016/j.neuroimage.2014.12.006>
- Rheault, F., Benedictis, A. D., Daducci, A., Maffei, C., Tax, C. M. W., Romascano, D., Caverzasi, E., Morency, F. C., Corrivetti, F., Pestilli, F., Girard, G., Theaud, G., Zemmoura, I., Hau, J., Glavin, K., Jordan, K. M., Pomiecko, K., Chamberland, M., Barakovic, M., ... Descoteaux, M. (2020). Tractostorm: The what, why, and how of tractography dissection reproducibility. *Human Brain Mapping*, *41*(7), 1859–1874. <https://doi.org/10.1002/hbm.24917>
- Richard, E., & Brayne, C. (2014). Mild cognitive impairment—Not always what it seems. *Nature Reviews Neurology*, *10*(3), 130–131. <https://doi.org/10.1038/nrneurol.2014.23>
- Riedel, B. C., Thompson, P. M., & Brinton, R. D. (2016). Age, APOE and sex: Triad of risk of Alzheimer's disease. *Journal of Steroid Biochemistry and*

- Molecular Biology*, 160, 134–147.  
<https://doi.org/10.1016/j.jsbmb.2016.03.012>
- Rippon, G., Eliot, L., Genon, S., & Joel, D. (2021). How hype and hyperbole distort the neuroscience of sex differences. *PLOS Biology*, 19(5), e3001253. <https://doi.org/10.1371/journal.pbio.3001253>
- Rippon, G., Jordan-Young, R., Kaiser, A., & Fine, C. (2014). Recommendations for sex/gender neuroimaging research: Key principles and implications for research design, analysis, and interpretation. *Frontiers in Human Neuroscience*, 8, 650. <https://doi.org/10.3389/fnhum.2014.00650>
- Ritchey, M., Libby, L. A., & Ranganath, C. (2015). Cortico-hippocampal systems involved in memory and cognition: The PMAT framework. In S. O'Mara & M. Tsanov (Eds.), *Progress in brain research* (Vol. 219, pp. 45–64). Elsevier. <https://doi.org/10.1016/bs.pbr.2015.04.001>
- Ritchey, M., Yonelinas, A. P., & Ranganath, C. (2014). Functional connectivity relationships predict similarities in task activation and pattern information during associative memory encoding. *Journal of Cognitive Neuroscience*, 26(5), 1085–1099. [https://doi.org/10.1162/jocn\\_a\\_00533](https://doi.org/10.1162/jocn_a_00533)
- Roberts, R. O., Aakre, J. A., Kremers, W. K., Vassilaki, M., Knopman, D. S., Mielke, M. M., Alhurani, R., Geda, Y. E., Machulda, M. M., Coloma, P., Schauble, B., Lowe, V. J., Jack, C. R., & Petersen, R. C. (2018). Prevalence and outcomes of amyloid positivity among persons without dementia in a longitudinal, population-based setting. *JAMA Neurology*, 75(8), 970–979. <https://doi.org/10.1001/jamaneurol.2018.0629>
- Robin, J. (2018). Spatial scaffold effects in event memory and imagination. *WIREs Cognitive Science*, 9(4), e1462. <https://doi.org/10.1002/wcs.1462>
- Robin, J., & Moscovitch, M. (2017). Familiar real-world spatial cues provide memory benefits in older and younger adults. *Psychology and Aging*, 32(3), 210–219. <https://doi.org/10.1037/pag0000162>
- Robin, J., & Olsen, R. K. (2019). Scenes facilitate associative memory and integration. *Learning & Memory*, 26(7), 252–261. <https://doi.org/10.1101/lm.049486.119>
- Robin, J., Rai, Y., Valli, M., & Olsen, R. K. (2019). Category specificity in the medial temporal lobe: A systematic review. *Hippocampus*, 29(4), 313–339. <https://doi.org/10.1002/hipo.23024>

- Robin, J., Wynn, J., & Moscovitch, M. (2016). The spatial scaffold: The effects of spatial context on memory for events. *Journal of Experimental Psychology: Learning, Memory, and Cognition*, *42*(2), 308–315. <https://doi.org/10.1037/xlm0000167>
- Rodrigue, K. M., Kennedy, K. M., Devous, M. D., Rieck, J. R., Hebrank, A. C., Diaz-Arrastia, R., Mathews, D., & Park, D. C. (2012).  $\beta$ -Amyloid burden in healthy aging: Regional distribution and cognitive consequences. *Neurology*, *78*(6), 387–395. <https://doi.org/10.1212/WNL.0b013e318245d295>
- Romero-Garcia, R., Whitaker, K. J., Váša, F., Seidlitz, J., Shinn, M., Fonagy, P., Dolan, R. J., Jones, P. B., Goodyer, I. M., Bullmore, E. T., & Vértes, P. E. (2018). Structural covariance networks are coupled to expression of genes enriched in supragranular layers of the human cortex. *NeuroImage*, *171*, 256–267. <https://doi.org/10.1016/j.neuroimage.2017.12.060>
- Rönnlund, M., Nyberg, L., Backman, L., & Nilsson, L.-G. (2005). Stability, growth, and decline in adult life span development of declarative memory: Cross-sectional and longitudinal data from a population-based study. *Psychology and Aging*, *20*(1), 3–18. <https://doi.org/10.1037/0882-7974.20.1.3>
- Rosen, V. M., Sunderland, T., Levy, J., Harwell, A., McGee, L., Hammond, C., Bhupali, D., Putnam, K., Bergeson, J., & Lefkowitz, C. (2005). Apolipoprotein E and category fluency: Evidence for reduced semantic access in healthy normal controls at risk for developing Alzheimer's disease. *Neuropsychologia*, *43*(4), 647–658. <https://doi.org/10.1016/j.neuropsychologia.2004.06.022>
- Rosenbaum, R. S., Gilboa, A., & Moscovitch, M. (2014). Case studies continue to illuminate the cognitive neuroscience of memory. *Annals of the New York Academy of Sciences*, *1316*(1), 105–133. <https://doi.org/10.1111/nyas.12467>
- RStudio Team. (2020). *RStudio: Integrated development environment for R* (Version 1.3.1093) [Computer software]. <http://www.rstudio.com/>
- Rubin, D. C., Deffler, S. A., & Umanath, S. (2019). Scenes enable a sense of reliving: Implications for autobiographical memory. *Cognition*, *183*, 44–56. <https://doi.org/10.1016/j.cognition.2018.10.024>
- Rubin, D. C., & Umanath, S. (2015). Event memory: A theory of memory for laboratory, autobiographical, and fictional events. *Psychological Review*, *122*(1), 1–23. <https://doi.org/10.1037/a0037907>

- Rugg, M. D., & Vilberg, K. L. (2013). Brain networks underlying episodic memory retrieval. *Current Opinion in Neurobiology*, *23*(2), 255–260. <https://doi.org/10.1016/j.conb.2012.11.005>
- Ruiz, N. A., Meager, M. R., Agarwal, S., & Aly, M. (2020). The medial temporal lobe is critical for spatial relational perception. *Journal of Cognitive Neuroscience*, *32*(9), 1780–1795. [https://doi.org/10.1162/jocn\\_a\\_01583](https://doi.org/10.1162/jocn_a_01583)
- Ryan, J. D., & Shen, K. (2020). The eyes are a window into memory. *Current Opinion in Behavioral Sciences*, *32*, 1–6. <https://doi.org/10.1016/j.cobeha.2019.12.014>
- Ryan, L., Cardoza, J. A., Barense, M. D., Kawa, K. H., Walletin-Flores, J., Arnold, W. T., & Alexander, G. E. (2012). Age-related impairment in a complex object discrimination task that engages perirhinal cortex. *Hippocampus*, *22*(10), 1978–1989. <https://doi.org/10.1002/hipo.22069>
- Sabuncu, M. R., Buckner, R. L., Smoller, J. W., Lee, P. H., Fischl, B., Sperling, R. A., & for the Alzheimer’s Disease Neuroimaging Initiative. (2012). The association between a polygenic Alzheimer score and cortical thickness in clinically normal subjects. *Cerebral Cortex*, *22*(11), 2653–2661. <https://doi.org/10.1093/cercor/bhr348>
- Safieh, M., Korczyn, A. D., & Michaelson, D. M. (2019). ApoE4: An emerging therapeutic target for Alzheimer’s disease. *BMC Medicine*, *17*, 64. <https://doi.org/10.1186/s12916-019-1299-4>
- Saksida, L. M., & Bussey, T. J. (2010). The representational-hierarchical view of amnesia: Translation from animal to human. *Neuropsychologia*, *48*(8), 2370–2384. <https://doi.org/10.1016/j.neuropsychologia.2010.02.026>
- Salami, A., Pudas, S., & Nyberg, L. (2014). Elevated hippocampal resting-state connectivity underlies deficient neurocognitive function in aging. *Proceedings of the National Academy of Sciences*, *111*(49), 17654–17659. <https://doi.org/10.1073/pnas.1410233111>
- Saleeba, C., Dempsey, B., Le, S., Goodchild, A., & McMullan, S. (2019). A student’s guide to neural circuit tracing. *Frontiers in Neuroscience*, *13*, 897. <https://doi.org/10.3389/fnins.2019.00897>
- Salminen, L. E., Conturo, T. E., Bolzenius, J. D., Cabeen, R. P., Akbudak, E., & Paul, R. H. (2016). Reducing CSF partial volume effects to enhance diffusion tensor imaging metrics of brain microstructure. *Technology & Innovation*, *18*(1), 5–20. <https://doi.org/10.21300/18.1.2016.5>

- Salthouse, T. A. (1996). The processing-speed theory of adult age differences in cognition. *Psychological Review*, 103(3), 403–428. <https://doi.org.abc.cardiff.ac.uk/10.1037/0033-295X.103.3.403>
- Salthouse, T. A. (2003). Memory aging from 18 to 80. *Alzheimer Disease & Associated Disorders*, 17(3), 162–167. <https://doi.org/10.1097/00002093-200307000-00008>
- Salthouse, T. A. (2009). When does age-related cognitive decline begin? *Neurobiology of Aging*, 30(4), 507–514. <https://doi.org/10.1016/j.neurobiolaging.2008.09.023>
- Salthouse, T. A. (2014). Selectivity of attrition in longitudinal studies of cognitive functioning. *The Journals of Gerontology: Series B*, 69(4), 567–574. <https://doi.org/10.1093/geronb/gbt046>
- Salthouse, T. A. (2019). Trajectories of normal cognitive aging. *Psychology and Aging*, 34(1), 17–24. <https://doi.org/10.1037/pag0000288>
- Salvadó, G., Grothe, M. J., Groot, C., Moscoso, A., Schöll, M., Gispert, J. D., Ossenkoppele, R., & for the Alzheimer's Disease Neuroimaging Initiative. (2021). Differential associations of APOE- $\epsilon$ 2 and APOE- $\epsilon$ 4 alleles with PET-measured amyloid- $\beta$  and tau deposition in older individuals without dementia. *European Journal of Nuclear Medicine and Molecular Imaging*, 48(7), 2212–2224. <https://doi.org/10.1007/s00259-021-05192-8>
- Salvato, G. (2015). Does apolipoprotein E genotype influence cognition in middle-aged individuals? *Current Opinion in Neurology*, 28(6), 612–617. <https://doi.org/10.1097/WCO.0000000000000262>
- Sando, S. B., Melquist, S., Cannon, A., Hutton, M. L., Sletvold, O., Saltvedt, I., White, L. R., Lydersen, S., & Aasly, J. O. (2008). APOE  $\epsilon$ 4 lowers age at onset and is a high risk factor for Alzheimer's disease; A case control study from central Norway. *BMC Neurology*, 8, 9. <https://doi.org/10.1186/1471-2377-8-9>
- Saunders, A. M., Strittmatter, W. J., Schmechel, D., George-Hyslop, P. H. S., Pericak-Vance, M. A., Joo, S. H., Rosi, B. L., Gusella, J. F., Lachlan, D. R. C.-M., Alberts, M. J., Hulette, C., Crain, B., Goldgaber, D., & Roses, A. D. (1993). Association of apolipoprotein E allele  $\epsilon$ 4 with late-onset familial and sporadic Alzheimer's disease. *Neurology*, 43(8), 1467–1472. <https://doi.org.abc.cardiff.ac.uk/10.1212/WNL.43.8.1467>

- Savalia, N. K., Agres, P. F., Chan, M. Y., Feczko, E. J., Kennedy, K. M., & Wig, G. S. (2016). Motion-related artifacts in structural brain images revealed with independent estimates of in-scanner head motion. *Human Brain Mapping, 38*(1), 472–492. <https://doi.org/10.1002/hbm.23397>
- Schacter, D. L., Benoit, R. G., & Szpunar, K. K. (2017). Episodic future thinking: Mechanisms and functions. *Current Opinion in Behavioral Sciences, 17*, 41–50. <https://doi.org/10.1016/j.cobeha.2017.06.002>
- Schafer, M., & Schiller, D. (2018). Navigating social space. *Neuron, 100*(2), 476–489. <https://doi.org/10.1016/j.neuron.2018.10.006>
- Scheltens, N. M. E., Tijms, B. M., Koene, T., Barkhof, F., Teunissen, C. E., Wolfsgruber, S., Wagner, M., Kornhuber, J., Peters, O., Cohn-Sheehy, B. I., Rabinovici, G. D., Miller, B. L., Kramer, J. H., Scheltens, P., & van der Flier, W. M. (2017). Cognitive subtypes of probable Alzheimer's disease robustly identified in four cohorts. *Alzheimer's & Dementia, 13*(11), 1226–1236. <https://doi.org/10.1016/j.jalz.2017.03.002>
- Scherf, K. S., Behrmann, M., & Dahl, R. E. (2012). Facing changes and changing faces in adolescence: A new model for investigating adolescent-specific interactions between pubertal, brain and behavioral development. *Developmental Cognitive Neuroscience, 2*(2), 199–219. <https://doi.org/10.1016/j.dcn.2011.07.016>
- Schilder, B. M., Petry, H. M., & Hof, P. R. (2020). Evolutionary shifts dramatically reorganized the human hippocampal complex. *Journal of Comparative Neurology, 528*(17), 3143–3170. <https://doi.org/10.1002/cne.24822>
- Schilling, K. G., Nath, V., Hansen, C., Parvathaneni, P., Blaber, J., Gao, Y., Neher, P., Aydogan, D. B., Shi, Y., Ocampo-Pineda, M., Schiavi, S., Daducci, A., Girard, G., Barakovic, M., Rafael-Patino, J., Romascano, D., Renonnet, G., Pizzolato, M., Bates, A., ... Landman, B. A. (2019). Limits to anatomical accuracy of diffusion tractography using modern approaches. *NeuroImage, 185*, 1–11. <https://doi.org/10.1016/j.neuroimage.2018.10.029>
- Schilling, K. G., Petit, L., Rheault, F., Remedios, S., Pierpaoli, C., Anderson, A. W., Landman, B. A., & Descoteaux, M. (2020). Brain connections derived from diffusion MRI tractography can be highly anatomically accurate-If we know where white matter pathways start, where they end, and where they do not go. *Brain Structure and Function, 225*(8), 2387–2402. <https://doi.org/10.1007/s00429-020-02129-z>

- Schilling, K. G., Rheault, F., Petit, L., Hansen, C. B., Nath, V., Yeh, F.-C., Girard, G., Barakovic, M., Rafael-Patino, J., Yu, T., Fischi-Gomez, E., Pizzolato, M., Ocampo-Pineda, M., Schiavi, S., Canales-Rodríguez, E. J., Daducci, A., Granziera, C., Innocenti, G., Thiran, J.-P., ... Descoteaux, M. (2021). Tractography dissection variability: What happens when 42 groups dissect 14 white matter bundles on the same dataset? *NeuroImage*, 243, 118502. <https://doi.org/10.1016/j.neuroimage.2021.118502>
- Schultz, A. P., Chhatwal, J. P., Hedden, T., Mormino, E. C., Hanseeuw, B. J., Sepulcre, J., Huijbers, W., LaPoint, M., Buckley, R. F., Johnson, K. A., & Sperling, R. A. (2017). Phases of hyperconnectivity and hypoconnectivity in the default mode and salience networks track with amyloid and tau in clinically normal individuals. *Journal of Neuroscience*, 37(16), 4323–4331. <https://doi.org/10.1523/JNEUROSCI.3263-16.2017>
- Scoville, W. B. (1954). The limbic lobe in man. *Journal of Neurosurgery*, 11(1), 64–66. <https://doi.org/10.3171/jns.1954.11.1.0064>
- Scoville, W. B., & Milner, B. (1957). Loss of recent memory after bilateral hippocampal lesions. *Journal of Neurology, Neurosurgery, and Psychiatry*, 20(1), 11–21. <https://doi-org.abc.cardiff.ac.uk/10.1136/jnnp.20.1.11>
- Sebastiani, P., Gurinovich, A., Nygaard, M., Sasaki, T., Sweigart, B., Bae, H., Andersen, S. L., Villa, F., Atzmon, G., Christensen, K., Arai, Y., Barzilai, N., Puca, A., Christiansen, L., Hirose, N., & Perls, T. T. (2019). APOE alleles and extreme human longevity. *The Journals of Gerontology: Series A*, 74(1), 44–51. <https://doi.org/10.1093/gerona/gly174>
- Seehaus, A. K., Roebroek, A., Chiry, O., Kim, D.-S., Ronen, I., Bratzke, H., Goebel, R., & Galuske, R. A. W. (2013). Histological validation of DW-MRI tractography in human postmortem tissue. *Cerebral Cortex*, 23(2), 442–450. <https://doi.org/10.1093/cercor/bhs036>
- Seeley, W. W. (2017). Mapping neurodegenerative disease onset and progression. *Cold Spring Harbor Perspectives in Biology*, 9(8), a023622. <https://doi.org/10.1101/cshperspect.a023622>
- Seeley, W. W., Crawford, R. K., Zhou, J., Miller, B. L., & Greicius, M. D. (2009). Neurodegenerative diseases target large-scale human brain networks. *Neuron*, 62(1), 42–52. <https://doi.org/10.1016/j.neuron.2009.03.024>
- Seidlitz, J., Váša, F., Shinn, M., Romero-Garcia, R., Whitaker, K. J., Vértes, P. E., Wagstyl, K., Kirkpatrick Reardon, P., Clasen, L., Liu, S., Messinger, A., Leopold, D. A., Fonagy, P., Dolan, R. J., Jones, P. B., Goodyer, I. M.,



- Raznahan, A., & Bullmore, E. T. (2018). Morphometric similarity networks detect microscale cortical organization and predict inter-individual cognitive variation. *Neuron*, *97*(1), 231–247. <https://doi.org/10.1016/j.neuron.2017.11.039>
- Selker, R. (2017). *medmod: Simple mediation and moderation analysis* (Version 1.0.0) [Computer software]. <https://CRAN.R-project.org/package=medmod>
- Selkoe, D. J. (1991). The molecular pathology of Alzheimer's disease. *Neuron*, *6*(4), 487–498. [https://doi.org/10.1016/0896-6273\(91\)90052-2](https://doi.org/10.1016/0896-6273(91)90052-2)
- Selkoe, D. J., & Hardy, J. (2016). The amyloid hypothesis of Alzheimer's disease at 25 years. *EMBO Molecular Medicine*, *8*(6), 595–608. <https://doi.org/10.15252/emmm.201606210>
- Serrano-Pozo, A., Das, S., & Hyman, B. T. (2021). APOE and Alzheimer's disease: Advances in genetics, pathophysiology, and therapeutic approaches. *The Lancet Neurology*, *20*(1), 68–80. [https://doi.org/10.1016/S1474-4422\(20\)30412-9](https://doi.org/10.1016/S1474-4422(20)30412-9)
- Serrano-Pozo, A., Frosch, M. P., Masliah, E., & Hyman, B. T. (2011). Neuropathological alterations in Alzheimer disease. *Cold Spring Harbor Perspectives in Medicine*, *1*(a006189). <https://doi.org/10.1101/cshperspect.a006189>
- Sharda, M., Khundrakpam, B. S., Evans, A. C., & Singh, N. C. (2016). Disruption of structural covariance networks for language in autism is modulated by verbal ability. *Brain Structure and Function*, *221*(2), 1017–1032. <https://doi.org/10.1007/s00429-014-0953-z>
- Sheldon, S., Farb, N., Palombo, D. J., & Levine, B. (2016). Intrinsic medial temporal lobe connectivity relates to individual differences in episodic autobiographical remembering. *Cortex*, *74*, 206–216. <https://doi.org/10.1016/j.cortex.2015.11.005>
- Shine, J. P., Hodgetts, C. J., Postans, M., Lawrence, A. D., & Graham, K. S. (2015). APOE-ε4 selectively modulates posteromedial cortex activity during scene perception and short-term memory in young healthy adults. *Scientific Reports*, *5*, 16322. <https://doi.org/10.1038/srep16322>
- Shinohara, M., Kanekiyo, T., Tachibana, M., Kurti, A., Shinohara, M., Fu, Y., Zhao, J., Han, X., Sullivan, P. M., Rebeck, G. W., Fryer, J. D., Heckman, M.

- G., & Bu, G. (2020). APOE2 is associated with longevity independent of Alzheimer's disease. *eLife*, *9*, e62199. <https://doi.org/10.7554/eLife.62199>
- Shrager, Y., Gold, J. J., Hopkins, R. O., & Squire, L. R. (2006). Intact visual perception in memory-impaired patients with medial temporal lobe lesions. *Journal of Neuroscience*, *26*(8), 2235–2240. <https://doi.org/10.1523/JNEUROSCI.4792-05.2006>
- Simonsohn, U. (2015). Small telescopes: Detectability and the evaluation of replication results. *Psychological Science*, *26*(5), 559–569. <https://doi.org/10.1177/0956797614567341>
- Sinclair, L. I., Pleydell-Pearce, C. W., & Day, I. N. M. (2017). Possible positive effect of the APOE  $\epsilon$ 2 allele on cognition in early to mid-adult life. *Neurobiology of Learning and Memory*, *146*, 37–46. <https://doi.org/10.1016/j.nlm.2017.10.008>
- Sirugo, G., Williams, S. M., & Tishkoff, S. A. (2019). The missing diversity in human genetic studies. *Cell*, *177*(1), 26–31. <https://doi.org/10.1016/j.cell.2019.02.048>
- Smith, S. M., Jenkinson, M., Johansen-Berg, H., Rueckert, D., Nichols, T. E., Mackay, C. E., Watkins, K. E., Ciccarelli, O., Cader, M. Z., Matthews, P. M., & Behrens, T. E. J. (2006). Tract-based spatial statistics: Voxelwise analysis of multi-subject diffusion data. *NeuroImage*, *31*(4), 1487–1505. <https://doi.org/10.1016/j.neuroimage.2006.02.024>
- Smith, S. M., & Nichols, T. E. (2009). Threshold-free cluster enhancement: Addressing problems of smoothing, threshold dependence and localisation in cluster inference. *NeuroImage*, *44*(1), 83–98. <https://doi.org/10.1016/j.neuroimage.2008.03.061>
- Smitha, K., Akhil Raja, K., Arun, K., Rajesh, P., Thomas, B., Kapilamoorthy, T., & Kesavadas, C. (2017). Resting state fMRI: A review on methods in resting state connectivity analysis and resting state networks. *The Neurology Journal*, *30*(4), 305–317. <https://doi.org/10.1177/1971400917697342>
- Snowden, J. S., Stopford, C. L., Julien, C. L., Thompson, J. C., Davidson, Y., Gibbons, L., Pritchard, A., Lendon, C. L., Richardson, A. M., Varma, A., Neary, D., & Mann, D. (2007). Cognitive phenotypes in Alzheimer's disease and genetic risk. *Cortex*, *43*(7), 835–845. [https://doi.org/10.1016/s0010-9452\(08\)70683-x](https://doi.org/10.1016/s0010-9452(08)70683-x)

- Soares, J., Marques, P., Alves, V., & Sousa, N. (2013). A hitchhiker's guide to diffusion tensor imaging. *Frontiers in Neuroscience*, 7, 31. <https://doi.org/10.3389/fnins.2013.00031>
- Son, G., Walther, D. B., & Mack, M. L. (2021). Scene wheels: Measuring perception and memory of real-world scenes with a continuous stimulus space. *bioRxiv*. <https://doi.org/10.1101/2020.10.09.333708>
- Song, J. W., Mitchell, P. D., Kolasinski, J., Ellen Grant, P., Galaburda, A. M., & Takahashi, E. (2015). Asymmetry of white matter pathways in developing human brains. *Cerebral Cortex*, 25(9), 2883–2893. <https://doi.org/10.1093/cercor/bhu084>
- Spaniol, J., Davidson, P. S. R., Kim, A. S. N., Han, H., Moscovitch, M., & Grady, C. L. (2009). Event-related fMRI studies of episodic encoding and retrieval: Meta-analyses using activation likelihood estimation. *Neuropsychologia*, 47(8), 1765–1779. <https://doi.org/10.1016/j.neuropsychologia.2009.02.028>
- Spencer, W. D., & Raz, N. (1995). Differential effects of aging on memory for content and context: A meta-analysis. *Psychology and Aging*, 10(4), 527–539. <https://doi.org/10.1037/0882-7974.10.4.527>
- Sperling, R. A., Laviolette, P. S., O'Keefe, K., O'Brien, J., Rentz, D. M., Pihlajamaki, M., Marshall, G., Hyman, B. T., Selkoe, D. J., Hedden, T., Buckner, R. L., Becker, J. A., & Johnson, K. A. (2009). Amyloid deposition is associated with impaired default network function in older persons without dementia. *Neuron*, 63(2), 178–188. <https://doi.org/10.1016/j.neuron.2009.07.003>
- Spreng, R. N., DuPre, E., Ji, J. L., Yang, G., Diehl, C., Murray, J. D., Pearlson, G. D., & Anticevic, A. (2019). Structural covariance reveals alterations in control and salience network integrity in chronic schizophrenia. *Cerebral Cortex*, 29(12), 5269–5284. <https://doi.org/10.1093/cercor/bhz064>
- Spreng, R. N., & Turner, G. R. (2013). Structural covariance of the default network in healthy and pathological aging. *Journal of Neuroscience*, 33(38), 15226–15234. <https://doi.org/10.1523/JNEUROSCI.2261-13.2013>
- Squire, L. R. (2009). The legacy of Patient H.M. for neuroscience. *Neuron*, 61(1), 6–9. <https://doi.org/10.1016/j.neuron.2008.12.023>

- Squire, L. R., & Zola-Morgan, S. (1991). The medial temporal lobe memory system. *Science*, 253(5026), 1380–1386. <https://doi.org/10.1126/science.1896849>
- Squire, L. R., & Zola, S. M. (1996). Structure and function of declarative and nondeclarative memory systems. *Proceedings of the National Academy of Sciences*, 93(24), 13515–13522. <https://doi.org/10.1073/pnas.93.24.13515>
- Squire, L. R., Stark, C. E. L., & Clark, R. E. (2004). The medial temporal lobe. *Annual Review of Neuroscience*, 27, 279–306. <https://doi.org/10.1146/annurev.neuro.27.070203.144130>
- Squire, L. R., & Wixted, J. T. (2011). The cognitive neuroscience of memory since H.M. *Annual Review of Neuroscience*, 34, 259–288. <https://doi.org/10.1146/annurev-neuro-061010-113720>
- Squire, L. R., & Dede, A. J. O. (2015). Conscious and unconscious memory systems. *Cold Spring Harbor Perspectives in Biology*, 7(3), a021667. <https://doi.org/10.1101/cshperspect.a021667>
- Staffaroni, A. M., Brown, J. A., Casaletto, K. B., Elahi, F. M., Deng, J., Neuhaus, J., Cobigo, Y., Mumford, P. S., Walters, S., Saloner, R., Karydas, A., Coppola, G., Rosen, H. J., Miller, B. L., Seeley, W. W., & Kramer, J. H. (2018). The longitudinal trajectory of default mode network connectivity in healthy older adults varies as a function of age and is associated with changes in episodic memory and processing speed. *Journal of Neuroscience*, 38(11), 2809–2817. <https://doi.org/10.1523/JNEUROSCI.3067-17.2018>
- Stangl, M., Achtzehn, J., Huber, K., Dietrich, C., Tempelmann, C., & Wolbers, T. (2018). Compromised grid-cell-like representations in old age as a key mechanism to explain age-related navigational deficits. *Current Biology*, 28(7), 1108–1115. <https://doi.org/10.1016/j.cub.2018.02.038>
- Stark, S. M., & Stark, C. E. L. (2017). Age-related deficits in the mnemonic similarity task for objects and scenes. *Behavioural Brain Research*, 333, 109–117. <https://doi.org/10.1016/j.bbr.2017.06.049>
- Stark, C. E. L., & Squire, L. R. (2000). Intact visual perceptual discrimination in humans in the absence of perirhinal cortex. *Learning & Memory*, 7(5), 273–278. <https://doi.org/10.1101/lm.35000>

- Starns, J. J., & Ratcliff, R. (2010). The effects of aging on the speed-accuracy compromise: Boundary optimality in the diffusion model. *Psychology and Aging, 25*(2), 377–390. <https://doi.org/10.1037/a0018022>
- Starns, J. J., & Ratcliff, R. (2012). Age-related differences in diffusion model boundary optimality with both trial-limited and time-limited tasks. *Psychonomic Bulletin & Review, 19*(1), 139–145. <https://doi.org/10.3758/s13423-011-0189-3>
- Steiger, J. H. (1980). Tests for comparing elements of a correlation matrix. *Psychological Bulletin, 87*(2), 245–251. <https://doi.org/10.1037/0033-2909.87.2.245>
- Stening, E., Persson, J., Eriksson, E., Wahlund, L.-O., Zetterberg, H., & Söderlund, H. (2017). Specific patterns of whole-brain structural covariance of the anterior and posterior hippocampus in young APOE  $\epsilon$ 4 carriers. *Behavioural Brain Research, 326*, 256–264. <https://doi.org/10.1016/j.bbr.2017.03.013>
- Stergiakouli, E., Martin, J., Hamshere, M. L., Heron, J., St Pourcain, B., Timpson, N. J., Thapar, A., & Davey Smith, G. (2017). Association between polygenic risk scores for attention-deficit hyperactivity disorder and educational and cognitive outcomes in the general population. *International Journal of Epidemiology, 46*(2), 421–428. <https://doi.org/10.1093/ije/dyw216>
- Stern, Y., Barnes, C. A., Grady, C., Jones, R. N., & Raz, N. (2019). Brain reserve, cognitive reserve, compensation, and maintenance: Operationalization, validity, and mechanisms of cognitive resilience. *Neurobiology of Aging, 83*, 124–129. <https://doi.org/10.1016/j.neurobiolaging.2019.03.022>
- Strittmatter, W. J., Saunders, A. M., Schmechel, D., Pericak-Vance, M., Enghild, J., Salvesen, G. S., & Roses, A. D. (1993). Apolipoprotein E: High-avidity binding to  $\beta$ -amyloid and increased frequency of type 4 allele in late-onset familial Alzheimer disease. *Proceedings of the National Academy of Sciences, 90*(5), 1977–1981. <https://doi.org/10.1073/pnas.90.5.1977>
- Suárez, L. E., Markello, R. D., Betzel, R. F., & Misic, B. (2020). Linking structure and function in macroscale brain networks. *Trends in Cognitive Sciences, 24*(4), 302–315. <https://doi.org/10.1016/j.tics.2020.01.008>
- Subramaniapillai, S., Rajagopal, S., Elshiekh, A., Pasvanis, S., Ankudowich, E., & Rajah, M. N. (2019). Sex differences in the neural correlates of spatial

- context memory decline in healthy aging. *Journal of Cognitive Neuroscience*, 31(12), 1895–1916. [https://doi.org/10.1162/jocn\\_a\\_01455](https://doi.org/10.1162/jocn_a_01455)
- Suri, S., Heise, V., Trachtenberg, A. J., & Mackay, C. E. (2013). The forgotten APOE allele: A review of the evidence and suggested mechanisms for the protective effect of APOE e2. *Neuroscience & Biobehavioral Reviews*, 37(10), 2878–2886. <https://doi.org/10.1016/j.neubiorev.2013.10.010>
- Suri, S., Mackay, C. E., Kelly, M. E., Germuska, M., Tunbridge, E. M., Frisoni, G. B., Matthews, P. M., Ebmeier, K. P., Bulte, D. P., & Filippini, N. (2015). Reduced cerebrovascular reactivity in young adults carrying the APOE ε4 allele. *Alzheimer's & Dementia*, 11(6), 648-657.e1. <https://doi.org/10.1016/j.jalz.2014.05.1755>
- Suzuki, W. A. (2009). Perception and the medial temporal lobe: Evaluating the current evidence. *Neuron*, 61(5), 657–666. <https://doi.org/10.1016/j.neuron.2009.02.008>
- Suzuki, W. A. (2010). Untangling memory from perception in the medial temporal lobe. *Trends in Cognitive Sciences*, 14(5), 195–200. <https://doi.org/10.1016/j.tics.2010.02.002>
- Suzuki, W. A., & Amaral, D. G. (1994). Topographic organization of the reciprocal connections between the monkey entorhinal cortex and the perirhinal and parahippocampal cortices. *Journal of Neuroscience*, 14(3), 1856–1877. <https://doi.org/10.1523/JNEUROSCI.14-03-01856.1994>
- Swainson, R., Hodges, J. R., Galton, C. J., Semple, J., Michael, A., Dunn, B. D., Iddon, J. L., Robbins, T. W., & Sahakian, B. J. (2001). Early detection and differential diagnosis of Alzheimer's disease and depression with neuropsychological tasks. *Dementia and Geriatric Cognitive Disorders*, 12(4), 265–280. <https://doi.org/10.1159/000051269>
- Szucs, D., & Ioannidis, J. P. A. (2017a). When null hypothesis significance testing is unsuitable for research: A reassessment. *Frontiers in Human Neuroscience*, 11, 390. <https://doi.org/10.3389/fnhum.2017.00390>
- Szucs, D., & Ioannidis, J. P. A. (2017b). Empirical assessment of published effect sizes and power in the recent cognitive neuroscience and psychology literature. *PLOS Biology*, 15(3), e2000797. <https://doi.org/10.1371/journal.pbio.2000797>
- Szucs, D., & Ioannidis, J. P. A. (2020). Sample size evolution in neuroimaging research: An evaluation of highly-cited studies (1990–2012) and of latest

- practices (2017–2018) in high-impact journals. *NeuroImage*, 221, 117164. <https://doi.org/10.1016/j.neuroimage.2020.117164>
- Takao, H., Abe, O., Yamasue, H., Aoki, S., Sasaki, H., Kasai, K., Yoshioka, N., & Ohtomo, K. (2010). Gray and white matter asymmetries in healthy individuals aged 21–29 years: A voxel-based morphometry and diffusion tensor imaging study. *Human Brain Mapping*, 32(10), 1762–1773. <https://doi.org/10.1002/hbm.21145>
- Talamini, L. M., & Gorree, E. (2012). Aging memories: Differential decay of episodic memory components. *Learning & Memory*, 19(6), 239–246. <https://doi.org/10.1101/lm.024281.111>
- Talboom, J. S., Håberg, A., De Both, M. D., Naymik, M. A., Schrauwen, I., Lewis, C. R., Bertinelli, S. F., Hammersland, C., Fritz, M. A., Myers, A. J., Hay, M., Barnes, C. A., Glisky, E., Ryan, L., & Huentelman, M. J. (2019). Family history of Alzheimer’s disease alters cognition and is modified by medical and genetic factors. *eLife*, 8, e46179. <https://doi.org/10.7554/eLife.46179>
- Tamnes, C. K., Roalf, D. R., Goddings, A.-L., & Lebel, C. (2018). Diffusion MRI of white matter microstructure development in childhood and adolescence: Methods, challenges and progress. *Developmental Cognitive Neuroscience*, 33, 161–175. <https://doi.org/10.1016/j.dcn.2017.12.002>
- Taylor, K. J., Henson, R. N. A., & Graham, K. S. (2007). Recognition memory for faces and scenes in amnesia: Dissociable roles of medial temporal lobe structures. *Neuropsychologia*, 45(11), 2428–2438. <https://doi.org/10.1016/j.neuropsychologia.2007.04.004>
- Therneau, T. M., Knopman, D. S., Lowe, V. J., Botha, H., Graff-Radford, J., Jones, D. T., Vemuri, P., Mielke, M. M., Schwarz, C. G., Senjem, M. L., Gunter, J. L., Petersen, R. C., & Jack, C. R. (2021). Relationships between  $\beta$ -amyloid and tau in an elderly population: An accelerated failure time model. *NeuroImage*, 242, 118440. <https://doi.org/10.1016/j.neuroimage.2021.118440>
- Therriault, J., Benedet, A. L., Pascoal, T. A., Mathotaarachchi, S., Chamoun, M., Savard, M., Thomas, E., Kang, M. S., Lussier, F., Tissot, C., Parsons, M., Qureshi, M. N. I., Vitali, P., Massarweh, G., Soucy, J.-P., Rej, S., Saha-Chaudhuri, P., Gauthier, S., & Rosa-Neto, P. (2020). Association of apolipoprotein E  $\epsilon$ 4 with medial temporal tau independent of amyloid- $\beta$ . *JAMA Neurology*, 77(4), 470–479. <https://doi.org/10.1001/jamaneurol.2019.4421>

- Thiebaut de Schotten, M., Dell'Acqua, F., Ratiu, P., Leslie, A., Howells, H., Cabanis, E., Iba-Zizen, M. T., Plaisant, O., Simmons, A., Dronkers, N. F., Corkin, S., & Catani, M. (2015). From Phineas Gage and Monsieur Leborgne to H.M.: Revisiting disconnection syndromes. *Cerebral Cortex*, *25*(12), 4812–4827. <https://doi.org/10.1093/cercor/bhv173>
- Thiebaut de Schotten, M., ffytche, D. H., Bizzi, A., Dell'Acqua, F., Allin, M., Walshe, M., Murray, R., Williams, S. C., Murphy, D. G. M., & Catani, M. (2011). Atlasing location, asymmetry and inter-subject variability of white matter tracts in the human brain with MR diffusion tractography. *NeuroImage*, *54*(1), 49–59. <https://doi.org/10.1016/j.neuroimage.2010.07.055>
- Thomas, C., Avidan, G., Humphreys, K., Jung, K., Gao, F., & Behrmann, M. (2009). Reduced structural connectivity in ventral visual cortex in congenital prosopagnosia. *Nature Neuroscience*, *12*(1), 29–31. <https://doi.org/10.1038/nn.2224>
- Thomas, C., Ye, F. Q., Irfanoglu, M. O., Modi, P., Saleem, K. S., Leopold, D. A., & Pierpaoli, C. (2014). Anatomical accuracy of brain connections derived from diffusion MRI tractography is inherently limited. *Proceedings of the National Academy of Sciences*, *111*(46), 16574–16579. <https://doi.org/10.1073/pnas.1405672111>
- Tolman, E. C. (1948). Cognitive maps in rats and men. *Psychological Review*, *55*(4), 189–208. <https://doi.org/10.1037/h0061626>
- Torgersen, J., Helland, C., Flaatten, H., & Wester, K. (2010). Reversible dyscognition in patients with a unilateral, middle fossa arachnoid cyst revealed by using a laptop based neuropsychological test battery (CANTAB). *Journal of Neurology*, *257*(11), 1909–1916. <https://doi.org/10.1007/s00415-010-5634-0>
- Tournier, J.-D., Calamante, F., Gadian, D. G., & Connelly, A. (2004). Direct estimation of the fiber orientation density function from diffusion-weighted MRI data using spherical deconvolution. *NeuroImage*, *23*(3), 1176–1185. <https://doi.org/10.1016/j.neuroimage.2004.07.037>
- Townsend, J. T., & Ashby, F. G. (1978). Methods of modeling capacity in simple processing systems. In J. Castellan & F. Restle (Eds.), *Cognitive theory* (Vol. 3, pp. 200–239). Erlbaum.
- Townsend, J. T., & Ashby, F. G. (1983). *Stochastic modeling of elementary psychological processes*. Cambridge University Press.



- Trachtenberg, A. J., Filippini, N., Cheeseman, J., Duff, E. P., Neville, M. J., Ebmeier, K. P., Karpe, F., & Mackay, C. E. (2012). The effects of APOE on brain activity do not simply reflect the risk of Alzheimer's disease. *Neurobiology of Aging*, *33*(3), 618.e1-618.e13. <https://doi.org/10.1016/j.neurobiolaging.2010.11.011>
- Trachtenberg, A. J., Filippini, N., Ebmeier, K. P., Smith, S. M., Karpe, F., & Mackay, C. E. (2012). The effects of APOE on the functional architecture of the resting brain. *NeuroImage*, *59*(1), 565–572. <https://doi.org/10.1016/j.neuroimage.2011.07.059>
- Tromp, D., Dufour, A., Lithfous, S., Pebayle, T., & Després, O. (2015). Episodic memory in normal aging and Alzheimer disease: Insights from imaging and behavioral studies. *Ageing Research Reviews*, *24*, 232–262. <https://doi.org/10.1016/j.arr.2015.08.006>
- Tsuchida, A., Laurent, A., Crivello, F., Petit, L., Pepe, A., Beguedou, N., Debette, S., Tzourio, C., & Mazoyer, B. (2021). Changes in regional white matter volumetry and microstructure during the post-adolescence period: A cross-sectional study of a cohort of 1,713 university students. *bioRxiv*, <https://doi.org/10.1101/2021.04.13.439695>
- Tu, S., Wong, S., Hodges, J. R., Irish, M., Piguet, O., & Hornberger, M. (2015). Lost in spatial translation—A novel tool to objectively assess spatial disorientation in Alzheimer's disease and frontotemporal dementia. *Cortex*, *67*, 83–94. <https://doi.org/10.1016/j.cortex.2015.03.016>
- Tuch, D. S., Reese, T. G., Wiegell, M. R., Makris, N., Belliveau, J. W., & Wedeen, V. J. (2002). High angular resolution diffusion imaging reveals intravoxel white matter fiber heterogeneity. *Magnetic Resonance in Medicine*, *48*(4), 577–582. <https://doi.org/10.1002/mrm.10268>
- Tucker-Drob, E. M. (2019). Cognitive aging and dementia: A life-span perspective. *Annual Review of Developmental Psychology*, *1*, 177–196. <https://doi.org/10.1146/annurev-devpsych-121318-085204>
- Tulving, E. (1972). Episodic and semantic memory. In E. Tulving & W. Donaldson (Eds.), *Organization of memory* (pp. 381–403). Academic Press.
- Tulving, E. (1983). *Elements of episodic memory*. Oxford University Press.
- Tulving, E. (2002). Episodic memory: From mind to brain. *Annual Review of Psychology*, *53*, 1–25. <https://doi.org/10.1146/annurev.psych.53.100901.135114>

- Tuminello, E. R., & Han, S. D. (2011). The apolipoprotein e antagonistic pleiotropy hypothesis: Review and recommendations. *International Journal of Alzheimer's Disease*, 2011, 726197. <https://doi.org/10.4061/2011/726197>
- Turk-Browne, N. B. (2019). The hippocampus as a visual area organized by space and time: A spatiotemporal similarity hypothesis. *Vision Research*, 165, 123–130. <https://doi.org/10.1016/j.visres.2019.10.007>
- Turney, I. C., Chesebro, A. G., Rentería, M. A., Lao, P. J., Beato, J. M., Schupf, N., Mayeux, R., Manly, J. J., & Brickman, A. M. (2020). APOE  $\epsilon$ 4 and resting-state functional connectivity in racially/ethnically diverse older adults. *Alzheimer's & Dementia: Diagnosis, Assessment & Disease Monitoring*, 12(1), e12094. <https://doi.org/10.1002/dad2.12094>
- Tyrrell, J., Zheng, J., Beaumont, R., Hinton, K., Richardson, T. G., Wood, A. R., Davey Smith, G., Frayling, T. M., & Tilling, K. (2021). Genetic predictors of participation in optional components of UK Biobank. *Nature Communications*, 12, 886. <https://doi.org/10.1038/s41467-021-21073-y>
- Ungar, L., Altmann, A., & Greicius, M. D. (2014). Apolipoprotein E, gender, and Alzheimer's disease: An overlooked, but potent and promising interaction. *Brain Imaging and Behavior*, 8(2), 262–273. <https://doi.org/10.1007/s11682-013-9272-x>
- Ungerleider, L. G., & Haxby, J. V. (1994). 'What' and 'where' in the human brain. *Current Opinion in Neurobiology*, 4(2), 157–165. [https://doi.org/10.1016/0959-4388\(94\)90066-3](https://doi.org/10.1016/0959-4388(94)90066-3)
- Ungerleider, L. G., & Mishkin, M. (1982). Two cortical visual systems. In D. J. Ingle, M. A. Goodale, & R. J. W. Mansfield (Eds.), *Analysis of visual behavior* (pp. 549–586). The MIT Press.
- United Nations. (2020). *World population ageing 2020—Highlights*. [https://www.un.org/development/desa/pd/sites/www.un.org.development.desa.pd/files/undesa\\_pd-2020\\_world\\_population\\_ageing\\_highlights.pdf](https://www.un.org/development/desa/pd/sites/www.un.org.development.desa.pd/files/undesa_pd-2020_world_population_ageing_highlights.pdf)
- Valk, S. L., Di Martino, A., Milham, M. P., & Bernhardt, B. C. (2015). Multicenter mapping of structural network alterations in autism. *Human Brain Mapping*, 36(6), 2364–2373. <https://doi.org/10.1002/hbm.22776>
- Van Beijsterveldt, C. E. M., van Boxtel, M. P. J., Bosma, H., Houx, P. J., Buntinx, F., & Jolles, J. (2002). Predictors of attrition in a longitudinal cognitive aging study: The Maastricht Aging Study (MAAS). *Journal of*

- Clinical Epidemiology*, 55(3), 216–223. [https://doi.org/10.1016/s0895-4356\(01\)00473-5](https://doi.org/10.1016/s0895-4356(01)00473-5)
- van den Heuvel, M. P., de Reus, M. A., Feldman Barrett, L., Scholtens, L. H., Coopmans, F. M. T., Schmidt, R., Preuss, T. M., Rilling, J. K., & Li, L. (2015). Comparison of diffusion tractography and tract-tracing measures of connectivity strength in rhesus macaque connectome. *Human Brain Mapping*, 36(8), 3064–3075. <https://doi.org/10.1002/hbm.22828>
- van der Vlies, A. E., Pijnenburg, Y. A. L., Koene, T., Klein, M., Kok, A., Scheltens, P., & van der Flier, W. M. (2007). Cognitive impairment in Alzheimer's disease is modified by APOE genotype. *Dementia and Geriatric Cognitive Disorders*, 24(2), 98–103. <https://doi.org/10.1159/000104467>
- Van Essen, D. C., & Dierker, D. L. (2007). Surface-based and probabilistic atlases of primate cerebral cortex. *Neuron*, 56(2), 209–225. <https://doi.org/10.1016/j.neuron.2007.10.015>
- van Strien, N. M., Cappaert, N. L. M., & Witter, M. P. (2009). The anatomy of memory: An interactive overview of the parahippocampal–hippocampal network. *Nature Reviews Neuroscience*, 10(4), 272–282. <https://doi.org/10.1038/nrn2614>
- Vandierendonck, A. (2017). A comparison of methods to combine speed and accuracy measures of performance: A rejoinder on the binning procedure. *Behavior Research Methods*, 49(2), 653–673. <https://doi.org/10.3758/s13428-016-0721-5>
- Vandierendonck, A. (2018). Further tests of the utility of integrated speed-accuracy measures in task switching. *Journal of Cognition*, 1(1), 8. <https://doi.org/10.5334/joc.6>
- Vandierendonck, A. (2021). On the utility of integrated speed-accuracy measures when speed-accuracy trade-off is present. *Journal of Cognition*, 4(1), 22. <https://doi.org/10.5334/joc.154>
- Vannini, P., Hedden, T., Huijbers, W., Ward, A., Johnson, K. A., & Sperling, R. A. (2013). The ups and downs of the posteromedial cortex: Age- and amyloid-related functional alterations of the encoding/retrieval flip in cognitively normal older adults. *Cerebral Cortex*, 23(6), 1317–1328. <https://doi.org/10.1093/cercor/bhs108>
- Vaughn, K. E., Cone, J., & Kornell, N. (2018). A user's guide to collecting data online. In H. Otani & B. L. Schwartz (Eds.), *Handbook of research methods*

- in human memory* (1st ed., pp. 354–373). Routledge. <https://doi.org/10.4324/9780429439957-20>
- Veldsman, M., Cheng, H.-J., Ji, F., Werden, E., Khlif, M. S., Ng, K. K., Lim, J. K. W., Qian, X., Yu, H., Zhou, J. H., & Brodtmann, A. (2020). Degeneration of structural brain networks is associated with cognitive decline after ischaemic stroke. *Brain Communications*, 2(2), fcaa155. <https://doi.org/10.1093/braincomms/fcaa155>
- Verghese, J., Lipton, R., & Ayers, E. (2017). Spatial navigation and risk of cognitive impairment: A prospective cohort study. *Alzheimer's & Dementia*, 13(9), 985–992. <https://doi.org/10.1016/j.jalz.2017.01.023>
- Verhagen, J., & Wagenmakers, E.-J. (2014). Bayesian tests to quantify the result of a replication attempt. *Journal of Experimental Psychology: General*, 143(4), 1457–1475. <https://doi.org/10.1037/a0036731>
- Villain, N., Chételat, G., Grassiot, B., Bourgeat, P., Jones, G., Ellis, K. A., Ames, D., Martins, R. N., Eustache, F., Salvado, O., Masters, C. L., Rowe, C. C., Villemagne, V. L., & the AIBL Research Group. (2012). Regional dynamics of amyloid- $\beta$  deposition in healthy elderly, mild cognitive impairment and Alzheimer's disease: A voxelwise PiB-PET longitudinal study. *Brain*, 135(7), 2126–2139. <https://doi.org/10.1093/brain/aws125>
- Villain, N., Desgranges, B., Viader, F., Sayette, V. de la, Mézenge, F., Landeau, B., Baron, J.-C., Eustache, F., & Chételat, G. (2008). Relationships between hippocampal atrophy, white matter disruption, and gray matter hypometabolism in Alzheimer's disease. *Journal of Neuroscience*, 28(24), 6174–6181. <https://doi.org/10.1523/JNEUROSCI.1392-08.2008>
- Villeneuve, S., Rabinovici, G. D., Cohn-Sheehy, B. I., Madison, C., Ayakta, N., Ghosh, P. M., La Joie, R., Arthur-Bentil, S. K., Vogel, J. W., Marks, S. M., Lehmann, M., Rosen, H. J., Reed, B., Olichney, J., Boxer, A. L., Miller, B. L., Borys, E., Jin, L.-W., Huang, E. J., ... Jagust, W. (2015). Existing Pittsburgh compound-B positron emission tomography thresholds are too high: Statistical and pathological evaluation. *Brain*, 138(7), 2020–2033. <https://doi.org/10.1093/brain/awv112>
- Vogel, J. W., Iturria-Medina, Y., Strandberg, O. T., Smith, R., Levitis, E., Evans, A. C., & Hansson, O. (2020). Spread of pathological tau proteins through communicating neurons in human Alzheimer's disease. *Nature Communications*, 11, 2612. <https://doi.org/10.1038/s41467-020-15701-2>

- Vogel, J. W., La Joie, R., Grothe, M. J., Diaz-Papkovich, A., Doyle, A., Vachon-Preseu, E., Lepage, C., Vos de Wael, R., Thomas, R. A., Iturria-Medina, Y., Bernhardt, B., Rabinovici, G. D., & Evans, A. C. (2020). A molecular gradient along the longitudinal axis of the human hippocampus informs large-scale behavioral systems. *Nature Communications*, *11*, 960. <https://doi.org/10.1038/s41467-020-14518-3>
- Vonk, J. M. J., Flores, R. J., Rosado, D., Qian, C., Cabo, R., Habegger, J., Louie, K., Allocco, E., Brickman, A. M., & Manly, J. J. (2019). Semantic network function captured by word frequency in nondemented APOE  $\epsilon 4$  carriers. *Neuropsychology*, *33*(2), 256–262. <https://doi.org/10.1037/neu0000508>
- Vos, S. B., Jones, D. K., Viergever, M. A., & Leemans, A. (2011). Partial volume effect as a hidden covariate in DTI analyses. *NeuroImage*, *55*(4), 1566–1576. <https://doi.org/10.1016/j.neuroimage.2011.01.048>
- Vuoksmaa, E., Palviainen, T., Lindgren, N., Rinne, J. O., & Kaprio, J. (2020). Accuracy of imputation for apolipoprotein E  $\epsilon$  alleles in genome-wide genotyping data. *JAMA Network Open*, *3*(1), e1919960. <https://doi.org/10.1001/jamanetworkopen.2019.19960>
- Wahl, M., Li, Y.-O., Ng, J., Lahue, S. C., Cooper, S. R., Sherr, E. H., & Mukherjee, P. (2010). Microstructural correlations of white matter tracts in the human brain. *NeuroImage*, *51*(2), 531–541. <https://doi.org/10.1016/j.neuroimage.2010.02.072>
- Wakana, S., Caprihan, A., Panzenboeck, M. M., Fallon, J. H., Perry, M., Gollub, R. L., Hua, K., Zhang, J., Jiang, H., Dubey, P., Blitz, A., van Zijl, P., & Mori, S. (2007). Reproducibility of quantitative tractography methods applied to cerebral white matter. *NeuroImage*, *36*(3), 630–644. <https://doi.org/10.1016/j.neuroimage.2007.02.049>
- Walhovd, K. B., Fjell, A. M., & Espeseth, T. (2014). Cognitive decline and brain pathology in aging—Need for a dimensional, lifespan and systems vulnerability view. *Scandinavian Journal of Psychology*, *55*(3), 244–254. <https://doi.org/10.1111/sjop.12120>
- Wang, L., Laviolette, P., O’Keefe, K., Putcha, D., Bakkour, A., Van Dijk, K. R. A., Pihlajamäki, M., Dickerson, B. C., & Sperling, R. A. (2010). Intrinsic connectivity between the hippocampus and posteromedial cortex predicts memory performance in cognitively intact older individuals. *NeuroImage*, *51*(2), 910–917. <https://doi.org/10.1016/j.neuroimage.2010.02.046>

- Wang, S.-F., Ritchey, M., Libby, L. A., & Ranganath, C. (2016). Functional connectivity based parcellation of the human medial temporal lobe. *Neurobiology of Learning and Memory*, *134*, 123–134. <https://doi.org/10.1016/j.nlm.2016.01.005>
- Wang, X., Bernhardt, B. C., Karapanagiotidis, T., De Caso, I., Gonzalez Alam, T. R. D. J., Cotter, Z., Smallwood, J., & Jefferies, E. (2018). The structural basis of semantic control: Evidence from individual differences in cortical thickness. *NeuroImage*, *181*, 480–489. <https://doi.org/10.1016/j.neuroimage.2018.07.044>
- Wang, X., Zhou, W., Ye, T., Lin, X., Zhang, J., & for Alzheimer's Disease Neuroimaging Initiative. (2019). Sex difference in the association of APOE4 with memory decline in mild cognitive impairment. *Journal of Alzheimer's Disease*, *69*(4), 1161–1169. <https://doi.org/10.3233/JAD-181234>
- Wang, Y.-T. T., Pascoal, T. A., Therriault, J., Kang, M. S., Benedet, A. L., Savard, M., Tissot, C., Lussier, F. Z., Arias, J. F., Mathotaarachchi, S., Rajah, M. N., Gauthier, S., Rosa-Neto, P., & for the Alzheimer's Disease Neuroimaging Initiative. (2021). Interactive rather than independent effect of APOE and sex potentiates tau deposition in women. *Brain Communications*, *3*(2), fcab126. <https://doi.org/10.1093/braincomms/fcab126>
- Watson, H. C., Wilding, E. L., & Graham, K. S. (2012). A role for perirhinal cortex in memory for novel object–context associations. *Journal of Neuroscience*, *32*(13), 4473–4481. <https://doi.org/10.1523/JNEUROSCI.5751-11.2012>
- Wechsler, D. (1997). *WAIS-III: Administration and scoring manual* (3rd ed.). The Psychological Corporation.
- Wechsler, D. (1998). *Wechsler Memory Scale: Administration and scoring manual*. The Psychological Corporation.
- Weiner, K. S., & Zilles, K. (2016). The anatomical and functional specialization of the fusiform gyrus. *Neuropsychologia*, *83*, 48–62. <https://doi.org/10.1016/j.neuropsychologia.2015.06.033>
- Weisgraber, K. H., Rall, S. C., & Mahley, R. W. (1981). Human E apoprotein heterogeneity. Cysteine-arginine interchanges in the amino acid sequence of the apo-E isoforms. *Journal of Biological Chemistry*, *256*(17), 9077–9083. [https://doi.org/10.1016/S0021-9258\(19\)52510-8](https://doi.org/10.1016/S0021-9258(19)52510-8)

- Weissberger, G. H., Nation, D. A., Nguyen, C. P., Bondi, M. W., & Han, S. D. (2018). Meta-analysis of cognitive ability differences by apolipoprotein e genotype in young humans. *Neuroscience & Biobehavioral Reviews*, *94*, 49–58. <https://doi.org/10.1016/j.neubiorev.2018.08.009>
- Westlye, E. T., Hodneland, E., Haász, J., Espeseth, T., Lundervold, A., & Lundervold, A. J. (2012). Episodic memory of APOE  $\epsilon$ 4 carriers is correlated with fractional anisotropy, but not cortical thickness, in the medial temporal lobe. *NeuroImage*, *63*(1), 507–516. <https://doi.org/10.1016/j.neuroimage.2012.06.072>
- Westlye, E. T., Lundervold, A., Rootwelt, H., Lundervold, A. J., & Westlye, L. T. (2011). Increased hippocampal default mode synchronization during rest in middle-aged and elderly APOE  $\epsilon$ 4 carriers: Relationships with memory performance. *Journal of Neuroscience*, *31*(21), 7775–7783. <https://doi.org/10.1523/JNEUROSCI.1230-11.2011>
- Wilcox, R. R., & Tian, T. S. (2011). Measuring effect size: A robust heteroscedastic approach for two or more groups. *Journal of Applied Statistics*, *38*(7), 1359–1368. <https://doi.org/10.1080/02664763.2010.498507>
- Wisdom, N. M., Callahan, J. L., & Hawkins, K. A. (2011). The effects of apolipoprotein E on non-impaired cognitive functioning: A meta-analysis. *Neurobiology of Aging*, *32*(1), 63–74. <https://doi.org/10.1016/j.neurobiolaging.2009.02.003>
- Wisniewski, T., & Drummond, E. (2020). APOE-amyloid interaction: Therapeutic targets. *Neurobiology of Disease*, *138*, 104784. <https://doi.org/10.1016/j.nbd.2020.104784>
- Wisse, L. E. M., Daugherty, A. M., Olsen, R. K., Berron, D., Carr, V. A., Stark, C. E. L., Amaral, R. S. C., Amunts, K., Augustinack, J. C., Bender, A. R., Bernstein, J. D., Boccardi, M., Bocchetta, M., Burggren, A., Chakravarty, M. M., Chupin, M., Ekstrom, A. D., de Flores, R., Insausti, R., ... la Joie, R. (2017). A harmonized segmentation protocol for hippocampal and parahippocampal subregions: Why do we need one and what are the key goals? *Hippocampus*, *27*(1), 3–11. <https://doi.org/10.1002/hipo.22671>
- Witter, M. P., & Amaral, D. G. (1991). Entorhinal cortex of the monkey: V. Projections to the dentate gyrus, hippocampus, and subicular complex. *The Journal of Comparative Neurology*, *307*(3), 437–459. <https://doi.org/10.1002/cne.903070308>

- Witter, M. P., Wouterlood, F. G., Naber, P. A., & Haeften, T. V. (2000). Anatomical organization of the parahippocampal-hippocampal network. *Annals of the New York Academy of Sciences*, *911*(1), 1–24. <https://doi.org/10.1111/j.1749-6632.2000.tb06716.x>
- Wolbers, T., & Wiener, J. M. (2014). Challenges for identifying the neural mechanisms that support spatial navigation: The impact of spatial scale. *Frontiers in Human Neuroscience*, *8*, 571. <https://doi.org/10.3389/fnhum.2014.00571>
- Wolk, D. A., Dickerson, B. C., & the Alzheimer's Disease Neuroimaging Initiative. (2010). Apolipoprotein E (APOE) genotype has dissociable effects on memory and attentional-executive network function in Alzheimer's disease. *Proceedings of the National Academy of Sciences*, *107*(22), 10256–10261. <https://doi.org/10.1073/pnas.1001412107>
- Wolters, F. J., Yang, Q., Biggs, M. L., Jakobsdottir, J., Li, S., Evans, D. S., Bis, J. C., Harris, T. B., Vasan, R. S., Zilhao, N. R., Ghanbari, M., Ikram, M. A., Launer, L., Psaty, B. M., Tranah, G. J., Kulminski, A. M., Gudnason, V., Seshadri, S., & Investigators, for the E.-C. (2019). The impact of APOE genotype on survival: Results of 38,537 participants from six population-based cohorts (E2-CHARGE). *PLOS ONE*, *14*(7), e0219668. <https://doi.org/10.1371/journal.pone.0219668>
- Woods, A. T., Velasco, C., Levitan, C. A., Wan, X., & Spence, C. (2015). Conducting perception research over the internet: A tutorial review. *PeerJ*, *3*, e1058. <https://doi.org/10.7717/peerj.1058>
- World Health Organisation. (2017). *Global action plan on the public health response to dementia 2017–2025*. <https://apps.who.int/iris/bitstream/handle/10665/259615/9789241513487-eng.pdf?sequence=1>
- Wright, P., Randall, B., Clarke, A., & Tyler, L. K. (2015). The perirhinal cortex and conceptual processing: Effects of feature-based statistics following damage to the anterior temporal lobes. *Neuropsychologia*, *76*, 192–207. <https://doi.org/10.1016/j.neuropsychologia.2015.01.041>
- Yamamoto, K., Tanei, Z.-I., Hashimoto, T., Wakabayashi, T., Okuno, H., Naka, Y., Yizhar, O., Fenno, L. E., Fukayama, M., Bito, H., Cirrito, J. R., Holtzman, D. M., Deisseroth, K., & Iwatsubo, T. (2015). Chronic optogenetic activation augments a $\beta$  pathology in a mouse model of Alzheimer disease. *Cell Reports*, *11*(6), 859–865. <https://doi.org/10.1016/j.celrep.2015.04.017>



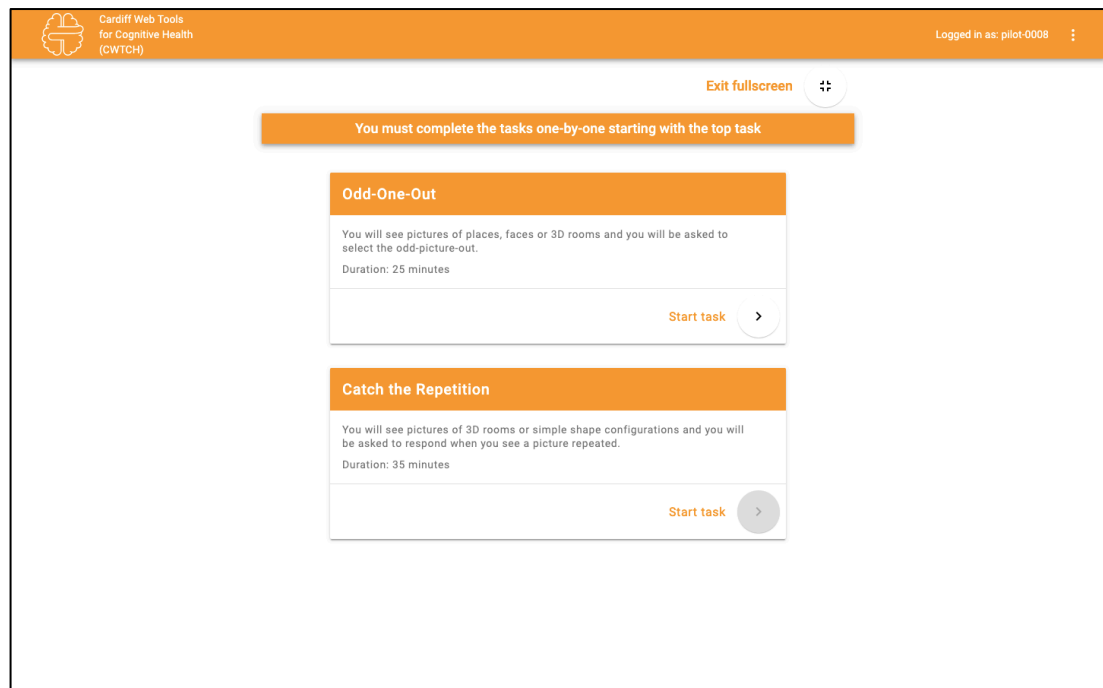
- Yang, C., Zhong, S., Zhou, X., Wei, L., Wang, L., & Nie, S. (2017). The abnormality of topological asymmetry between hemispheric brain white matter networks in Alzheimer's disease and mild cognitive impairment. *Frontiers in Aging Neuroscience*, 9, 261. <https://doi.org/10.3389/fnagi.2017.00261>
- Yarkoni, T., Poldrack, R. A., Nichols, T. E., Van Essen, D. C., & Wager, T. D. (2011). Large-scale automated synthesis of human functional neuroimaging data. *Nature Methods*, 8(8), 665–670. <https://doi.org/10.1038/nmeth.1635>
- Yeatman, J. D., Dougherty, R. F., Ben-Shachar, M., & Wandell, B. A. (2012). Development of white matter and reading skills. *Proceedings of the National Academy of Sciences*, 109(44), E3045–E3053. <https://doi.org/10.1073/pnas.1206792109>
- Yee, Y., Fernandes, D. J., French, L., Ellegood, J., Cahill, L. S., Vousden, D. A., Spencer Noakes, L., Scholz, J., van Eede, M. C., Nieman, B. J., Sled, J. G., & Lerch, J. P. (2018). Structural covariance of brain region volumes is associated with both structural connectivity and transcriptomic similarity. *NeuroImage*, 179, 357–372. <https://doi.org/10.1016/j.neuroimage.2018.05.028>
- Yeo, B. T., Krienen, F. M., Sepulcre, J., Sabuncu, M. R., Lashkari, D., Hollinshead, M., Roffman, J. L., Smoller, J. W., Zöllei, L., Polimeni, J. R., Fischl, B., Liu, H., & Buckner, R. L. (2011). The organization of the human cerebral cortex estimated by intrinsic functional connectivity. *Journal of Neurophysiology*, 106(3), 1125–1165. <https://doi.org/10.1152/jn.00338.2011>
- Yeung, L.-K., Ryan, J. D., Cowell, R. A., & Barense, M. D. (2013). Recognition memory impairments caused by false recognition of novel objects. *Journal of Experimental Psychology: General*, 142(4), 1384–1397. <https://doi.org/10.1037/a0034021>
- Yohai, V. J. (1987). High breakdown-point and high efficiency robust estimates for regression. *The Annals of Statistics*, 15(2), 642–656. <https://doi.org/10.1214/aos/1176350366>
- Yonelinas, A. P. (2002). The nature of recollection and familiarity: A review of 30 years of research. *Journal of Memory and Language*, 46(3), 441–517. <https://doi.org/10.1006/jmla.2002.2864>
- Yu, J.-T., Tan, L., & Hardy, J. (2014). Apolipoprotein E in Alzheimer's Disease: An update. *Annual Review of Neuroscience*, 37, 79–100. <https://doi.org/10.1146/annurev-neuro-071013-014300>

- Yu, J.-T., Xu, W., Tan, C.-C., Andrieu, S., Suckling, J., Evangelou, E., Pan, A., Zhang, C., Jia, J., Feng, L., Kua, E.-H., Wang, Y.-J., Wang, H.-F., Tan, M.-S., Li, J.-Q., Hou, X.-H., Wan, Y., Tan, L., Mok, V., ... Vellas, B. (2020). Evidence-based prevention of Alzheimer's disease: Systematic review and meta-analysis of 243 observational prospective studies and 153 randomised controlled trials. *Journal of Neurology, Neurosurgery, and Psychiatry*, *91*(11), 1201–1209. <https://doi.org/10.1136/jnnp-2019-321913>
- Yuan, P., & Grutzendler, J. (2016). Attenuation of  $\beta$ -amyloid deposition and neurotoxicity by chemogenetic modulation of neural activity. *Journal of Neuroscience*, *36*(2), 632–641. <https://doi.org/10.1523/JNEUROSCI.2531-15.2016>
- Yushkevich, P. A., Amaral, R. S. C., Augustinack, J. C., Bender, A. R., Bernstein, J. D., Boccardi, M., Bocchetta, M., Burggren, A. C., Carr, V. A., Chakravarty, M. M., Chetelat, G., Daugherty, A. M., Davachi, L., Ding, S.-L., Ekstrom, A. D., Geerlings, M. I., Hassan, A., Huang, Y., Iglesias, E., ... Zeineh, M. M. (2015). Quantitative comparison of 21 protocols for labeling hippocampal subfields and parahippocampal subregions in in vivo MRI: Towards a harmonized segmentation protocol. *NeuroImage*, *111*, 526–541. <https://doi.org/10.1016/j.neuroimage.2015.01.004>
- Yushkevich, P. A., López, M. M., Martín, M. M. I. de O., Ittyerah, R., Lim, S., Ravikumar, S., Bedard, M. L., Pickup, S., Liu, W., Wang, J., Hung, L. Y., Lasserre, J., Vergnet, N., Xie, L., Dong, M., Cui, S., McCollum, L., Robinson, J. L., Schuck, T., ... Insausti, R. (2021). Three-dimensional mapping of neurofibrillary tangle burden in the human medial temporal lobe. *Brain*, *awab262*. <https://doi.org/10.1093/brain/awab262>
- Zeidman, P., & Maguire, E. A. (2016). Anterior hippocampus: The anatomy of perception, imagination and episodic memory. *Nature Reviews Neuroscience*, *17*(3), 173–182. <https://doi.org/10.1038/nrn.2015.24>
- Zhao, J., Thiebaut de Schotten, M., Altarelli, I., Dubois, J., & Ramus, F. (2016). Altered hemispheric lateralization of white matter pathways in developmental dyslexia: Evidence from spherical deconvolution tractography. *Cortex*, *76*, 51–62. <https://doi.org/10.1016/j.cortex.2015.12.004>
- Zheng, L., Duan, J., Duan, X., Zhou, W., Chen, C., Li, Y., Chen, J., Zhou, W., Wang, Y.-J., Li, T., & Song, W. (2016). Association of apolipoprotein E (ApoE) polymorphism with Alzheimer's disease in Chinese population. *Current Alzheimer Research*, *13*(8), 912–917. <https://doi.org/10.2174/1567205013666160401115307>

- Zheng, L. J., Lin, L., Schoepf, U. J., Varga-Szemes, A., Savage, R. H., Zhang, H., Wang, Y. F., Zhang, X. Y., Luo, S., Liu, Y., Yang, G. F., Lu, G. M., & Zhang, L. J. (2021). Different posterior hippocampus and default mode network modulation in young APOE  $\epsilon$ 4 carriers: A functional connectome-informed phenotype longitudinal study. *Molecular Neurobiology*, *58*(6), 2757–2769. <https://doi.org/10.1007/s12035-021-02292-2>
- Zhong, J. Y., & Moffat, S. D. (2018). Extrahippocampal contributions to age-related changes in spatial navigation ability. *Frontiers in Human Neuroscience*, *12*, 272. <https://doi.org/10.3389/fnhum.2018.00272>
- Zielinski, B. A., Gennatas, E. D., Zhou, J., & Seeley, W. W. (2010). Network-level structural covariance in the developing brain. *Proceedings of the National Academy of Sciences*, *107*(42), 18191–18196. <https://doi.org/10.1073/pnas.1003109107>
- Zokaei, N., Board, A. G., Slavkova, E., Mackay, C. E., Nobre, A. C., & Husain, M. (2021). Superior short-term memory in APOE  $\epsilon$ 2 carriers across the age range. *Behavioural Brain Research*, *397*, 112918. <https://doi.org/10.1016/j.bbr.2020.112918>
- Zokaei, N., Čepukaitytė, G., Board, A. G., Mackay, C. E., Husain, M., & Nobre, A. C. (2019). Dissociable effects of the apolipoprotein-E (APOE) gene on short- and long-term memories. *Neurobiology of Aging*, *73*, 115–122. <https://doi.org/10.1016/j.neurobiolaging.2018.09.017>
- Zola-Morgan, S., Squire, L. R., & Ramus, S. J. (1994). Severity of memory impairment in monkeys as a function of locus and extent of damage within the medial temporal lobe memory system. *Hippocampus*, *4*(4), 483–495. <https://doi.org/10.1002/hipo.450040410>
- Zwaan, R. A., Etz, A., Lucas, R. E., & Donnellan, M. B. (2018). Improving social and behavioral science by making replication mainstream: A response to commentaries. *Behavioral and Brain Sciences*, *41*, e157. <https://doi.org/10.1017/S0140525X18000961>

## Appendix

### 6.1. Chapter 2: The task menu from the CWTCH research platform



*Note.* The task menu from the CWTCH research platform is shown. As made clear by the instruction at the top of the screen, participants were required to complete the top task first. Until this was done, the option to start the bottom task was inhibited (i.e. “greyed out”). The order in which participants completed the tasks was random. To improve accessibility, the spatial n-back task was referred to as the “Catch the Repetition” task.

## 6.2. Chapter 2: Family history of dementia questionnaire

This questionnaire asks about family history of dementia. We wish to know whether a first-degree relative has ever been diagnosed with dementia. First-degree relatives include biological parents (mother, father), siblings (sister, brother) and offspring (daughter, son). It does not include grandparents, cousins and so forth. For the purpose of this questionnaire, we will only ask about biological parents and siblings.

For clarity, the term dementia refers to a group of symptoms that may include problems with memory, thinking speed, problem solving or language. There are several different causes of dementia, although the most common are Alzheimer's disease, vascular dementia, dementia with Lewy bodies and frontotemporal dementia (also known as Pick's disease).

By providing this information, we will be better able to understand whether variations in our genes influence perception and memory abilities independent of family history of dementia.

Please provide your responses below by selecting the appropriate boxes (yes/no). If you do not know the answer, or if the question is not applicable to you (e.g. because you do not have any biological siblings), please select NA as your response.

*Has one of your biological parents (mother, father) ever been diagnosed with dementia?*

Yes [ ]

No [ ]

NA [ ]

*Have any of your biological siblings (sister, brother) ever been diagnosed with dementia?*

Yes [ ]

No [ ]

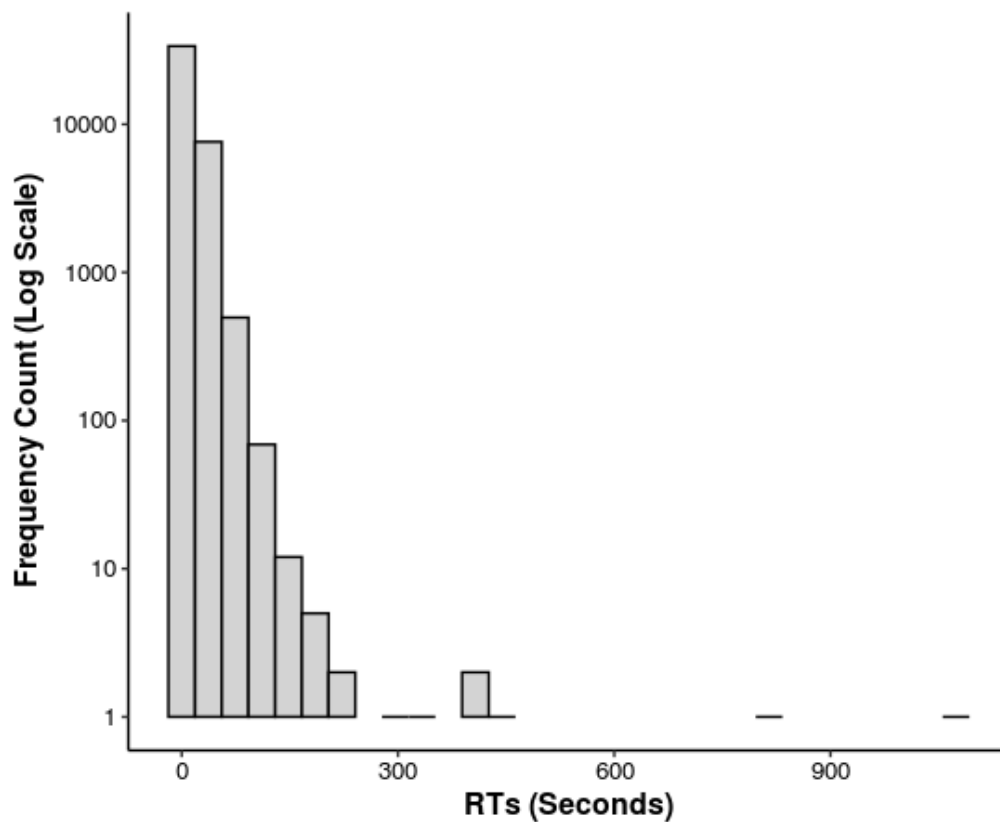
NA [ ]

### 6.3. Chapter 2: Correspondence between directly measured and imputed *APOE* genotypes

Directly Measured	Imputed					Total
	$\epsilon 2/\epsilon 2$	$\epsilon 2/\epsilon 3$	$\epsilon 3/\epsilon 3$	$\epsilon 3\epsilon 4$	$\epsilon 4/\epsilon 4$	
$\epsilon 2/\epsilon 2$	2	0	1	0	0	3
$\epsilon 2/\epsilon 3$	0	41	9	2	1	53
$\epsilon 3/\epsilon 3$	2	7	237	17	0	263
$\epsilon 3/\epsilon 4$	0	3	22	67	0	92
$\epsilon 4/\epsilon 4$	0	0	1	1	4	6
Total	4	51	270	87	5	417

*Note.* Of the 710 participants for whom *APOE* genotype (except  $\epsilon 2/\epsilon 4$ ) was successfully imputed (see Figure 2.2), 417 also had directly measured *APOE* genotype data available (58.73%). Values represent the total number of participants within each particular combination of directly measured and imputed *APOE* genotypes. Overall correspondence was relatively high (84.17%), which is largely consistent with prior reports (for relevant examples, see Lupton et al., 2018; Oldmeadow et al., 2014; Radmanesh et al., 2014; Vuoksimaa et al., 2020).

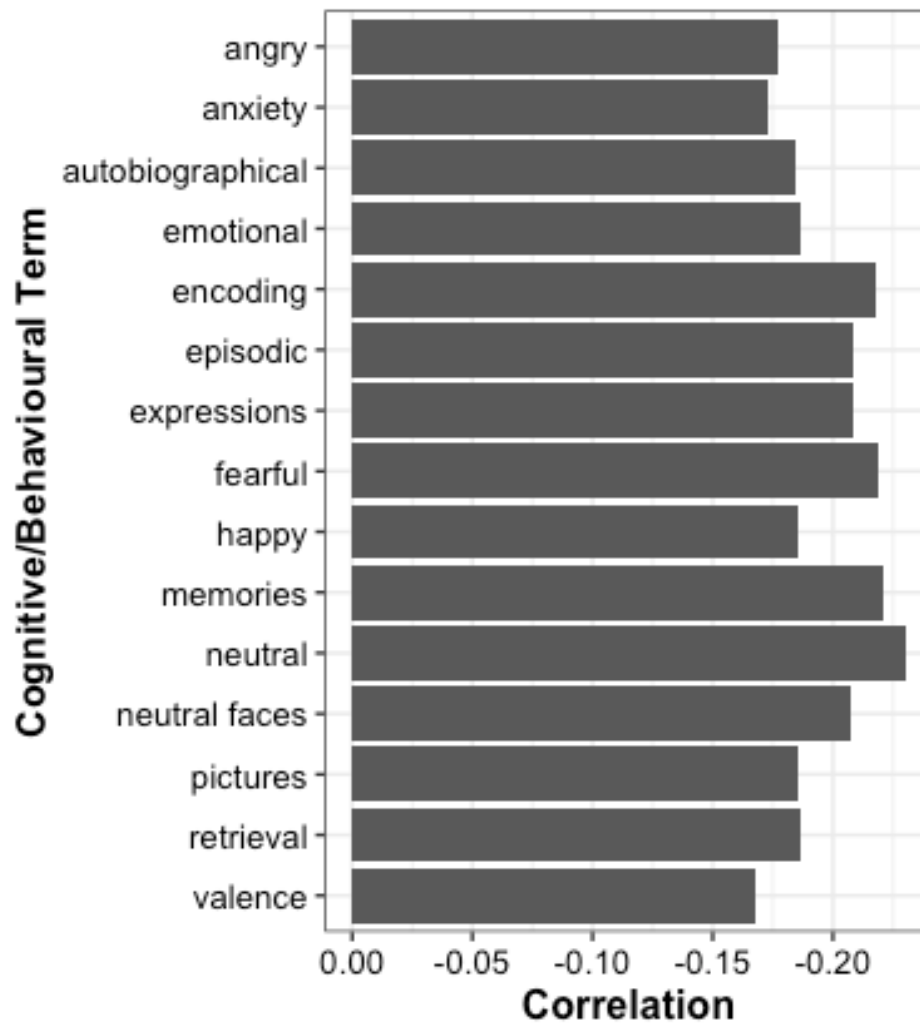
#### 6.4. Chapter 2: Distribution of all RTs – collapsed across participants – on the four-choice oddity task



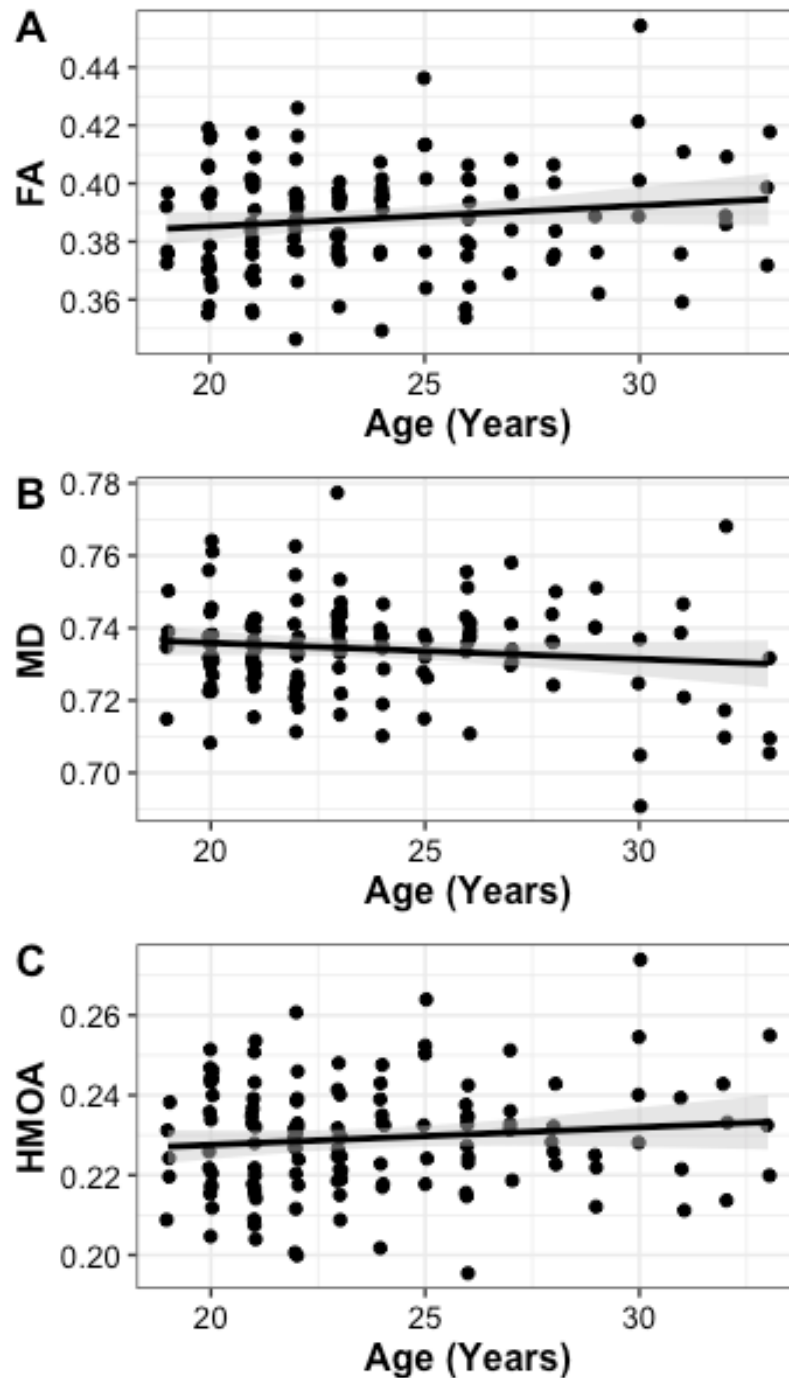
*Note.* The distribution of all trial-level RTs ( $N = 41,920$ ) – across participants and regardless of condition – is shown. To facilitate interpretation, the y-axis has been log-transformed. As can be seen, there were a relatively large number of slow trials (>30 seconds) on the four-choice oddity task. In fact, the maximum observed value – shown here – was 1074 seconds (i.e. 17.9 minutes).



### 6.5. Chapter 3: Correlations between cognitive/behavioural terms and the unthresholded BSR map



*Note.* Correlations between the top 15 cognitive/behavioural terms associated with the unthresholded BSR map, as determined by NeuroSynth, are shown. All correlations were negative as the majority of voxels in the unthresholded BSR maps were negative. As such, stronger, more negative correlations represent terms that are more commonly associated with the observed pattern.

**6.6. Chapter 4: Association between age and PHCB microstructure (FA, MD, HMOA)**

*Note.* The association between age and PHCB FA (A), MD (B), and HMOA (C) is shown. A small amount of jitter has been added to each point for clarity. For FA and HMOA, the association was positive (but relatively weak). For MD, the association was negative (but relatively weak). However, as can be seen, there were relatively few participants aged 25 years or above in the current sample, and even fewer aged 30 years or above. This limits the ability to draw meaningful inferences from the cross-sectional data.